

# Possibilities of timber high-rise

A parametric study on the possibilities of timber high-rise in The Netherlands  
A. van Rhijn



# Possibilities of timber high-rise

A parametric study on the possibilities of timber high-rise in  
The Netherlands

by

A. van Rhijn

to obtain the degree of Master of Science  
at the Delft University of Technology,  
to be defended publicly on Wednesday March 11, 2020.

Student number:	4163257	
Project duration:	February 2019 - March 2020	
Thesis committee:	prof. dr. ir. J. W. G. van de Kuilen	TU Delft chairman
	dr. ir. G. J. P. Ravenshorst	TU Delft
	dr. ir. M.A.N. Hendriks	TU Delft
	ir. P. Timmerman	Arcadis

An electronic version of this thesis is available at <http://repository.tudelft.nl/>.



# Preface

This report presents my graduation research to finish my masters Structural Engineering at Delft University of Technology, which I have enjoyed with great pleasure.

First of all I would like to thank my daily supervisor dr.ir. Ravenshorst for guiding my through the research and having long conversations to answer all the questions I had throughout the year. Also I would like to thank the other members of the graduation committee, prof.dr.ir. van de Kuilen and dr.ir. M.A.N. Hendriks for their enthusiasm and critical view during the meetings we had.

Thanks to all the colleagues from Arcadis for their hospitality and the opportunity to graduate at their company. In particular I would like to thank Pieter Timmerman for helping me on daily base and sharing his expertise and knowledge. Secondly, I would like to express my gratitude to Michael van Telgen and Igor Pećanac for their great support on all aspects involving parametric design.

I have the good fortune in life to have wonderful friends who always support me, for which I am immensely grateful. A special thanks to Petra for all her love and support during the majority of my studies. I could not have done this without you.

*Arthur van Rhijn*  
*Rotterdam, March 2020*



# Summary

Sustainability is an important aspect in the construction industry nowadays and therefore timber is interesting to use as it is considered a sustainable building material. With the development of mass timber engineered products such as glued and cross laminated timber, there are more and more possibilities to use timber as a structural element, but this material is not yet widely used in high-rise buildings. Recent research has shown different aspects to take into account when using timber. Due to the lightweight, high flexibility and strength, attention must be paid to the dynamic behaviour and the high horizontal deflections of the top levels of the building due to wind [2, 51, 59].

This thesis aims to give an insight on the possibilities of timber high-rise structures by making use of a parametric model. Therefore, the following research questions will be examined:

- *How can a parametric model be used to examine the possibilities of timber high-rise?*
- *What are the possibilities of timber high-rise regarding maximum building height in The Netherlands?*

A parametric model is used to generate the structural model, which enables you to easily change certain parameters to gain a quick insight into the consequences of these changes on the behaviour of the structure. The model is developed in the program Autodesk Dynamo, where a plug-in developed by the company Arcadis is used to connect Dynamo to a FEA application called RFEM to be able to check the generated structure on relevant criteria.

The parametric model is able to design a building which has certain dimensions and lateral stability systems which can be changed. It is chosen to implement lateral stability systems consisting of shear core(s), a diagrid and a tube, which can be used either independently or combined. The connections between the elements can not be modelled with a finite stiffness using the Arcadis plug-in. Therefore, several assumptions had to be made to encounter for the characteristics of the connections. The Young's modulus of the structural elements are modified to take into account the stiffness of the connections and openings in surfaces if present.

To check if the parametric model gives satisfying results, a case study is performed on the BrockCommons Tallwood House. This showed that the parametric model gives satisfactory results.

A parametric study is performed to check the possibilities of timber high-rise regarding maximum building height in The Netherlands. An office building with a width of 32.4 metres, a depth of 28.8 metres with a specific floor plan and connection characteristics is used. Optimal configurations regarding compressive and tensile resistance of connections between structural elements are resolved using MATLAB and the reduction of Young's modulus of the elements is determined using the specific connection characteristics.

The connections used in the parametric study are compared to commonly used connections regarding strength and stiffness. Furthermore, an insight is given on the influence of the stiffness of the connections on the structure.

The maximum building heights are investigated for stability systems consisting of either a shear core, diagrid, tube or a combination of 2 stability systems. Results show that a 4-storey diagrid system with infinite stiff connections can reach the greatest height of 187.2 metres. No additional measures had to be taken to ensure that each structure complied with the maximum acceleration limit for office buildings. Finally, a comparison is made between the stability systems with regard to total timber volume and steel mass usage.



# Contents

<b>Summary</b>	<b>v</b>
<b>List of Figures</b>	<b>ix</b>
<b>List of Tables</b>	<b>xiii</b>
<b>1 Introduction</b>	<b>1</b>
1.1 Introduction to timber high-rise . . . . .	1
1.2 Introduction to parametric design . . . . .	3
1.3 Problem description . . . . .	4
1.4 Objectives. . . . .	4
1.5 Methodology . . . . .	4
<b>2 Background information</b>	<b>7</b>
2.1 Lateral stability and gravitational systems for high-rise . . . . .	7
2.2 Timber as a structural material . . . . .	8
2.3 Timber connections. . . . .	11
2.4 Introduction to parametric design . . . . .	13
<b>3 Design and verification of the structure</b>	<b>19</b>
3.1 Loads on structure . . . . .	19
3.2 Stresses . . . . .	24
3.3 Buckling . . . . .	26
3.4 Deformation . . . . .	27
3.5 Global initial sway imperfections . . . . .	28
3.6 Vibration . . . . .	28
3.7 Fire safety. . . . .	30
3.8 Connections . . . . .	34
<b>4 Development of parametric model</b>	<b>41</b>
4.1 Global design . . . . .	41
4.2 Setup of parametric model in Dynamo and RFEM . . . . .	43
4.3 Method of using the parametric model . . . . .	51
<b>5 Case study: Brock Commons Tallwood House</b>	<b>53</b>
5.1 General information . . . . .	53
5.2 Load-bearing structure . . . . .	53
5.3 Detailing . . . . .	54
5.4 Parametric model of the building . . . . .	55
5.5 Structural analysis results . . . . .	57
5.6 Conclusion . . . . .	59
<b>6 Parametric study on timber high-rise in The Netherlands</b>	<b>61</b>
6.1 Basic principles of the design . . . . .	61
6.2 Characteristics of columns . . . . .	62
6.3 Characteristics of diagonals. . . . .	64
6.4 Properties of floors . . . . .	71
6.5 Characteristics of stability core . . . . .	73
6.6 Characteristics of facade elements . . . . .	80
6.7 Characteristics of foundation . . . . .	88
6.8 Fire safety design . . . . .	88
<b>7 Background on connections</b>	<b>91</b>
7.1 Connections between members . . . . .	91

7.2	Shear connection between corners of walls . . . . .	94
7.3	Tension and shear connections between stacked walls . . . . .	99
<b>8</b>	<b>Results of parametric study</b>	<b>105</b>
8.1	Structure with concrete stability core . . . . .	105
8.2	Structure with CLT stability core . . . . .	108
8.3	Structure with diagrid using glued-in threaded rods connections . . . . .	111
8.4	Structure with diagrid using steel plates and dowel connections . . . . .	115
8.5	Structure with tube system . . . . .	118
8.6	Structure with combined stability systems . . . . .	120
<b>9</b>	<b>Comparison between the stability systems</b>	<b>123</b>
9.1	Maximum building height and slenderness . . . . .	123
9.2	Timber material usage . . . . .	125
9.3	Steel material usage . . . . .	128
9.4	Comparison with other stability systems . . . . .	129
<b>10</b>	<b>Conclusions and Recommendations</b>	<b>133</b>
10.1	Conclusions. . . . .	133
10.2	Recommendations . . . . .	135
	<b>Bibliography</b>	<b>137</b>
<b>A</b>	<b>Connections</b>	<b>141</b>
A.1	MATLAB script for determining strength of slotted-in steel plates and dowels connection . . . . .	141
A.2	MATLAB script for determining strength of glued-in rod connection . . . . .	143
A.3	MATLAB script for determining maximum strength of slotted-in steel plates and dowels connection . . . . .	144
A.4	Maximum strength of slotted-in steel plates and dowels connection . . . . .	147
A.5	MATLAB script for determining maximum strength of glued-in rods connection . . . . .	149
A.6	Maximum strength of glued-in rods connection . . . . .	151
A.7	MATLAB script for determining shear resistance of screwed connection . . . . .	153
<b>B</b>	<b>Structural elements calculations</b>	<b>155</b>
B.1	Structural analysis of floor beam . . . . .	155
B.2	Strength of glued-in rod connection of Brockcommons Tallwood Building . . . . .	156
B.3	Shear strength of screwed corner connection . . . . .	156
B.4	Tensile strength of glued-in rods connection . . . . .	157
B.5	Separating function of wall assembly . . . . .	158
B.6	Connection study . . . . .	162
<b>C</b>	<b>Dynamo model overview</b>	<b>169</b>
C.1	Dynamo model overview . . . . .	170
C.2	Dynamo model custom node . . . . .	171
C.3	Dynamo model facade element research . . . . .	173
<b>D</b>	<b>Parametric study results</b>	<b>175</b>
D.1	RFEM results for structure with concrete stability core . . . . .	176
D.2	RFEM results for structure with CLT stability core. . . . .	177
D.3	RFEM results for diagrid structure with glued-in rods connections . . . . .	178
D.4	RFEM results for diagrid structure with steel plates and dowels connections . . . . .	181
D.5	RFEM results for structure with tube system . . . . .	184
D.6	RFEM results for structures with multiple stability systems . . . . .	185
D.7	Timber volume for different type of stability systems . . . . .	186
D.8	Steel mass for different type of stability systems. . . . .	187

# List of Figures

1.1	Stadthaus, London [40]	1
1.2	LifeCycle Tower One [17]	2
1.3	Treet, Bergen [2]	2
1.4	Mjøstårnet, Brumunddal [1]	3
1.5	Nationaal Militair Museum [6]	4
2.1	Lateral stability and gravitational systems for high-rise	7
2.2	Glued laminated timber [22, 43]	9
2.3	Cross-laminated timber [4, 37]	10
2.4	Joints with glued-in rods [52]	11
2.5	Methods to fabricate connections with glued rods [14]	12
2.6	Joint with steel nails [55]	12
2.7	Joint with steel plates and dowels [4, 39]	13
2.8	Joint with adhesive (XEPOX) [53]	13
2.9	GenerativeComponents [11], Grasshopper [11] and Autodesk Dynamo	14
2.10	Dynamo file with different elements	14
2.11	Background 3D preview of Dynamo file	15
2.12	Member node	16
2.13	Support node	16
2.14	Load and load case nodes	16
2.15	ModelToRFEM node	17
2.16	Dynamo model exported to RFEM	17
2.17	Nodes for result data	17
3.1	The use of partial safety factors and $k_{mod}$ to ensure limit states [4]	20
3.2	Different wind zones in The Netherlands	21
3.3	Velocity pressure distributed over the building	22
3.4	Different zones for a building	23
3.5	Stress-strain diagram for clear wood [4]	25
3.6	Deflection components [4]	27
3.7	Global initial sway imperfection [30]	28
3.8	Acceptable accelerations for specific frequencies [16]	29
3.9	Definition of the reduced cross-section method [31]	31
3.10	Values for $k_0$ for protected member	31
3.11	Charring depth for unprotected and protected timber member	32
3.12	Basic insulation value [20]	33
3.13	Basic protection value [20]	33
3.14	Failure modes for dowel connections with 2 steel plates [47]	35
3.15	The values of $l_{v,i}$ and $l_{t,i}$	36
3.16	Spacing and edge/end distances for dowel connections in tension	36
3.17	Spacing and edge/end distances for dowel connections in compression	37
3.18	Defined distances for connection with glued-in rods [19]	38
3.19	Failure mechanism for glued-in threaded rod in shear	39
4.1	Global design of the different stability systems	42
4.2	Overview of the Dynamo custom node	44
4.3	Column and connections in series	45
4.4	Modelling the columns in RFEM	45
4.5	Modelling the columns in RFEM	46

4.6	Modelling the core in RFEM . . . . .	46
4.7	Divisions of the bottom core walls . . . . .	47
4.8	Modelling the diagrid in RFEM . . . . .	47
4.9	Modelling the facade elements in RFEM . . . . .	48
4.10	Modelling permanent loads in RFEM . . . . .	49
4.11	Modelling the wind loads in RFEM . . . . .	49
4.12	Loads applied to the floors . . . . .	50
4.13	Modelling combination of systems in RFEM . . . . .	50
4.14	Method of using the parametric model . . . . .	52
5.1	Side-views of the Brock Commons Tallwood House [45] . . . . .	53
5.2	Floorplan of the Brock Commons Tallwood House [45] . . . . .	54
5.3	Connections column to concrete podium and column to column [48] . . . . .	54
5.4	Floor to core connection [48] . . . . .	55
5.5	Type X gypsum layers around a column [45] . . . . .	55
5.6	RFEM model of Brockcommons Tallwood Building . . . . .	57
5.8	Maximum compression and tension forces . . . . .	58
5.9	Maximum acceleration of the top level of the Brock Commons building . . . . .	59
6.1	Floor plan of the building without any lateral stability system . . . . .	62
6.2	Maximum tension force in 700x700mm member with glued-in rod connection . . . . .	63
6.3	Detail of connection between 400x400mm columns using glued-in threaded rods . . . . .	64
6.4	Maximum compression and tension force in dowel connection for 700x700mm member . . . . .	65
6.5	Maximum compression and tension force in dowel connection for different column dimensions . . . . .	66
6.6	Stiffness of different connection configurations . . . . .	67
6.7	Detail of connection between diagonals using slotted-in steel plates and dowels . . . . .	69
6.8	Detail of connection between diagonals using glued-in threaded rods . . . . .	70
6.9	Decrease of compression resistance due to buckling . . . . .	71
6.10	Floor plan for each storey of the building . . . . .	72
6.11	Reinforcement of concrete core elements . . . . .	74
6.12	Connections of core walls in CLT . . . . .	75
6.13	Dimensions and symbols of mechanically jointed beams theory . . . . .	76
6.14	Core dimensions for determining effective bending stiffness . . . . .	77
6.15	Effective bending stiffness for core with corner connections in x- and y-directions . . . . .	77
6.16	Effective bending stiffness for core with corner connections . . . . .	78
6.17	Resistance to compression and shear for toothed connection . . . . .	79
6.18	Detail of connection between sides of facade elements . . . . .	81
6.19	Parametric model for investigating influence of opening in facade . . . . .	82
6.20	Stiffness reduction due to openings in facade elements . . . . .	82
6.21	Reduced stiffness of a CLT wall panel with an opening . . . . .	83
6.22	Method of Dujic compared to RFEM results . . . . .	83
6.23	RFEM model overview for determining bending stiffness reduction . . . . .	84
6.24	Bending stiffness reduction due to connections at the sides of the facade elements . . . . .	85
6.25	Facade dimensions for determining effective bending stiffness . . . . .	85
6.26	Effective facade flange width . . . . .	86
6.27	Reduction of bending stiffness due to corner connections . . . . .	86
6.28	Total bending stiffness reduction of facade surface . . . . .	87
6.29	Concentration of compressive and tensile stresses between the openings . . . . .	88
6.30	Deflections due to stiffness of the structure and foundation . . . . .	88
6.31	Reduction of compressive resistance for different fire safety levels . . . . .	89
6.32	Char layer depth for different fire protective layer thicknesses . . . . .	89
6.33	Separating function for different wall thicknesses . . . . .	90
7.1	Side views of different commonly used connections between timber members . . . . .	92
7.2	Modelling the member combined with a connection with finite stiffness . . . . .	93
7.3	Contribution of a connection to the total vertical deformation . . . . .	94
7.4	Side views of commonly used connection between wall segments to transfer shear forces . . . . .	95

7.5	Connection strength and stiffness for different connections . . . . .	96
7.6	Top view of the investigated structure . . . . .	97
7.7	Contribution of connections to total horizontal displacements in y-direction . . . . .	98
7.8	Contribution of connections to total horizontal displacements in x-direction . . . . .	98
7.9	Overview of tension connections between wall elements . . . . .	99
7.10	Models as used to determine influence of vertical connection stiffness on the structures . . . . .	101
7.11	Contribution of connection to total horizontal displacements of 10-metres width wall . . . . .	102
7.12	Contribution of connection to total horizontal displacements of 20-metres width wall . . . . .	102
7.13	Models as used to determine influence of vertical connection stiffness on the structures . . . . .	103
7.14	Contribution of connection to total horizontal displacements of 10-metres width wall . . . . .	104
8.1	Core properties for different building heights . . . . .	106
8.2	Unity check of core stresses for different building heights . . . . .	106
8.3	Column dimensions for different building heights . . . . .	107
8.4	Increase in core size for 18-storey and 20-storey building . . . . .	107
8.5	Maximum accelerations of top level for different building heights . . . . .	108
8.6	Core properties for different building heights . . . . .	108
8.7	Unity check of core stresses for different building heights . . . . .	109
8.8	Stresses in the core walls . . . . .	110
8.9	Column dimensions for different building heights . . . . .	110
8.10	Maximum accelerations of top level for different building heights . . . . .	111
8.11	Definition of the angle of a diagonal . . . . .	111
8.12	Diagonal size for each diagrid . . . . .	113
8.13	Forces in diagonals . . . . .	113
8.14	Column dimensions for all diagrid types . . . . .	114
8.15	Maximum acceleration of the top level for each diagrid type . . . . .	115
8.16	Diagonal size for each diagrid . . . . .	116
8.17	Column dimensions for different building heights . . . . .	117
8.18	Maximum acceleration of the top level for each diagrid type . . . . .	117
8.19	Column size for different building heights . . . . .	118
8.20	Unity checks of stresses . . . . .	119
8.21	Stresses in facade . . . . .	119
8.22	Max acceleration of the top level . . . . .	120
8.23	Unity checks for different stresses . . . . .	121
8.24	Maximum acceleration of the top level . . . . .	122
9.1	Maximum building height for each type of stability system . . . . .	123
9.2	Maximum building height for combinations of stability systems . . . . .	124
9.3	Volume of timber per type of stability system . . . . .	126
9.4	Distribution of volume for different type of stability systems . . . . .	127
9.5	Steel volume for different building heights . . . . .	128
9.6	Distribution of steel mass per stability system . . . . .	129
9.7	Comparison between completed buildings and results from parametric study . . . . .	130
A.1	Compression and tension strength for 300x300mm and 400x400mm member . . . . .	147
A.2	Compression and tension strength for 500x500mm and 600x600mm member . . . . .	147
A.3	Compression and tension strength for 700x700mm and 800x800mm member . . . . .	147
A.4	Compression and tension strength for 900x900mm and 1000x1000mm member . . . . .	148
A.5	Compression and tension strength for 1100x1100mm and 1200x1200mm member . . . . .	148
A.6	Tensile strength for 300x300mm and 400x400mm member . . . . .	151
A.7	Tensile strength for 500x500mm and 600x600mm member . . . . .	151
A.8	Tensile strength for 700x700mm and 800x800mm member . . . . .	151
A.9	Tensile strength for 900x900mm and 1000x1000mm member . . . . .	152
A.10	Tensile strength for 1100x1100mm and 1200x1200mm member . . . . .	152
B.1	Simply supported floor beam . . . . .	155
B.2	Column connection of Brockcommons Tallwood Building . . . . .	156

---

B.3	Position coefficients of exposed wall assembly . . . . .	158
B.4	Position coefficients of unexposed wall assembly . . . . .	159
B.5	Join coefficients for wall assembly . . . . .	160
C.1	Dynamo model overview . . . . .	170
C.2	Dynamo custom node overview . . . . .	171
C.3	Dynamo window research . . . . .	173

# List of Tables

2.1	Material properties of different materials . . . . .	8
2.2	Strength classes for GLT [18] . . . . .	9
2.3	Characteristic values for different properties of C24 . . . . .	10
2.4	Characteristic values for Parallam PSL 2.0E Column [62] . . . . .	11
2.5	Plug-ins for Grasshopper and Dynamo to perform a structural analysis [8] . . . . .	14
3.1	Combination factors $\psi$ for an office building . . . . .	20
3.2	Values of $k_{mod}$ for different load-duration and service classes for solid timber, glulam and CLT [4] . . . . .	20
3.3	$\nu_{b,0}$ for different wind zones in The Netherlands . . . . .	21
3.4	Roughness length for different terrain categories in The Netherlands [27] . . . . .	22
3.5	External pressure coefficients . . . . .	23
3.6	Human perception levels [42] . . . . .	29
3.7	Basic insulation and protection values for different materials . . . . .	34
3.8	Minimum spacing and edge/end distances for a dowel connection [31] . . . . .	37
4.1	Load combinations for ULS and SLS . . . . .	43
5.1	Material properties for RFEM model of Brock Commons Tallwood House . . . . .	56
5.2	Dynamo input values . . . . .	56
6.1	Dynamo input values . . . . .	61
6.2	Characteristics of the connections for different columns sizes . . . . .	63
6.3	Maximum compression and tension forces of a connection with glued-in rods for different column dimensions . . . . .	64
6.4	Characteristics of the connections for the different column dimensions . . . . .	66
6.5	Maximum compression and tension forces of a dowel connection for different column dimensions . . . . .	67
6.6	Ratios between columns and columns with connections . . . . .	68
6.7	Equivalent in-plane stiffness of a CLT plate . . . . .	73
6.8	Maximum spans for different plate thicknesses . . . . .	73
6.9	Strength properties of concrete core . . . . .	74
6.10	Normalised stiffness for different building heights . . . . .	78
6.11	Strength properties of CLT core elements . . . . .	80
6.12	Normalised stiffness for different building heights . . . . .	87
7.1	Properties of different columnn connections . . . . .	93
7.2	ctc for all shear connections . . . . .	96
7.3	Strength and stiffness properties of connections . . . . .	100
8.1	Inputs for different diagrids . . . . .	112
8.2	Maximum height of combined stability systems . . . . .	120
9.1	Maximum building height and slenderness of single stability systems . . . . .	125
9.1	Maximum building height and slenderness of combined stability systems . . . . .	125
9.2	Completed buildings and other case studies [10, 36, 50] . . . . .	130
9.3	Results from parametric study . . . . .	131
B.1	Structural calculations of the floor beam . . . . .	155
B.2	Calculation of resistance of glued-in rod connection . . . . .	156
B.3	Shear strength of screwed corner connection . . . . .	157

B.4	Tensile resistance of glued-in rods . . . . .	157
B.5	Separating function for 135 millimetres thick wall . . . . .	160
B.6	Separating function for 225 millimetres thick wall . . . . .	161
B.7	Separating function for 315 millimetres thick wall . . . . .	161
B.8	Separating function for 405 millimetres thick wall . . . . .	161
B.9	Separating function for 495 millimetres thick wall . . . . .	162
B.10	Calculation of resistance of glued-in rod connection . . . . .	162
B.11	Compression and tension of the net timber area . . . . .	163
B.12	Compression and tension of the net timber area . . . . .	163
B.13	Resistance of dowels (both dowel failure and embedment failure) . . . . .	163
B.14	Block shear and plug shear failure . . . . .	163
B.15	Tension in the net area of the steel plates . . . . .	164
B.16	Strength and stiffness of TTV240 . . . . .	165
B.17	Strength and stiffness of TTN240 . . . . .	165
B.18	Strength and stiffness of TTS240 . . . . .	165
B.19	Strength of connection E . . . . .	165
B.20	Strength and stiffness of connection F . . . . .	166
B.21	Strength and stiffness of connection G . . . . .	166
B.22	Strength of connection B . . . . .	167
B.23	Calculation of resistance of glued-in rod connection . . . . .	167
B.24	Strength of connection B . . . . .	167
B.25	Strength of connection D . . . . .	168
B.26	Strength of connection E . . . . .	168

# 1

## Introduction

As the title of this thesis states, 2 topics are involved in this research, namely timber high-rise structures and parametric design. A short introduction is given to both subjects.

### 1.1. Introduction to timber high-rise

Sustainability is an important aspect in the construction industry nowadays. Therefore, more buildings are being built using timber as a construction material as it is considered sustainable due to its low embodied energy and its ability to store carbon dioxide. Timber is also getting more interesting to use because of the development of mass timber engineered products, such as glued and cross laminated timber, which have better strength and stiffness properties compared to ordinary wood. Although wood is a combustible material, it will keep its structural integrity due to a charred layer which will protect the inner layers of the material. Timber could therefore be a suitable construction material to be used in high-rise buildings.

Nearly 30 mass timber buildings over 8 stories tall are completed, under construction or in late-phase design in 2014 and in the last 5 years, another 19 8 stories tall buildings have been completed [15]. Some timber buildings which are already built will be briefly discussed.

#### 1.1.1. Stadthaus, London, England

Stadthaus is a residential building located in London consisting of 9 stories. It is the first building made out of only cross-laminated timber panels. Not only is CLT used for walls and floors, but also for staircases and lift cores. The building houses a total of 29 apartments and also an office is located on the ground floor.

Each timber element was prefabricated and cut-outs for windows and doors were already applied before transported to the construction site. Therefore, they could be put in place immediately, which resulted in a very short construction time of only 49 weeks, 20 weeks less than a construction of a similar building made out of concrete would take [58].

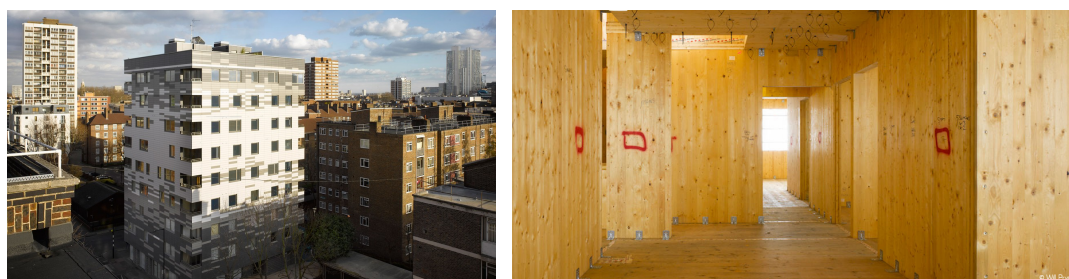


Figure 1.1: Stadthaus, London [40]

### 1.1.2. LifeCycle Tower One, Dornbirn, Austria

The LifeCycle tower One is an office building which consists of a wood-concrete composite structural system located in Dornbirn (Austria). The building has 8 stories, is 24 metres in length and 13 metres in width. The staircase core, situated on one side of the building, is made of reinforced concrete. Due to fire prevention regulations in the Austrian building regulations, a staircase made of timber was not allowed by the authorities.

The facade elements are prefabricated using recycled material. Due to the fact that this building has prefabricated building modules, the erection time was 8 days after the foundation and stair case were finished, which is half the time of a traditional building made of concrete.



Figure 1.2: LifeCycle Tower One [17]

### 1.1.3. "Treet", Bergen, Norway

"Treet" is 14-storey high residential building located at Bergen, Norway and houses 62 apartments. The structure contains load-carrying Glulam trusses and 2 intermediate strengthened levels, the so called "power stories". These levels have a prefabricated concrete slab. The main function of these slabs is to increase the total mass of the building. The apartments are prefabricated residential modules which are placed on each strengthened level. A maximum of 4 modules are put on top of each other. The load-carrying trusses are placed along the facade and gives the buildings its lateral stiffness. The elevator shafts, staircases and internal walls are made of CLT. They do not incorporate with the stability system of the building.

The cross-sections of the load-bearing structure are increased to obtain a fire resistance of 90 minutes. All elements are connected using slotted-in steel plates and dowels.



Figure 1.3: Treet, Bergen [2]

### 1.1.4. Mjøstårnet, Brumunddal, Norway

Mjøstårnet in Brumunddal is a residential building finished in 2019. It has a height of 85.4 metres and is therefore the world's tallest timber building. The building has 18 storeys which houses apartments, a hotel

and offices.

The main load bearing structure consists of glulam trusses which are located in the facade, combined with internal columns and beams. The trusses transfer vertical and horizontal forces to the foundation. All members are connected using a steel plate with dowels. CLT walls are used to carry the elevator shafts and staircases.

The floors are made of prefabricated wooden slabs, which are called Trä8 elements made by Moelven. The 7 upper floors have an additional concrete finishing layer is added to satisfy the comfort criteria and acoustics requirements.

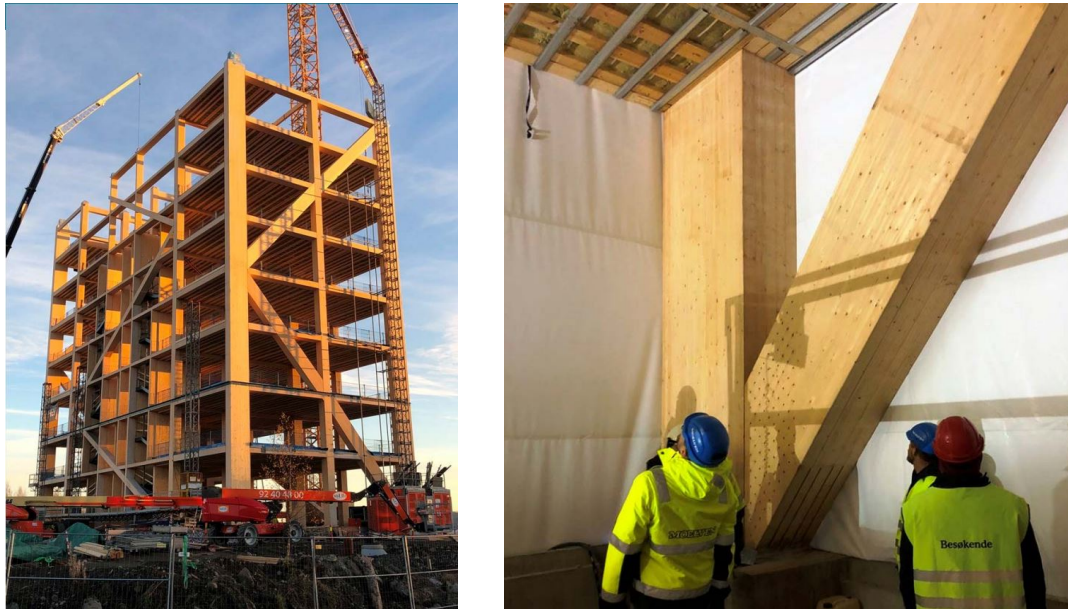


Figure 1.4: Mjöstårnet, Brumunddal [1]

## 1.2. Introduction to parametric design

Parametric software has been used mostly for architectural purposes, but structural engineers recently started to use this technology as well. It allows you to generate a structural design by using algorithms which are defined using certain parameters. This can be done without the use of programming code by making use of visual functions, where the results can directly be seen as a graphical representation. Therefore, also non-experienced programmers will be able to use such parametric software packages. Parametric design is being used more and more in practice due to the following advantages [8]:

- Complex geometries, boundary conditions and load cases are easy to generate.
- It enables you to make an infinite number of variants by making use of different parameters in a short amount of time.
- Parametric models can be reused in different projects, which saves time and thus money.

These software packages allow you to generate a design, but is unable to check the design on structural requirements. Therefore, it is necessary to connect the parametric software package to structural analysis software, which can examine stresses and deformations.

For example, a parametric model is used during the design phase of the load bearing structure of the 'Nationaal Militair Museum' in Soest, The Netherlands. It was used to optimise the dead weight of the roof structure and to minimise the amount of columns needed [6].



Figure 1.5: Nationaal Militair Museum [6]

### 1.3. Problem description

Recent research has shown different aspects to take into account when using timber as a construction material for high-rise. Due to the lightweight, high flexibility and strength, attention must be paid to the dynamic behaviour and the high horizontal deflections of the top levels of the building due to wind. This has been demonstrated in research done on existing residential buildings with a timber lateral stability system like Treet [2, 59] and on buildings with a concrete stability core and timber load-bearing columns [51, 62].

Although these studies have shown that these problems exist, it is still not clear which building heights are within the possibilities of timber structures without these problems occurring. It will be very useful to use a parametric model to be able to easily change certain parameters of a structure and thereby gain a quick insight into the consequences of these changes.

### 1.4. Objectives

#### 1.4.1. Main research question

Following section 1.3, this will lead to the main research questions:

- How can a parametric model be used to examine the possibilities of timber high-rise?
- What are the possibilities regarding maximum building height of timber high-rise in The Netherlands?

#### 1.4.2. Sub questions

The following sub questions will be examined to get an inside on the problems of the main questions:

- What are important aspects for high-rise timber structures?
- What are the criteria for ultimate and serviceability limit state for high-rise timber structures?
- How can a parametric model be created to be used in combination with a finite element software package?
- What are the limitations of using a parametric model to analyse a timber high-rise structure?
- What aspects determine the building height limits of a high-rise timber structure?

### 1.5. Methodology

In order to answer the research questions, first the characteristics of timber high-rise are examined in chapter 2. Therefore, different stability systems often used for high-rise in general are elaborated. Next, properties of timber construction materials, such as glued and cross laminated timber, and connection which are often used in timber structures are studied. Furthermore, the possibilities regarding parametric design are looked at in aspect to structural design. Therefore, a connection between parametric and finite element analysis

(FEA) software is examined.

A timber building must be designed according to the criteria for ultimate and serviceability limit state described by the Eurocode and other relevant codes which are used in The Netherlands. In chapter 3, the rules and requirements provided by these codes are looked further into.

A parametric model will be made which can generate structures with different stability systems. This is done by using the program Dynamo, which can collaborate with the FEA software RFEM using a plug-in made by the company Arcadis. This is elaborated in chapter 4. With the structural calculations done by RFEM, the relevant criteria described in chapter 3 can be checked.

In chapter 5, the results the parametric model generates are checked whether or not it produces satisfactory results by performing a case study. An already existing timber high-rise building named BrockCommons Tallwood House, located in Vancouver, will be examined using the parametric model.

To analyse the possibilities of a timber high-rise building regarding maximum building height, first the basic principles of the design are explained in chapter 6. Then the characteristics of all connection used in the structure are determined. An optimization is performed using MATLAB in order to obtain the properties of connection which give the highest resistance to compression, tension and shear forces. The stiffness of the different specific connections are cooperated into the design by adapting the Young's modulus of the structural elements.

In chapter 7, connections which are commonly used are explained and compared with the specific connections assumed in chapter 6. The influence of the stiffness of the connections on the structure is explained for connections between members and between walls.

Finally, in chapter 8 and chapter 9 the possibilities regarding maximum building height for different stability systems is investigated. The results are discussed with regard to element dimensions, stresses and dynamic behaviour. The configurations of the different stability systems, together with combinations of different systems, are then compared on material usage.



# 2

## Background information

In this chapter, background information is given on timber high-rise and parametric design. First, different stability systems used in high-rise are identified, after which the characteristics of timber and timber engineered products are investigated. Some types of connections commonly used in timber structures are being discussed and the possibilities of parametric design are presented.

### 2.1. Lateral stability and gravitational systems for high-rise

The term high-rise can have many definitions. For example, the Cambridge Dictionary describes it as 'a tall modern building with many floors' [49] and the Encyclopaedia Britannica calls a building high-rise when its a 'multi-storey building tall enough to require the use of a system of mechanical vertical transportation' [13]. Emporis provides a clearer definition, they state that 'a high-rise building is a structure whose architectural height is between 35 and 100 metres' and that buildings can furthermore be defined as high-rise when it has a minimum of 12 floors and the height is not known or when it has fewer than 40 floors and the height is unknown [21].

Different structural systems can be used which provide sufficient stiffness to withstand lateral and gravity loads. These systems can be considered as vertical cantilever beams fixed in the ground. The cantilever beam has to carry vertical gravity loads, due to dead and live loads, and lateral wind with possible earthquake loads. A couple of widely used stability systems are described. Often some of these stability systems are combined to obtain even greater stiffness.

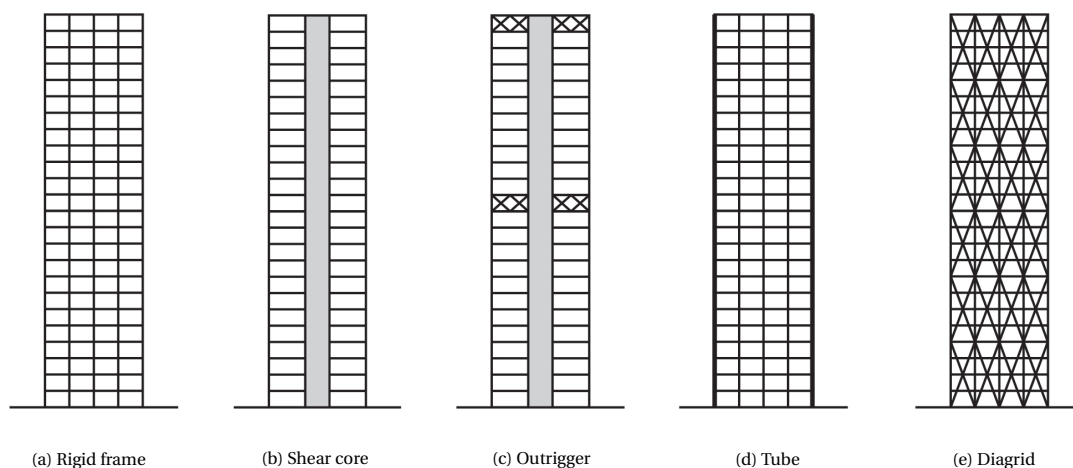


Figure 2.1: Lateral stability and gravitational systems for high-rise

### 2.1.1. Rigid frame system

A rigid frame system is a system which consist of load resisting columns connected with horizontal members by using a rigid connection. The vertical and lateral loads are resisted by bending of the beams and the columns, therefore no bracings are required. The stiffness of this system is mainly determined by the bending rigidity of the beams and columns and the rigidity of the connections between those beams and columns.

### 2.1.2. Shear wall system

A shear wall system is a system which consist of continuous vertical walls which carry the lateral and gravitational loads. These walls are often placed in the core of the building and will act as vertical cantilevers. They are mostly made of reinforced concrete, but can also be made out of timber panels. The shear wall system can be combined with the rigid frame system, thus when the floors and columns have a rigid connection with the core, these can provide additional stiffness to the structure.

### 2.1.3. Outrigger system

The outrigger system is a system which consist of (an) outrigger(s) connected to a core. This outrigger makes it possible to induce additional tension and compression forces in the outer columns and thus reduces the overturning moment in the core. This results in a more stiff structure. The outriggers are generally made of steel trusses or reinforced concrete walls.

### 2.1.4. Tube system

The tube system is a system for which the building is designed to act as a hollow cantilever perpendicular to the ground. The exterior of the building, known as the load-bearing facade, consists of elements which are joined. This results in shear deformation of these elements, which are unequally distributed due to shear lag, and compression/tension due to bending deformation. They can be made of concrete, steel, timber or a composite.

### 2.1.5. Diagrid system

The diagrid system is a system which has a framework composed of elements that intersect in a diagonal pattern. The diagonals act as a lattice girder. Due to these diagonals, there is no need for additional rigid columns or cores for stability. Frequently, the diagrid framework is applied in the facade.

## 2.2. Timber as a structural material

Timber has a lower strength, but a better weight to strength ratio compared to reinforced concrete or steel. Because of this, it is possible to create very light structures compared to structures made out of traditional materials. On the other hand, timber has a lower Young's modulus compared to the other materials. In Table 2.1 a comparison of different construction materials is shown.

Table 2.1: Material properties of different materials

Material	Bending strength $f_m$ ( $N/mm^2$ )	Density $\rho$ ( $kg/m^3$ )	Ratio $\rho/f_m$
Timber	20	400	20
Steel	300	7850	26
Reinforced concrete	40	2400	60

Timber is an orthotropic material, which means that this material has different properties in different directions, for example parallel or perpendicular to the grain. These properties are often described in longitudinal, radial and tangential directions. For example, timber is significantly stronger in the longitudinal direction than in the tangential and radial directions. Also, the shrinkage and swelling behaviour of the timber differs in all directions. For example, the tangential shrinkage is about twice as high as that of the radial direction.

To improve the behaviour of the timber on anisotropy, mass timber engineered products are being developed. The most used products are glued laminated timber and cross laminated timber. These products have higher stiffness and strength compared to traditional wood and have better shrinkage behaviour.

### 2.2.1. Glued Laminated Timber

Glued laminated timber (GLT or Glulam) is a timber engineered product made out of boards stacked on top of each other parallel to the grain. They are glued together using an adhesive. This allows for larger cross-sections than possible with regular sawn wood. Weak points like knots have less influence on the overall cross-section and thus GLT products have a better homogeneity than regular timber. GLT can be made of various wood species like pine, fir and larch, but mostly spruce is used.

Sawn timber with a large cross-section can have large pith and shrinkage cracks and therefore moisture can penetrate the wood easily. With glued laminated timber you can simply remove any deformations formed during the drying process and thus these problems can be reduced.



Figure 2.2: Glued laminated timber [22, 43]

GLT is specified in different strength classes depending on the mean compressive strength. These classes are shown in Table 2.2. The suffix *h* means that the Glulam is homogeneous, where a suffix *c* implies that the Glulam consists of different timber classes.

Table 2.2: Strength classes for GLT [18]

$N/mm^2$	GL24h	GL24c	GL28h	GL28c	GL32h	GL32c	GL36h	GL36c
$f_{m,g,k}$	24	24	28	28	32	32	36	36
$f_{t,0,g,k}$	16.5	14	19.5	16.5	22.5	19.5	26	22.5
$f_{t,90,k}$	0.5	0.5	0.5	0.5	0.5	0.5	0.5	0.5
$f_{c,0,g,k}$	24	21	26.5	24	29	26.5	31	29
$f_{c,90,k}$	2.7	2.4	3.0	2.7	3.3	3.0	3.6	3.3
$f_{v,k}$	3.5	3.5	3.5	3.5	3.5	3.5	3.5	3.5
$E_{0,mean}$	11600	11600	12600	12600	13700	13700	14700	14700
$E_{90,mean}$	390	320	420	390	460	420	490	460
$G_{mean}$	720	590	780	720	850	780	910	850
$kg/m^3$								
$\rho_{g,k}$	380	350	410	380	430	410	450	430

### 2.2.2. Cross-Laminated Timber

Cross-laminated timber (CLT) is a timber engineered product made out of lumber boards stacked at 90 degree angle to each other, which are then glued together using an adhesive. Often an uneven number of layers is used to obtain a symmetrical cross-section. The layers are connected with finger-joints in longitudinal direction. Most of the time, CLT is made of spruce, but panels can also be made of fir, pine or larch. The maximum sizes of a single CLT plate are 3 metres in width, 18 metres in length and can have a maximum total thickness of 500mm [7]. CLT plates are often fabricated by using C24 boards. The characteristic values for the different properties of C24 plates are shown in Table 2.3.

Table 2.3: Characteristic values for different properties of C24

Strength and stiffness properties in $N/mm^2$		C24
Bending edgewise	$f_{m,k}$	24
Tension parallel to the grain	$f_{t,0,k}$	14.5
Tension perpendicular to the grain	$f_{t,90,k}$	0.4
Compression parallel to the grain	$f_{c,0,k}$	21
Compression perpendicular to the grain	$f_{c,90,k}$	2.5
Shear	$f_{v,k}$	4.0
Mean modulus of elasticity	$E_{0,mean}$	11000
0.05% percentile modulus of elasticity	$E_{0.05}$	9600
5% modulus of elasticity	$E_{0.05}$	740
Density in $kg/m^3$		
Characteristic density	$\rho_k$	350

Due to the fact that this product has layers in different directions, it can transfer loads on all sides and this results in a great use for large wall and floor panels. Another advantage is that CLT is not very sensitive to moisture change and creep.



Figure 2.3: Cross-laminated timber [4, 37]

### 2.2.3. Parallel Strand Lumber

Parallel Strand Lumber (PSL) is a timber engineered product made of wooden strands. They are made of waste veneers from the production of plywood. Cuts around 23 mm wide and 2.5 metres long are made from the veneer sheets and positioned in the longitudinal direction of the beam or column. The cuts are then pressed together and glued. Because of this process, it is possible to produce beams and columns with almost infinite length.

PSL has high strength and stiffness properties, which is also depicted in Table 2.4, where the characteristic values for Parallam PSL 2.0E are shown.

Table 2.4: Characteristic values for Parallam PSL 2.0E Column [62]

Strength and stiffness properties in $N/mm^2$	Parallam PSL 2.0E Column	
Bending edgewise	$f_{m,k}$	59
Tension parallel to the grain	$f_{t,0,k}$	10
Compression parallel to the grain	$f_{c,0,k}$	32
Compression perpendicular to the grain	$f_{c,90,k}$	2.8
Shear	$f_{v,k}$	2.5
Mean modulus of elasticity	$E_{0,mean}$	14300
Shear modulus of elasticity	$G_{0,mean}$	530
Density in $kg/m^3$		
Characteristic density	$\rho_k$	500

## 2.3. Timber connections

Timber connections often determines the overall strength of the structure and their stiffness will also have a great influence on the overall behaviour of the structure. Therefore, generally the connections are the critical factors in the design of a structure [38]. There are many possibilities on how to make timber-to-timber connections and timber-to-steel connections, which all have different advantages and disadvantages regarding strength and stiffness.

In the following section, the most used structural elements to connect timber elements are described and also typical connection layouts are described.

### 2.3.1. Joint with glued-in rods

Timber members can be connected by using rods. The rods, often made of either steel or fibre-reinforced plastic (FRP), can be applied both parallel and perpendicular to the grain of the timber. They are often threaded and glued to the timber member by making use of an adhesive. Epoxy has the best performance on pull-out strength and is most commonly used in Europe [56]. The rods can connect the members directly, but can also be welded to a steel plate, which is shown in Figure 2.4.

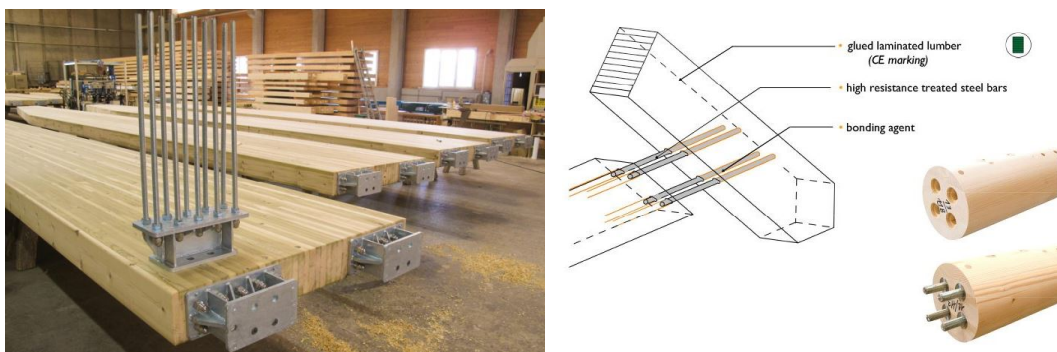


Figure 2.4: Joints with glued-in rods [52]

To build such a connection, first a hole must be drilled in the timber member which is approximately 1 to 4 millimetres larger than the diameter of the rod. Subsequently, there are 2 ways to finish the connection. In the first method, the adhesive is poured inside the hole, after which the rod can be inserted. The second method uses a additional hole at the side of the member, where the adhesive can be inserted. Both methods are shown in Figure 2.5.

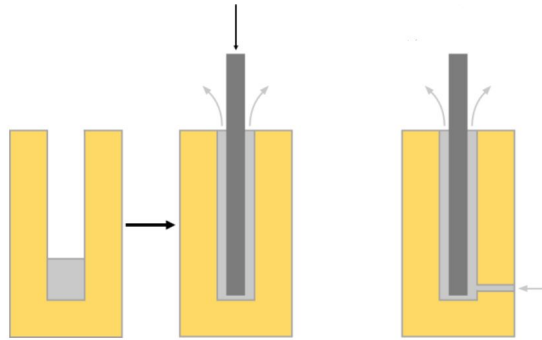


Figure 2.5: Methods to fabricate connections with glued rods [14]

### 2.3.2. Joints with nails

Nails are often used in timber connections, because they are easy to manufacture and can easily be put into place. They perform well when used in nail groups and when exposed to earthquakes. Nails have bad performance on withstanding forces in the shank direction. Especially when nails are used in combination with high density timber, sometimes pre-drilling is required to prevent splitting of the wood or buckling of the nail.

Nails can be used to connect timber to timber, but often additional steel components such as perforated steel plates are used. In Figure 2.6, a joint with nails is shown which uses a steel plate to connect 2 timber elements and in Figure 2.6, a steel plate is used to transfer tension forces to a concrete slab.



Figure 2.6: Joint with steel nails [55]

### 2.3.3. Joints with bolts and dowels

A joint with bolts or dowels consist of pre-drilled holes where bolts or dowels are inserted. If bolts are used, an additional head, nut and washer are added. The holes can be drilled 1 mm larger than the dowel diameter. These joints are able to transfer large forces and can be used to obtain a high rigidity.

To obtain a high strength connection between 2 different timber elements, often additional steel plates are used. These steel plates are placed in the centre of the element by making a cut and then dowels are put in holes created in both the timber and steel plate. Self-drilling dowels can be used for up to 3 steel plates, each up to 5 mm thick or 1 steel plate with a maximum thickness of 10 mm.



Figure 2.7: Joint with steel plates and dowels [4, 39]

### 2.3.4. Joint with self-tapping screws

Connections with self-tapping screws are ideal to use for connecting steel and timber elements to other timber elements, but it could also be used for timber-to-timber connections. Self-tapping screws can resist high loads in the direction parallel to the screw axis. This is because the thread of the screw provides an effective bond between the screw and the timber. The screws can also be used to transfer forces perpendicular to the screw axis, the threaded of the screw then contributes to the load-carrying capacity because of the rope effect.

Just as joints with nails, self-tapping screws can also be used in combination with steel components. For example, screws can be used together with brackets to transfer shear forces or with steel plates to provide tensile resistance.

### 2.3.5. Joint with adhesive

Timber elements can be glued together using an adhesive on the contact surface between those elements. The adhesive fills the joint between the different timber parts and ensures that the adhesion is as strong as the timber material itself. It is also possible to add an adhesive between timber and a steel components as with an XEPOX connection [53].

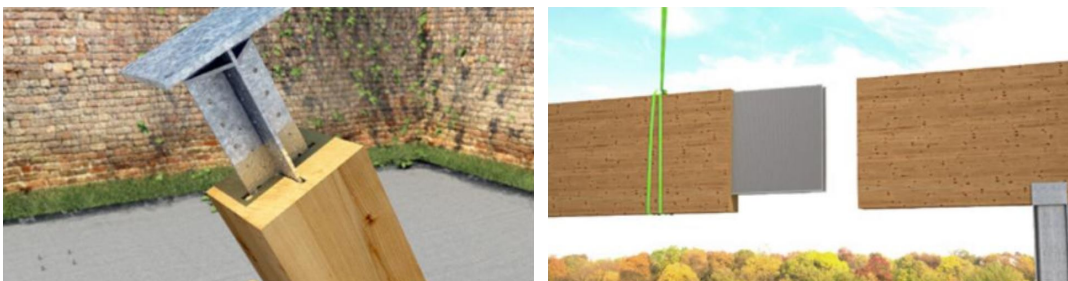


Figure 2.8: Joint with adhesive (XEPOX) [53]

## 2.4. Introduction to parametric design

Various software packages for parametric design are on the market at this moment. The most used programs are:

- **GenerativeComponents:** This program is developed by the company Bentley Systems and was introduced in 2003. It is free stand-alone software which can be used in combination with CAD software, such as Bentley Systems MicroSystem or AutoDesk AutoCAD.
- **Grasshopper:** It is developed by Robert McNeel and appeared in 2007. It runs within the Rhinoceros 3D application, which is a CAD program also developed by Robert McNeel & Associates. To speed up the process of developing models in Grasshopper, a large amount of plug-ins are available on the web.
- **Autodesk Dynamo:** This is a stand-alone application, but can also be used simultaneously with Autodesk Revit. The program is free to use. Because it's open-source, several plug-ins are available on the web.

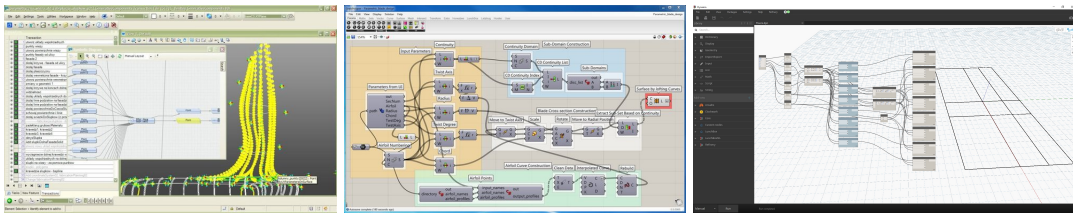


Figure 2.9: GenerativeComponents [11], Grasshopper [11] and Autodesk Dynamo

As already mentioned in section 1.2, these applications are not able to check the design on structural requirements. Therefore, several plug-ins are developed to connect the parametric software packages with structural analysis programs. An overview of available plug-ins for Grasshopper and Dynamo is given in Table 2.5.

Table 2.5: Plug-ins for Grasshopper and Dynamo to perform a structural analysis [8]

Program	Plug-in name	
Grasshopper	Kangaroo	Built-in Grasshopper
	Karamba 3D	Built-in Grasshopper
	GeometryGym	Connects to either Oasys GSA, Robot, ETABS, SCIA Engineer or SAP2000
	Grasshopper-Tekla Live Link	Connects with Tekla Structures
Autodesk Dynamo	Structural analysis	Uses Robot Structural Software
	Arcadis plug-in	Connects with Dlubal RFEM

### 2.4.1. Parametric design software package

The parametric design software package used in this thesis is called Dynamo. This software enables users to create their own custom-built tools. In Dynamo you can use different elements to obtain a parametric design. A typical Dynamo file is shown in Figure 2.10, where different elements are displayed and subsequently the functions of these elements are described.

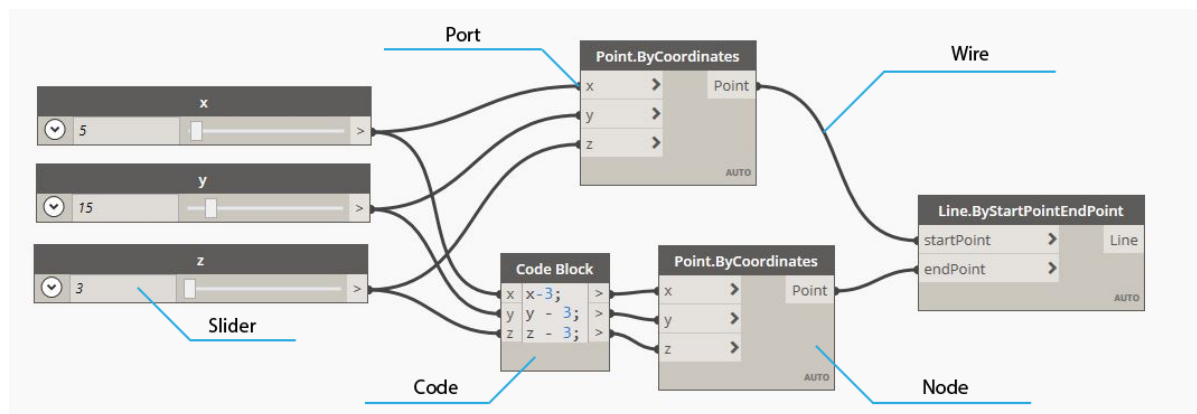


Figure 2.10: Dynamo file with different elements

#### Work space

The work space is the area where you can place nodes and connect them using wires.

#### Node

A node is an object which can either be an element like lines or points, or operations. The node has inputs and outputs which can be connected using wires.

#### Wire

Wires enable you to create a connection between the in- and output of nodes and thus transfer different kind of information between the nodes.

### Port

Ports represent the input and output of a node. The input ports are on the left side and the output ports are on the right side of the node. Therefore, normally a file is built up from left to right.

### Code

Instead of using nodes which represent different functions, Dynamo allows you to use programming code. This code can be written in a Code block. When using variables, these will show up as input ports and every line of code can be used as output.

### Slider

Sliders allow you to visually change a parameter by moving the slider left and right. You can give the slider a start value, an interval and an end value.

### Custom nodes

Dynamo allows you to build custom nodes. This custom node is nothing more than a container which contains other nodes and custom nodes. When executing a custom node, all the nodes inside this custom node will be executed.

### Background 3D preview

Behind the work space, the result of the connected nodes is shown. The result of the nodes shown in Figure 2.10 is displayed in Figure 2.11.

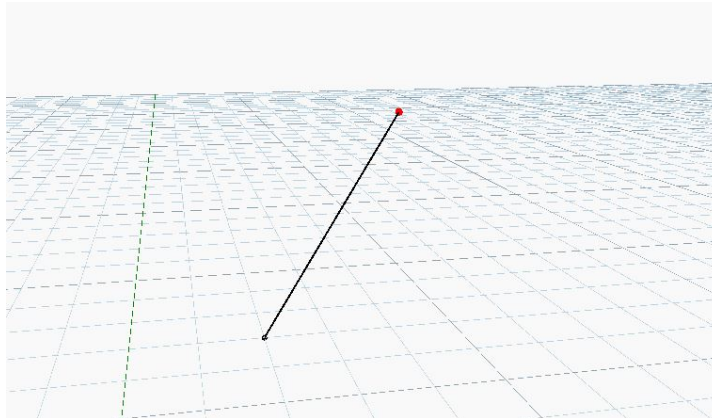


Figure 2.11: Background 3D preview of Dynamo file

## 2.4.2. Structural analysis software

The structural analysis software which will be further used is called RFEM from the company Dlubal. In order to generate and analyse a structure in RFEM using Dynamo, a plug-in had to be made because Dynamo does not provide this functionality.

Michael van Telgen from the company Arcadis [61] and Igor Pečanac [8] are working on this plug-in, which allows you to assign different structural properties to the geometry made in Dynamo and apply loads to this geometry. This can then be imported into RFEM, where a structural analysis can be performed [61].

To do so, the plugin has different nodes which are explained below.

### Member element

The plugin allows you to convert lines made in Dynamo to members in RFEM. You can assign different properties to this member, namely material, cross section, rotation angle and the boundary conditions (hinged or rigid). A special node is made for the specific materials concrete, steel and timber, for which you can choose different classes. Cross sections can be picked from the cross sections nodes, such as steel sections (for example HEA and IPE profiles) and rectangular shaped timber cross sections. This node is shown in Figure 2.12.

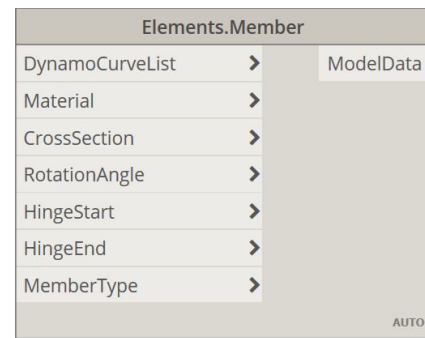


Figure 2.12: Member node

### Surface element

The plugin also enables you to convert surfaces created in Dynamo to surface elements in RFEM. You can assign the surface thickness, the material and the eccentricity to this element.

### Node element

Points which are made in Dynamo can be converted to nodes in RFEM. You can then apply nodal forces and support conditions to these nodes.

### Support

Supports can be added by applying the support boundary conditions to a RFEM node. It is possible to restrain translations of all axes and the rotations around each axes can either be chosen hinged or rigid. This node is shown in Figure 2.13.

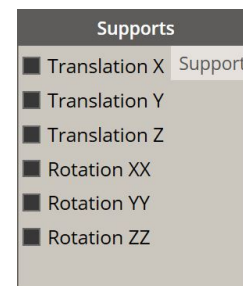


Figure 2.13: Support node

### Loads and load case

The plug-in allows you to add different loads to the structure. At this moment, it is possible to apply nodal loads, surface loads and self weight in all directions. These loads can then be sorted in several load cases, which can be used in different combination loads as determined in section 3.1 by using the Load Combination node.

### Load combinations

The Load Combination load allows you to assign different load combinations for ULS and SLS to the model by using the defined load cases. The different load cases are inputted and load factors can be applied. The node gives an option to calculate the load combination using a linear or a non-linear analysis.

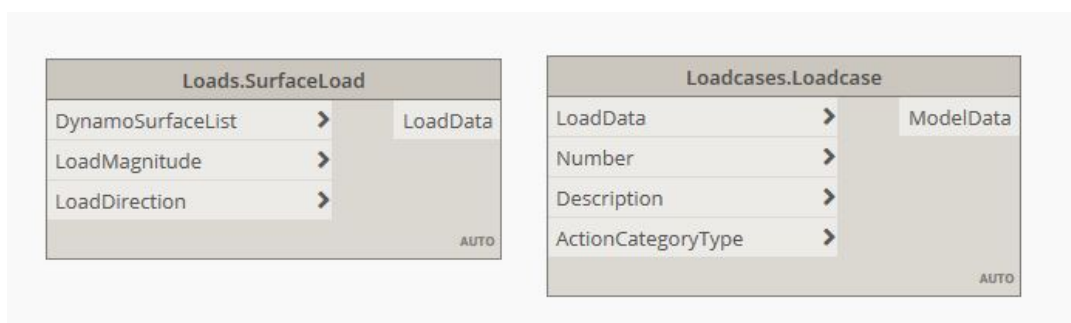


Figure 2.14: Load and load case nodes

Export model to RFEM

All generated members, supports and loads are combined in a list with model data. This model data can then be put in the node ModelToRFEM to export it to RFEM. This node allows you to start the structural calculations immediately.

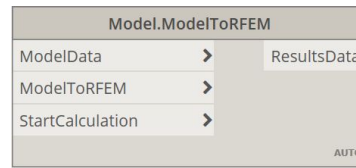


Figure 2.15: ModelToRFEM node

In Figure 2.16 a member which is generated in RFEM is shown. The Dynamo file displayed in Figure 2.11 is used, after which other Dynamo nodes are used to assign a cross section to the line, add a support to one side and attach a point load to the other side.

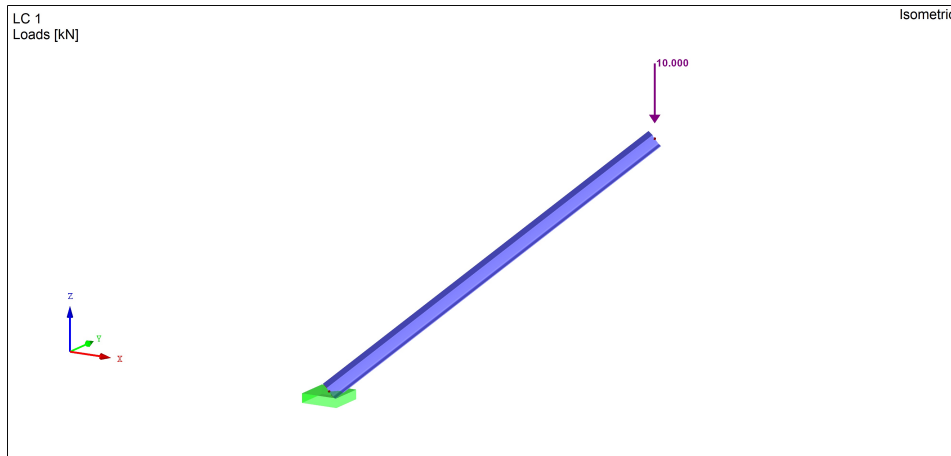


Figure 2.16: Dynamo model exported to RFEM

Results

When a structural calculation is started, RFEM will return the results to the Dynamo model. Different nodes are provided which can read the result data. At this moment, it is possible to get member deformation, member internal forces, surface deformation, surface design forces, surface internal forces and nodal deformation. The members or surfaces for which you want the data to be shown can be selected in the InputMembers or InputSurfaces input. A couple of these nodes are shown in Figure 2.17.

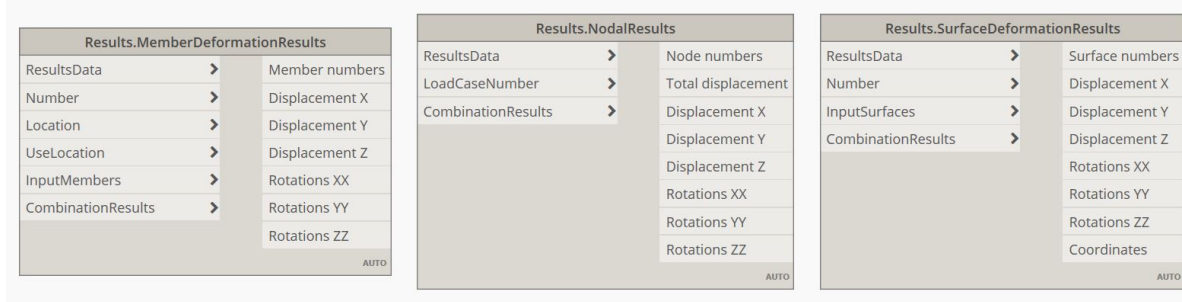


Figure 2.17: Nodes for result data



# 3

## Design and verification of the structure

To design and verify the structure generated by a parametric model, different codes, national annexes from the Eurocode and reports which are used in The Netherlands are adopted.

### 3.1. Loads on structure

NEN-EN 1990-1-1 [23] describes 2 types of limit states, the so called Ultimate Limit State (ULS) and the Serviceability Limit State (SLS). The ULS is a state which the structure must fulfil to ensure personal and structural safety. The SLS is a state which the structure must fulfil to ensure requirements for use of the building.

The design value  $X_d$  of a material property of timber with characteristic value  $X_k$  can be described as:

$$X_d = k_{mod} \cdot \frac{X_k}{\gamma_M} \quad (3.1)$$

where  $\gamma_M$  is a partial safety factor. For timber the partial safety factor in ULS is equal to 1.25, while for SLS it is equal to 1.0. For connections, the partial safety factor is equal to 1.3.  $k_{mod}$  takes into account load duration and moisture content of the material.

To design and verify a high-rise building according to the Eurocode, loads such as permanent load, variable load and horizontal wind loads need to be considered. For each of the limit states, a decisive combination of loads is defined. For the ULS this combination is equal to the more adverse of:

$$\sum \gamma_{G,j} G_{k,j} + \gamma_{Q,1} \psi_{0,1} Q_{k,1} + \sum \gamma_{Q,i} \psi_{0,i} Q_{k,i} \quad (3.2)$$

$$\sum \xi \gamma_{G,j} G_{k,j} + \gamma_{Q,1} Q_{k,1} + \sum \gamma_{Q,i} \psi_{0,i} Q_{k,i} \quad (3.3)$$

The first term represents the design value for the permanent load. The second term expresses the design value of the leading variable load and the third term is the design combination value of all other variable loads. The partial safety factors  $\gamma$  take into account possible unfavourable uncertainties. High-rise buildings need to be designed for consequence class 3 (CC3), which takes into account the possible consequences of failure in terms of loss of human life or potential economical losses. Using CC3, this leads to the following load combinations in ULS:

$$\sum 1.5 G_{k,j} + 1.65 \psi_{0,1} Q_{k,1} + \sum 1.65 \psi_{0,i} Q_{k,i} \quad (3.4)$$

$$\sum 1.3 G_{k,j} + 1.65 Q_{k,1} + \sum 1.65 \psi_{0,i} Q_{k,i} \quad (3.5)$$

For the SLS this combination is equal to:

$$\sum G_{k,j} + Q_{k,1} + \sum \psi_{0,i} Q_{k,i} \quad (3.6)$$

The combination factors  $\psi$  take into account the fact that maximum variable loads are unlikely to occur at the same time and thus these loads, expect for one variable load, can be reduced by a certain factor. These

factors for different types of variable loads according to the Dutch annex of NEN-EN1990 [24] are shown in Table 3.1, in this case specifically for an office building.

Table 3.1: Combination factors  $\psi$  for an office building

Action	$\psi_0$	$\psi_1$	$\psi_2$
Imposed loads	0.5	0.5	0.3
Snow loads	0	0.2	0.0
Wind loads	0	0.2	0.0

At all time, the limit states must not be exceeded. Therefore, in the ultimate limit state, the design values for the loads must not exceed the design values of the resistances and in the serviceability limit states, the design values for the loads do not exceed limit values. This is shown in a graphical way in Figure 3.1.

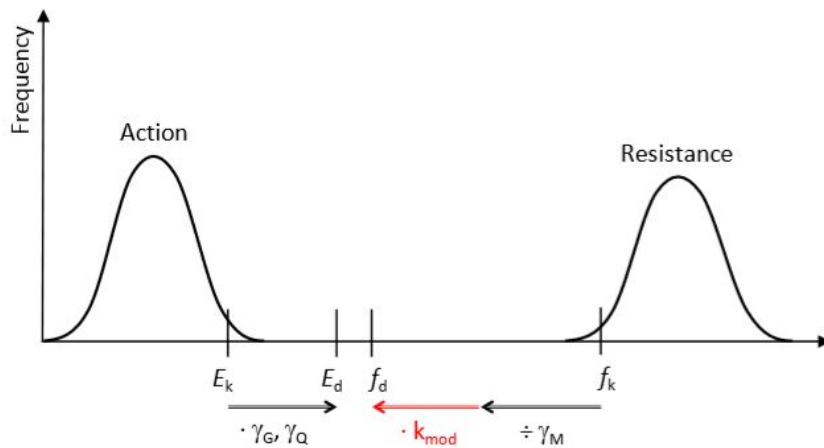


Figure 3.1: The use of partial safety factors and  $k_{mod}$  to ensure limit states [4]

The factor  $k_{mod}$  depends on the service class of the structure and the load-duration class. The service class takes into account the temperature and moisture content for which the timber is exposed to. For example, service class 1 states that the moisture content in most softwoods does not exceed 12%. For service class 3, no limit for moisture content is given. In Table 3.2 the different values for  $k_{mod}$  are shown for different service- and load-duration classes.

Table 3.2: Values of  $k_{mod}$  for different load-duration and service classes for solid timber, glulam and CLT [4]

Load-duration class	Duration	Examples for loads	$k_{mod}$ for service class:	
			1 and 2	3
Permanent	More than 10 years	Self-weight	0.6	0.5
Long-term	From 6 month to 10 years	Storage	0.7	0.55
Medium-term	From 1 week to 6 months	Imposed floor load	0.8	0.65
Short-term	Less than one week	Snow, wind	0.9	0.7
Instantaneous		Accidental load	1.1	0.9

### 3.1.1. Wind load

The wind load can be calculated according to NEN-EN 1991-1-4 [26]. In order to calculate the load, first the basic wind velocity needs to be calculated using the formula:

$$v_b = c_{dir} \cdot c_{season} \cdot v_{b,0} \quad (3.7)$$

where  $c_{dir}$  is the directional factor and  $c_{season}$  is the season factor. Both factors can be assumed to be equal to 1.0. The basic wind velocity  $v_{b,0}$  is defined as the average 10-minute wind velocity at a height of 10 meter

and is determined for 3 different zones in The Netherlands. These areas are shown on the map in Figure 3.2.

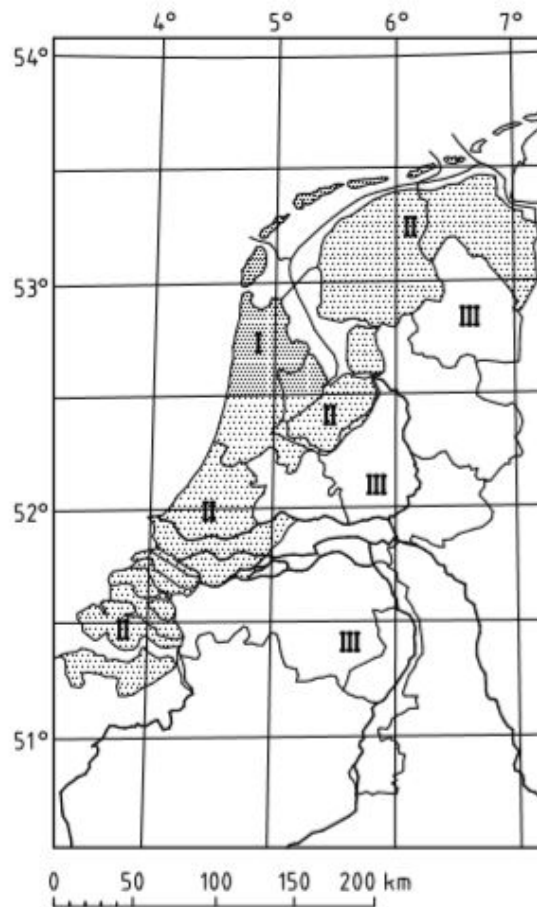


Figure 3.2: Different wind zones in The Netherlands

For each of these zones the basic wind velocity is defined and is shown in Table 3.3.

Table 3.3:  $v_{b,0}$  for different wind zones in The Netherlands

Windgebied	I	II	III
$v_{b,0}$ (m/s)	29.5	27.0	24.5

Next, the mean wind velocity at height  $z$  can be determined using:

$$v_m(z) = c_f(z) \cdot c_0(z) \cdot v_b \quad (3.8)$$

where  $c_f(z)$  is the roughness factor and  $c_0(z)$  is the orography factor. The orography factor can be assumed 1.0 and for buildings higher than 10 metres and lower than 200 metres the roughness factor is:

$$c_f(z) = k_r \cdot \ln\left(\frac{z}{z_0}\right) \quad (3.9)$$

where  $z_0$  is the roughness length and  $k_r$  is the terrain factor which is equal to:

$$k_r = 0.19 \cdot \left(\frac{z_0}{z_{0,||}}\right)^{0.07} \quad (3.10)$$

where  $z_{0,||}$  is equal to 0.05. To determine the value of  $z_0$ , NEN-EN 1991-1-4 [26] gives a table with different terrain categories, which is shown in Table 3.4.

Table 3.4: Roughness length for different terrain categories in The Netherlands [27]

Terrain category		$z_0$	$z_{min}$
0	Sea or coastal environment	0.005	1
II	Unbuilt environment	0.2	4
III	Urban environment	0.5	7

To calculate the peak velocity pressure, first the turbulence intensity  $I_v(z)$  needs to be determined.

$$I_v(z) = \frac{k_I}{c_0(z) \ln(z/z_0)} \quad (3.11)$$

where  $k_I$  is the turbulence factor, which is equal to 1.0.

$$q_p(z) = [1 + 7 \cdot I_v(z)] \cdot \frac{1}{2} \cdot \rho \cdot v_m^2(z) \quad (3.12)$$

where  $\rho$  is the air density ( $1.25 \text{ kg/m}^3$ ). For buildings higher than 2 times the width, according to the Eurocode [26] the velocity pressure is distributed over the building as shown in Figure 3.3.

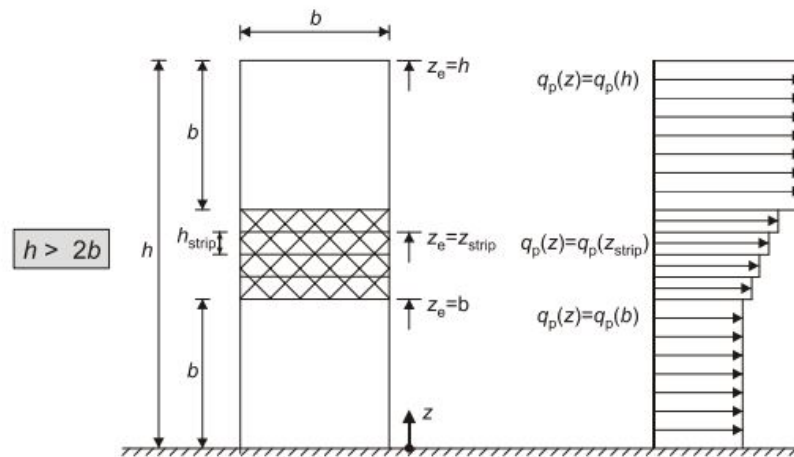


Figure 3.3: Velocity pressure distributed over the building

The peak velocity pressure needs to be multiplied with an additional factor called the external pressure coefficient, which is defined for different zones of the building and the structural factor  $c_s c_d$ . These zones and the corresponding factors are shown in figure 3.4.

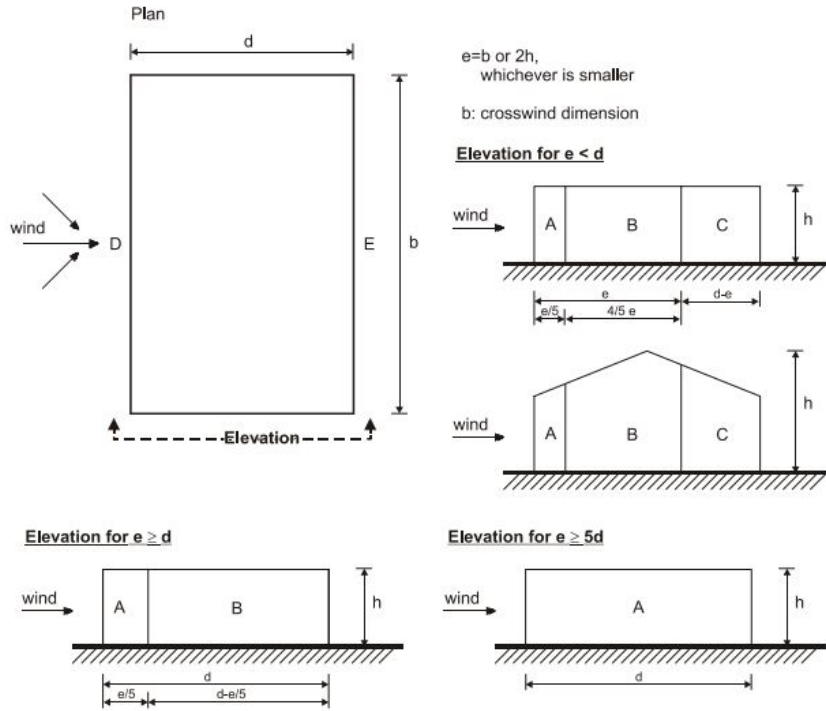


Figure 3.4: Different zones for a building

The recommended values for the external pressure coefficients are shown in Table 3.5.

Table 3.5: External pressure coefficients

Zone	A	B	C	D	E
$h/d = 5$	-1.2	-0.8	-0.5	+0.8	-0.7
$h/d = 1$	-1.2	-0.8	-0.5	+0.8	-0.5
$h/d \leq 0.25$	-1.2	-1.4	-0.5	+0.7	-0.3

The structural factor  $c_s c_d$  is defined as:

$$c_s c_d = \frac{1 + 2 \cdot k_p \cdot I_v(z_s) \cdot \sqrt{B^2 + R^2}}{1 + 7 \cdot I_v(z_s)} \quad (3.13)$$

$B^2$  is the background factor and takes into account the lack of full correlation of the pressure on the structure:

$$B^2 = \frac{1}{1 + \frac{3}{2} \cdot \sqrt{\left(\frac{b}{L(z_s)}\right)^2 + \left(\frac{h}{L(z_s)}\right)^2 + \left(\frac{b}{L(z_s)} \cdot \frac{h}{L(z_s)}\right)^2}} \quad (3.14)$$

The turbulent length scale  $L(z)$  considers the average gust size for natural winds. For buildings below 200 metres and higher than 10 metres, the scale can be calculated with the following formula:

$$L(z) = L_t \cdot \left(\frac{z}{z_t}\right)^\alpha \quad (3.15)$$

with a reference height of  $z_t = 200m$ , a reference length scale of  $L_t = 300m$  and  $\alpha = 0.67 + 0.05 \ln(z_0)$ .

$R^2$  is the resonance response factor which takes into account the turbulence in resonance:

$$R^2 = \frac{\pi^2}{2 \cdot \delta} \cdot S_L(z_s, n_{1,x}) \cdot K_s(n_{1,x}) \quad (3.16)$$

The non-dimensional power spectral density function  $S_L(z, n)$  represents the wind distribution over frequencies and can be expressed as:

$$S_L(z, n) = \frac{n \cdot S_v(z, n)}{\sigma_v^2} = \frac{6.8 \cdot f_L(z, n)}{(1 + 10.2 \cdot f_L(z, n))^{5/3}} \quad (3.17)$$

where  $S_v(z, n)$  is the one-sided variance spectrum and  $f_L(z, n) = \frac{n \cdot L(z)}{v_m(z)}$  is the non-dimensional frequency, where  $n = n_{1,x}$  is the natural frequency of the structure.

The peak factor  $k_p$  is equal to:

$$k_p = \max(\sqrt{2 \cdot \ln(v \cdot T)} + \frac{0.6}{\sqrt{2 \cdot \ln(v \cdot T)}}, 3) \quad (3.18)$$

where  $T$  is the averaging time for the mean wind velocity ( $T = 600 \text{seconds}$ ) and  $v$  is the up-crossing frequency:

$$v = n_{1,x} \frac{R^2}{B^2 + R^2} \geq 0.08 \text{Hz} \quad (3.19)$$

where  $\delta$  is the total logarithmic decrement of damping and  $K_s$  is the size reduction function, which is formulated as:

$$K_s(n) = \frac{1}{1 + \sqrt{(G_y \cdot \phi_y)^2 + (G_z \cdot \phi_z)^2 + (\frac{2}{\pi} \cdot G_y \cdot \phi_y \cdot G_z \cdot \phi_z)^2}} \quad (3.20)$$

$$\phi_y = \frac{c_y \cdot b \cdot n}{v_m(z_s)} \quad (3.21)$$

$$\phi_z = \frac{c_z \cdot h \cdot n}{v_m(z_s)} \quad (3.22)$$

The decay constant  $c_y$  and  $c_z$  are equal to 11.5. The constant  $G_y$  and  $G_z$  are related to the mode shape variation along the horizontal y-axis and vertical z-axis. For a uniform horizontal mode shape variation and a linear vertical mode shape variation of a building,  $G_y = 1/2$  and  $G_z = 3/2$ .

The damping of the system is  $\delta = \delta_s + \delta_a + \delta_d$ , which is the sum of the the structural damping, aerodynamic damping and damping due to special equipment, such as tuned mass dampers.

When the modal displacement is the same for every height  $z$ , the following equation can be used for the aerodynamic damping:

$$\delta_a = \frac{c_f \cdot \rho \cdot b \cdot v_m(z_s)}{2 \cdot n_1 \cdot m_e} \quad (3.23)$$

$m_e$  is the mass of the building per unit of height.

The structural damping of different structural types is given in NEN-EN 1991-1-4 [26]. For timber buildings, no specific value is shown, however a factor is given for timber bridges which is equal to 0.06 to 0.12.

## 3.2. Stresses

When clear wood is exposed to a load, a clear stress-strain diagram can be determined, shown in Figure 3.5.

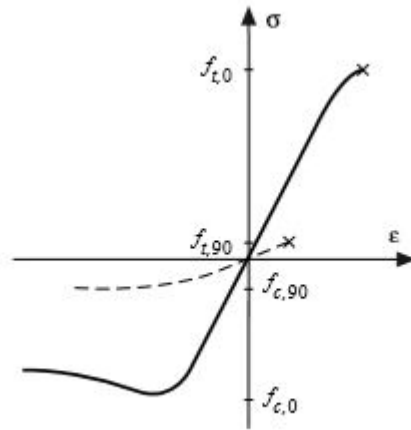


Figure 3.5: Stress-strain diagram for clear wood [4]

As can be seen, clear wood has a better resistance to tension ( $f_{t,0}$ ) than to compression ( $f_{c,0}$ ). The stress-strain curve stops abruptly when exposed to tension, which means that the wood fails brittle. When a compressive force is applied, plastic behaviour can be observed.

The dashed line shows the behaviour of the material when exposed to load perpendicular to the grain, which is worse than the behaviour when compressive or tensile stresses are applied parallel to the grain. The tensile strength perpendicular to the grain is depending on the volume of the specimen, since pre-existing cracks and growth irregularities strongly influence the strength.

Timber members need to resist normal forces, bending moments and shear forces, which need to fulfil the following expressions according to NEN-EN 1995-1-1 [31].

### 3.2.1. Normal force

When a normal force is applied parallel to the grain, a simple expression is used to check the resistance.

$$\sigma_{c,0,d} < f_{c,0,d} \quad (3.24)$$

where  $\sigma_{c,0,d} = N_{Ed}/A$ .

When a normal force is applied perpendicular to the grain, an additional factor  $k_{c,90}$  is used.

$$\sigma_{c,90,d} \leq k_{c,90} \cdot f_{c,90,d} \quad (3.25)$$

### 3.2.2. Bending moment

For bending, a distinction is made for members subjected to bending and axial tension and members subjected to bending and axial compression.

For a combination of bending and axial tension, the following expressions should be met:

$$\frac{\sigma_{t,0,d}}{f_{t,0,d}} + \frac{\sigma_{m,y,d}}{f_{m,y,d}} + k_m \cdot \frac{\sigma_{m,z,d}}{f_{m,z,d}} \leq 1.0 \quad (3.26)$$

$$\frac{\sigma_{t,0,d}}{f_{t,0,d}} + k_m \cdot \frac{\sigma_{m,y,d}}{f_{m,y,d}} + \frac{\sigma_{m,z,d}}{f_{m,z,d}} \leq 1.0 \quad (3.27)$$

For a combination of bending and axial compression, the following expressions should be met:

$$\left(\frac{\sigma_{c,0,d}}{f_{c,0,d}}\right)^2 + \frac{\sigma_{m,y,d}}{f_{m,y,d}} + k_m \cdot \frac{\sigma_{m,z,d}}{f_{m,z,d}} \leq 1.0 \quad (3.28)$$

$$\left(\frac{\sigma_{c,0,d}}{f_{c,0,d}}\right)^2 + k_m \cdot \frac{\sigma_{m,y,d}}{f_{m,y,d}} + \frac{\sigma_{m,z,d}}{f_{m,z,d}} \leq 1.0 \quad (3.29)$$

In these expressions,  $k_m$  is used to take into consideration the re-distribution of stresses and the effect of inhomogeneities in the cross-section. The factor is equal to 0.7 for solid timber, glulam and LVL. For other timber products or when  $h/b > 4$ , this factor is equal to 1.0.

The bending moment stress capacity of a beam may be multiplied by a factor  $k_h$ , which is for normal wood equal to:

$$k_h = \left(\frac{150}{h}\right)^{0.2} \leq 1.3 \quad (3.30)$$

For laminated wood products, this equation is equal to:

$$k_h = \left(\frac{600}{h}\right)^{0.1} \leq 1.1 \quad (3.31)$$

### 3.2.3. Shear force

For a rectangular cross-section, the maximum value of the shear stress can be calculated as:

$$\tau = 1.5 * V_d / A \quad (3.32)$$

Cracks have a negative influence on the shear strength of the cross-section and therefore the width of the member has to be reduced with a factor  $k_{cr}$ . This factor  $k_{cr}$  is equal to 1.0 for a prismatic cross-section [34].

## 3.3. Buckling

According to NEN-EN 1995-1-1 [31], the load-bearing capacity of a slender structural member exposed to a compressive force can be determined by using a buckling curve. Buckling curves give a relation between the slenderness of the column and its characteristic load-bearing capacity.

The relative slenderness can be determined as follows:

$$\lambda_{rel,y} = \frac{\lambda_y}{\pi} \cdot \sqrt{\frac{f_{c,0,k}}{E_{0,05}}} \quad (3.33)$$

$$\lambda_{rel,z} = \frac{\lambda_z}{\pi} \cdot \sqrt{\frac{f_{c,0,k}}{E_{0,05}}} \quad (3.34)$$

As can be seen in the equation, for determining the buckling capacity the lower quantile values for stiffness are used. For buckling about the y-axis,  $\lambda_y$  and  $\lambda_{rel,y}$  are used, while for buckling about the z-axis  $\lambda_z$  and  $\lambda_{rel,z}$  are used.

The slenderness of the column is equal to:

$$\lambda = \frac{l_{ef}}{i} \quad (3.35)$$

where  $i$  is the radius of gyration, which is defined as the square root of the moment of inertia divided by the cross section area. For a column pinned at both sides,  $l_{ef}$  is equal to its actual length  $l$ .

The following conditions should be met for  $\lambda_{rel,y} \leq 0.3$  and  $\lambda_{rel,z} \leq 0.3$ :

$$\left(\frac{\sigma_{c,0,d}}{f_{c,0,d}}\right)^2 + \frac{\sigma_{m,y,d}}{f_{m,y,d}} + k_m \cdot \frac{\sigma_{m,z,d}}{f_{m,z,d}} \leq 1.0 \quad (3.36)$$

$$\left(\frac{\sigma_{c,0,d}}{f_{c,0,d}}\right)^2 + k_m \cdot \frac{\sigma_{m,y,d}}{f_{m,y,d}} + \frac{\sigma_{m,z,d}}{f_{m,z,d}} \leq 1.0 \quad (3.37)$$

If  $\lambda_{rel,y} > 0.3$  and  $\lambda_{rel,z} > 0.3$ , the following conditions should be met:

$$\frac{\sigma_{c,0,d}}{k_{c,y} \cdot f_{c,0,d}} + \frac{\sigma_{m,y,d}}{f_{m,y,d}} + k_m \cdot \frac{\sigma_{m,z,d}}{f_{m,z,d}} \quad (3.38)$$

$$\frac{\sigma_{c,0,d}}{k_{c,z} \cdot f_{c,0,d}} + k_m \cdot \frac{\sigma_{m,y,d}}{f_{m,y,d}} + \frac{\sigma_{m,z,d}}{f_{m,z,d}} \quad (3.39)$$

where:

- $k_c = \frac{1}{k + \sqrt{k^2 - \lambda_{rel}^2}}$
- $k = 0.5 \cdot (1 + \beta_c \cdot (\lambda_{rel} - 0.3) + \lambda_{rel}^2)$
- $\beta_c$  is a coefficient for members, which for Glulam and LVL is equal to 0.1.

### 3.4. Deformation

The deformation of a timber structure can be divided into different portions as seen in Figure 3.6.

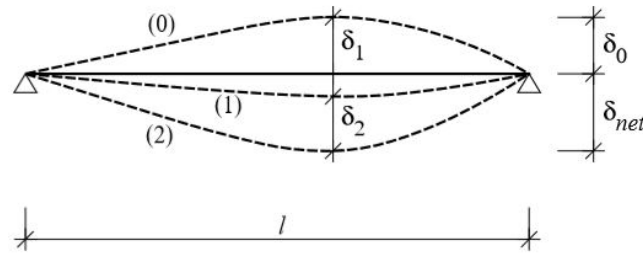


Figure 3.6: Deflection components [4]

where:

- $\delta_0$  is the pre-camber in the unloaded state.
- $\delta_1$  is the deflection due to permanent load immediately after the load is applied.
- $\delta_2$  is the deflection due to variable load and an additional deflection due to time-depended behaviour of the timber due to load.

For deflections of floors, the following limiting values are established in The Netherlands according to the Dutch annex of NEN-EN 1990-1-1:

- $\delta_{net} < 3/1000 \cdot l_{rep}$
- $l_{rep}$  is equal to the span for a simple supported beam
- $l_{rep}$  is equal to 2 times the length of the cantilever for a cantilever beam.

Creep behaviour of timber elements is a complex process and is influenced by several factors. For example, the higher the moisture content in the material, the larger the creep.

Because it is not feasible to use complex models to predict the creep behaviour for design of a timber structure, a simplification can be used which is described in the Eurocode. For structures which consist of elements and connections which have the same creep behaviour, the following equation can be used [5]:

$$u_{fin} = u_{fin,G} + u_{fin,Q_1} + \sum u_{fin,Q_i} \quad (3.40)$$

where:

- $u_{fin,G} = u_{inst,G}(1 + k_{def})$  for the permanent load
- $u_{fin,Q,1} = u_{inst,Q,1}(1 + \psi_{2,1}k_{def})$  for the leading variable load
- $u_{fin,Q,i} = u_{inst,Q,i}(\psi_{0,i} + \psi_{2,1}k_{def})$  for other variable loads

NEN-EN 1990-1-1 [28] describes for the SLS a maximum allowed horizontal displacement of the whole building of  $\frac{1}{500} \cdot h$ , where  $h$  is the total height of the building. A limit is also set for the inter-storey drift. The drift is defined as:

$$\delta = (\Delta_2 - \Delta_1)/h \quad (3.41)$$

where  $\Delta_1$  is the horizontal displacement of a specific floor and  $\Delta_2$  is the horizontal displacement of the floor above the floor which corresponds with  $\Delta_1$ .  $h$  is the storey height. The Eurocode sets a limit of the drift to  $1/400$ .

### 3.5. Global initial sway imperfections

An initial sway imperfection has to be taken into account for frames which are sensitive to buckling in a sway mode. This global initial sway imperfection is determined in NEN-EN 1993-1-1 [30].

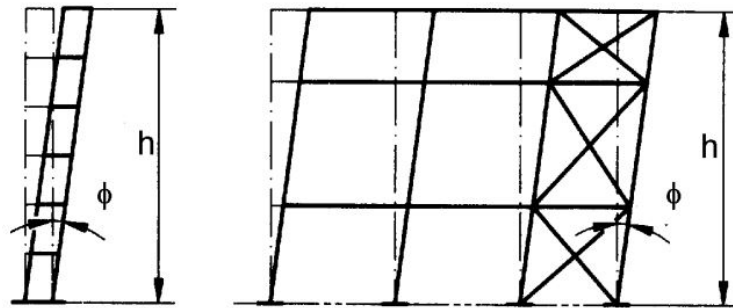


Figure 3.7: Global initial sway imperfection [30]

In this figure, the angle  $\phi$  is equal to:

$$\phi = \phi_0 \alpha_h \alpha_m \quad (3.42)$$

where:

- $\phi_0 = 1/200$  is the basic value
- $\alpha_h = \frac{2}{\sqrt{h}}$ , but  $2/3 \leq \alpha_h \leq 1.0$ .
- $h$  is the height of the structure
- $\alpha_m = \sqrt{0.5 \cdot (1 + \frac{1}{m})}$  is a reduction factor for the number of columns in a row.

This sway can be taken into account by adding an additional horizontal force on each level to the structure, which is equal to the vertical force applied to this level multiplied by  $\phi$ .

### 3.6. Vibration

Vibrations due to wind can be annoying for people. These vibrations can cause people to feel uncomfortable and they can even get sick. The effect of these accelerations on humans are shown in Table 3.6.

Table 3.6: Human perception levels [42]

Range	Acceleration ( $m/s^2$ )	Effect
1	< 0.05	Humans cannot perceive motion
2	0.05-0.10	Sensitive people can perceive motion; hanging objects may move slightly
3	0.10-0.25	Majority of people will perceive motion, level of motion may effect desk work, long-term exposure may produce motion sickness
4	0.25-0.40	Desk work becomes difficult or almost impossible, ambulation still possible
5	0.40-0.50	People strongly perceive motion, difficult to walk naturally, standing people may lose balance
6	0.50-0.60	Most people cannot tolerate motion and are unable to walk naturally
7	0.60-0.70	People cannot walk or tolerate motion
8	> 0.85	Objects begin to fall and people may be injured

The Dutch annex of NEN-EN 1990-1-1 [28] describes limitations of the acceleration for certain frequencies of the building. For buildings higher than 20 metres and a width less than the height of the building, the acceleration of the structure has to be checked. These limitations are shown in Figure 3.8.

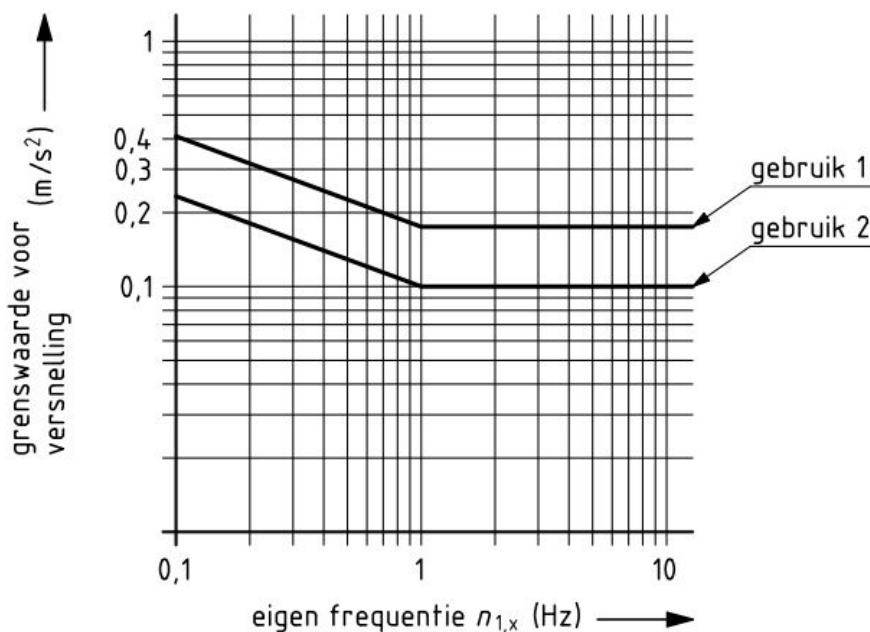


Figure 3.8: Acceptable accelerations for specific frequencies [16]

Line 1 represents the limitation of the acceleration of the top level for office buildings, line 2 represents the limitation for residential buildings.  $f_0$  is equal to the fundamental frequency of the building in Hz.

The first natural frequency of a building with multiple stories can be estimated in the following way:

$$n_{1,x} = \frac{46}{h} \quad (3.43)$$

in Hz, where  $h$  is the height of the structure.

To determine the acceleration of the top level of a building the Dutch annex of NEN-EN 1990-1-1 [28] is used. The formula is based on a report made by TNO, which takes into account a foundation with a low rotational stiffness [60]. This gives the following formula:

$$a_{wind} = 1.6 \cdot \frac{\phi_2 \cdot \rho_{vw,1} \cdot c_{pe} \cdot b_m}{\rho_l} \quad (3.44)$$

$\phi_2$  is the dynamic factor for vibrations caused by the wind, which is equal to:

$$\phi_2 = \sqrt{\frac{0.0344(n_{1,x})^{-2/3}}{D(1 + 0.12n_{1,x}h)(1 + 0.2n_{1,x}b_m)}} \quad (3.45)$$

$\rho_{vw,1}$  is the value of the varying part of the wind pressure.

$$\rho_{vw,1} = 100 \cdot \ln\left(\frac{h}{0.2}\right) \quad (3.46)$$

$c_{pe}$  is the sum of the external wind pressure coefficients (see Figure 3.4 and Table 3.5) and  $b_m$  is the width of the building perpendicular to the direction of the wind.  $\rho_l$  is the total mass of the building including household contents per unit of height.  $D$  is the damping coefficient of the building. For buildings with a natural frequency lower than 1 Hz this coefficient is equal to 0.01.

### 3.7. Fire safety

Buildings need to be designed in such a way that they provide an acceptable level of fire safety and minimise risks from heat and smoke. Therefore, NEN-EN 1995-1-1 describes different objectives, namely:

"The construction works must be designed and built in such a way, that in the event of an outbreak of fire

- the load-bearing resistance of the construction can be assumed for a specified period of time;
- the generation and spread of fire and smoke within the works is limited;
- the spread of fire to neighbouring construction works is limited;
- the occupants can leave the works or can be rescued by other means;
- the safety of rescue teams is taken into consideration". [31]

In this thesis, 2 aspects are taken into account, namely the resistance of the load-bearing structure during a fire event and limiting the spread of fire and smoke within the building. This can be obtained by making use of passive and active measurements, where only the passive measurements are discussed in this thesis.

The first aspect uses the reduced cross-section method to calculate the resistance of the load-bearing structure during a fire event. The second aspect can be investigated by examining the separating function of wall and floor assemblies.

#### 3.7.1. Reduced cross-section method

When timber burns, part of the wood will char and thus will lose its load bearing function. The cross-sections of the different parts of the structure will decrease. The charring layer will then isolate and protect the remaining inner material. Therefore, the fire safety behaviour of a timber structure is good. Also extra fire protective cladding can be added to the members, so it takes longer for the timber to start charring.

To calculate the load bearing capacity of the remaining structure, the reduced cross-section method as described in NEN-EN 1995-1-2 [32] can be used. This method takes into account the thickness of the charring layer and an additional layer thickness which lost its strength and stiffness due to the heat of the fire.

The definition of this method is shown in Figure 3.9.

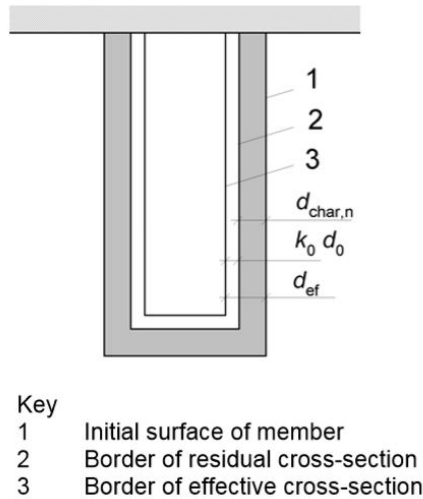


Figure 3.9: Definition of the reduced cross-section method [31]

The effective cross-section can be calculated by reducing the initial cross-section by:

$$d_{ef} = d_{char,n} + k_0 \cdot d_0 \tag{3.47}$$

with  $d_0 = 7\text{ mm}$ .  $d_{char,n}$  is the notional design charring depth which includes the effects of corner rounding and is equal to:

$$d_{char,n} = \beta_n \cdot t \tag{3.48}$$

where  $\beta_n$  is the notional charring rate and  $t$  is the time in minutes for which the timber is burning.

For glued laminated timber with a characteristic density  $\geq 290\text{ kg/m}^3$ ,  $\beta_n = 0.7\text{ mm/min}$ . For unprotected surfaces,  $k_0$  is equal to 1.0. When gypsum as a fire protective cladding is used, the time after which the protected timber starts charring should be taken as:

$$t_{ch} = 2.8 \cdot h_p - 14 \tag{3.49}$$

where  $h_p$  is the thickness of the cladding. For protected members with  $t_{ch} > 20$  min,  $k_0$  will vary linearly during the interval  $t = 0$  to  $t = t_{ch}$ , as can be seen in figure 3.10.

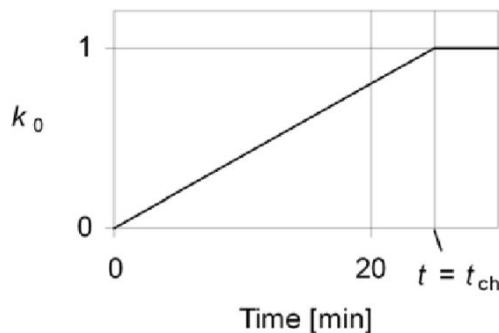


Figure 3.10: Values for  $k_0$  for protected member

When charring of the protected timber has started, the charring rate is multiplied by a factor  $k_3$ , which is equal to 2. After time  $t_a$  the charring rate will be the notional charring rate  $\beta_n$ .  $t_a$  can be determined in the

following way:

$$t_a = \min \left\{ \begin{array}{l} 2 \cdot t_f \\ \frac{25}{k_3 \cdot \beta_n} + t_f \end{array} \right. \quad (3.50)$$

The charring depth of an unprotected and a protected timber member over time are shown in figure 3.11.

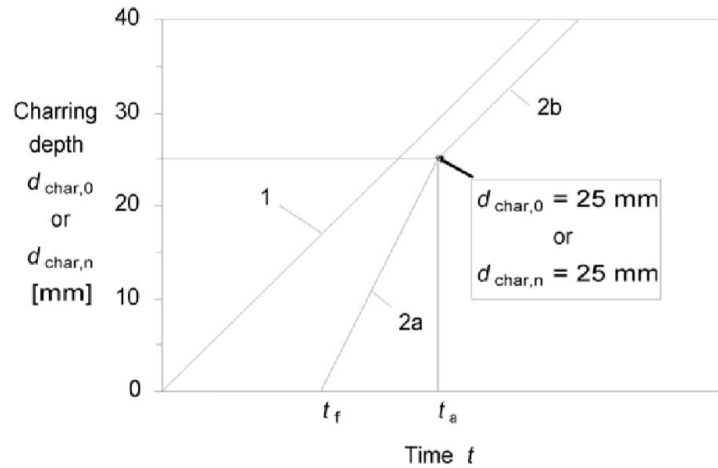


Figure 3.11: Charring depth for unprotected and protected timber member

To verify if the reduced cross section still satisfies the conditions during fire, the design value for the load bearing capacity should be taken as:

$$R_{d,t,fi} = \eta \cdot \frac{R_{20}}{\gamma_{M,fi}} \quad (3.51)$$

where  $\eta$  is a conversion factor used when verifying connections,  $R_{20}$  is the 20% fractile value of the resistance and  $\gamma_{M,fi}$  is the partial safety factor during fire.

The 20% fractile of the resistance is equal to:

$$R_{20} = k_{fi} \cdot f_k \quad (3.52)$$

$k_{fi}$  is a factor which is 1.25 for solid timber and 1.1 for glued-laminated timber,  $f_k$  is the characteristic resistance.

To determine the total effect of the loads acting on the member, during fire a reduction factor can be used:

$$E_{d,fi} = \eta_{fi} \cdot E_d \quad (3.53)$$

where  $E_d$  is the design value of the loads under normal conditions. According to the Dutch National Annex [33], the value of the factor  $\eta_{fi}$  is equal to 0.45.

### 3.7.2. Separating function of wall and floor assemblies

Walls should meet the requirements for resistance, integrity and insulation when these walls fulfil a load-bearing function combined with a separating function. The separating function gives a period for which an element can keep its separating function between fire compartment during a fire event.

Therefore, the elements should meet the condition:

$$t_{ins} \geq t_{req} \quad (3.54)$$

where:

- $t_{ins}$  is the time taken for the temperature to reach a rise of 140 degree Celsius over the whole exposed surface and the maximum temperature rise at any point of that surface to not exceed 180 degree Celsius.

- $t_{req}$  is the required time of fire resistance of the surface.

The Eurocode describes a method to analyse the insulation of a wall assembly. The method calculates the contribution of each individual layer of a wall segment to the separating function. Therefore, it uses a basic insulation value of the layer, a position coefficient and a joint coefficient. The values which the Eurocode gives for the basic insulation values of different materials are only valid for verification of a fire resistance up to 60 minutes [32].

A guideline is made by the European research project FireInTimber, which also describes values for verification of a fire resistance of a wall assembly. Because the main function of the different layers is to protect the adjacent layer, [20] introduces, in addition to the basic insulation value, a basic protection value of the layers.

This basic protection value describes the time for a layer to have an average temperature rise of 250 degree Celsius and a maximum temperature rise at any point on the surface of 270 degree Celsius. The basic insulation value describes the time for a layer to have an average temperature rise of 140 degree Celsius and a maximum temperature rise at any point on the surface of 180 Celsius. The definition of these values are visualized in Figure 3.12 and Figure 3.13.

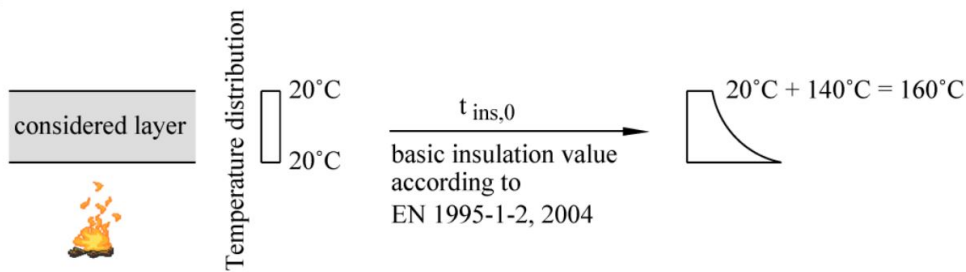


Figure 3.12: Basic insulation value [20]

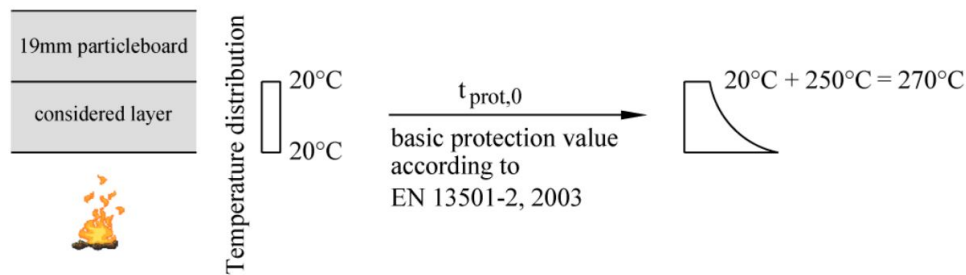


Figure 3.13: Basic protection value [20]

To calculate the total insulation time of a wall assembly, the sum of the basic protection values for all layers except for the layer with the greatest distance to the fire must be used along with the basic insulation value of the layer furthest from the fire. Thus:

$$t_{prot,i} = (t_{prot,0,i} \cdot k_{pos,exp,i} \cdot k_{pos,unexp,i} + \Delta t_i) \cdot k_{j,i} \tag{3.55}$$

$$t_{ins,n} = (t_{ins,0,n} \cdot k_{pos,exp,n} + \Delta t_n) \cdot k_{j,n} \tag{3.56}$$

[20] gives the basic insulation value and basic protection value for different materials. These values are shown in Table 3.7.

Table 3.7: Basic insulation and protection values for different materials

Material	Basic insulation value $t_{ins,0,n}$ [min]	Basic protection value $t_{prot,0,i}$ [min]
Gypsum plasterboard, gypsum fibre board	$24 \cdot (\frac{h_i}{15})^{1.4}$	$30 \cdot (\frac{h_i}{15})^{1.2}$
Solid timber, cross-laminated timber, LVL	$19 \cdot (\frac{h_i}{20})^{1.4}$	$30 \cdot (\frac{h_i}{20})^{1.1} \leq \frac{h_i}{\beta_0}$
Particleboard, fibreboard	$22 \cdot (\frac{h_i}{15})^{1.4}$	$24 \cdot (\frac{h_i}{15})^{1.4} \leq \frac{h_i}{\beta_0}$
OSB, plywood	$16 \cdot (\frac{h_i}{20})^{1.4}$	$23 \cdot (\frac{h_i}{20})^{1.1} \leq \frac{h_i}{\beta_0}$
Stone wool insulation with $\rho \geq 0$ $26kg/m^3$	0	$0.3 \cdot h_i^{(0.75 \cdot \log \rho_i - \rho_i / 400)}$
Glass wool insulation with $\rho \geq 0$ $15kg/m^3$	0	for $h_i < 40mm$ : 0 for $h_i \geq 40mm$ : $(0.0007 \cdot \rho_i + 0.046) \cdot h_i + 13 \leq 30$

[20] also describes the values for the position coefficients and joint coefficients. For example, when wall assemblies are connected using a single finger joint, the joint coefficient is equal to 0.4. The values for the position and joint coefficient are shown in Appendix B.5.1 and Appendix B.5.2 respectively.

### 3.8. Connections

In this report three typical connections are examined, namely a connection with slotted-in steel plates and dowels, a connection with glued-in rods and a connection with screws. For these specific connection types, the strength and stiffness properties are discussed.

#### 3.8.1. Slotted-in steel plates and dowels connection

First the strength properties of the connection are examined and then the stiffness of such a connection is discussed.

##### Strength

It is considered that both the steel and timber can reach plasticity. The maximum compressive or tensile resistance is reached when either the timber fails, the steel dowels reach plastic failure or the steel plates fail.

A connection is examined which consists of 2 slotted-in steel plates combined with multiple dowels. For such a connection with more than 1 steel plate, the maximum resistance is not explicitly mentioned in the Eurocode. Pedersen [47] has determined a total of 7 failure modes for connections with 2 plates, which are shown in figure 3.14. These failure modes describe both failure of the timber, dowels and steel plates.

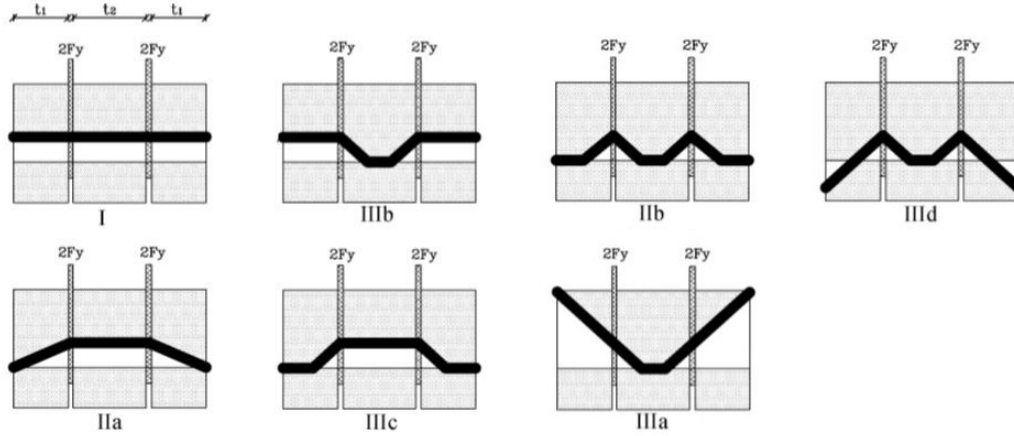


Figure 3.14: Failure modes for dowel connections with 2 steel plates [47]

The maximum compressive or tensile resistance for each of these failure modes can be calculated as follows:

$$F_{failure} = \min \begin{cases} \frac{1}{4}(2t_1 + t_2) \cdot d \cdot f_h & \text{Mode I} \\ (-\frac{1}{2}t_1 + \frac{t_2}{4} + \sqrt{\frac{1}{2}t_1^2 + \frac{M_y}{d \cdot f_h}}) \cdot d \cdot f_h & \text{Mode IIa} \\ \sqrt{4 \cdot M_y \cdot d \cdot f_h} & \text{Mode IIb} \\ (\frac{1}{2}t_1 + \frac{1}{2}\sqrt{t_1^2 + \frac{2 \cdot M_y}{d \cdot f_h}}) \cdot d \cdot f_h & \text{Mode IIIa} \\ (\sqrt{\frac{M_y}{d \cdot f_h}} + \frac{1}{2}t_1) \cdot d \cdot f_h & \text{Mode IIIb} \\ (\sqrt{\frac{M_y}{d \cdot f_h}} + \frac{1}{4}t_2) \cdot d \cdot f_h & \text{Mode IIIc} \\ (-\frac{1}{2}t_1 + \sqrt{\frac{1}{2}t_1^2 + \frac{M_y}{d \cdot f_h}} + \sqrt{\frac{M_y}{d \cdot f_h}}) \cdot d \cdot f_h & \text{Mode IIId} \end{cases} \quad (3.57)$$

where  $M_y$  is equal to the plastic moment resistance of a single dowel,  $d$  is the diameter of a dowel and  $f_h$  is the embedment strength of the timber with a characteristic density of  $\rho_k$ , which is equal to:

$$f_{h,k} = 0.082(1 - 0.01 \cdot d)\rho_k \quad (3.58)$$

The maximum force described above applies to each shear plane. This connection has 4 shear planes in total, thus the decisive failure mode found in Equation 3.57 is multiplied by 4.

Not all dowel columns will be fully effective, therefore an effective number of dowel columns has to be used, which is equal to:

$$n_{ef} = \min(n_{columns}; n_{columns}^{0.9} \cdot (\frac{\alpha_1}{13d})^{1/4}) \quad (3.59)$$

where  $n_{columns}$  are the number of dowel columns parallel to the grain.

Finally, the maximum force in the dowels can be calculated as:

$$F_{max,dowels} = n_{ef} \cdot 4 \cdot F_{failure} \cdot n_{rows} \quad (3.60)$$

Furthermore, failure of the net timber area, failure of the steel plate due to compression or tension and block and plug shear failure of the dowel group have to be checked. The net timber area is the area of the timber member reduced by the area the holes made for the dowels and the steel plates. Thus:

$$F_{max,c} = f_{c,0,k} \cdot A_{net,timber} \quad (3.61)$$

$$F_{max,t} = f_{t,0,k} \cdot A_{net,timber} \quad (3.62)$$

Failure of the steel plate will occur when the material reaches its yield strength  $f_y$ . Therefore, the following equation has to be fulfilled:

$$F_{max,plates,1} = f_y * t_{steelplates} * b_{steelplates} \quad (3.63)$$

where  $t_{steelplates}$  is the total thickness of the steel plates and  $b_{steelplates}$  is the width of the steel plates.

The net area of the steel plate can also fail when loaded in tension.

$$F_{max,plates,2} = \frac{0.9 \cdot f_u \cdot A_{net}}{\gamma_{M,2}} \quad (3.64)$$

Block shear and plug shear failure has to be taken into account. The main part of the member will tear away from the connection and a fracture along the perimeter of the fastener area will occur. The Eurocode [31] states that the maximum value of the block shear and plug shear failure has to be taken, which is:

$$F_{max,blockplug} = \max \begin{cases} 1.5 A_{net,t} \cdot f_{t,0,k} \\ 0.7 A_{net,v} \cdot f_{v,k} \end{cases} \quad (3.65)$$

The values for the net shear and tensile areas are marked in Figure 3.15.

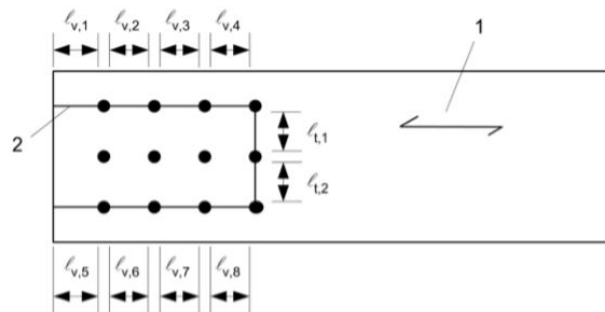


Figure 3.15: The values of  $l_{v,i}$  and  $l_{t,i}$

where:

- $L_{net,v} = \sum_i l_{v,i}$
- $L_{net,t} = \sum_i l_{t,i}$
- $A_{net,t} = L_{net,t} \cdot t$
- $A_{net,v} = L_{net,v} \cdot t$

When designing a connection with steel plates and dowels, the minimum spacing and end distances of the dowels should be considered. These spacing and end distances take into account the diameter of the dowels and the direction of the load. The distances  $\alpha_1$ ,  $\alpha_2$ ,  $\alpha_3$  and  $\alpha_4$  are shown in Figure 3.16 and Figure 3.17.

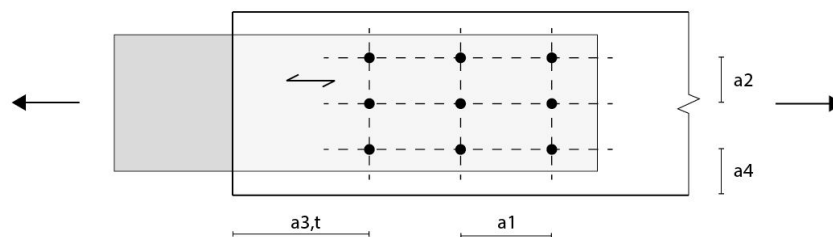


Figure 3.16: Spacing and edge/end distances for dowel connections in tension

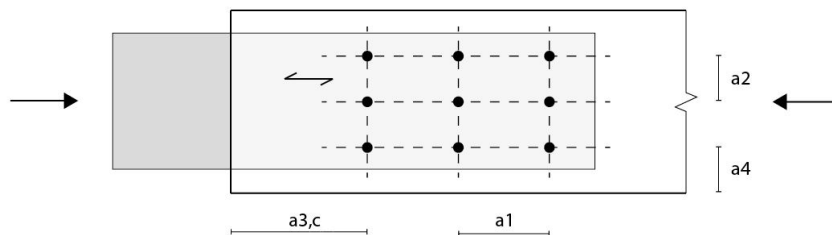


Figure 3.17: Spacing and edge/end distances for dowel connections in compression

The values of the different distances are shown in table 3.8 for either compression or tension in the connection.

Table 3.8: Minimum spacing and edge/end distances for a dowel connection [31]

Spacing and edge/end distances	Angle	Minimum spacing or edge/end distance
$\alpha_1$ (parallel to grain)	$0^\circ \leq \alpha \leq 360^\circ$	$(3 + 2 \cos \alpha )d$
$\alpha_2$ (perpendicular to grain)	$0^\circ \leq \alpha \leq 360^\circ$	$3d$
$\alpha_{3,t}$ (loaded end)	$-90^\circ \leq \alpha \leq 90^\circ$	$\max(7d; 80\text{mm})$
$\alpha_{3,c}$ (unloaded end)	$90^\circ \leq \alpha \leq 150^\circ$	$\max(\alpha_{3,t}  \sin \alpha ); 3d$
	$150^\circ \leq \alpha \leq 210^\circ$	$3d$
	$210^\circ \leq \alpha \leq 270^\circ$	$\max(\alpha_{3,t}  \sin \alpha )d; 3d$
$\alpha_{4,t}$ (loaded edge)	$0^\circ \leq \alpha \leq 180^\circ$	$\max(2 + 2 \sin \alpha)d; 3d$
$\alpha_{4,c}$ (unloaded edge)	$180^\circ \leq \alpha \leq 360^\circ$	$3d$

#### Stiffness

The connection is not infinite stiff and will therefore have a certain stiffness. This stiffness is determined by the properties of the timber and the diameter of the dowel. The stiffness of a single dowel is calculated using the slip modulus  $K_{ser}$  which is equal to:

$$K_{ser} = \rho_m^{1.5} \cdot d / 23 \quad (3.66)$$

per shear plane per fastener. Two steel plates give the dowel a total of 4 shear plates, thus the equation above may be multiplied by 4. Furthermore, when a connection between timber and steel is examined, the value  $\rho_m$  may be doubled. The total stiffness of the connection is equal to  $K_{ser}$  multiplied by the number of dowels.

#### 3.8.2. Connection with glued-in rods

The Eurocode does not discuss connections with glued-in rods, but the German national annex for Eurocode 5 does describe a method to determine the maximum axial force in a glued-in threaded rod.

#### Strength

The minimum distances between each rod and the minimum distance from a rod to the edge are defined as  $a_2$  is  $5 \cdot d$  and  $a_{2,c}$  is  $2.5 \cdot d$  for rods which are axially loaded.

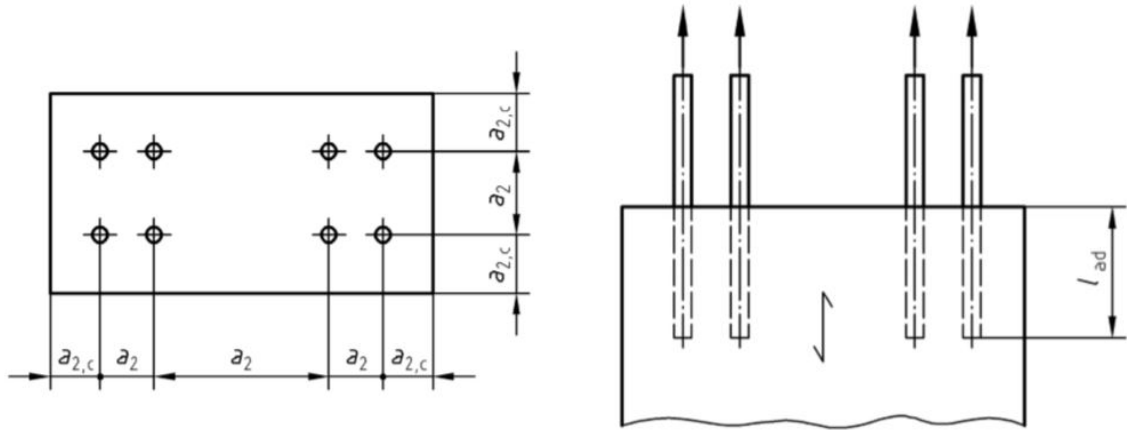


Figure 3.18: Defined distances for connection with glued-in rods [19]

The maximum force per rod can be determined as:

$$F_{ax,Rd} = \min(f_{y,d} \cdot A_{ef}; \pi \cdot d \cdot l_{ad} \cdot f_{k1,d}) \quad (3.67)$$

where:

- $f_{y,d}$  is the yield strength of the rods
- $A_{ef}$  is the effective area of a rod
- $d$  is the diameter of a single rod
- $l_{ad}$  is the adhesive length of the rod
- $f_{k1,d}$  is the value for the bond joint strength

The adhesive length of the rod should be at least:

$$l_{ad,min} = \max(0.5 \cdot d^2; 10 \cdot d) \quad (3.68)$$

Furthermore the rod should meet the requirement that its slenderness is between 7 and 15. The slenderness is defined as the length of the rod divided by its diameter.

The bond joint strength is determined for different lengths of the rod.

$$f_{k1,d} = \begin{cases} 4.0 & l_{ad} \leq 250 \\ 5.25 - 0.005 \cdot l_{ad} & 250 < l_{ad} \leq 500 \\ 3.5 - 0.0015 \cdot l_{ad} & 500 < l_{ad} \leq 1000 \end{cases} \quad (3.69)$$

where  $l_{ad}$  is in mm and  $f_{k1,d}$  is in  $N/mm^2$ .

To determine the maximum force perpendicular to the rod, the Johansen equations can be used, which takes into account the yield and withdrawal strength of the fastener and the embedment strength of the timber.

The failure mechanisms shown in Figure 3.19 are considered.

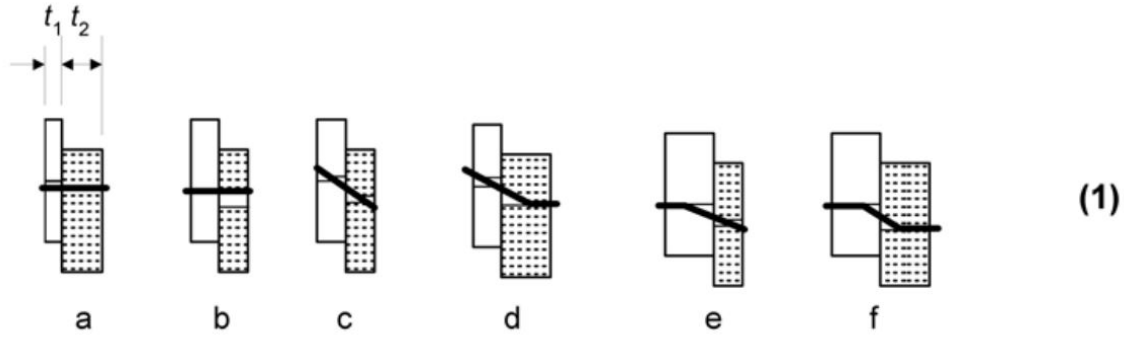


Figure 3.19: Failure mechanism for glued-in threaded rod in shear

The maximum shear force in a single rod is determined using the following formulas:

$$F_{v,Rk} = \min \begin{cases} f_{h,1,k} t_1 d & (a) \\ f_{h,2,k} t_2 d & (b) \\ \frac{f_{h,1,k} t_1 d}{1+\beta} \left[ \sqrt{\beta + 2\beta^2 \left[ 1 + \frac{t_2}{t_1} + \left( \frac{t_2}{t_1} \right)^2 \right]} - \beta \left( 1 + \frac{t_2}{t_1} \right) \right] + \frac{F_{ax,Rk}}{4} & (c) \\ 1.05 \frac{f_{h,1,k} t_1 d}{2+\beta} \left[ \sqrt{2\beta(1+\beta) + \frac{4\beta(2+\beta)M_{y,Rk}}{f_{h,1,k} d t_1^2}} - \beta \right] + \frac{F_{ax,Rk}}{4} & (d) \\ 1.05 \frac{f_{h,1,k} t_2 d}{2+\beta} \left[ \sqrt{2\beta(1+\beta) + \frac{4\beta(2+\beta)M_{y,Rk}}{f_{h,1,k} d t_2^2}} - \beta \right] + \frac{F_{ax,Rk}}{4} & (e) \\ 1.15 \frac{2\beta}{1+\beta} \sqrt{2M_{y,Rk} f_{h,1,k} d} + \frac{F_{ax,Rk}}{4} & (f) \end{cases} \quad (3.70)$$

with:

- $\beta = \frac{f_{h,2,k}}{f_{h,1,k}}$
- The embedment strength of the timber  $f_{h,1,k}$  should be replaced by  $\frac{f_{h,1,k}}{k_h \cdot \sin(\alpha)^2 + \cos(\alpha)^2}$  if the angle  $\alpha$  between the screw and the direction of the grain is greater than 0.
- $k_h = 1.35 + 0.015d$  for soft wood.

For failure mechanisms c,d,e and f, a contribution  $F_{ax,Rk}/4$  can be seen, which is the contribution from the rope effect, while the first term of the equation represents the Johansen part. For dowels this contribution must be limited to 0% of the Johansen part.

#### Stiffness

For connections with glued-in rods which are axially loaded, the stiffness can be assumed infinite. This is not the case when the rods are loaded perpendicular to its axis. For glued-in rods, the same formula is used as the stiffness of a dowel, defined in Equation 3.66. In this case, the rod will have a single shear plane and thus the value  $K_{ser}$  is not multiplied by an additional factor.

#### 3.8.3. Connection with screws

Screwed connections can be loaded either in tension or shear. The maximum tensile resistance is described by the maximum axial resistance of the screws. For the single screw, the maximum axial force is equal to:

$$F_{ax,Rd} = n_{ef} \cdot (\pi \cdot d \cdot l_{ef})^{0.8} \cdot f_{ax,\alpha,k} \quad (3.71)$$

where:

- $f_{ax,\alpha,k} = \frac{f_{ax,k}}{\sin^2(\alpha) + 1.5\cos^2(\alpha)}$
- $f_{ax,k} = 3.6 \cdot 10^{-3} \rho_k^{1.5}$
- $\alpha$  is the angle between the screw and the direction of the grain.

To calculate the maximum shear capacity, the Johansen formulas still hold. To use these formulas, the maximum axial force of a single screw is used. The contribution of the rope effect should be limited to 100% of the Johansen part for screws.

Instead of using this formula, manufacturers often give characteristic values for screws brought on the market. For example, Rothoblaas has a catalogue with different screws and connectors and their corresponding characteristics [54].

# 4

## Development of parametric model

In this chapter, the setup of the parametric model is elaborated. The parametric model is able to design a building which has certain dimensions and lateral stability systems which can be changed. It is chosen to implement lateral stability systems consisting of shear core(s), a diagrid and a tube in the model, which can be used either separately or combined. The different stability systems and the setup of the model is further discussed.

### 4.1. Global design

Every system consists of a structure where columns are placed in a certain grid. Floors are added on each level, which are simply supported by the columns. The different stability systems can then be added to this structure.

#### Shear core system

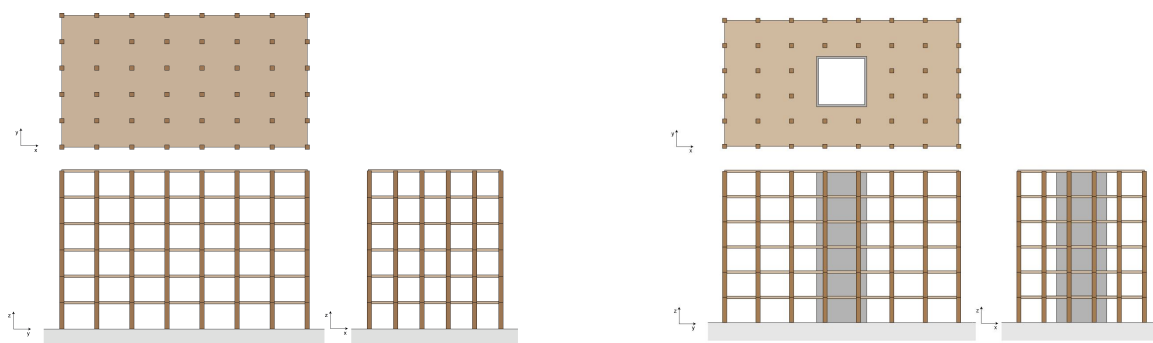
The shear core system has one or more cores added to the structure, which can be made of different materials, for example reinforced concrete or CLT plates. The columns which would be placed inside the core area are removed and also the columns which would intersect with the core walls are deleted.

#### Diagrid system

The diagrid system has a diagrid added to the structure and is placed in the facade. The diagonals replace the columns situated on the perimeter of the structure and consists of diagonally intersecting members. They are connected in each intersection.

#### Tube system

When using a tube system, the columns on the perimeter of the structure are replaced by load-bearing elements which consist of CLT plates with optional openings in the centre. Consequently, this system cannot be used combined with the diagrid system. The load-bearing elements are connected such that they are able to transfer horizontal and vertical loads to the foundation.



(a) Column plan with floors

(b) Stability core system

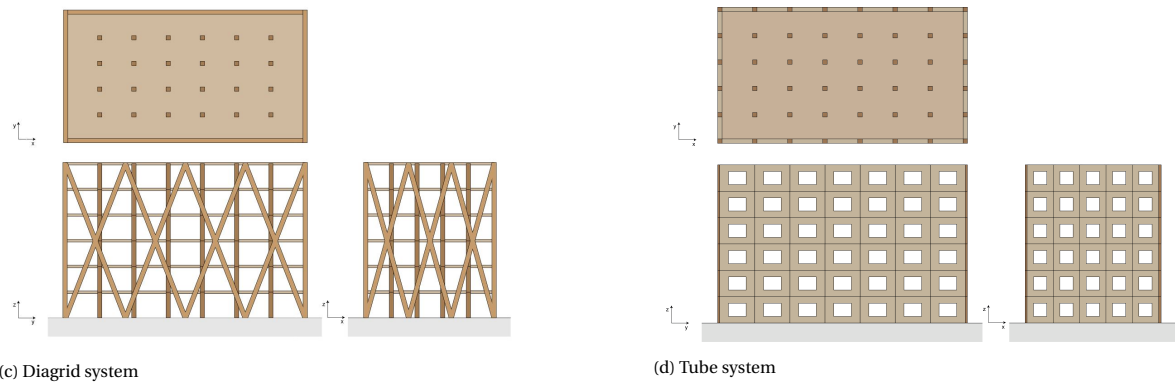


Figure 4.1: Global design of the different stability systems

#### 4.1.1. Loads

The loads acting on the structure can be divided in different groups, namely:

- Permanent actions:
  - Dead load
  - Additional dead load
- Variable actions:
  - Live loads
  - Snow load
  - Wind loads

##### Permanent actions

Two permanent actions are considered in the parametric model, namely dead load and additional dead load. The dead load which has to be taken into account is the self weight of the load-bearing structure. It is modelled as a distributed load in the direction of the gravitational field, assuming  $g = 9.81 m/s^2$ . An additional dead load is used to take into account the self weight of the facade, which is present on all edges of each floor. Therefore a line load is applied to the edges of all floor surfaces which corresponds to the weight of the facade. Furthermore, a surface load which corresponds with the self weight of additional structural components, such as finishing of floors and ceilings, can be applied to the floor surfaces.

##### Variable actions

Three different variable actions are considered in the parametric model, namely live loads, wind loads and roof loading. These loads will be applied as a surface load in both vertical and horizontal direction on the floor surfaces.

- A live load is added to the floors because the building has a residential or office function. For residential usage this load is equal to  $1.75 kN/m^2$  and for office usage this load is equal to  $2.5 kN/m^2$  [25]. To take into account partition walls, an additional load can be added to the live loads. For example, when using a light partition wall system, this load is equal to  $0.5 kN/m^2$ . The whole live load is added to the upper 2 floors, while for all other floors the live load is multiplied by factor  $\psi_0$ .
- The wind loads are calculated according to NEN-EN 1991-1-4 [26], which is explained in subsection 3.1.1. The horizontal wind loads will act on the edges of the different floors, while the vertical wind loads are distributed over the upper floor.
- A load of  $1 kN/m^2$  is applied to the roof.
- A snow load is added to the roof of the building. This snow load is a linear distributed load over the surface with a value of  $0.56 kN/m^2$ . This value is used in the Netherlands [29].

In addition to the permanent and variable actions, horizontal forces are applied to all floors, which encounter for the global initial sway imperfection described in section 3.5. These forces are equal to  $\phi \cdot F$  where  $F$  is the total force on the floors, consisting of permanent and variable actions.

### Load combinations

For these actions, different load combinations can be determined for the ULS and SLS as discussed in section 3.1. These combinations are then used to calculate stresses and deflections. Table 4.1 shows all the load combinations for ULS and SLS. For ULS, also combinations with favourable dead weight load actions are considered.

Table 4.1: Load combinations for ULS and SLS

Load combination	ULS	SLS
1	$1.5 * LC1$	LC1
2	$1.5 * LC1 + 1.65 * 0.5 * LC4$	LC1 + LC2
3	$1.3 * LC1 + 1.65 * LC2$	LC1 + LC3
4	$1.3 * LC1 + 1.65 * LC3$	LC1 + LC2 + 0.5 * LC4
5	$1.3 * LC1 + 1.65 * LC2 + 1.65 * 0.5 * LC4$	LC1 + LC3 + 0.5 * LC4
6	$1.3 * LC1 + 1.65 * LC3 + 1.65 * 0.5 * LC4$	LC1 + LC4
7	$1.3 * LC1 + 1.65 * LC4$	LC1 + 0.5 * LC4 + LC5
8	$1.3 * LC1 + 1.65 * LC5$	LC1 + LC5
9	$1.3 * LC1 + 1.65 * 0.5 * LC4 + 1.65 * LC5$	
10	$0.9 * LC1$	
11	$0.9 * LC1 + 1.65 * 0.5 * LC4$	
12	$0.9 * LC1 + 1.65 * LC2$	
13	$0.9 * LC1 + 1.65 * LC3$	
14	$0.9 * LC1 + 1.65 * LC2 + 1.65 * 0.5 * LC4$	
15	$0.9 * LC1 + 1.65 * LC3 + 1.65 * 0.5 * LC5$	
16	$0.9 * LC1 + 1.65 * LC4$	
17	$0.9 * LC1 + 1.65 * LC5$	
18	$0.9 * LC1 + 1.65 * 0.5 * LC4 + 1.65 * LC5$	

where:

- LC1 is the load case for permanent actions
- LC2 is the load case for wind loads in global y-direction
- LC3 is the load case for wind loads in global x-direction
- LC4 is the load case for live loads on floors
- LC5 is the load case for loads on roof

## 4.2. Setup of parametric model in Dynamo and RFEM

The parametric model consists of a custom node which generates the structure as a whole and outputs member forces and displacements. The custom node has different inputs which can be used to obtain the desired structure. The Dynamo workspace is shown in Appendix C.1.

To design the different lateral stability systems, the structure is divided into different components which are generated in groups in Dynamo. The custom node workspace is shown in Figure 4.2, but can also be found as a larger image in Appendix C.2. The different groups to generate the components are columns, floors, core, diagrid, facade and forces which are presented in the next sections. The groups are labelled in Figure 4.2 and these labels can be found behind each group name in the remainder of this section.

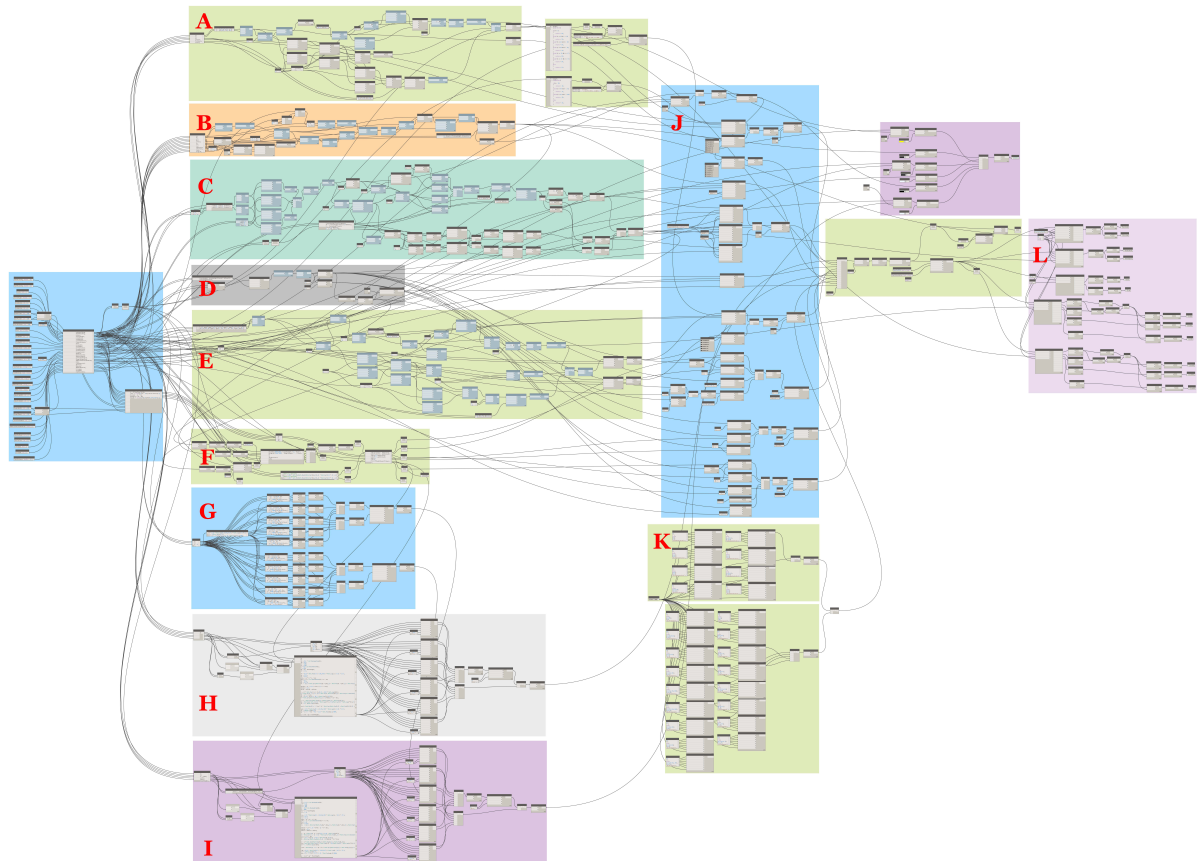


Figure 4.2: Overview of the Dynamo custom node

#### 4.2.1. Columns (B)

The columns are placed in a grid. The distance between the columns is determined by the width and depth of the structure and the amount of columns in width and depth of the building, which is determined by the input of the model. The columns are placed on each level and connected using a hinge on both sides. Supports are placed at the bottom of the columns on the base floor, which restrain translation in x,y and z-direction and rotation around the z-axis. The same material and cross-section properties are assigned to each column, which can be provided as input.

At this moment of writing, springs can not be modelled using the Arcadis add-on. Therefore, only timber columns are generated in RFEM with the connections modelled as hinges on both ends. However, this would imply that these connections are infinitely stiff in the direction of the column, while there are connections where this is not the case. For example, when a connection with steel plates and dowels is used, the connections have a certain stiffness. To take into account this effect, the E-modulus of the column material should be modified in RFEM. The modified E-modulus can be calculated by considering a column with connections on both sides as 3 springs which are placed in series, as shown in Figure 4.3.

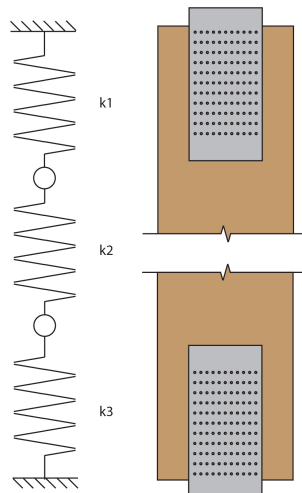


Figure 4.3: Column and connections in series

To determine the modified stiffness of the column, the equivalent spring stiffness is calculated as follows:

$$\frac{1}{k_{eq}} = \frac{1}{k_1} + \frac{1}{k_2} + \frac{1}{k_3} \quad (4.1)$$

where  $k_1$  and  $k_3$  represent the connection stiffness  $K_{ser}$  and  $k_2$  represents the stiffness of the column, which is equal to  $EA/l$ .

In Figure 4.4 different column configurations as generated in RFEM are shown.

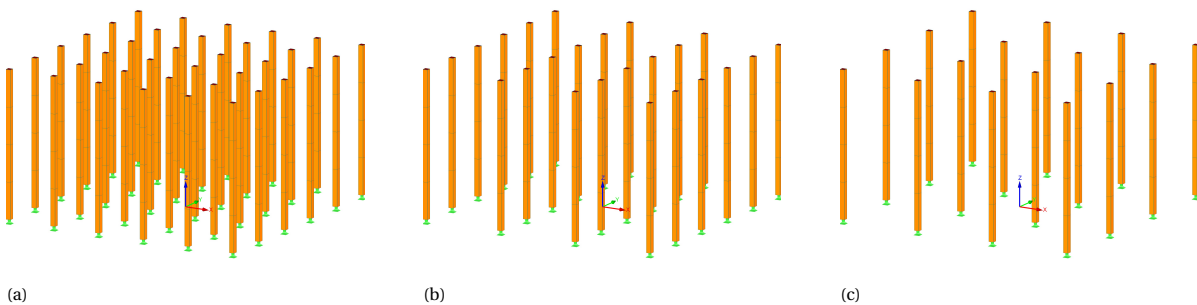


Figure 4.4: Modelling the columns in RFEM

#### 4.2.2. Floors (D)

At every level, a surface is added that has a width and depth equal to those of the building. The height between each storey can be chosen and also the number of storeys is variable. The surface is connected to all present columns, cores and diagonals. Each floor is made of the same material and has a certain thickness, which are provided as input. On the perimeter of the surfaces, a line hinge is applied. This line hinge ensures that when facade elements are added, the connection between these elements and the floor surfaces is hinged.

Figure 4.5 shows 3 models which consist of different storey heights and number of storeys.

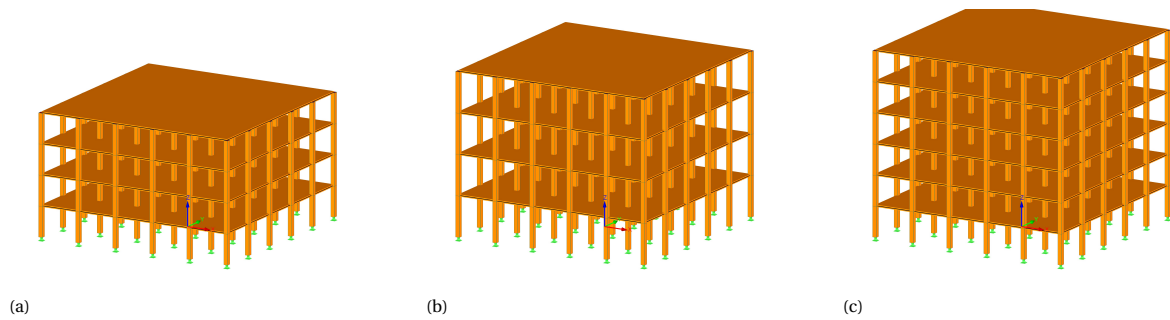


Figure 4.5: Modelling the columns in RFEM

### 4.2.3. Core (E)

One or more cores can be added by using the core switch in the input group. The position(s) of the core(s) can be determined by using the x and y-coordinates input. Also the width and depth of the core can be changed and the thickness of the core walls is variable. Parts of the core walls can be removed, so that U-shaped cores can be created. The columns, which would be placed if no core was present, are removed. Furthermore, columns which are placed within 850 millimetres from the core will be removed to assure that the cross-sections of the columns do not intersect with the core walls. The material of the core walls can be changed to either concrete or timber. It is only possible to apply an isotropic material to the surfaces, therefore the in-plane stiffness of the CLT plates must be used.

Different variations of cores are presented in Figure 4.6.

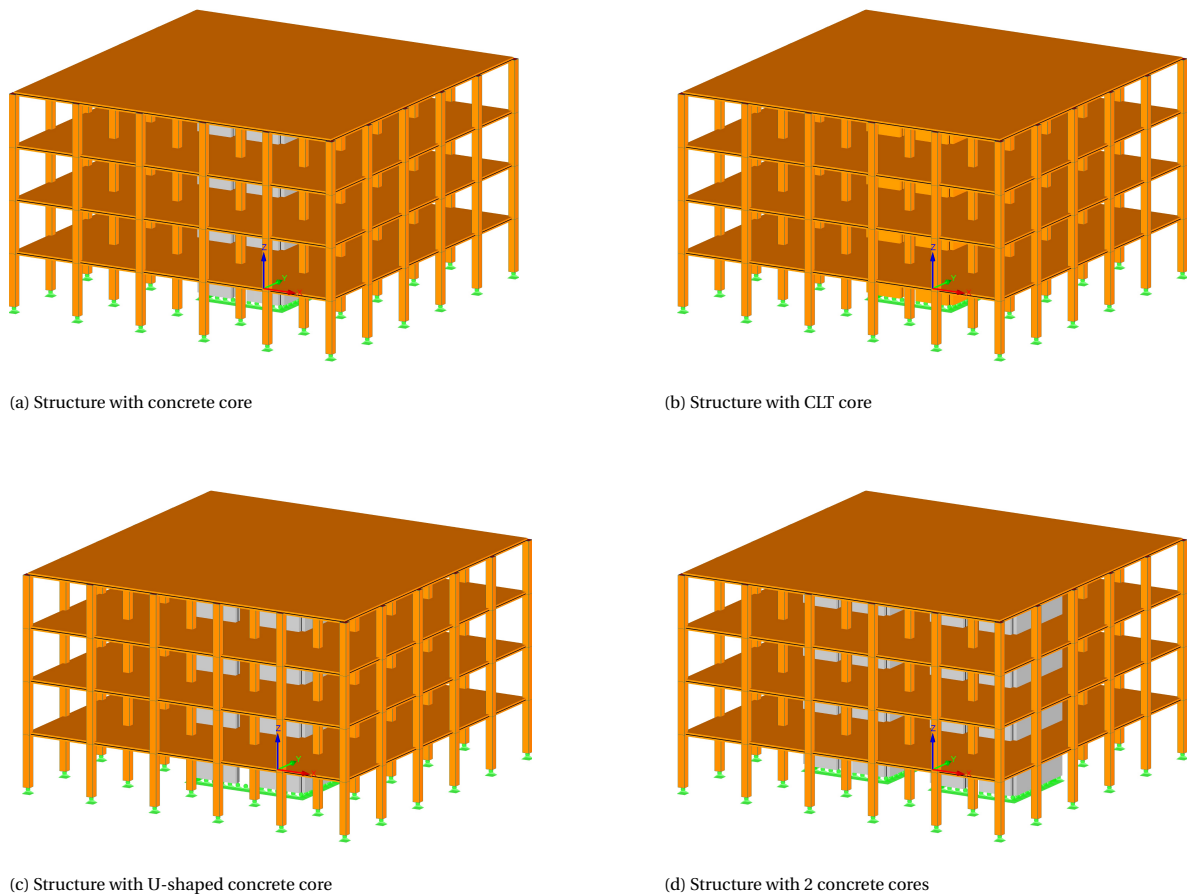


Figure 4.6: Modelling the core in RFEM

The core walls can in reality consist of multiple elements, which have to be connected. These connections can

be located in the corners of the cores and between core walls on each floor. Depending on the connections considered, these connections may not be infinite stiff in all directions, while the walls in the RFEM model are connected using a hinged connection. Due to the fact that also in this case these connections cannot be modelled as a spring using the Arcadis add-on, the Young's modulus of the walls must be adapted to include these connection stiffness.

The reduction of the Young's modulus of the walls due to the connection stiffness is depended on the properties of the walls and connections and the building height. The influence of the connection stiffness can be determined by hand using the theory of mechanically jointed beams provided by the Eurocode or in FEM software by creating a model with and without implemented connection stiffness and then compare these models.

To determine the correct stresses in the surface and thus neglect the influence of singularities near the edges, at the bottom the surface is divided into small rectangles. The maximum stresses in the surface can be calculated by averaging the stresses in each rectangle and taking the maximum of these average values. At the bottom of the walls, supports are added which restrain translation in x, y and z-direction. The divided core wall surfaces and supports can be seen in Figure 4.7.

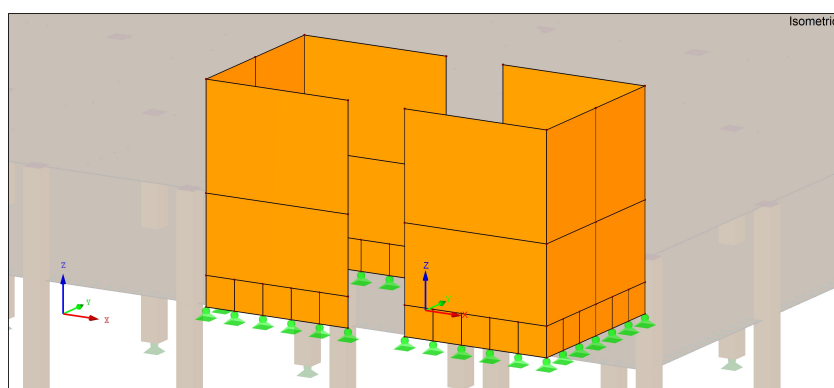


Figure 4.7: Divisions of the bottom core walls

#### 4.2.4. Diagrid (C)

A diagrid can be applied to the structure by using the diagrid switch in the input group. The number of diagonals which are placed is determined by the amount of diagonals in width and depth provided as input. The height of a diagonal is controlled by the amount of floors per diagonal. All diagonals are made of the same material and have the same cross-section properties.

The RFEM output is shown in Figure 4.8.

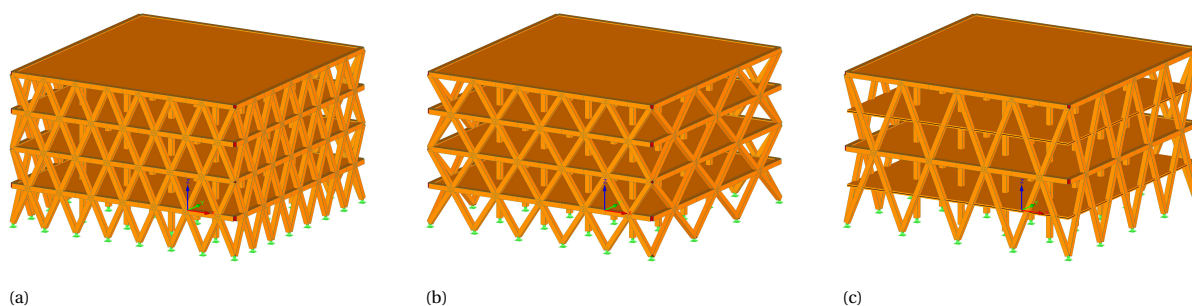


Figure 4.8: Modelling the diagrid in RFEM

As also seen for the columns, the diagonals will consist of members with hinges on both ends. To encounter for a finite connection stiffness in the direction of the diagonal, the E-modulus of the diagonal material should

be modified in RFEM. This can be done in the same way as described in subsection 4.2.1.

#### 4.2.5. Tube system (A)

The load-bearing facade elements are modelled as surfaces which are placed on all sides of each storey. Because it is desirable to have a hinged connection between the facade surfaces and floor surfaces, line hinges are applied to the perimeters of the facade surfaces. Also for these surfaces it is only possible to apply an isotropic material, therefore the in-plane stiffness of the CLT plates must be used.

The facade will consist of multiple elements, which have to be connected. These connections can be located in the corners of the building, between the different elements in vertical direction and between the elements in horizontal direction on each floor. Furthermore, windows could be present in the facade. Depending on the connections considered, these connections may not be infinite stiff in all directions, while the facade is modelled as a single surface without windows and therefore uses infinite stiff connections. Also in this case the connections cannot be modelled as a spring using the Arcadis add-on, therefore the Young's modulus of the walls must be adapted to include these connection stiffness and possible windows in the facade. The same methods as described for the core elements can be used to determine the reduction of the Young's modulus due to the connections stiffness.

To calculate the maximum stresses in the facade surface, the same method is applied as used for the core elements, discussed in subsection 4.2.3. Therefore, also the bottom of the facade surfaces is divided into smaller rectangles and supports are added, which restrain translation in x, y and z-direction. This is displayed in Figure 4.9.

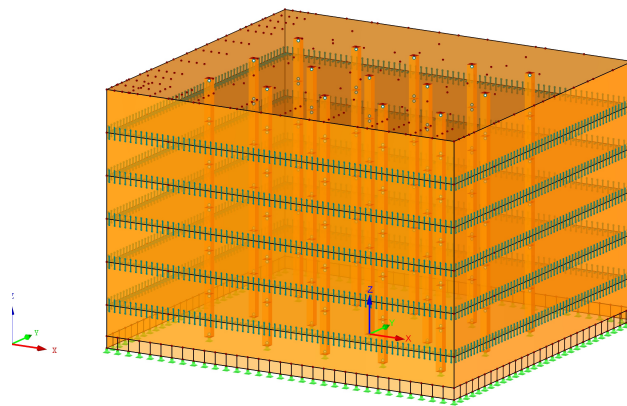
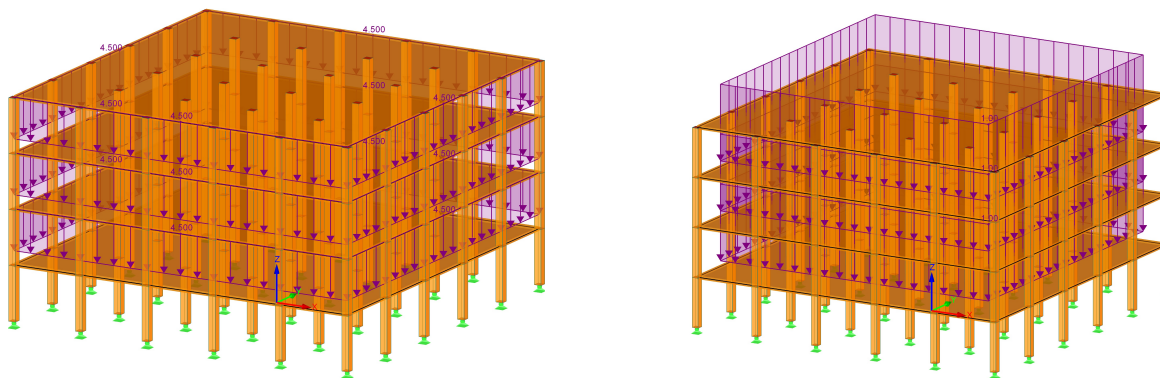


Figure 4.9: Modelling the facade elements in RFEM

#### 4.2.6. Forces (F,H,I,J,L)

Several forces have to be applied to the structure to take into account dead weight, wind loads and variable loading. To apply the dead weight of the facade to the structure, a vertical line load is applied to the edges of the floor surfaces. Also an additional permanent load is applied to all floors.

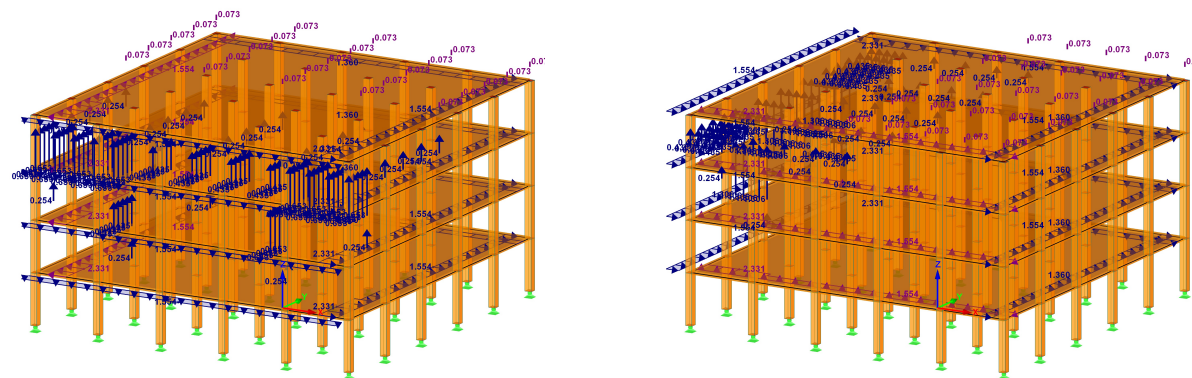


(a) Permanent load due to the facade

(b) Additional permanent load

Figure 4.10: Modelling permanent loads in RFEM

Two load cases are created to apply wind loads on the structure for 2 directions, namely x- and y-direction. The horizontal loads are applied to the edge of the floors by using a line load. The loads on the roofs due to the wind are modelled by using nodal forces. Each wind area (E, G, H, I) is divided into 25 points and vertical nodal forces are put on these points, where each nodal force represents a small part of the total wind load.

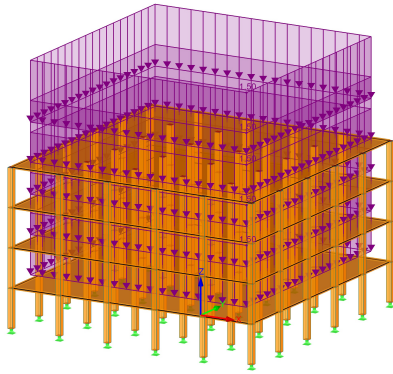


(a) Applied loads for wind in x-direction

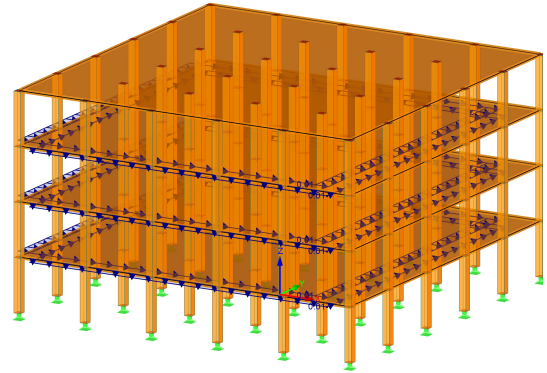
(b) Applied loads for wind in y-direction

Figure 4.11: Modelling the wind loads in RFEM

Live loads are applied to each floor, which is shown in Figure 4.12a. These loads will have a horizontal component due to the global initial sway imperfections. Therefore these loads are applied to these floors as well, as can be seen in Figure 4.12b. For both loads, surface loads are used.



(a) Live loads applied to the floors



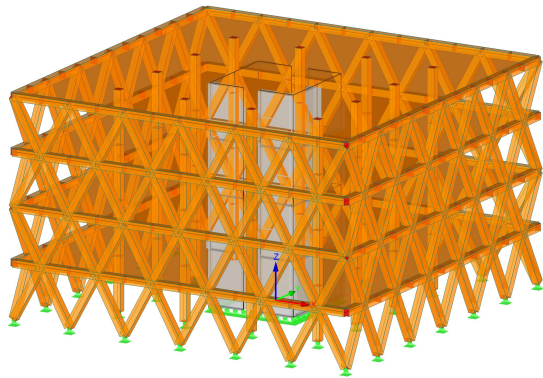
(b) Horizontal loads due to the global initial sway imperfections

Figure 4.12: Loads applied to the floors

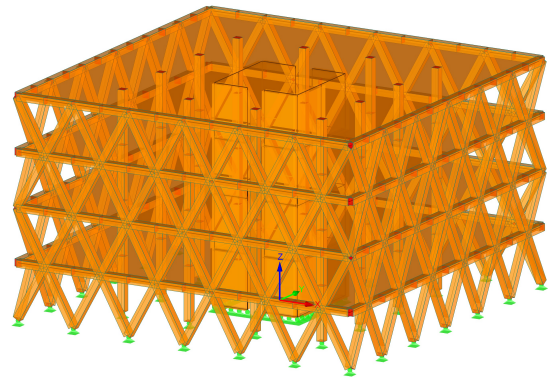
#### 4.2.7. Combination of systems

The different stability systems can be combined. For example, a diagrid system can be combined with either a concrete or CLT core. Also, a facade can be combined with both cores. Combining a diagrid with a facade will not give desirable results.

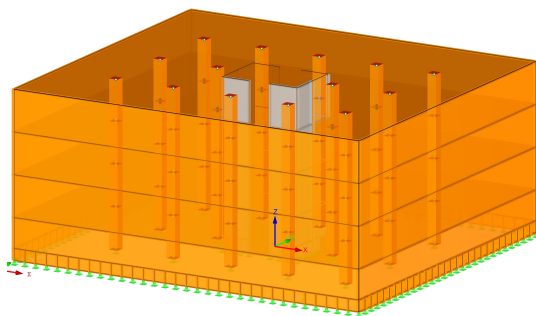
The different combinations are depicted in Figure 4.13.



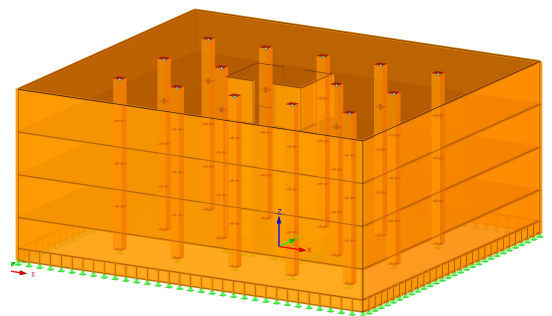
(a) Concrete core combined with diagrid system



(b) CLT core combined with diagrid system



(c) Concrete core combined with tube system



(d) CLT core combined with tube system

Figure 4.13: Modelling combination of systems in RFEM

#### 4.2.8. Export to RFEM and analysis of stresses and deformations (J,L)

After the Dynamo model is generated, it will be exported to RFEM. A structural calculation can be started by setting the switch *Start Calculation* to true. This calculation can either be linear or non-linear, depending on the load combinations defined. The results of the structural calculation can now be examined in RFEM or Dynamo and checked if they meet the requirements in SLS and ULS. When using Dynamo to examine the results, only a limited amount of available results provided in RFEM can be viewed in Dynamo.

It should be noted that exporting the model to RFEM, running the structural calculation and transferring back the results to Dynamo can take a very long time (>1 hour) if a very large model or a model consisting of many surfaces is used. Hence, as a result the model will contain many elements that which cause a great amount of data to be exchanged between the programs, which ensures a long time required for the information to be transferred.

### 4.3. Method of using the parametric model

To use the parametric model in order to get sufficient results, some steps have to be taken. First, the dimensions of the building and floors have to be set as input. The dimensions of the building include width, depth and storey height of the structure, but also the number of columns in width and depth and the dimensions of the columns. Furthermore, the floor properties can be adjusted, such as thickness and material. Next, the type of stability system has to be chosen and the dimensions of the elements of the stability system must be inputted. For a system with a core, the width, depth and thickness of the core must be set.

Subsequently, the connections have to be determined for the columns, diagonals and/or walls. The connection strength and stiffness have to be calculated by hand. Because stiffness of connections cannot be applied in the model due to restrictions of the Arcadis add-on, the material stiffness of the stability elements have to be adjusted in such a way that the connection of the stiffness is taken into account.

By hitting the Run button, the structure is generated by Dynamo and exported to RFEM. A structural analysis will be executed, which can take some time depending on the size of the structure. Next, you can choose to either use RFEM or Dynamo to check the design according to ULS and SLS requirements. The connections can be checked by using the member forces in the columns and diagonals and stresses in the wall elements. The deformations can be checked in SLS and the eigenfrequency and maximum acceleration of the top floor is calculated.

The whole method of using the parametric model is shown as a flow chart in Figure 4.14.

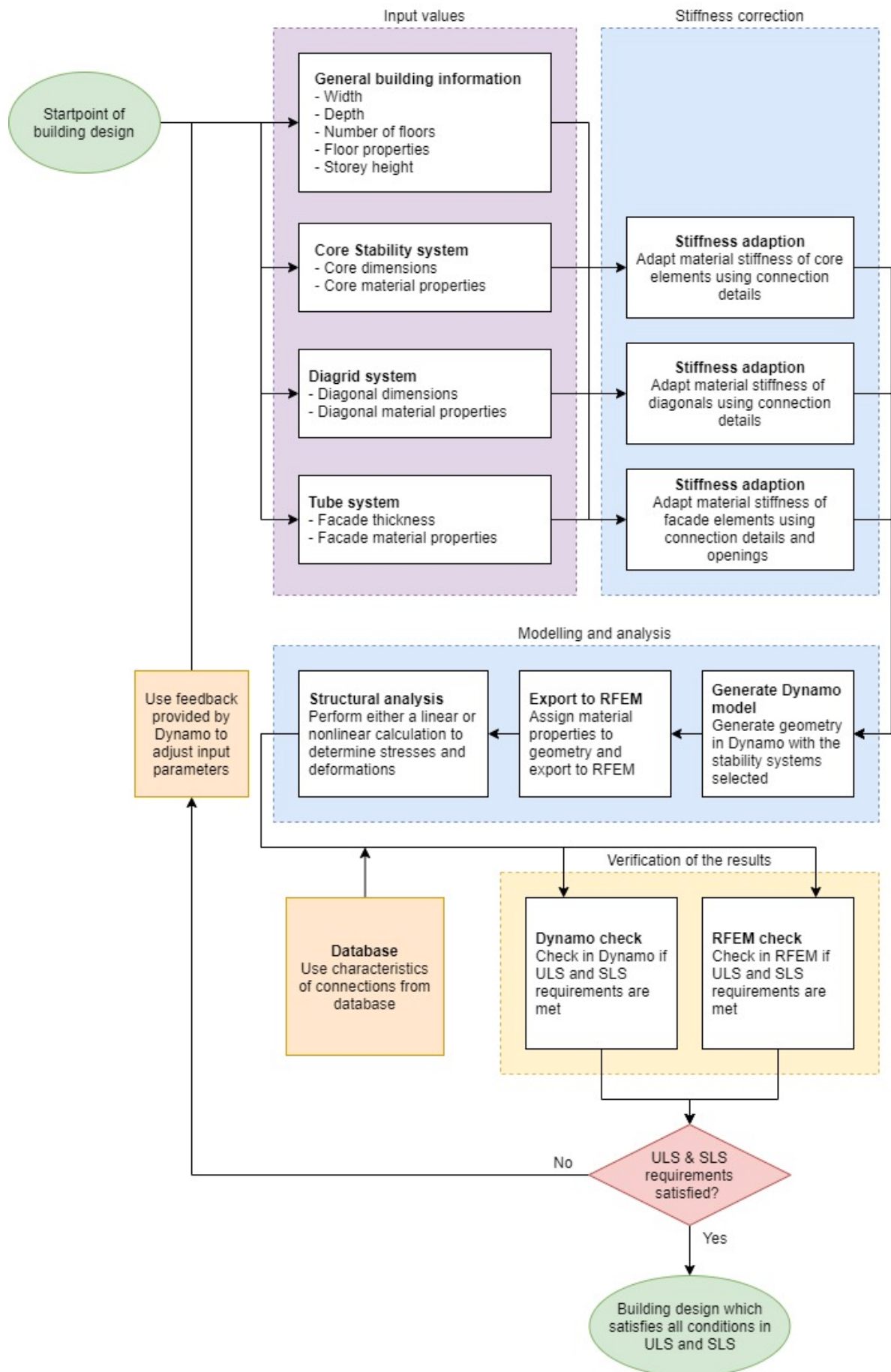


Figure 4.14: Method of using the parametric model

# 5

## Case study: Brock Commons Tallwood House

To check if the parametric model gives satisfying results, a case study is performed on the Brock Commons Tallwood House. First the building will be discussed together with its load-bearing structure and detailing. Next, the structure of this building will be generated using the parametric model. The results which the model produces will be compared with results available of this building.

### 5.1. General information

The Brock Commons Tallwood House is a student residence building at the University of Columbia in Vancouver. It consists of 18 stories, which gives it a height of 54 metres. It houses 404 students in studio and four-bed units with public places on the ground floor and a lounge on the top floor.



Figure 5.1: Side-views of the Brock Commons Tallwood House [45]

### 5.2. Load-bearing structure

The floor plan of the building is shown in Figure 5.2, where the load-bearing structure is visible. The building has a width of 56 metres and a depth of 15 metres.

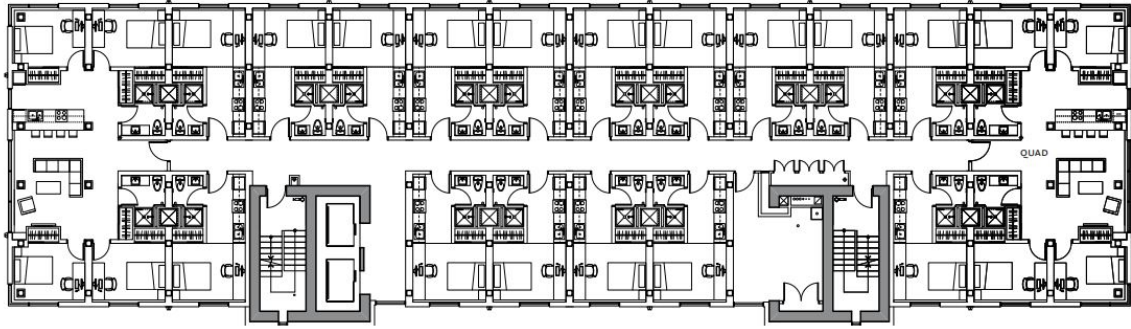


Figure 5.2: Floorplan of the Brock Commons Tallwood House [45]

A concrete podium is placed on the ground floor. This is done to create large spans between the concrete columns in order to get a large open area. On top of these concrete columns a 600 mm thick concrete slab is placed, which supports the timber structure. The building has 2 concrete cores, which provide lateral stability and resist seismic forces. These cores house stairs, elevator shafts and mechanical services. It is cast in-situ and has a thickness of 450 millimetres.

GLT and PSL columns carry the vertical loads together with the concrete cores to the foundation. These columns are placed in a grid measuring 4 by 2.85 metres. On the lower levels, from levels 2 to 9, the dimensions 265 by 265 millimetres are used, while on the upper levels, levels 9 to 18, the dimensions are 265 by 215 millimetres. Between stories 2 and 5, the columns are made of PSL, others are made of GL24h.

The floors are built using CLT slabs, which have a thickness of 169 millimetres. They have a width of 2.85 metres and have varied lengths. The panels function as diaphragms. To increase the weight of the building and stiffness of the CLT floors, a 40 millimetres thick concrete topping is added. This topping also improves acoustic performance. The CLT is directly supported by the columns.

### 5.3. Detailing

Columns are connected using a steel section. Threaded rods are glued into the column and a thick steel plate is welded to these rods. A round hollow steel piece is used to connect the steel plates at the ends of the columns. The floor slabs lay on top of the steel plate and are bolted by four rods. Therefore, the vertical loads can be transferred directly from column to column, while the vertical and shear forces of the floor slab can be supported by the column as well. Such a connection is also used to connect the columns to the concrete podium, but the rods at the lower steel plate are fixed in the concrete.

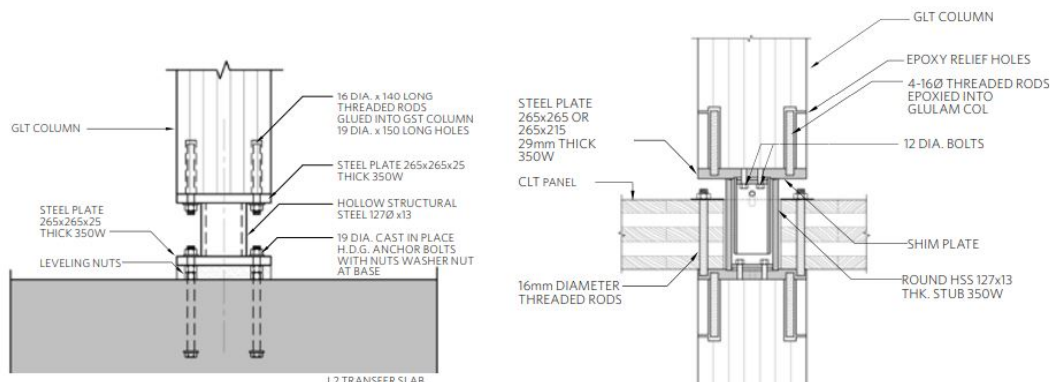


Figure 5.3: Connections column to concrete podium and column to column [48]

The CLT panels are connected to the concrete core using a steel angle that is welded to a steel plate. This

plate is fixed in the concrete. The steel angle can resist both vertical and shear forces. To transfer the lateral loads, which are present due to the diaphragm function of the floor, drag straps are attached. Bolts are used to connect the drag straps to faceplates, which are bolted to the core.

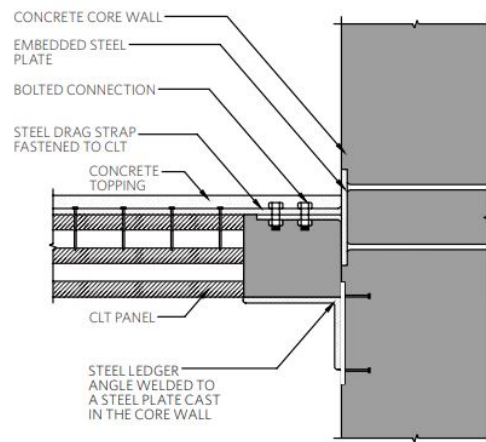


Figure 5.4: Floor to core connection [48]

Fire protection is a very important aspect in the design of the Brock Commons Tallwood House. Active and passive fire protection is used to achieve a sufficient fire safety. By taking passive fire safety measures, the probability that structural elements fail before occupants can exit the building is prevented, as well as the spread of the fire between different stories. These measures consist of a full encapsulation of the timber structure in multiple layers of gypsum. These layers, made of Type X gypsum, give the load bearing structure a fire-resistance rating of 2 hour, which is required according to the building codes. A total of 3 gypsum layers with a total thickness of 48 millimetres is used at the column, as can be seen in Figure 5.5. Also the concrete topping on top of the CLT floor slabs give additional fire-resistance rating.



Figure 5.5: Type X gypsum layers around a column [45]

The building has an automatic sprinkler system, which has a 20000 litre water-tank located in the bottom of the building. The tank allows the sprinklers to work for 30 minutes.

## 5.4. Parametric model of the building

### 5.4.1. Model input

The parametric model is used to generate the structure in RFEM. Some assumptions had to be made in order to do so:

- The parametric model allows you to only generate storeys with the same storey height. For this reason, the concrete podium cannot be used and is therefore replaced by a storey with timber columns of 3 metres in height. Because all stories have a height of 3 metres and a total of 18 storeys is used, the building will still reach a total height of 54 metres.
- Because the model only allows you to assign the same cross-section and material to each column, it is considered that all columns have the dimensions and material of the columns which are situated

between floors 2 and 5. Hence, the columns will have a width and depth of 265 millimetres and are made of Parallam PSL 2.0E.

- The cores of the Brock Commons Tallwood House do not have a clear rectangular shape. It consists of 2 walls per core in the depth, 2 walls per core in the width with an opening in it and some additional small walls. Therefore, each concrete core is represented by 2 U-shaped concrete elements with a thickness of 450 millimetres. Between those elements a gap of 1.0 meter in the width of the building is applied. The cores are made of C40/50 and it is assumed that this concrete is cracked. Because the concrete is poured in-situ, no reduction is applied to the E-modulus of the core material to encounter for stiffness of connections.
- The floor slabs are made of CLT consisting of 5 layers. An additional dead load of  $1.0 \text{ kN/m}^2$  is applied to the floor to encounter for the concrete topping. The stiffness of the floor is determined in Table 6.7, where a floor with a height of 130 millimetres is considered, thus a stiffness of  $2947 \text{ N/mm}^2$  is used.

All material properties are displayed in Table 5.1.

Table 5.1: Material properties for RFEM model of Brock Commons Tallwood House

		Parallam PSL 2.0E	Concrete C40/50 (cracked)	CLT	
Design Modulus of Elasticity	$E_d$	11400	11667	2358	$\text{N/mm}^2$
Design Shear modulus	$G_d$	424	5833	982	$\text{N/mm}^2$
Poisson's ratio	$\nu$	12.49	0.0	0.2	(-)
Specific weight	$\gamma$	5	25	5	$\text{kN/m}^3$

With all the assumptions taken into consideration, the following inputs were used to generate the model.

Table 5.2: Dynamo input values

Description	Value	
Width building	56	m
Depth building	15	m
Levels	18	
Storey height	3	m
Columns in width	15	
Column in depth	6	
Width column	265	mm
Depth column	265	mm
Column material	Parallam PSL 2.0 E	
Floor thickness	130	mm
Core width	6.5	m
Core depth	6.5	m
Core x-position	[-14, 14]	m
Core y-position	-4	m
Core gap in x	1	m
Core material	Cracked C40/50	
Core thickness	450	mm
Additional floor load	1.0	$\text{kN/m}^2$

The result in RFEM is presented in Figure 5.6.

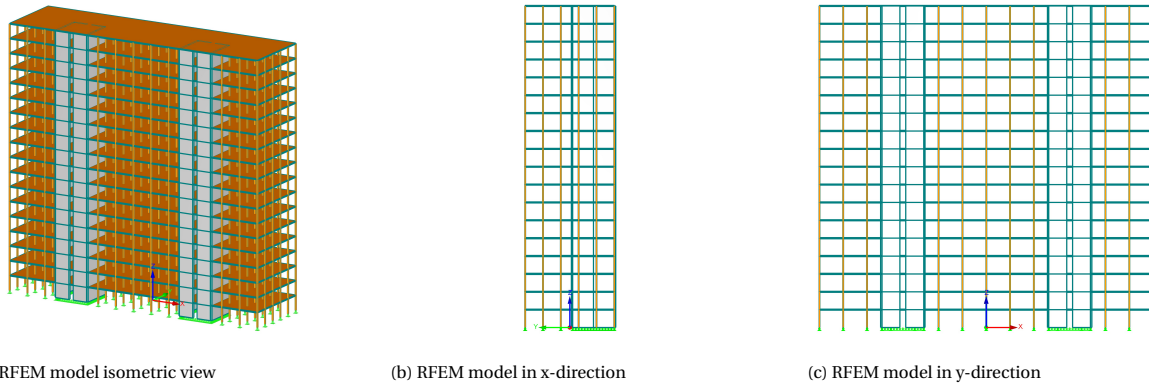


Figure 5.6: RFEM model of Brockcommons Tallwood Building

### 5.4.2. Connections

The columns are connected using glued-in rods. A total of 4 threaded rods is used, which have a length of 140 millimetres and a diameter of 16 millimetres. The fire protective layer, which is added to all sides of the columns, give a char layer depth of 12 millimetres after 120 minutes of fire. The properties of the material of the column are shown in Table 2.4. All steel parts in the connection are made of S355.

In Appendix B.2 the maximum compression and tension forces which can be taken up by the connection are calculated. It is determined that the maximum compression force is equal to 1383kN and the maximum tension force is equal to 69kN.

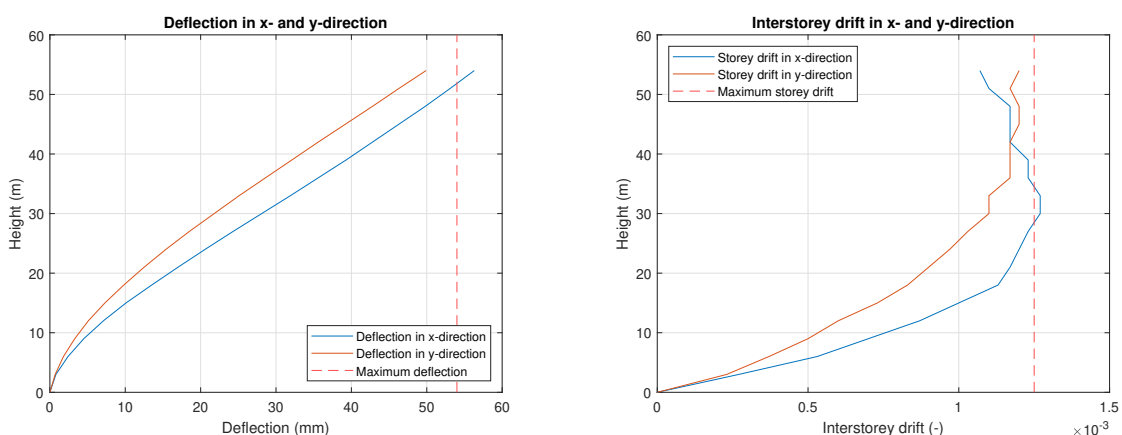
## 5.5. Structural analysis results

The results of the structural analysis are checked using RFEM. All load combinations are calculated using a second-order analysis. All the results will be further discussed.

### 5.5.1. Deflection of the structure

The deflection of the structure in SLS is determined for each level in both horizontal directions. The stiffness of the foundation is not taken into account, therefore instead of using a maximum horizontal deflection of  $h/500$ , a maximum of  $h/1000$  is used.

These deflections and the maximum allowed deflection are shown in Figure 5.7a.



(a) Deflections

(b) Interstorey drift

So the unity checks for horizontal deflections are:

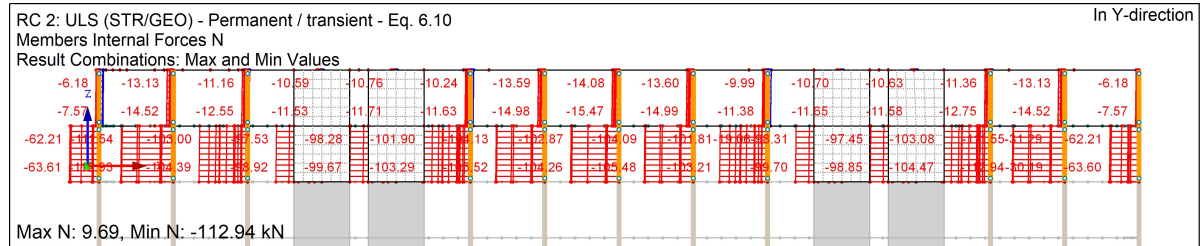
$$UC_{deflection,x} = \frac{56.4}{54} = 1.04$$

$$UC_{deflection,y} = \frac{50.7}{54} = 0.94$$

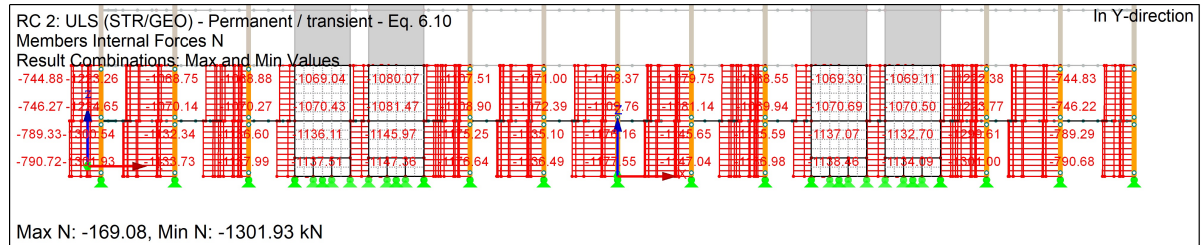
As can be seen, the building slightly exceeds the conditions for maximum deflection and inter-storey drift in x-direction. This can be caused by the fact that it is assumed that the foundation contributes to half of the total deflection, which is a conservative assumption. Therefore, the results regarding deflection are satisfying, because the unity checks are close to 1.0.

### 5.5.2. Forces in the structure

The maximum forces in ULS are determined for each column. The maximum compression forces occur at the first level, while the maximum tension forces occur at the top level. The results for the lowest and top level are displayed in Figure 5.8a and Figure 5.8b respectively.



(a) Maximum forces at the top level



(b) Maximum forces at the first level

Figure 5.8: Maximum compression and tension forces

The corresponding maximum values are 1302 kN in compression and 10 kN in tension. Hence, the unity check values are:

- $UC_{compression} = 1302/1383 = 0.94$
- $UC_{tension} = 9/69 = 0.13$

The stresses which occur in the core walls are:

- $\sigma_{compression} = -6.69 N/mm^2$
- $\sigma_{tension} = 2.34 N/mm^2$
- $\sigma_{shear} = 1.40 N/mm^2$

The stresses are lower than the strength properties and therefore, only minimum reinforcement is required.

### 5.5.3. Dynamics of the structure

To check the acceleration of the top level of the building, the method described in section 3.6 is used. The natural frequency is calculated using the mass of the building, the additional weight on the floor slabs and the quasi-permanent load, which is equal to 0.4 times the live loads on the floor. The natural frequency is therefore approximately:

$$f_0 = 46/h = 46/54 = 0.85 \text{ Hz}$$

These maximum acceleration of the top level is calculated and plotted in Figure 5.9, where also the limitations for accelerations according to the Eurocode are shown.

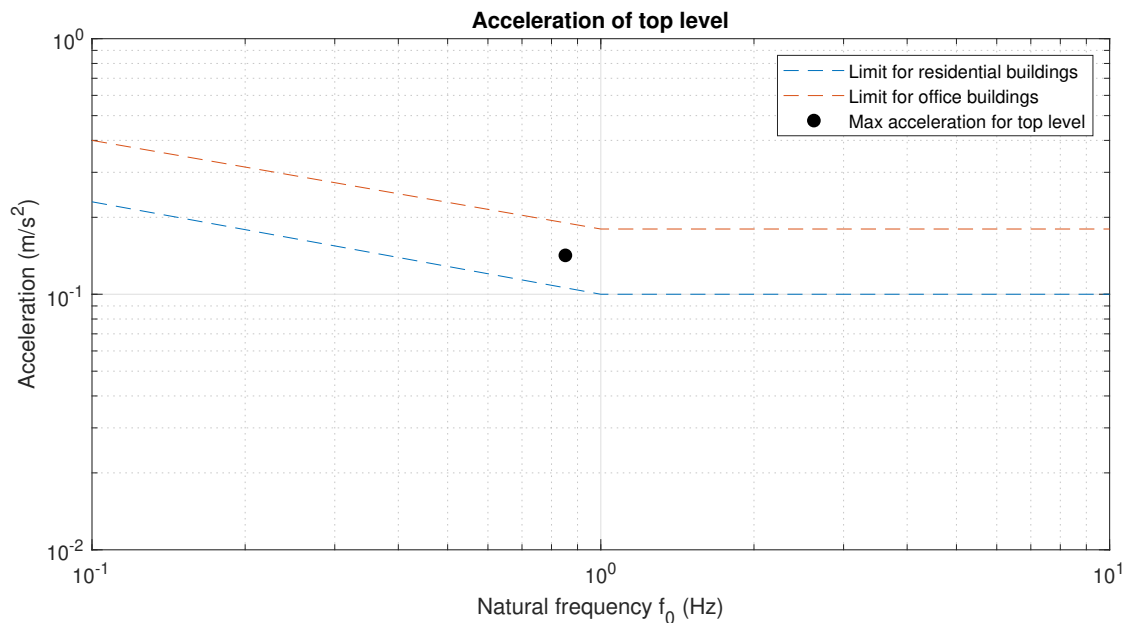


Figure 5.9: Maximum acceleration of the top level of the Brock Commons building

The building has a first mode frequency of 0.5 Hz and is designed to limit the top level accelerations due to wind to 1.5 percent of the gravity acceleration, which is equal to  $0.15 \text{ m/s}^2$  [44]. From the parametric model follows that the building has a natural frequency of 0.85 Hz and a maximum acceleration of  $0.14 \text{ m/s}^2$ . The maximum acceleration is almost equal to the values according to the designer, but the frequency is slightly different. It can be seen that the maximum acceleration does not satisfy the Eurocode requirements for residential buildings.

## 5.6. Conclusion

Using the parametric model, it is possible to generate and validate the Brock Commons Tallwood House. To do so, several assumptions had to be made.

It is only possible to generate identical storeys. Therefore, it was not possible to generate the concrete podium and thus this is replaced by a storey with timber columns. Also the columns have the same dimensions at all levels, while in reality these columns will become slightly smaller at a certain level. These differences will have small influence on the mass and stiffness of the building.

The columns at the lowest level have the correct dimensions and material and at that location the highest compression forces occur. Therefore it is considered that this assumption is acceptable. The concrete podium would add additional mass to the building, but this mass is only a small portion of the total mass of the building and therefore it is assumed that this will not have a big influence on the behaviour of the building.

The core is not generated exactly like how the core looks in reality. By making use of a gap in the core wall, the cores will be represented by 2 U-shaped elements. These elements are comparable to the core shape used in reality and thus can be applied in such a way. The cores provide enough stiffness to satisfy the conditions for horizontal deformation of the structure and inter-storey drift in SLS. The unity checks for horizontal deformation are close to 1.0 (1.04 and 0.94 respectively), which is desirable. It slightly exceeds the conditions for maximum deflection in x-direction, which is caused by the fact that a conservative approach regarding foundation stiffness is used.

Also the unity checks for compression and tension satisfy the conditions in ULS. The building does not satisfy the conditions for the maximum acceleration of the top level according to the Eurocode, but the eigenfrequency and maximum acceleration of the top level are comparable to those found by the designer of the building.

Hence, these results and therefore the parametric model are adequate.

# 6

## Parametric study on timber high-rise in The Netherlands

In this chapter, the basic principles of the design are set up to be used in the parametric study. Furthermore, the connections between the columns, diagonals and wall elements are elaborated. To do so, a calculation is performed using MATLAB to obtain the optimal characteristics of the connections regarding strength and stiffness. The effect of the presence of connections and facade windows on the stiffness of the structural elements is checked and assumptions are made regarding foundation stiffness and fire safety design.

### 6.1. Basic principles of the design

A building with a width of 32.4 metres and a depth of 28.8 metres is assumed and serves as an office building. A commonly used grid spacing in The Netherlands of 1.8 metres is used. The structure has 7 columns in width and 5 columns in depth. It is considered that beams are placed in the direction of the depth of the building, hence the beams have a span of 7.2 metres. CLT floor slabs are placed perpendicular to the beams, which give them a span of 5.4 metres. An additional dead floor load of  $1.0\text{ kN/m}^2$  is applied. Therefore, 5 layer floor slabs with a height of 225 millimetres are used. It is assumed that the facade has a weight of  $1.5\text{ kN/m}^2$ . The building is designed for consequence class 3. All structural elements must therefore have a fire resistance of at least 120 minutes and all wall elements must have a separating function of 120 minutes.

The inputs which are valid for all stability systems are summarised in Table 6.1.

Table 6.1: Dynamo input values

Description	Value	
Width building	32.4	m
Depth building	28.8	m
Storey height	3.6	m
Columns in width	7	
Column in depth	5	
Floor thickness	225	mm
Additional floor load	1.0	$\text{kN/m}^2$

The floor plan for the building without any lateral stability system is shown in Figure 6.1.

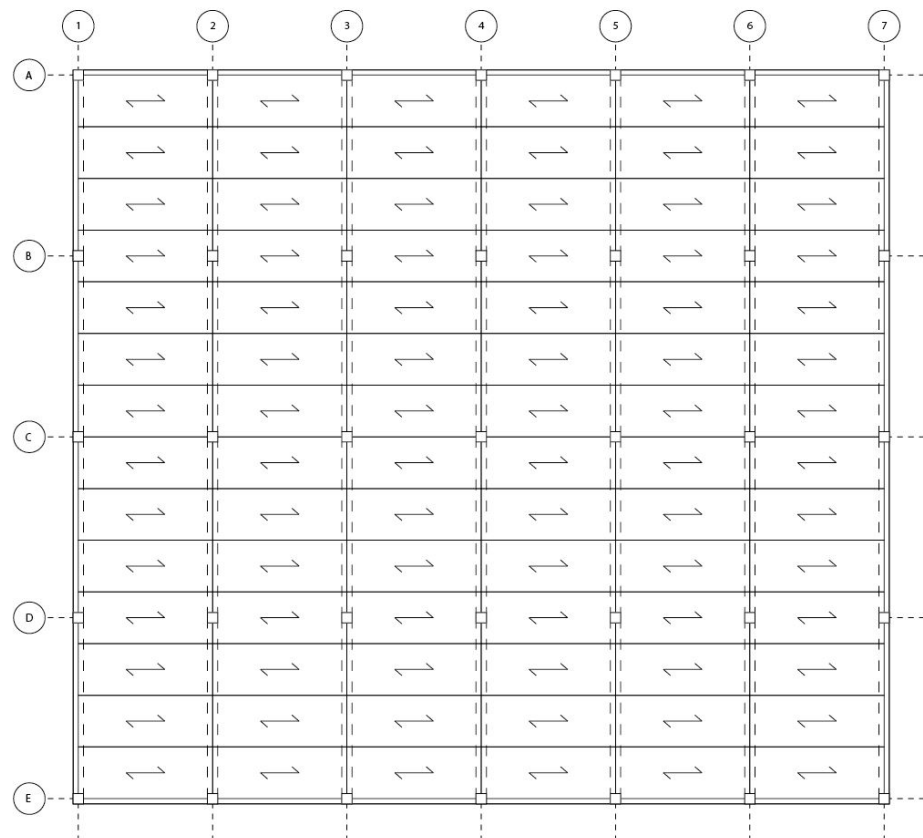


Figure 6.1: Floor plan of the building without any lateral stability system

To ensure sufficient office area compared to the total area of the building, a minimum net floor area of 75% is set. Therefore, the total area of the core must not exceed 25% of the total area of the building. In the core, a gap of 2 metres in width is considered which results in a core consisting of 2 U-forms. The minimum width of core is 7 metres and the minimum depth 5 metres to provide space for elevators and staircases.

To transfer forces between the columns, diagonals, core walls and facade elements, in the following sections specific connection are described, which are not all commonly used at the moment. Therefore, in in chapter 7 some more in-depth information on commonly used connections and the specific connections considered in the parametric study is given .

## 6.2. Characteristics of columns

To join the columns, a connection is uses which transfers tension forces by glued-in rods and compression forces by a steel plate. In subsection 3.8.2 it is described how the strength of such a connection can be calculated. To calculate the strength MATLAB can be used as presented in Appendix A.2. This connection is chosen because it provides high compressive resistance, good tension resistance and is easily and quickly to assemble.

The minimum spacing and edge/end distances, which are displayed in Figure 3.18, are used. The rods are placed at a minimum distance to the edge of the column that is equal to the char layer thickness which corresponds with the fire resistance of the member.

For this connection, a research has been performed to determine the configurations of the connection for different column dimensions such that the tension and compression resistance are maximized. The MATLAB script which is used is given in Appendix A.5. All results of this research are displayed in Appendix A.6.

First the material properties of the connecting members and glued-in threaded rods are inputted. Next, the

minimum edge spacing is determined by taking the lesser value of the minimum edge spacing and the char layer depth during fire. Next, the dowel diameter is varied between 6 and 30 millimetres and the maximum rod length is set to the width of the member. The results for which the slenderness of the rod is not between the given values are removed. All the results are finally plotted in a single graph.

For this result, a column made of GL24h without any fire protective layers is used, which has to withstand a fire of 120 minutes without failure. The column dimensions range from 300 to 1200 millimetres. The tension resistance of the connection is determined by the glued-in rods, while the compression resistance is determined by the compression resistance of the timber. In Figure 6.2, the result is shown for a 700x700mm column.

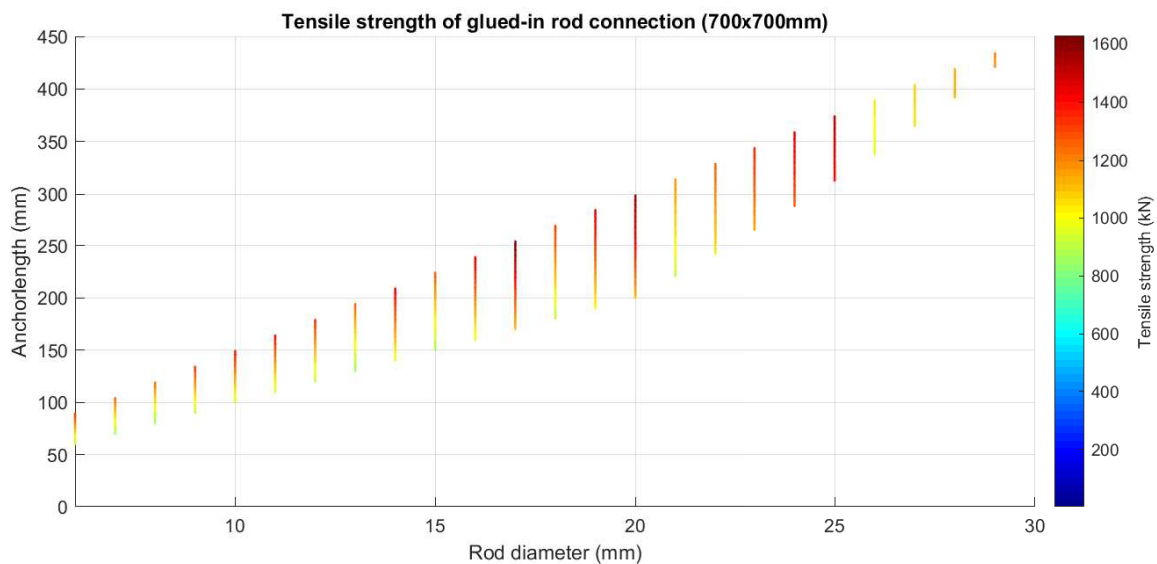


Figure 6.2: Maximum tension force in 700x700mm member with glued-in rod connection

The maximum compression strength is used with the corresponding tension resistance. The characteristics of the connections for different column dimensions which are used are shown in Table 6.2.

Table 6.2: Characteristics of the connections for different columns sizes

Dimensions (mm)	Number of rods	Rod diameter (mm)	Rod length (mm)
300 x 300	4	23	300
400 x 400	9	21	314
500 x 500	16	21	314
600 x 600	16	27	404
700 x 700	49	17	254
800 x 800	49	20	299
900 x 900	144	13	194
1000 x 1000	100	18	269
1100 x 1100	196	14	209
1200 x 1200	144	18	269

The maximum compressive and tensile strengths of each connection setup are displayed in Table 6.3.

Table 6.3: Maximum compression and tension forces of a connection with glued-in rods for different column dimensions

Dimensions (mm x mm)	Max compression (kN)	Max tension (kN)
300 x 300	817	200
400 x 400	2363	422
500 x 500	3692	751
600 x 600	5317	1090
700 x 700	7237	1628
800 x 800	9452	2127
900 x 900	11963	2808
1000 x 1000	14769	3655
1100 x 1100	17871	4435
1200 x 1200	21268	5264

A typical detail of 2 columns which are connected can be seen in Figure 6.3. The columns have dimensions 400x400 millimetres and a connection is used which gives the highest compressive and tensile resistance. The threaded rods can be applied to the timber in advance. A steel plate is attached to these rods, to which a steel connecting part can be attached using bolts.

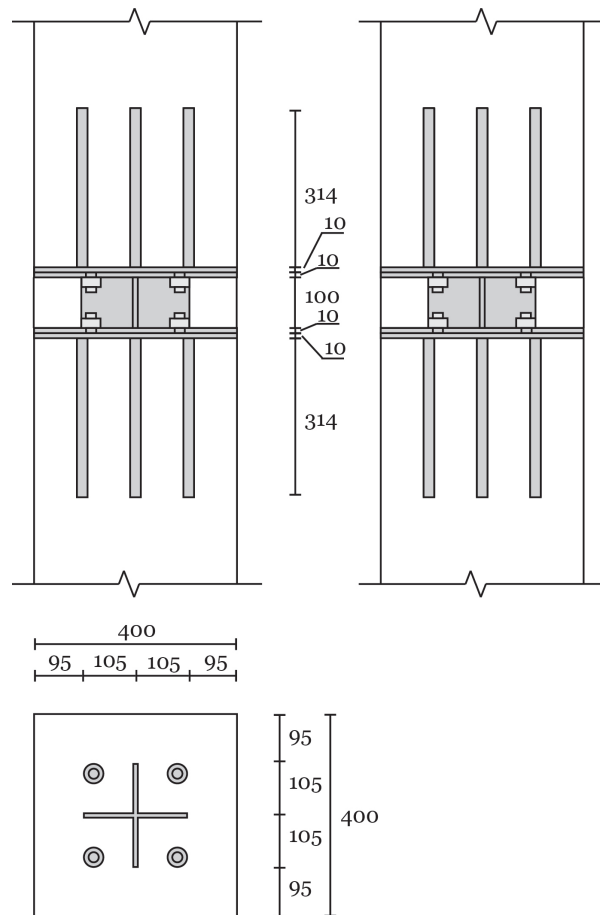


Figure 6.3: Detail of connection between 400x400mm columns using glued-in threaded rods

### 6.3. Characteristics of diagonals

To connect the diagonals, a distinction is made between diagonals connected using slotted-in steel plates and dowels and diagonals connected using glued-in threaded rods. The connection using slotted-in steel plates and dowels is considered, because this connection gives high tensile resistance and good compressive resistance. However, this connection will not be infinitely stiff and thus provide additional deformation in

comparison with the connection using glued-in threaded rods, which is assumed to be rigid. Despite that, the connection using glued-in threaded rods has a lower tensile strength compared to a connection with slotted-in steel plates and dowels. Because these connections have advantages and disadvantages relative to each other, they will both be investigated.

### 6.3.1. Diagonal with connection using slotted-in steel plates and dowels

A connection with slotted-in steel plates and dowels can be used to attach the diagonals. The strength of this connection is determined as explained in subsection 3.8.1. These formulas are put in a MATLAB script to calculate the connection strength in tension and compression. This script is presented in Appendix A.1.

According to the Eurocode, the dowel diameter has to be at least 6 millimetres and at most 30 millimetres. For the 2 steel plates, no minimum and maximum dimensions are given regarding thickness, length and width. The minimum spacing and edge/end distances, which are shown in Table 3.8, are used. The steel plate is placed at a distance to the edge of the member equal to the char layer depth during fire.

A research has been performed to determine the configurations of the connection for different column dimensions such that the tension and compression resistance are maximized. MATLAB is used to calculate these values. First the material properties of the connecting members, dowels and steel plates are inputted. Next, the width of the steel plate is set to the width of the column reduced by the char layer depth during fire. Then the steel plate thickness and the diameter of the dowels are varied. The maximum number of dowel rows and columns is determined by using the minimum spacing between the dowels and the maximum length of the connection. All failure modes are considered and the maximum compressive and tensile strength of the connection is calculated. All results are finally plotted in a single graph.

The result of this research is shown, which represents a column made of GL24h without any fire protective layers, which has to withstand a fire of 120 minutes without failure. The column dimensions range from 300 to 1200 millimetres with an interval of 100 millimetres. This maximum value is chosen to take into account the make-ability of the column. In Figure 6.4, the result is shown for a column with dimensions 700 by 700 millimetres.

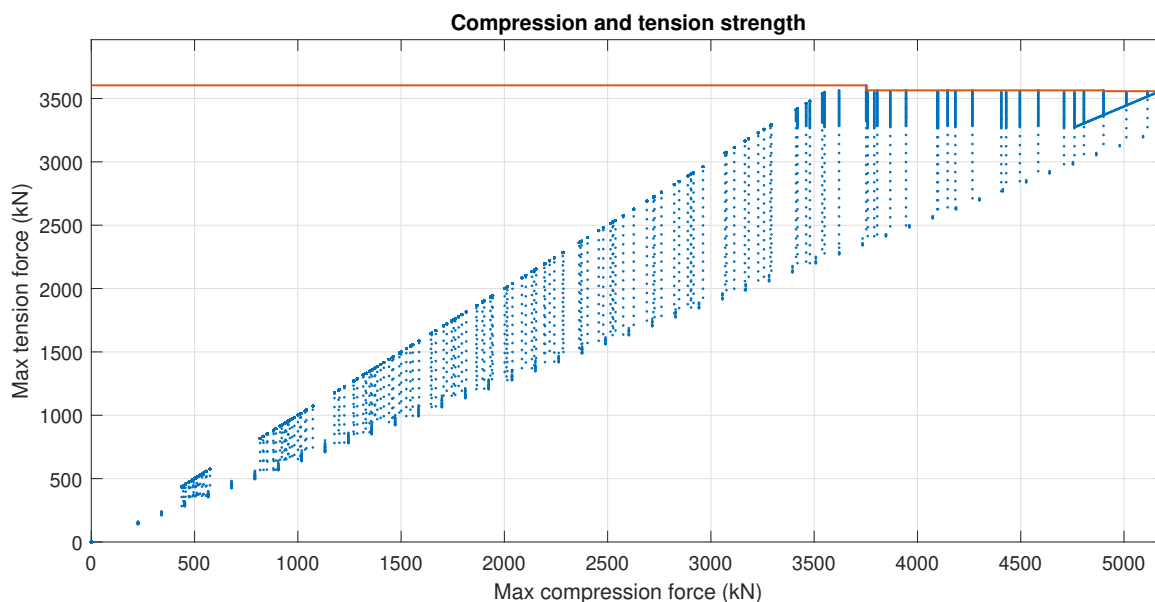


Figure 6.4: Maximum compression and tension force in dowel connection for 700x700mm member

Each dot represents a specific configuration of the connection, which gives a certain compression resistance with a corresponding tension resistance. An orange line is drawn which displays the maximum tension resistance for a certain minimum value of the compression resistance. The results for each individual column size are shown in Appendix A.4.

In Figure 6.5 the maximum resistances for all column sizes are shown.

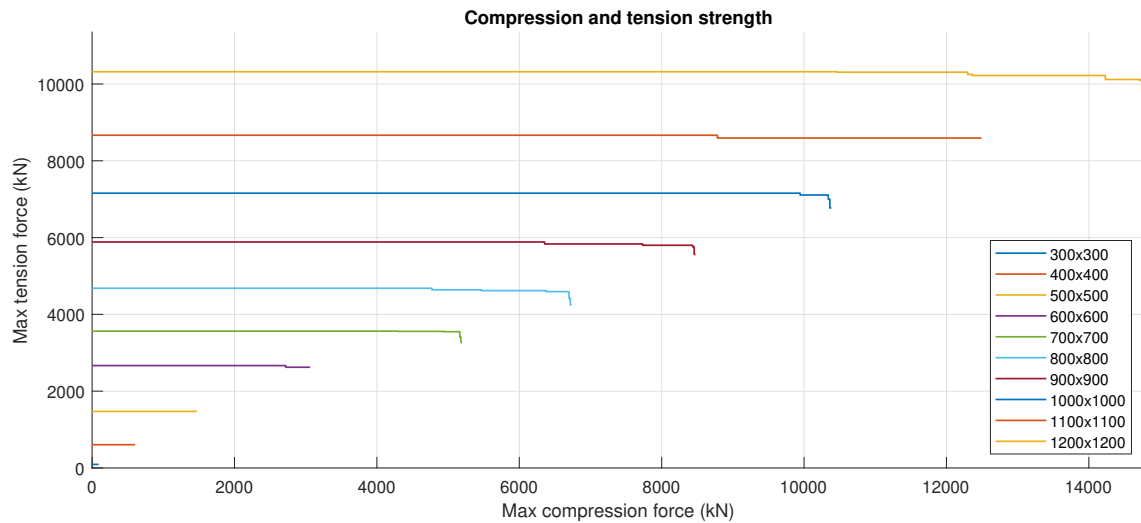


Figure 6.5: Maximum compression and tension force in dowel connection for different column dimensions

As can be seen, the tension resistance becomes slightly less when the compression resistance increases. It is expected that the compression forces which occur in the connection will be higher than the tension forces, due to the fact that the dead weight of the structure will lower the tension forces.

The maximum compression strength is used with the corresponding tension resistance. The characteristics of the connections for the different column dimensions which are used are shown in Table 6.4.

Table 6.4: Characteristics of the connections for the different column dimensions

Dimensions (mm)	Dowel rows	Dowel columns	Total dowels	Dowel diameter (mm)	Connection length (mm)	Steel plate thickness (mm)
300 x 300	5	5	25	6	280	3
400 x 400	11	9	99	6	400	10
500 x 500	16	12	192	6	490	18
600 x 600	22	15	330	6	580	23
700 x 700	23	16	368	7	685	23
800 x 800	21	14	294	9	745	26
900 x 900	18	13	234	12	888	28
1000 x 1000	19	12	228	13	897	30
1100 x 1100	20	12	240	14	966	32
1200 x 1200	18	12	216	17	1173	34

The corresponding maximum compressive and tensile strengths of each connection setup are presented in Table 6.5.

Table 6.5: Maximum compression and tension forces of a dowel connection for different column dimensions

Dimensions (mm x mm)	Max compression (kN)	Max tension (kN)
300 x 300	85	86
400 x 400	595	596
500 x 500	1545	1546
600 x 600	3336	2623
700 x 700	5204	3274
800 x 800	6749	4448
900 x 900	8525	5605
1000 x 1000	10452	6831
1100 x 1100	12545	8141
1200 x 1200	14945	9653

The stiffness of these connections have to be taken into account and therefore the stiffness of the column and the stiffness of the column including the connections are compared. First the stiffness of the connection has to be determined for all connection configurations presented in Figure 6.5. The results are displayed in Figure 6.6.

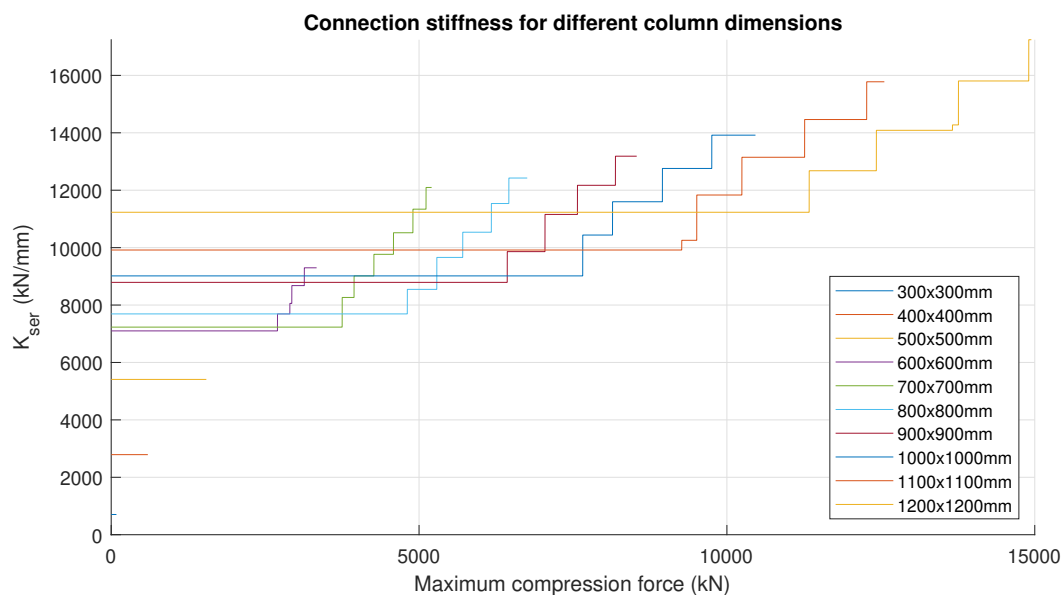


Figure 6.6: Stiffness of different connection configurations

As can be seen, the stiffness of the connections will increase when the size of the column increases. This is expected, because for larger columns, more and bigger dowels are used, which gives the connection more stiffness. Therefore, also the stiffness increases when the resistance of the connection is higher.

The equivalent stiffness is calculated for the different column dimensions with a length of 3600 millimetres. After that, the ratios between the stiffness of the column with connections and without are determined. The stiffness of the column has to be multiplied by the average value of these ratios in the parametric model.

The results are displayed in Table 6.6.

Table 6.6: Ratios between columns and columns with connections

Column size (mm)	$K_{ser}$ (kN/mm)	EA/l (kN/mm)	$K_{eq}$ (kN/mm)	Ratio (-)
300	704	288	158	0.55
400	2789	511	386	0.73
500	5409	799	617	0.77
600	9297	1150	922	0.80
700	12096	1565	1243	0.79
800	12425	2044	1538	0.75
900	13185	2588	1858	0.72
1000	13918	3194	2189	0.69
1100	15777	3865	2594	0.67
1200	17242	4600	3000	0.65
Mean value				0.71

Hence, when columns made of GL24h with a length 3600 millimetres are used, it is sufficient to reduce the stiffness of the column by a factor 0.70 to take into account the stiffness of the connections. The influence of the connection stiffness will decrease if the length of the column increases. When the column length is doubled, the reduction factor will be equal to 0.8 and will further increase to 0.9 for a column length of 14.4 metres. A conservative approach is used and therefore a reduction factor of 0.7 is used for all lengths.

A typical detail of a connection between different diagonals is shown in Figure 6.7. The diagonal used in the detail has dimensions 400x400 millimetres and configuration of the dowels is such that the highest compressive resistance is reached. The steel plates and dowels can be applied to the timber in advance. A steel plate is attached to these rods, to which a steel connecting part can be attached using bolts to connect all the members. The steel plate has several stiffeners to prevent local buckling. The steel plate and stiffeners are covered by timber plates on both sides, these protect the steel during a fire event.

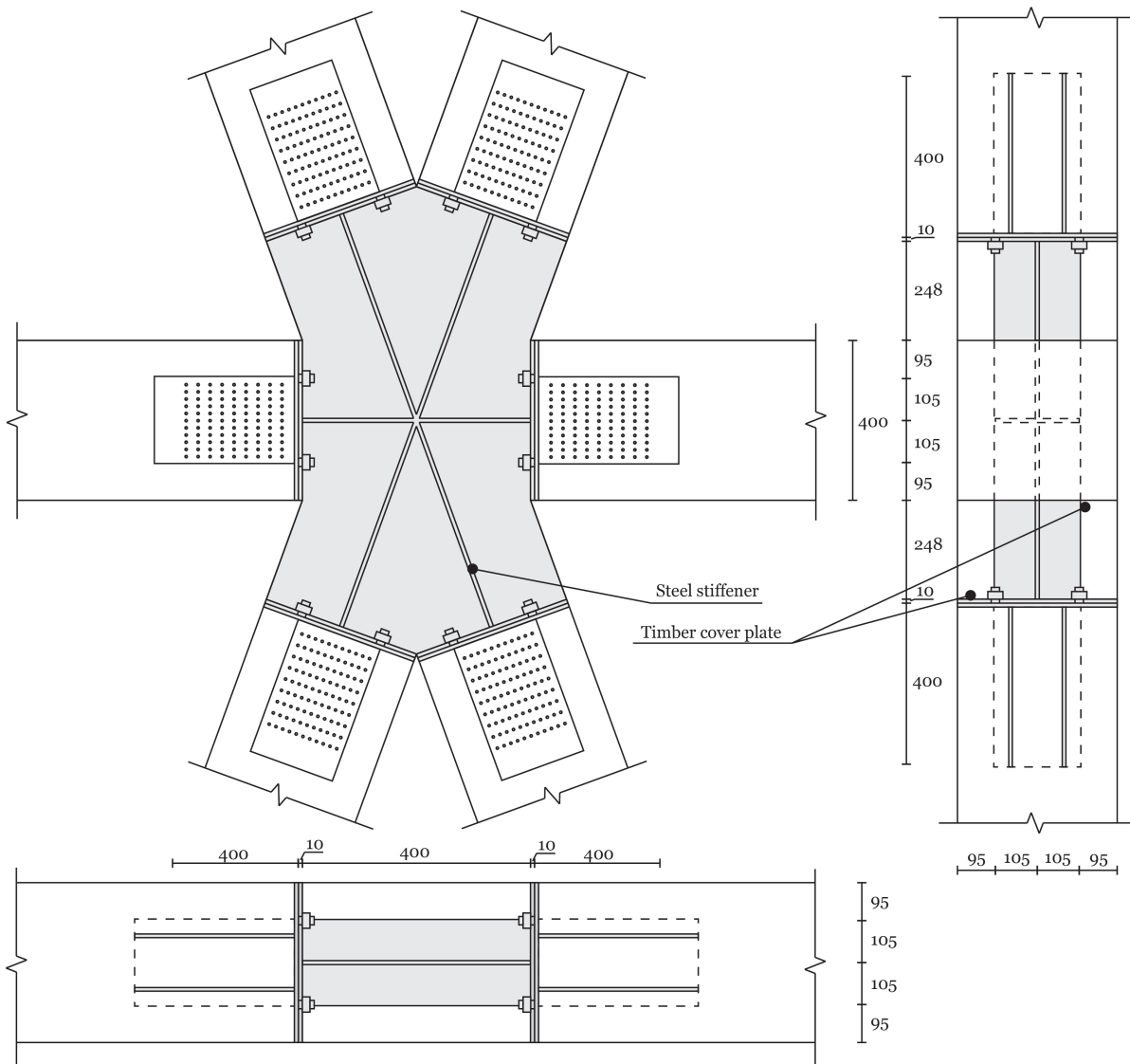


Figure 6.7: Detail of connection between diagonals using slotted-in steel plates and dowels

**6.3.2. Diagonal with connection using glued-in threaded rods**

Diagonals can also be connected using glued-in threaded rods. The strength of this connection is already determined in section 6.2.

A typical detail for this connection is displayed in Figure 6.8, where the diagonals have dimensions 400x400 millimetres. The threaded rods can be applied to the timber in advance. A steel plate is attached to these rods, to which a steel connecting part can be attached using bolts to connect all the members. The steel plate has several stiffeners to prevent local buckling. The steel plate and stiffeners are covered by timber plates on both sides, these protect the steel during a fire event.

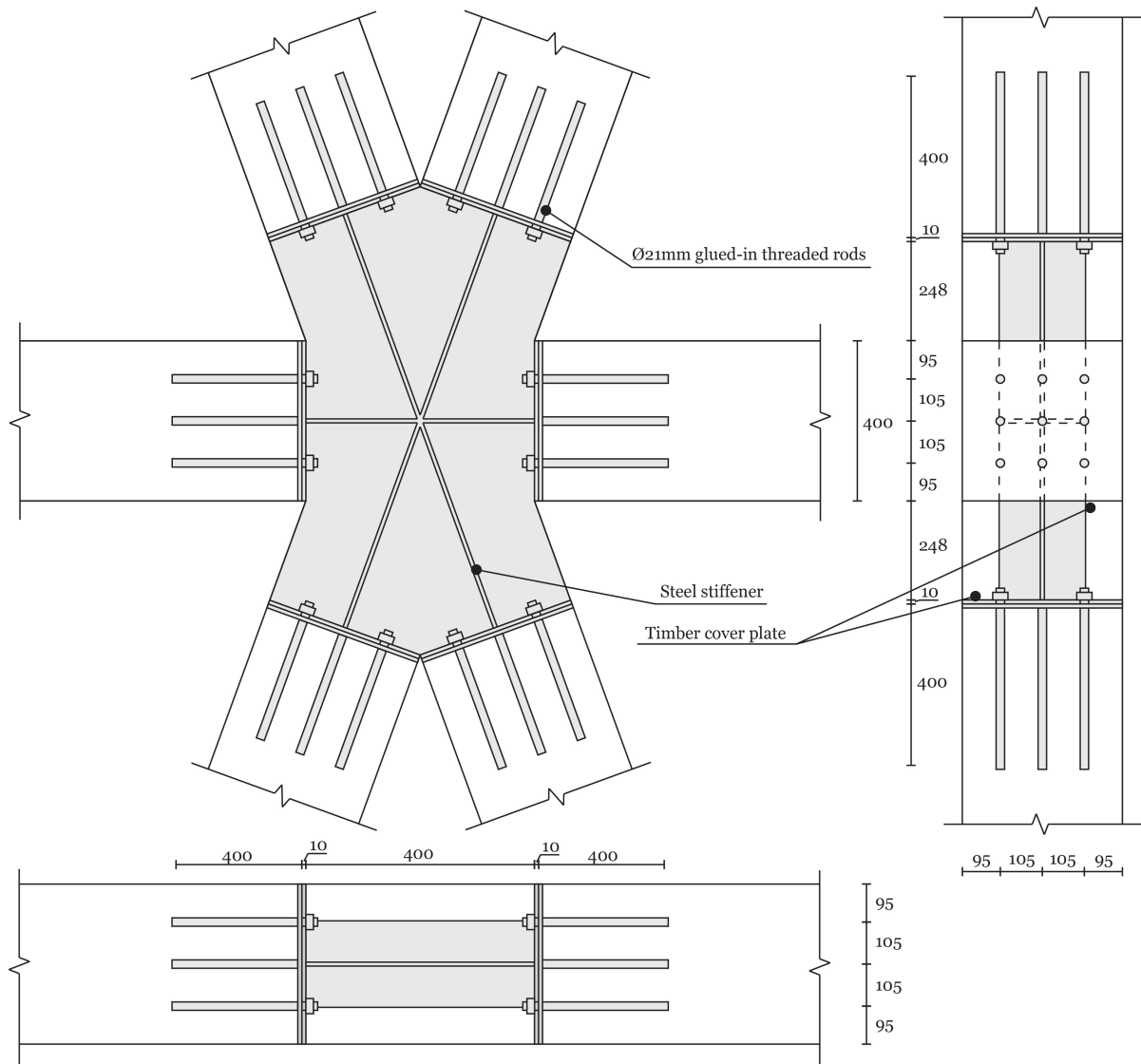


Figure 6.8: Detail of connection between diagonals using glued-in threaded rods

### 6.3.3. Buckling

The load-bearing capacity of a structural member can decrease due to the fact that buckling occurs before the maximum compressive stress is reached. This decrease is checked for a squared column with a buckling length of 3600 millimetres and a width of 300 millimetres to 1200 millimetres. The result is displayed in Figure 6.9.

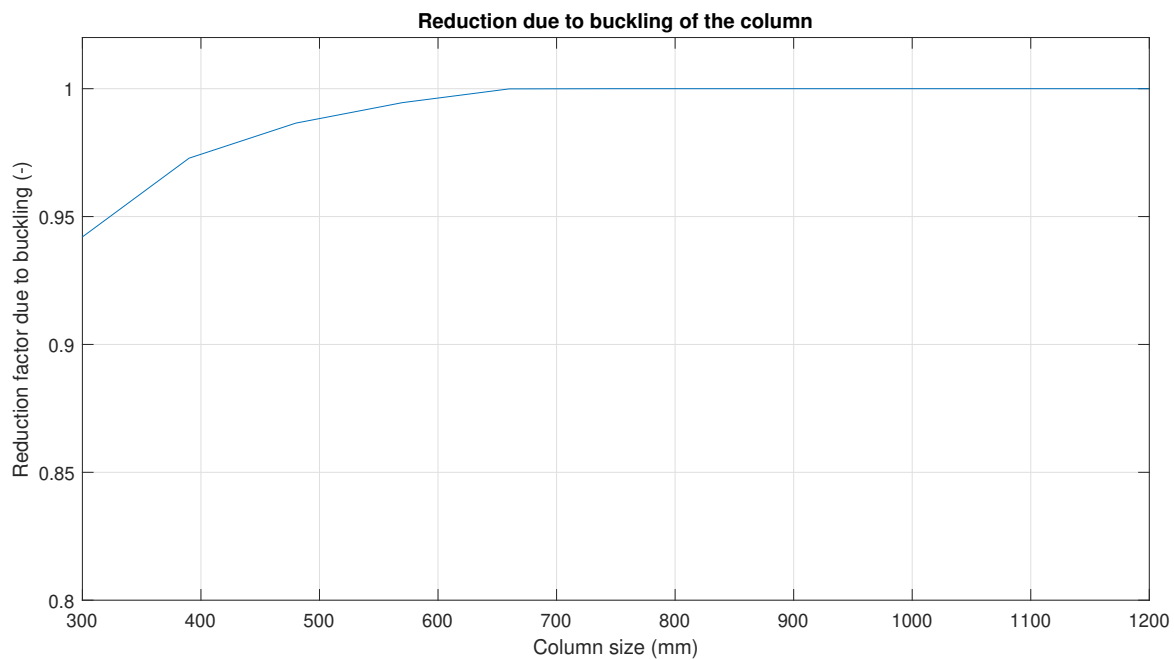


Figure 6.9: Decrease of compression resistance due to buckling

There will be a small decrease of compressive resistance due to buckling. However, this decrease is negligibly small. Furthermore, the connections of these members will have a smaller resistance than the members themselves due to the fact that the safety factors used for calculating the resistance of connections are greater than the safety factors used for determining the resistance of members. Buckling of members is therefore negligible and will not be further taken into account.

## 6.4. Properties of floors

Floors are placed on each storey between the columns and the facade. It is considered that these floors are supported on 2 edges by making use of timber beams. These beams are placed between the columns and the facade elements. The floor slabs are made of CLT plates. In longitudinal direction these plates are tied using metal connectors.

The typical floor plan of each storey of the building is shown in Figure 6.10.

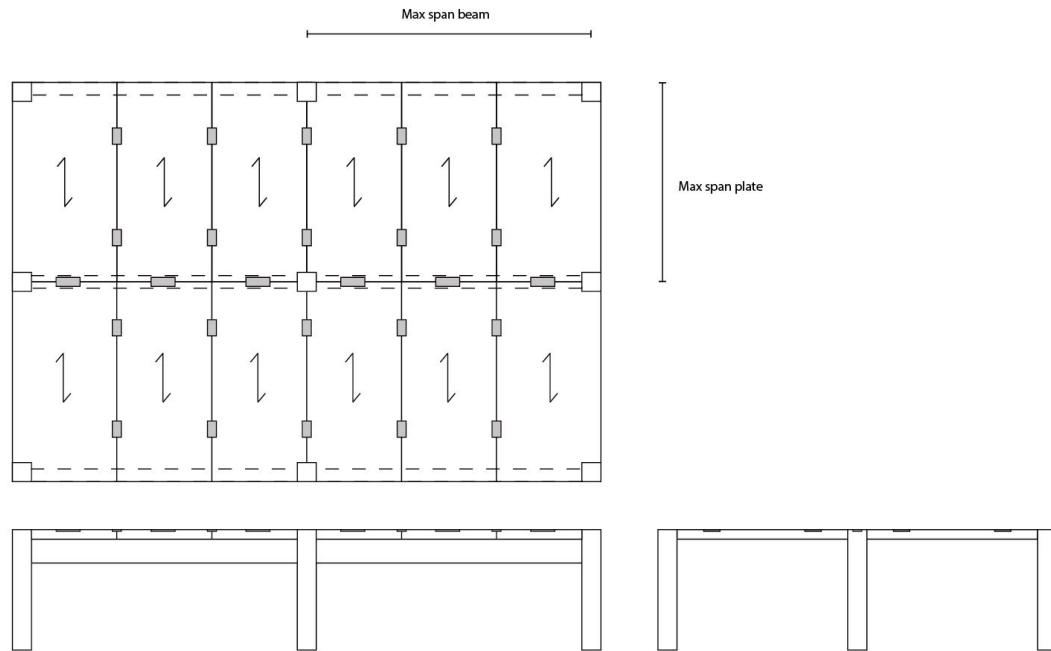


Figure 6.10: Floor plan for each storey of the building

The maximum span of a timber slab is based on data provided by a CLT plate manufacturer [41]. For example, when an office building is considered using a simply supported CLT floor slab consisting of 5 layers, a total thickness of 225mm and a super imposed dead load  $1 \text{ kN/m}^2$ , a maximum floor span of 5.7 metres is achievable.

The maximum span of the beams is determined by assuming a maximum height of the beam of 700 millimetres. This height is chosen to guarantee enough operating height at each storey. It is considered that the beam is simply supported on each column with a minimum support length of 150 mm. The width of the beam will have a maximum value of 400 millimetres to provide sufficient support area for the floor slabs.

Calculations have been done to determine the maximum span of the beam, which can be seen in Appendix B.1. The maximum span of the beam is set at 8 metres.

#### 6.4.1. Floor stiffness

The in-plane stiffness of the slab is considered to be the stiffness of the surface. This stiffness is determined by performing a calculation, where an equivalent stiffness is calculated. The Young's modulus of each layer in its orientation is multiplied by its thickness and then divided by the total thickness of the slab. The results for the cross section in both directions of the plate are shown in Table 6.7.

Table 6.7: Equivalent in-plane stiffness of a CLT plate

Layer (mm)			$E_1, E_3$	$E_2$	h	$E_{eq,1}$	$E_{eq,2}$				
1	2	3	( $N/mm^2$ )	( $N/mm^2$ )	(mm)	( $N/mm^2$ )	( $N/mm^2$ )				
20	20	20	11000	370	60	7457	3913				
20	35	20	11000	370	75	6039	5331				
20	45	20	11000	370	85	5372	5998				
35	35	35	11000	370	105	7457	3913				
35	45	35	11000	370	115	6840	4530				
45	35	45	11000	370	125	8024	3346				
45	45	45	11000	370	135	7457	3913				
Layer (mm)					$E_1, E_3, E_5$	$E_2, E_4$					
1	2	3	4	5							
20	20	20	20	20	11000	370	100	6748	4622		
35	20	20	20	35	11000	370	130	7729	3641		
35	20	35	20	35	11000	370	145	8068	3302		
45	20	20	20	45	11000	370	150	8165	3205		
45	20	35	20	45	11000	370	165	8423	2947		
45	20	45	20	45	11000	370	175	8570	2800		
45	35	35	35	45	11000	370	195	7184	4186		
45	35	45	35	45	11000	370	205	7370	4000		
45	45	45	45	45	11000	370	225	6748	4622		
Layer (mm)							$E_1, E_3, E_5, E_7$	$E_2, E_4, E_6$			
1	2	3	4	5	6	7					
35	35	35	35	35	35	35	11000	370	245	6444	4926
45	35	35	35	35	35	45	11000	370	265	6788	4582
45	35	35	45	35	35	45	11000	370	275	6555	4815
45	35	45	45	45	35	45	11000	370	295	6856	4514
45	45	45	45	45	45	45	11000	370	315	6444	4926
									Average	7178	4192

The highest equivalent Young's modulus can be used when compression and tensile stresses occur in the direction of the odd numbered layers, while the lowest equivalent Young's modulus must be used when these stresses occur in the direction of the even numbered layers.

#### 6.4.2. Floor deflection

The maximum deflection of the CLT plate is governed by the data provided by a CLT manufacturer [41]. For different thicknesses of a CLT plate, the maximum allowed span is given. Therefore, the following thicknesses are used for different span lengths, as shown in Table 6.8. These thicknesses are based on a live load of  $3kN/m^2$  and an additional dead load on the floor of  $1kN/m^2$ .

Table 6.8: Maximum spans for different plate thicknesses

Panel	Layer (mm)							h (mm)	$E_{eq,1}$ ( $N/mm^2$ )	$E_{eq,2}$ ( $N/mm^2$ )	Span	
	1	2	3	4	5	6	7				min (m)	max (m)
CL3/135	45	45	45					135	7457	3913	0	3.9
CL5/225	45	45	45	45	45			225	6748	4622	3.9	5.7
CL7/315	45	45	45	45	45	45	45	315	6444	4926	5.7	6.9

### 6.5. Characteristics of stability core

A distinction is made between a stability core made of concrete and a core made of CLT.

### 6.5.1. Concrete core

A minimum thickness of the concrete core elements of 250 millimetres and a maximum thickness of 500 millimetres is assumed. The maximum value is picked to limit the usage of concrete, so that the majority of the construction material remains timber. The core is poured in-situ and made of C40/50.

It is assumed that the concrete is cracked. Therefore, a reduction in stiffness is applied. The Eurocode states that for cracked concrete the Poisson's ratio of the material changes from 0.2 to 0.0. No further detailed calculation has been done to determine the stiffness of the cracked concrete core(s), however the Eurocode describes a simplified formula to determine the stiffness:

$$EI \approx 0.4E_{cd}I_c \quad (6.1)$$

where  $E_{cd}$  is the design value for the Young's modulus of the concrete and  $I_c$  is the moment of inertia of the core. To include this decrease in stiffness, a reduction of 60% on the Young's modulus of the core material is applied in the model. The Young's modulus of uncracked C40/50 is given by RFEM and equals  $35000\text{N}/\text{mm}^2$ .

Next, the resistance to compression, tension and shear forces of the core have to be determined. The resistance to tension and shear is determined by the reinforcement. A maximum of 2% of the core area is used for lateral reinforcement and FeB500 is chosen. The shear stress must be less than the maximum shear stress which may occur when shear reinforcement is used, defined in [35]:

$$\tau_2 = 0.24 \cdot (1 - f_{ck}/250) \cdot f_{cd} = 5.4\text{N}/\text{mm}^2 \quad (6.2)$$

For concrete C40/50,  $f_{ck}$  will be equal to  $40\text{N}/\text{mm}^2$  and  $f_{cd}$  will be equal to  $40/1.5 = 26.67\text{N}/\text{mm}^2$ .

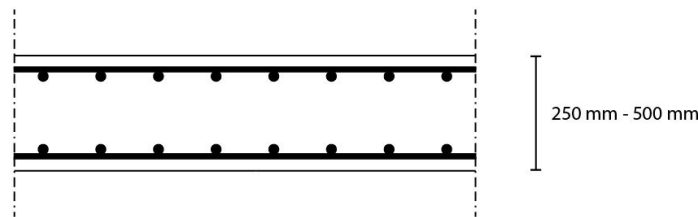


Figure 6.11: Reinforcement of concrete core elements

Hence, the maximum allowed stresses are summarised in Table 6.9:

Table 6.9: Strength properties of concrete core

Compression strength	$f_{c,max}$	26.67	$\text{N}/\text{mm}^2$
Tensile strength	$f_{t,max}$	8.7	$\text{N}/\text{mm}^2$
Shear strength	$f_{v,max}$	5.4	$\text{N}/\text{mm}^2$

### 6.5.2. CLT core

The CLT core walls are connected in the corners using counter sunk head self-tapping fully threaded wood screws. These screws have a diameter of 10 millimetres and a length of 800 millimetres. These properties are chosen, because these are available on the market [9]. Two screws will be placed next to each other to improve the stiffness and strength of the connection compared to a connection with a single screw. The diameter of the screw does not influence the stiffness of the connection if the minimum spacing of the screws is used. Therefore, the connections are uniformly distributed over the whole height of the core walls and the minimum spacing distance of  $5d = 50\text{mm}$  is used.

A fixed thickness of 495 millimetres is used for the elements, which is equal to 11 timber layers with a thickness of 45 millimetres each. It is assumed that each side of the core can be constructed using a single plate. For example, a core consisting of 2 U-shapes will contain 6 CLT plates per level.

The CLT core walls are stacked vertically and connected using a toothed connection combined with glued-in threaded rods. The teeth will transfer shear forces, while the rods will provide tensile resistance. By using this specific connection, it can be assumed that this connection is fully rigid and will therefore not cause additional stiffness reduction of the core walls.

In Figure 6.12 the position of the walls, screws and glued-in threaded rods are shown.

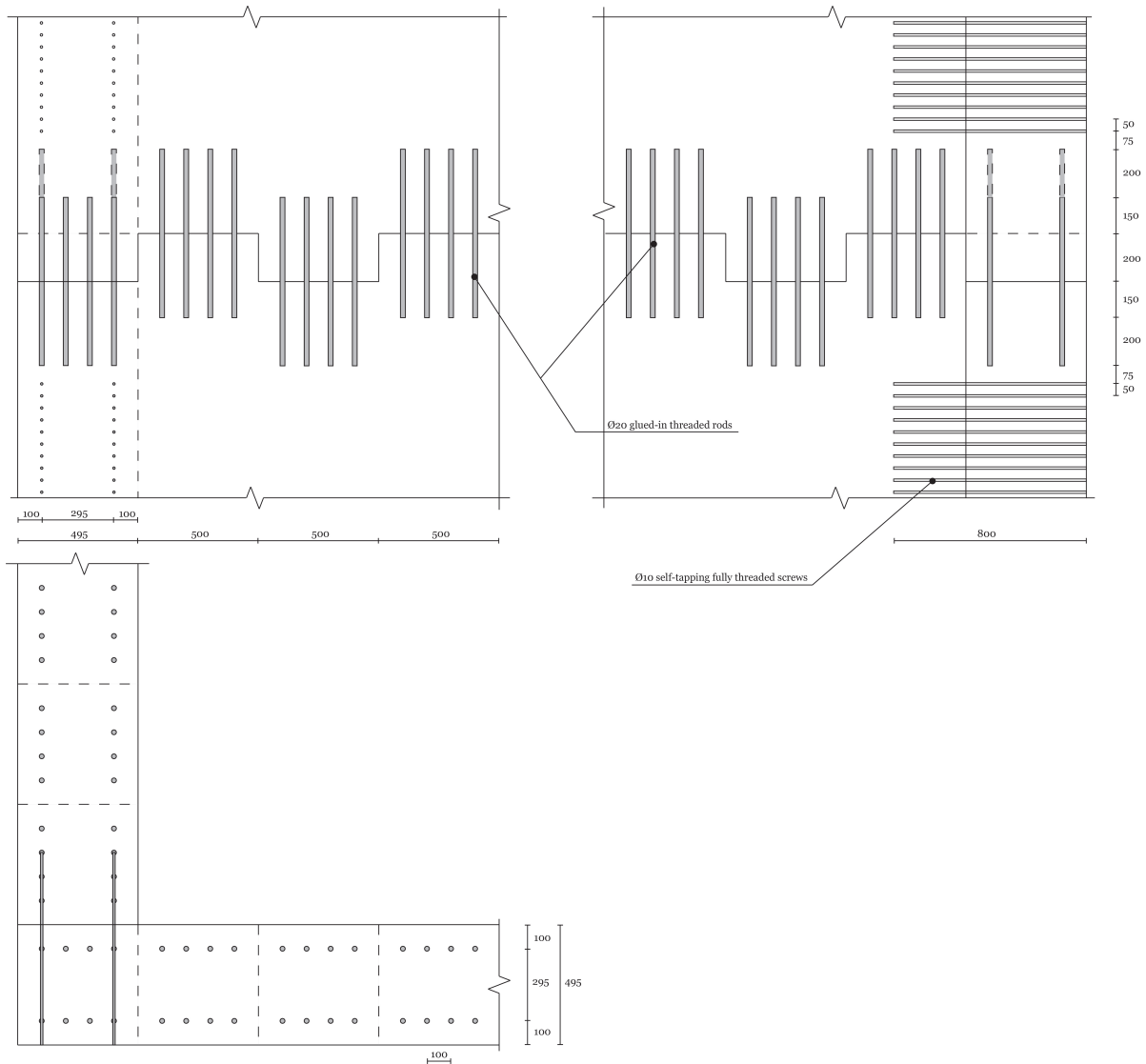


Figure 6.12: Connections of core walls in CLT

The in-plane stiffness of the elements is assumed, as described in subsection 6.4.1. For a 11-layers 495mm thick CLT plate with 6 layers in the vertical direction and 5 layers in the horizontal direction, the equivalent Young's modulus is equal to:

$$E_{eq,1} = (6 \cdot 45 \cdot 11000 + 5 \cdot 45 \cdot 370) / 495 = 6168 N/mm^2 \tag{6.3}$$

The corner connections are not fully rigid and as a result will cause a reduction in bending stiffness of the core walls. Applying a hinge along the corners with stiffness properties equal to the properties of the applied connections in the model would be ideal, however the Arcadis add-on does not have this functionality (yet). Consequently, to account for this effect a reduction to the Young's modulus is determined by applying the theory of mechanically jointed beams provided by the Eurocode. The dimensions and symbols used by this

theory are depicted in Figure 6.13. The effective bending stiffness is determined for bending around both x- and y-axis. The horizontal toothed connection is assumed to be fully rigid.

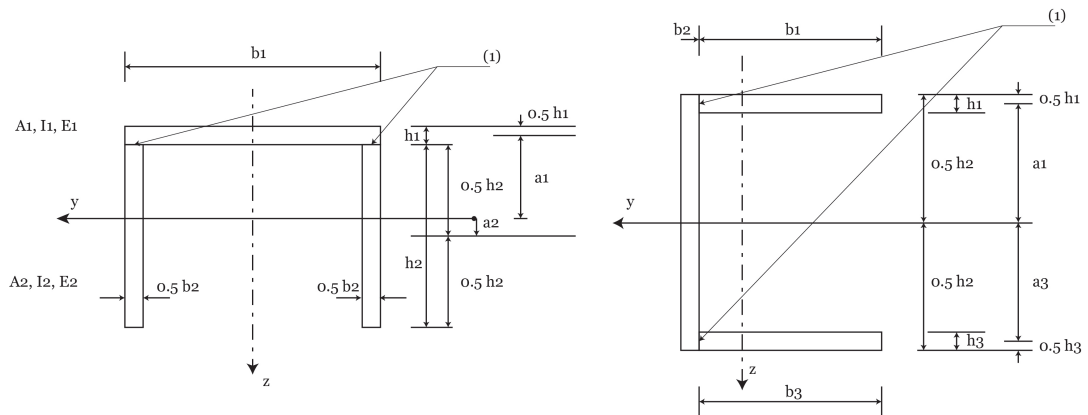


Figure 6.13: Dimensions and symbols of mechanically jointed beams theory

The effective bending stiffness can be calculated using the following formula:

$$(EI)_{ef} = \sum_{i=1}^3 (E_i I_i + \gamma_i E_i A_i a_i^2) \quad (6.4)$$

where:

- $A_i = b_i h_i$
- $I_i = \frac{b_i h_i^3}{12}$
- $\gamma_2 = 1$
- $\gamma_i = [1 + \pi^2 E_i A_i s_i / (K_i l^2)]^{-1}$

The distance  $a_2$  should be taken as:

$$a_2 = \frac{\gamma_1 E_1 A_1 (h_1 + h_2) - \gamma_3 E_3 A_3 (h_2 + h_3)}{2 \sum_{i=1}^3 \gamma_i E_i A_i} \quad (6.5)$$

The stiffness of the connection can be determined using the information given in Figure 6.12. Two screws are used next to each other, which both have a single shear plane and a spacing of  $5 \cdot d = 50$  millimetres. Therefore, the connection stiffness is equal to:

$$K_{ser} = \frac{2 \cdot d \cdot \rho_m^{1.5} / 23}{5 \cdot d} = 186 N/mm^2 \quad (6.6)$$

where the mean density of CLT is equal to  $485 kg/m^3$  [57].

The effective bending stiffness depends on both the dimensions of the core and the length of the beam, which is in this case the height of the building. Because the core of the building can be considered as a cantilever, this length may be multiplied by 2. Therefore, the effective bending stiffness is calculated for different building heights and core dimensions.

Figure 6.14a and Figure 6.14b show 2 variants which are used for the core dimensions. These are such that the moment of inertia around both axes are equal.

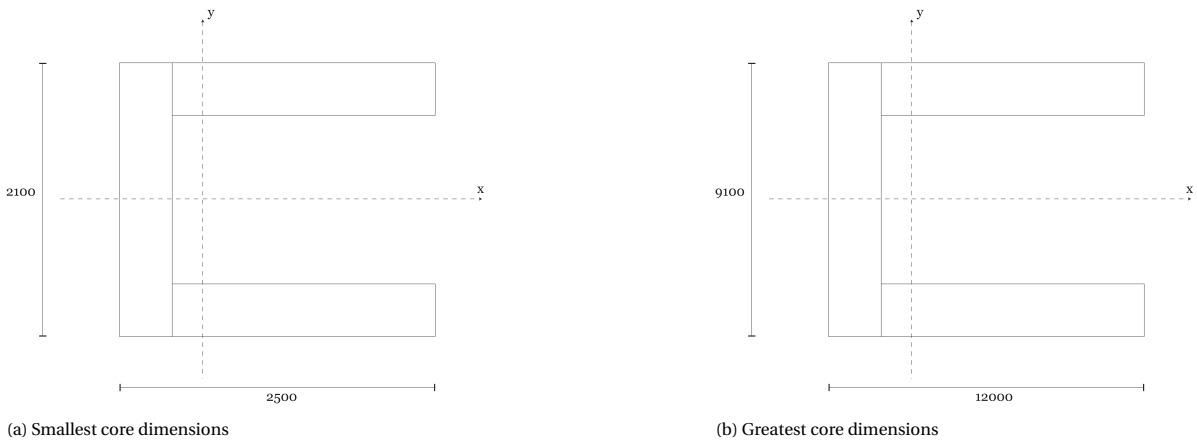


Figure 6.14: Core dimensions for determining effective bending stiffness

The results for the effective bending stiffness, which are expressed as the normalised stiffness, are plotted in Figure 6.15. The normalised stiffness is the ratio between the effective bending stiffness and the bending stiffness of a core with the same dimensions, but with rigid connections instead.

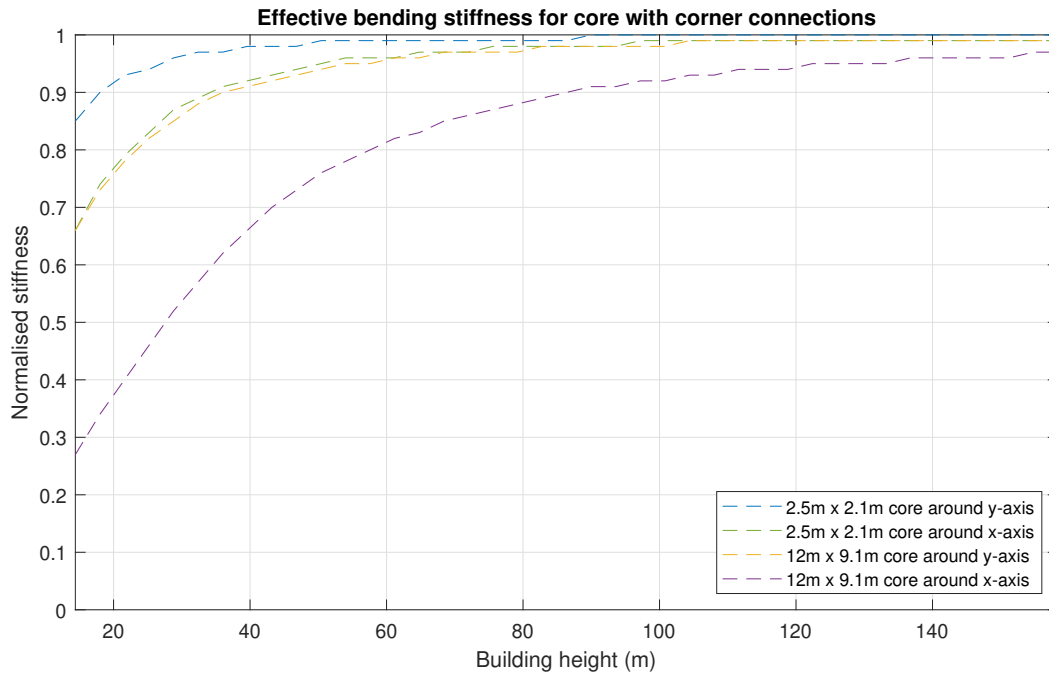


Figure 6.15: Effective bending stiffness for core with corner connections in x- and y-directions

As can be seen, the effective bending stiffness around the x-axis is lower compared to the y-axis, but will increase when the height of the building increases. It is more likely that a smaller core is used for low buildings and a core with greater dimensions is used for higher buildings. It is therefore assumed that the average values of the results give sufficient results in all cases.

The average values are plotted in Figure 6.16.

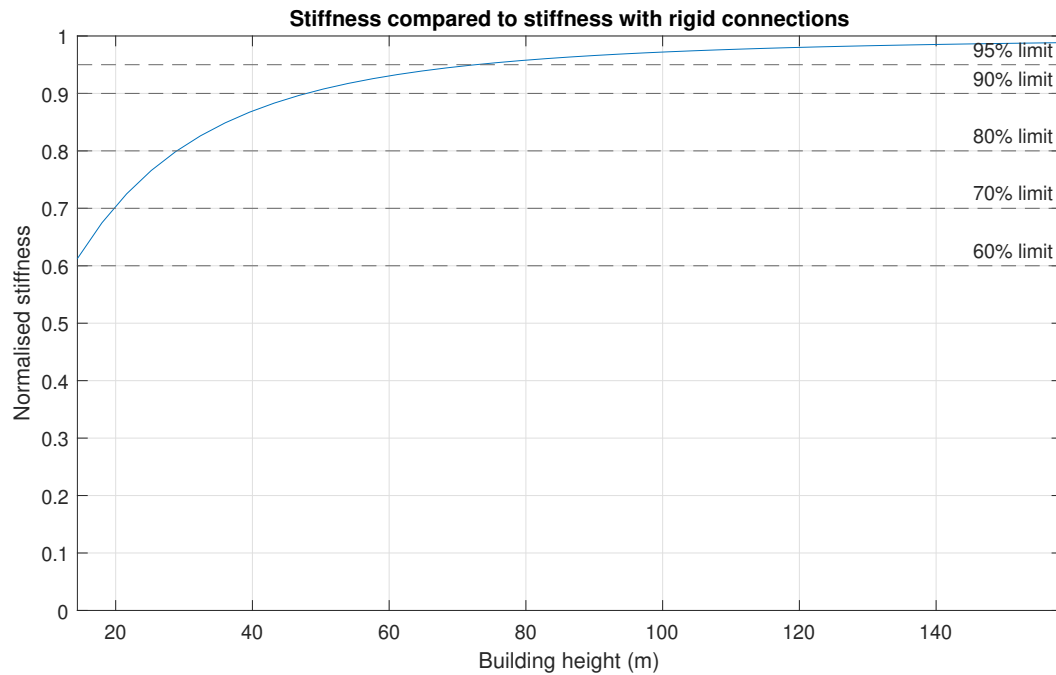


Figure 6.16: Effective bending stiffness for core with corner connections

Dynamo can only apply material properties which have been added in advance to the RFEM material database. Therefore, several reduced values for the stiffness properties of the material are added to the database, namely for 60% of the bending stiffness with rigid connections up to 95%. The parametric model will check the building height and apply the correct stiffness to the core elements. These effective bending stiffness are shown in Table 6.10.

Table 6.10: Normalised stiffness for different building heights

Building height interval (m)	Normalised stiffness (-)
$h \leq 20$	0.60
$20 < h \leq 29$	0.70
$29 < h \leq 47$	0.80
$47 < h \leq 76$	0.90
$h > 76$	0.95

The strength properties of the core elements can be divided in compression, tension and shear resistance, which are defined by the different components of the connections. The compression resistance is determined by the compression strength of the CLT material, while the tension resistance is solved by using the tension strength of the glued-in threaded rods. The shear resistance is based on the shear strength of the toothed connection and also the shear strength of the corner connection is examined.

#### Compression resistance of CLT

To determine the compression resistance of the CLT, it is assumed that only the timber layers whose fibres are in the direction of the compression force provide compression resistance. The compression force will act in vertical direction, thus when a CLT element with 11 layers is used, 6 layers will provide compression resistance. The compression resistance is therefore:

$$f_{c,Rd} = \frac{0.8 \cdot 6 \cdot 45 \cdot 24}{495 \cdot 1.3} = 8.06 \text{ N/mm}^2 \quad (6.7)$$

### Tension resistance of glued-in threaded rod

To determine the tensile resistance of the connections, first the tensile resistance of a single rod is calculated. This is done by using the formulas provided in subsection 3.8.2 and by considering the spacing between the rods of 100 millimetres. This is shown in Appendix B.4. So:

$$f_{t,Rd} = 1.91 N/mm^2 \quad (6.8)$$

### Shear resistance of toothed connection

The core plates are coupled at the bottom and top by cut teeth, so that shear forces can be transferred to the next plate. In order to use the maximum shear resistance of the CLT plate, the height of the tooth must be sufficiently large. In Figure 6.17 this concept is shown. The compression resistance which occurs at the side of the tooth (displayed as a red line) must be greater than the shear resistance of the CLT, located at the green dashed line.

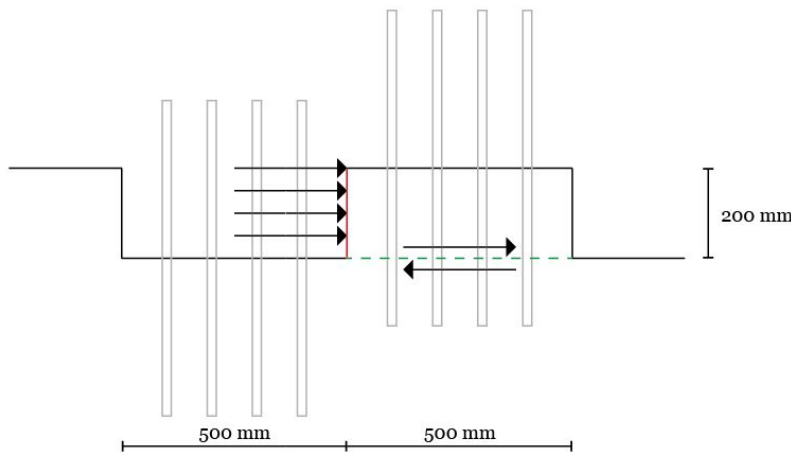


Figure 6.17: Resistance to compression and shear for toothed connection

The shear resistance is equal to:

$$F_{v,Rd} = k_{mod} \cdot f_{v,k} / \gamma_M \cdot A = 0.8 \cdot 3.5 / 1.3 \cdot 495 \cdot 500 = 533 kN \quad (6.9)$$

The compression resistance is determined by the layers whose fibres are placed horizontally, which is a total of 5 layers. The compression resistance is thus:

$$F_{c,Rd} = k_{mod} \cdot A \cdot f_{c,0,k} / \gamma_M = 0.8 \cdot 5 \cdot 45 \cdot 24 \cdot / 1.3 \cdot h = 3.32h \quad (6.10)$$

Hence, for  $F_{v,Rd} = F_{c,90,Rd}$ , the minimum height of the 161 millimetres, so a height of 200 millimetres is used.

In Figure 6.17 it can be seen that the green line represents half of the total length of the connection, thus the maximum shear stress must be divided by 2. Therefore:

$$f_{v,Rd} = k_{mod} \cdot f_{v,k} / \gamma_M / 2 = 0.8 \cdot 3.5 / 1.3 / 2 = 1.12 N/mm^2 \quad (6.11)$$

### Shear resistance of corner connection

The shear resistance of the corner connection is determined by the shear strength of the screws. This is shown in Appendix B.3, where first the axial resistance of a screw is calculated, after which the shear resistance of a screw can be determined. By using the number of screws next to each other and the spacing between the screws, the shear resistance of the connection can be calculated.

$$f_{v,Rd} = 0.86 N/mm^2 \quad (6.12)$$

To summarize, the different strength properties of the core elements are as follows:

Table 6.11: Strength properties of CLT core elements

Compression strength	8.06	$N/mm^2$
Tensile strength	1.91	$N/mm^2$
Shear strength	1.12	$N/mm^2$
Shear strength corner	0.86	$N/mm^2$

To check if the wall can reach its full compressive resistance, buckling of the wall is checked.

- $I_{eff} = 6424313 mm^3$
- $A = 495 mm$
- $i = \sqrt{I_{eff}/A} = 113.92$
- $\lambda_y = l_{eff}/i = 31.60$
- $f_{c,0,k} = 24 N/mm^2$
- $E_{0,05} = 6700 N/mm^2$
- $\lambda_{rel} = 0.60$
- $k_y = 0.69$
- $k_{c,y} = 0.96$

There will be a small decrease of compressive resistance due to buckling. However, the connections between the wall elements have a smaller resistance than the walls themselves due to the fact that the safety factors used for calculating the resistance of connections are greater than the safety factors used for determining the resistance of the walls. Buckling of the walls is therefore negligible and will not be further taken into account.

## 6.6. Characteristics of facade elements

Facade elements can be placed in the facade. These elements consists of a CLT plate where an opening has been made in the centre, so that a window can be placed. The top and bottom of the elements are connected in the same way as the core elements are connected, as shown in Figure 6.12. At the corners of the building, the facade elements are also connected in the same way as the core elements.

Because the width and depth of the building are greater than the maximum size of a single CLT plate, the facade will consist of multiple facade elements. Therefore, these elements need to be connected at their sides. These connections are displayed in Figure 6.18.

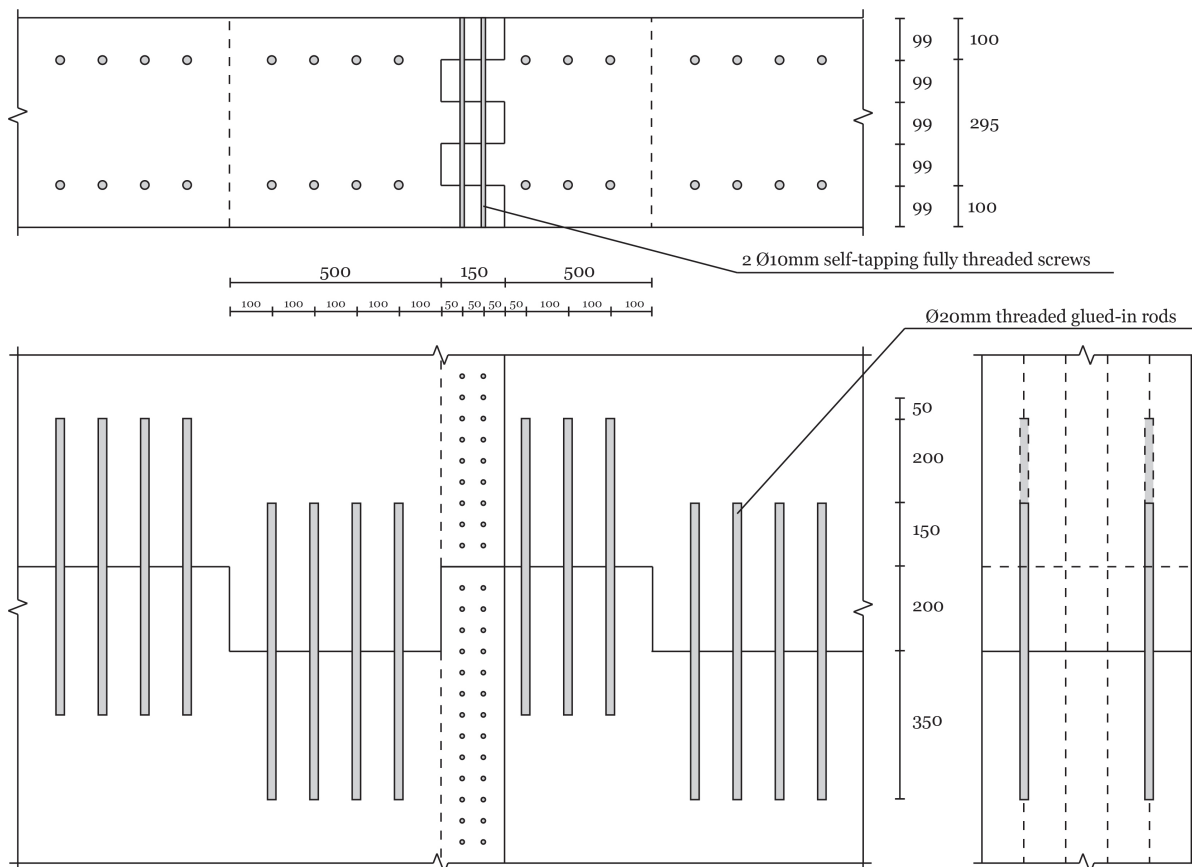


Figure 6.18: Detail of connection between sides of facade elements

The corner connections and the connections between the sides of the elements are not fully rigid and as a result will cause a reduction in bending stiffness of the facade elements. Also, it is assumed that an opening will be present in the plate, which causes bending stiffness reduction. The elements will be modelled as a single surface. Therefore, it must be investigated what the stiffness of the element with connections and an opening is compared to a fully closed surface with rigid connections.

First the influence of an opening in the CLT plate is investigated. This is done by making use of a simple parametric model for which the width and height of the element and the ratios width of the opening to width of the element and height of the opening to height of the element can be inputted. The models will consist of 3 elements placed next to each other. They are shown in Figure 6.19. The Dynamo script used for this research is shown in Appendix C.3.

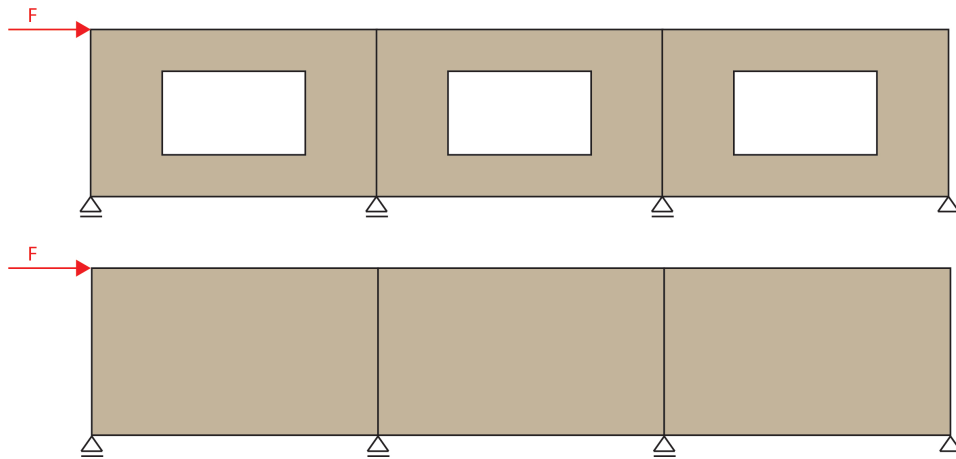


Figure 6.19: Parametric model for investigating influence of opening in facade

A horizontal load is applied to the top left corner of the facade elements. A parametric study is performed where for different width and opening ratios the horizontal deflections are calculated for both elements. These horizontal deflections are then compared to determine the decrease of stiffness due to the presence of these openings.

In Figure 6.20 these results are presented, where the stiffness reduction factors are shown for different height ratios and width ratios.

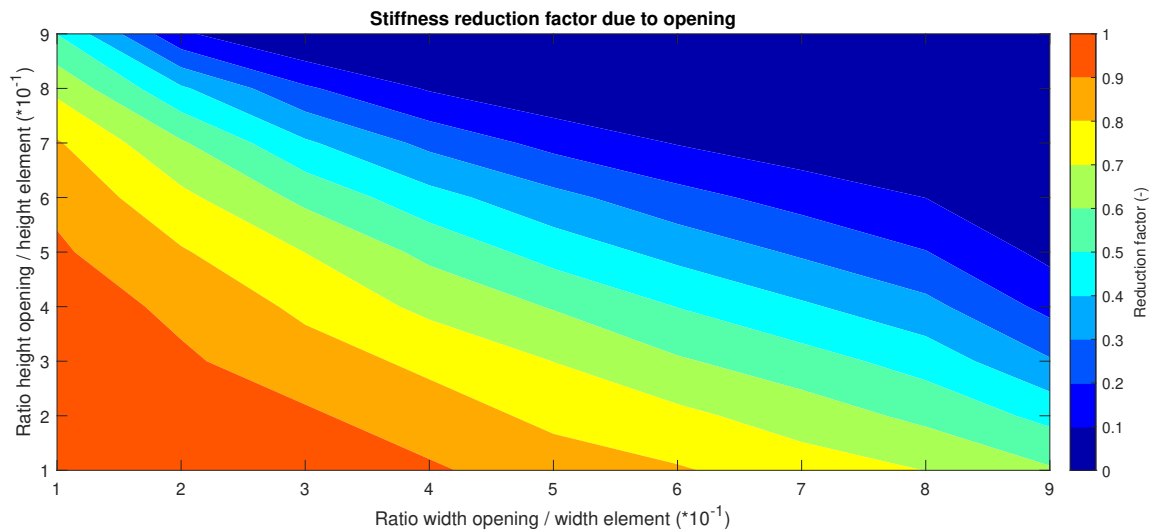


Figure 6.20: Stiffness reduction due to openings in facade elements

To verify these results, the values are compared with values which can be found in literature. Dujic et al. [12] investigated the behaviour of CLT wall panels with different opening locations and proposed a method to calculate the reduced stiffness of the CLT wall panels due to openings. In Figure 6.21 a segment with an opening is shown, where the definitions of different components are depicted.



Figure 6.21: Reduced stiffness of a CLT wall panel with an opening

The stiffness of the element with opening can be calculated using the following formula:

$$K_{opening} = K_{full} \cdot \frac{r}{2-r} \quad (6.13)$$

where  $K_{opening}$  and  $K_{full}$  represent the stiffness of CLT walls with and without openings respectively.  $r$  is defined as the panel area ratio, which is equal to:

$$r = \frac{H \sum L_i}{H \sum L_i + \sum A_i} \quad (6.14)$$

where  $H$  is the height of the wall,  $\sum L_i$  the summation of the length of full wall height segments and  $\sum A_i$  the summation of the area of all openings. According to Figure 6.21,  $A_i$  is equal to  $l_w \cdot h_w$ .

Next, the stiffness reduction is calculated for openings where the ratio width of the opening to width of facade element is equal to the ratio height of the opening to height of facade element. The results for the method of Dujic and the RFEM results are plotted in Figure 6.22.

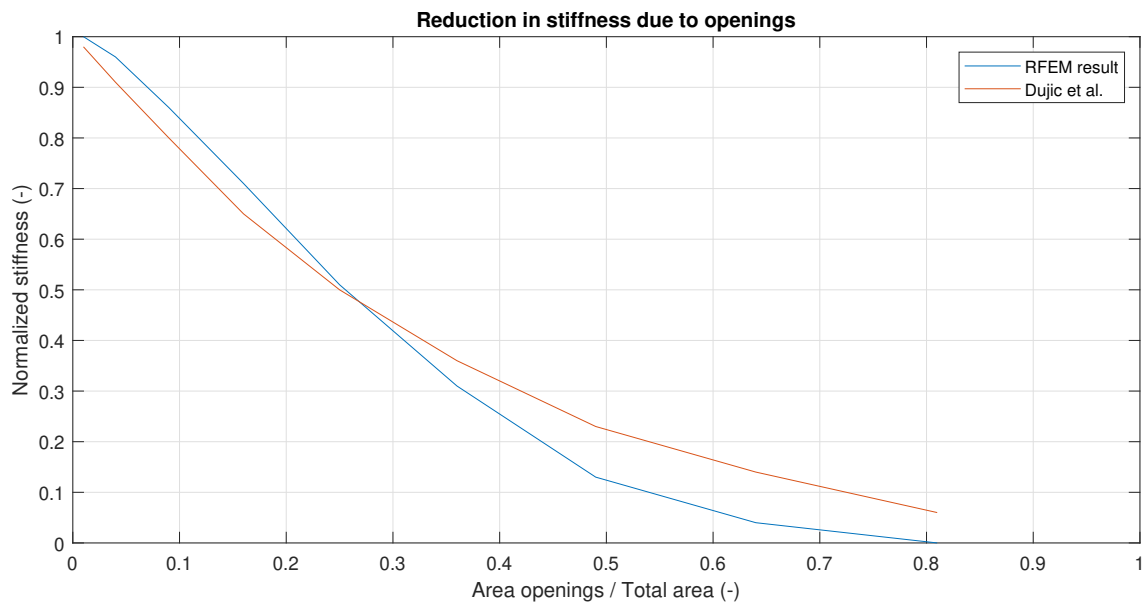


Figure 6.22: Method of Dujic compared to RFEM results

The results by RFEM and Dujic are similar and therefore the reduction of stiffness determined by RFEM to include windows in CLT plates can be used.

The stiffness of the vertical connections at the sides of the elements have to be taken into account as well. To investigate the influence of the connection stiffness on the total bending stiffness of the facade, a model is made with vertical springs between the different facade elements and a model is created with rigid connections between the elements. Two facade configurations are tested, namely a facade which consists of 4 elements with a width of 7.2 metres and a facade which is made of 6 elements with a width of 5.4 metres. The model using 6 elements is depicted in Figure 6.23.

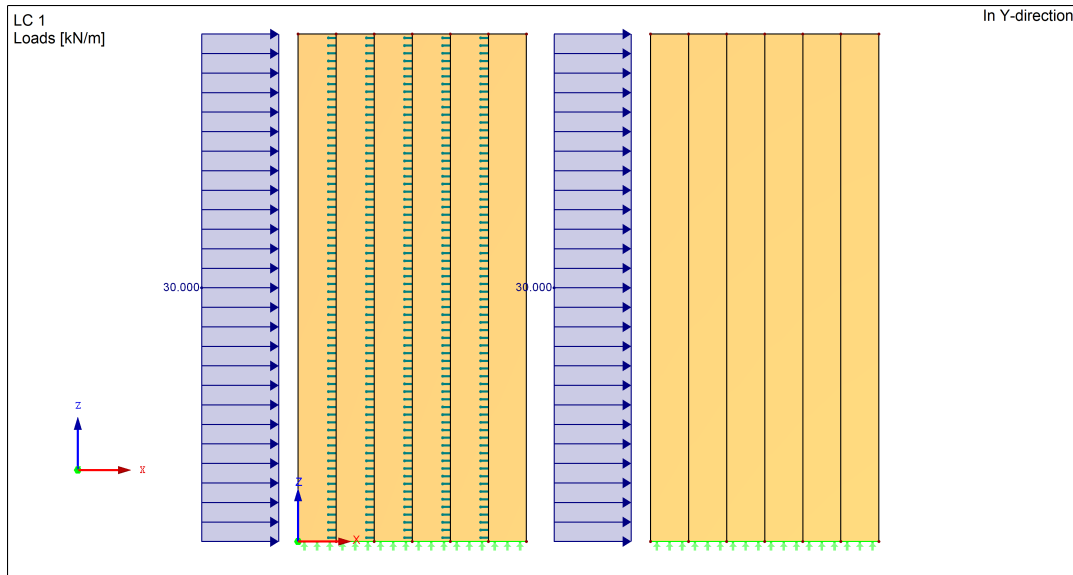


Figure 6.23: RFEM model overview for determining bending stiffness reduction

Each line hinge represents a connection shown in Figure 6.18, thus the vertical spring constant of the line hinge can be calculated. Each connection consist of 2 screws with a total of 8 shear planes.

$$K_{spring} = \frac{8 \cdot \rho_k^{1.5} \cdot d / 23}{5 \cdot d} = \frac{8 \cdot \rho_k^{1.5}}{23 \cdot 5} = 743 \text{ N/mm}^2 \quad (6.15)$$

where  $\rho_m = 485 \text{ kg/m}^3$ .

The reduction of bending stiffness is determined using the ratio between the horizontal displacements of the top of both facades. This is done for building heights up to 150 metres. The results are shown in Figure 6.24.

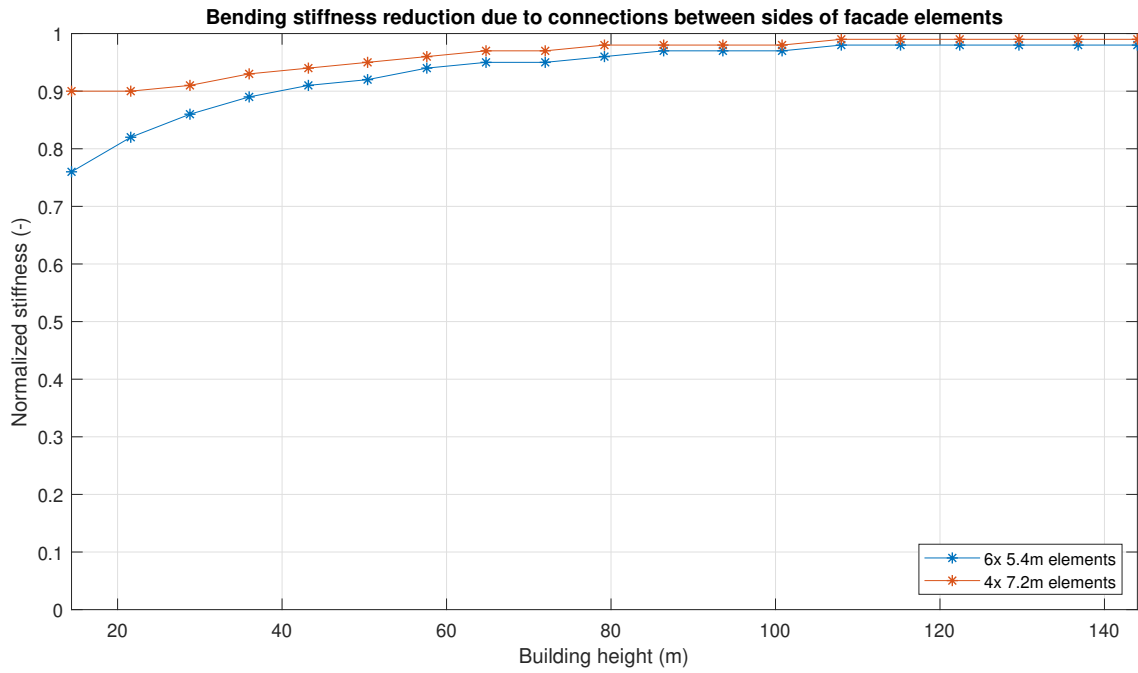


Figure 6.24: Bending stiffness reduction due to connections at the sides of the facade elements

The connections in the corners of the building are not fully rigid as well and as a result will cause reduction in bending stiffness of the facade elements. To determine the stiffness reduction, also for the facade the theory of mechanically jointed beams is used. The dimensions and symbols used by this theory are displayed in Figure 6.25.

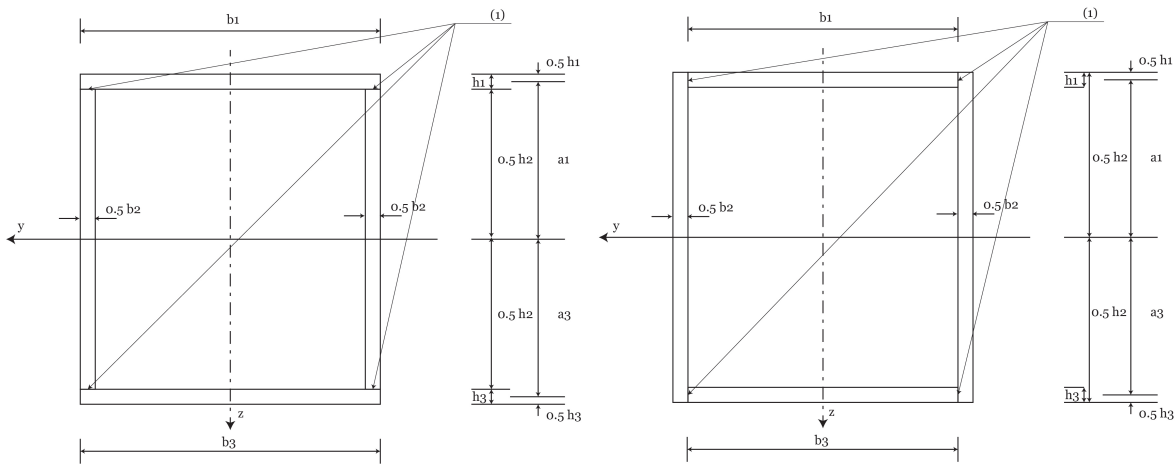


Figure 6.25: Facade dimensions for determining effective bending stiffness

The reduction in bending stiffness is calculated using a building with a width of 32.4 metres and a depth of 28.8 metres. The configuration of the corner connections is the same as that of the CLT cores and therefore the stiffness, defined in Equation 6.6, is:

$$K_{spring} = 186 N/mm^2 \tag{6.16}$$

The facade will not be fully effective in resisting bending moments, because of the large dimensions compared to the thickness. Therefore, the flange width is replaced by an effective flange width, which is illustrated in Figure 6.26.

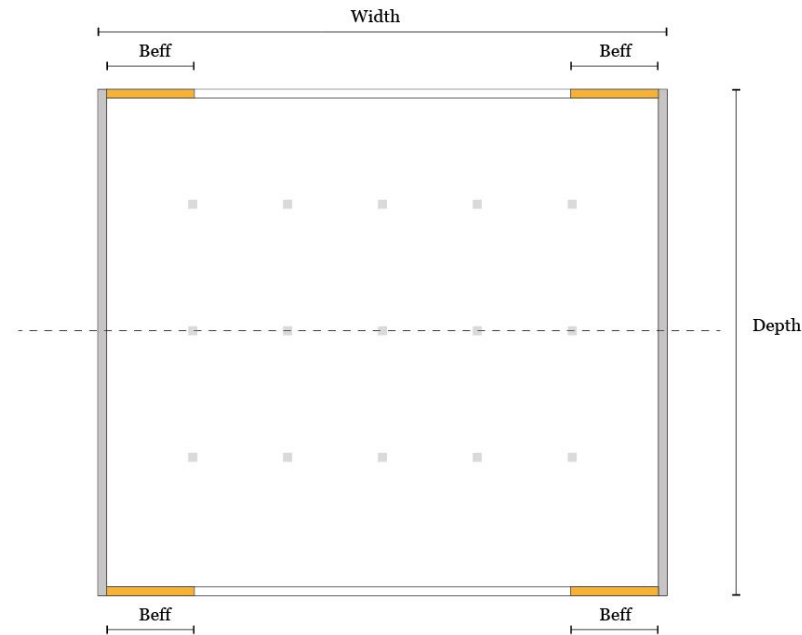


Figure 6.26: Effective facade flange width

The effective width will be equal to the lesser of [3]:

- Half of the width of the building
- 1/10 of the height of the building

The effective bending stiffness is calculated around both x- and y-axis. The results are displayed in Figure 6.27.

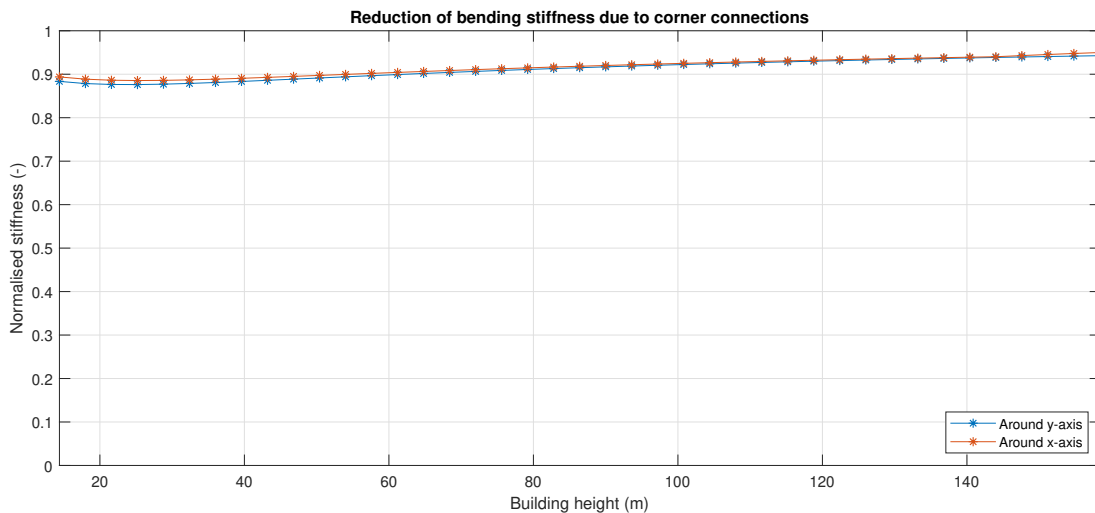


Figure 6.27: Reduction of bending stiffness due to corner connections

The reduction of bending stiffness is almost equal for both axis. A stiffness reduction of around 10% can be seen for buildings lower than 60 metres, this reduction will decrease for greater building heights. Because the reductions around both axis are almost equal, the lowest value of the normalised stiffness will be further used.

The normalized stiffness found for applying openings, vertical connections at the sides of the elements and connections in the corners are multiplied in order to get a combined normalized stiffness for different building heights. The result of this multiplication is depicted in Figure 6.28.

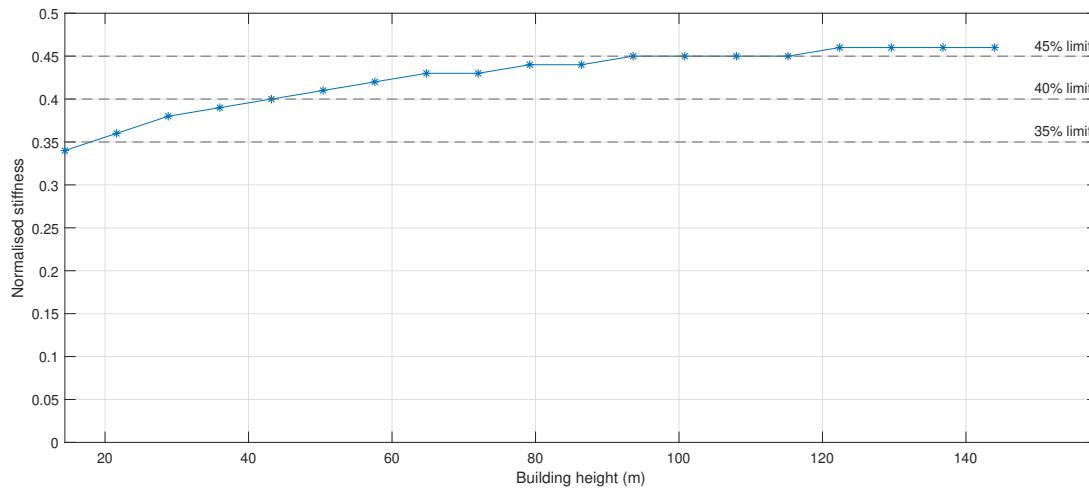


Figure 6.28: Total bending stiffness reduction of facade surface

To assign the material with the correct properties, several reduced values for the stiffness properties are added to the RFEM database, namely for 30% of the bending stiffness compared to the bending stiffness with rigid connections up to 45%. Just like with the core walls, the parametric model will check the building height and apply the correct material properties to the facade elements. The effective bending stiffness are shown in Table 6.12.

Table 6.12: Normalised stiffness for different building heights

Building height interval (m)	Normalised stiffness (-)
$h \leq 19$	0.30
$19 < h \leq 41$	0.35
$41 < h \leq 104$	0.40
$h > 104$	0.45

The strength properties of the corner connections of the facade elements are similar to those of the core elements, because the same connections are used. The vertical connections between the different facade elements however are slightly different. They use the same screws as used for the corner connections, but these screws have 4 shear planes instead of 1. Because there are no formulas available to determine the strength of such a connection, the same connection strength is considered for this connection as for the corner connections.

Furthermore, an assumption has to be made concerning the stress distribution due to the openings. Because of these openings, the stresses can only be transferred using the wall area between the openings. The shear stresses will then be redistributed again over all shear connections between the elements, while the compression and tensile stresses will remain concentrated among the areas between the windows. This is graphical representation is given in Figure 6.29, where the forces acting on top of the facade elements are shown in the associated support reactions. To take these concentrated stresses into account, the calculated compressive and tensile stresses at the bottom of the elements are multiplied by 2. As for the core walls, there will be no reduction of the compressive resistance due to buckling.

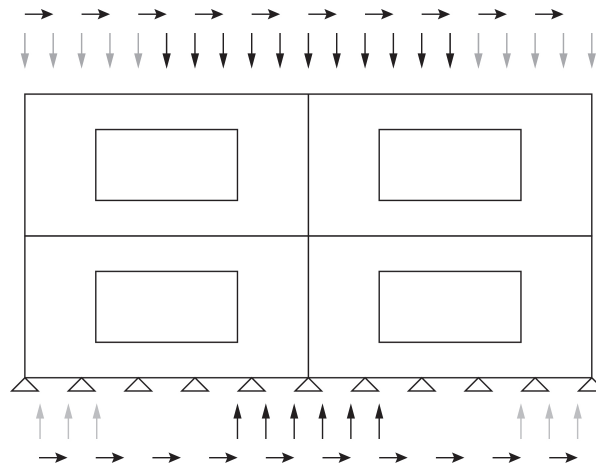


Figure 6.29: Concentration of compressive and tensile stresses between the openings

## 6.7. Characteristics of foundation

It is assumed that the structure is simply supported, but in reality the structure is connected to a foundation, which isn't infinitely stiff. The foundation will have a certain stiffness in x-, y- and z-direction and also a rotational stiffness.

The structure will have a deflection due to both the stiffness of the structure and the stiffness of the foundation. This is shown in Figure 6.30. The distance  $d_1$  represents the deformation due to stiffness of the structure, the distance  $d_2$  shows the deformation due to the rotational stiffness of the foundation.

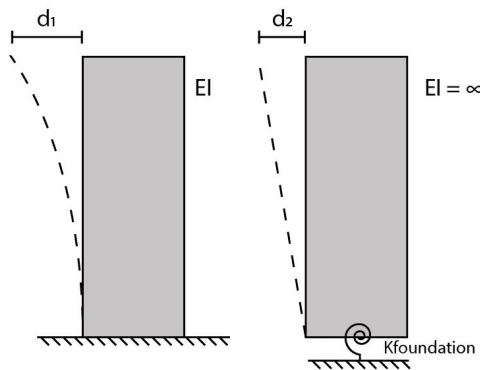


Figure 6.30: Deflections due to stiffness of the structure and foundation

No calculations are done regarding the stiffness of the foundation. It is considered that the deformation  $d_1$  will be 50% of the total deformation and  $d_2$  will be 50% respectively. Therefore, instead of using a maximum horizontal deformation of  $1/500h$  according to the SLS requirements, a value of  $1/1000h$  is used to encounter for the rotational stiffness of the foundation. It is assumed that the stiffness in x- and y-direction are infinite.

## 6.8. Fire safety design

To encounter for the fire safety of all the members, the methods explained in section 3.7 are used. In Figure 6.31 the reduction of the compressive resistance of a Glulam member with dimensions of 200 millimetres up to 500 millimetres which should be applied is demonstrated for different fire safety levels.

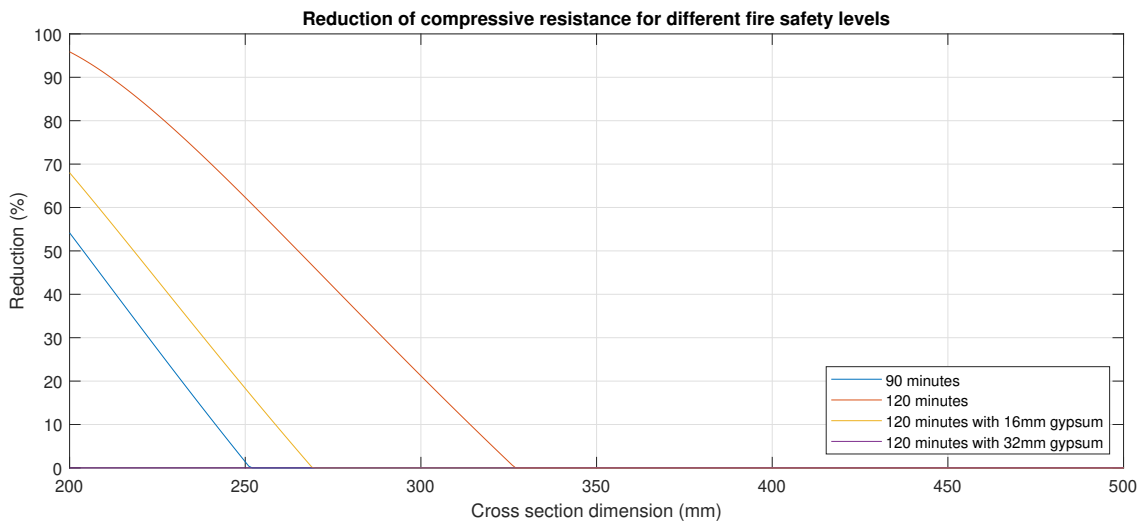


Figure 6.31: Reduction of compressive resistance for different fire safety levels

When using a column with dimensions 300x300 millimetres, a reduction of the compressive resistance of 21% should be applied. If a gypsum layer of 32 millimetres is placed on all sides of the member, no reduction is required for every dimension. For unprotected columns, no reduction should be applied when the width and depth of the columns exceeds 326 millimetres.

Including the fire resistance to members influences the strength of the connections. This is because the connections should be placed within parts which are not affected in case of a fire situation. In other words, the char layer depth has a large influence on the configuration of the connection.

In Figure 6.32 the maximum char layer depth is determined for different fire protective layer thicknesses and a fire resistance between 0 and 120 minutes. For example, when an unprotected column is used where a dowel connection is applied to, the steel plate(s) should be placed at a minimum distance of 91 millimetres from the edge of the column on both sides and also the dowels should be placed the same distance inwards. It is likely that this will cause a reduction of the maximum amount of dowels which can be applied to the steel plate and thus influences the strength of the connection.

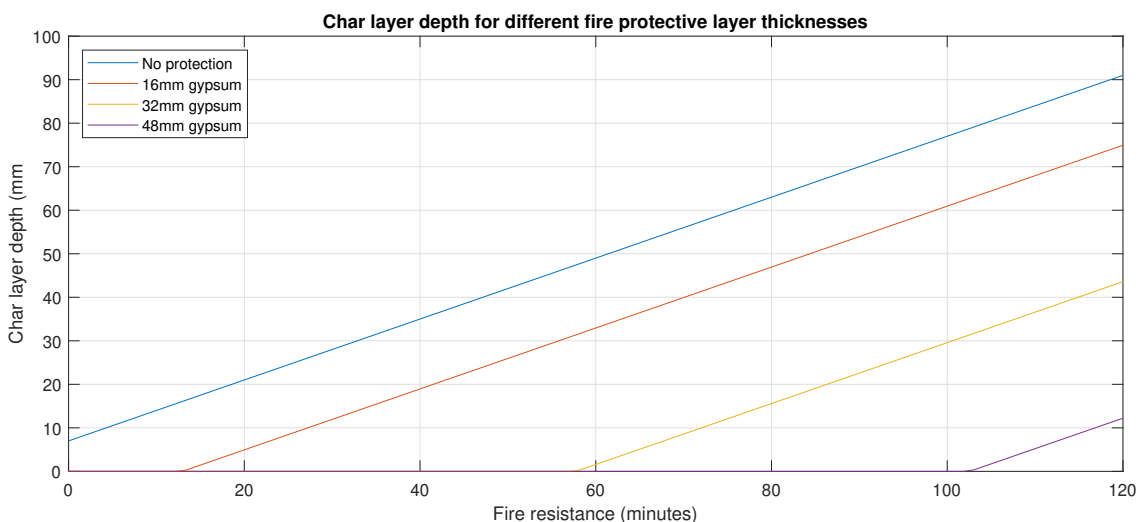


Figure 6.32: Char layer depth for different fire protective layer thicknesses

The separating function of a wall assembly can be calculated using the method described in section 3.7. In

Figure 6.33 the separating function is shown for different wall thicknesses with timber layers of 45 millimetres where no fire protective layers are applied. It is assumed that each layer of the CLT represents a separate layer of the wall assembly.

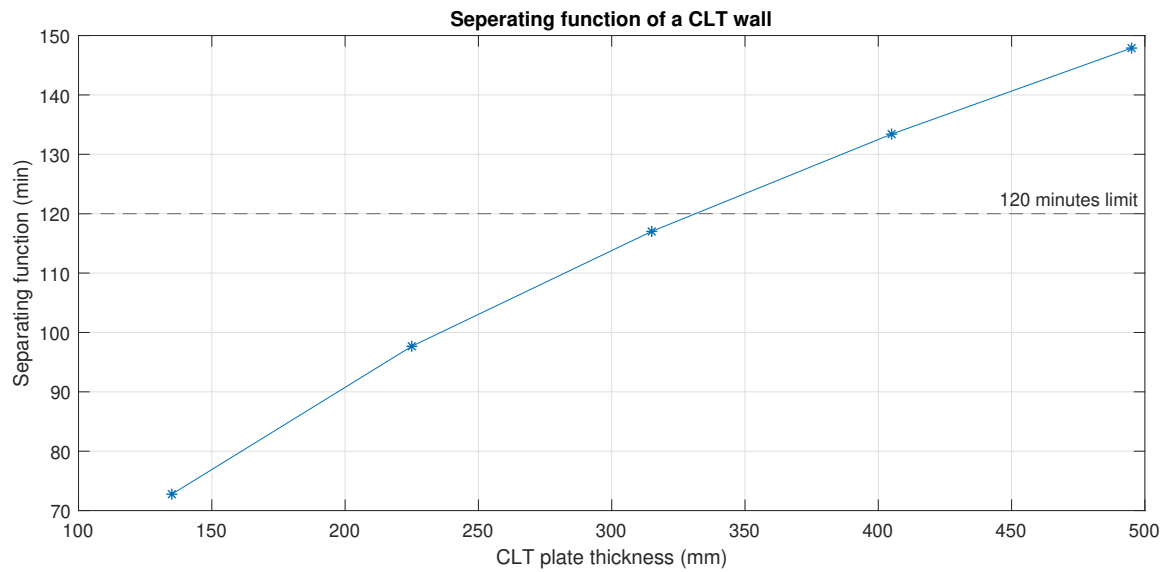


Figure 6.33: Separating function for different wall thicknesses

As can be seen, if a wall assembly requires a separating function of 120 minutes, a minimum wall thickness of 330 millimetres is required.

# 7

## Background on connections

In chapter 6, several specific connections are chosen to be used in the parametric model. However, these connections are not commonly used at the moment and therefore it is useful to compare the properties of these connections with connections normally used in structures. This is done for both connections between columns and diagonals and the connections between wall elements, where both the strength and stiffness properties are compared. The influence of the stiffness of the connections on the structure is also investigated. The calculations made to determine the strength and stiffness of the connections are shown in Appendix B.6.

### 7.1. Connections between members

The connections between members, such as columns and diagonals, are used to transfer compression and tension forces. Different connections which are commonly used are shown in Figure 7.1. Still several variations of these connections are possible, where only a few are considered, but it still gives a good insight on the behaviour of these types of connections.

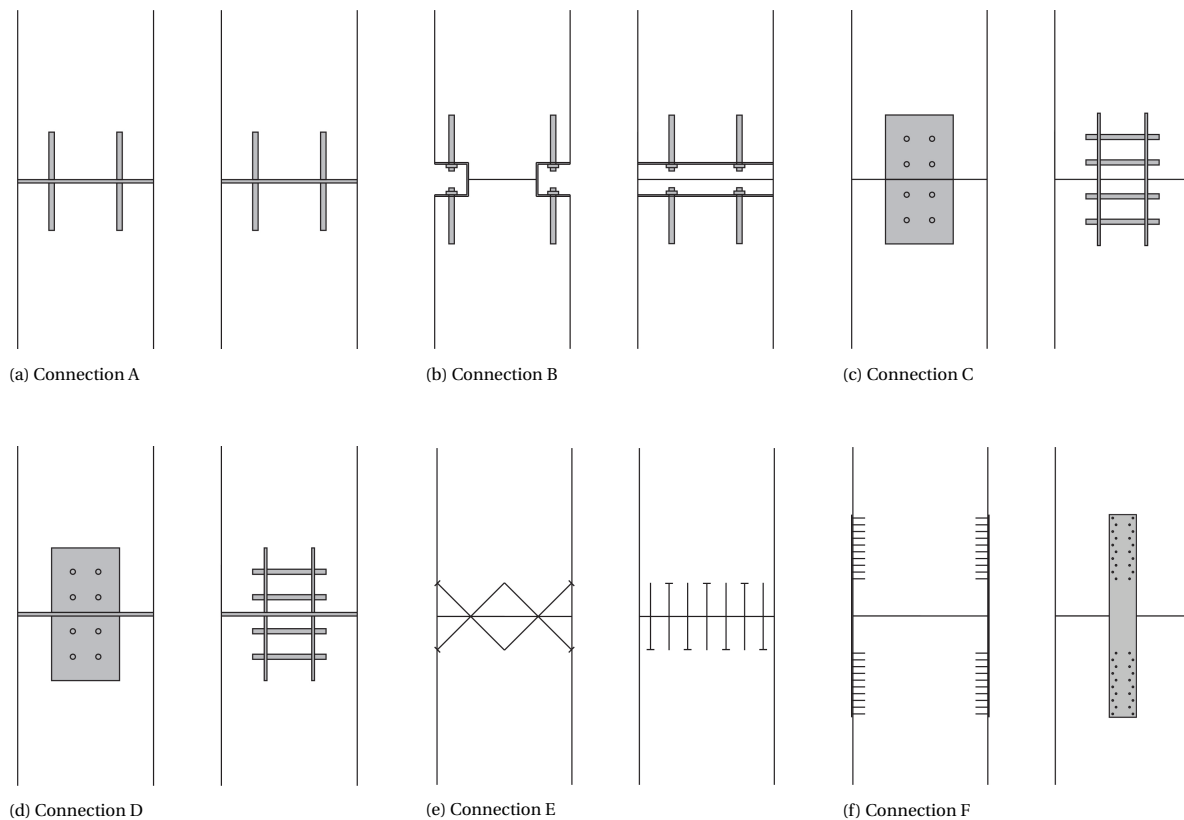




Figure 7.1: Side views of different commonly used connections between timber members

The connections can be described as follows:

- Connection A: To take up tension forces, 4 glued-in threaded rods are used. Compression is transferred via the steel plate between the 2 members. In this case, the rods have a diameter of 16 millimetres and a length of 140 millimetres, the same as the connection discussed in section 5.3.
- Connection B: This connection also has 4 glued-in threaded rods, however these rods are attached to a steel profile using bolts. Because of this, the rods can already be glued in the timber before the members are being placed on site. The compression forces are transferred using the reduced timber area between the steel profiles.
- Connection C: Steel plates are used in this connection, wherein 4 dowels are placed. The steel plates and dowels are used to transfer both compression and tension forces.
- Connection D: The connection is similar to connection C, but an additional steel end plate is attached to the end of the 2 existing steel plates. Therefore, compression forces can be transferred using the steel end plate and the dowels are used to carry tension forces to provide tension resistance.
- Connection E: The connection consists of 14  $\phi 11$  mm full threaded screws with cylindrical head which are applied in a 45 degrees angle from both up- and downwards direction. The screws have a length of 300 millimetres. They can take up tension forces, while the timber transfers the compression forces.
- Connection F: In this case, perforated plates combined with anker nails provided by the company Rothoblaas [54] are used to transfer tension forces. These plates have a width of 80 millimetres, a thickness of 1.5 millimetres and a total length of 600 millimetres. The plates are applied on 2 sides of the member, where 20  $\phi 4$  mm nails with a length of 40 millimetres are applied to each plate.
- Connection G: The same holds for this connection as for connection C, but this connection uses more and smaller dowels. This connection has the optimised configuration determined in subsection 6.3.1.
- Connection H: This connection uses 9 glued-in threaded rods to take up the tension forces and the steel end plate to transfer compression forces. The rods have a diameter of 21 millimetres and a length of 314 millimetres, the same as the optimised configuration determined in section 6.2

### 7.1.1. Strength and stiffness properties

For all connections described in the list above, the design strength can be determined. Also, some connections will have a certain stiffness in the direction parallel to the member. The calculations can be found in Appendix B.6.1, while all results are shown in Table 7.1.

Table 7.1: Properties of different column connections

Connection	Compression resistance (kN)	Tension resistance (kN)	Stiffness parallel to member (kN/mm)
A	2363	69	$\infty$
B	1182	69	$\infty$
C	115	115	141
D	2363	115	141
E	2363	81	72
F	2363	92	74
G	595	596	1395
H	2363	422	$\infty$

For connection A, D, E, F and H, the maximum compression resistance is equal to the resistance of the timber material. The maximum compression in connection B is half the resistance of connection A because of the reduction of the timber area in the connection due to the steel profiles. For connection C and G, the compression forces are transferred by the dowels, which results in a lower compression resistance compared to the other connections.

Most connections show a similar resistance to tension, where connection A and B have the lowest resistance of 69 kN and connection C and D have the highest resistance. It is clear that the optimised connections examined in subsection 6.3.1 and section 6.2 have a much higher resistance to tension of 596 kN and 422 kN respectively.

Regarding stiffness of the connections, connection A, B and H can assumed to be infinite stiff. The connections with steel plates and dowels will give a stiffness equal to 282 kN/mm for connection C and D and 2789 kN/mm for connection G. Connection E, using screws, and connection F, using perforated plates with anchor nails, have a stiffness of 72 and 74 kN/mm respectively.

### 7.1.2. Influence of connection stiffness on structure

The influence of the connections on the behaviour of the members is checked for multiple connection stiffness and member lengths. This is done by considering a member with length  $L$  which is loaded by a force  $F$ . The connection is modelled as a spring at the bottom of the member with spring stiffness  $K_{ser}$ . This is shown in Figure 7.2.

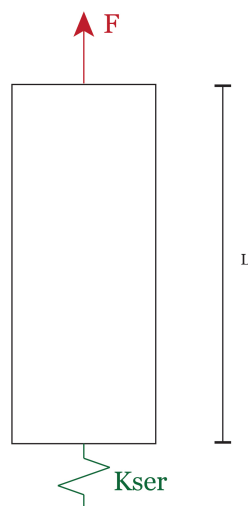


Figure 7.2: Modelling the member combined with a connection with finite stiffness

The spring stiffness is varied from 100 kN/mm to 2000 kN/mm, because these values were found in this

section for typical connections. The length of the member varies from 3 metres to 14 metres. The contribution of the connection to the total vertical displacement of the top of the member is determined and the results are shown in Figure 7.3.

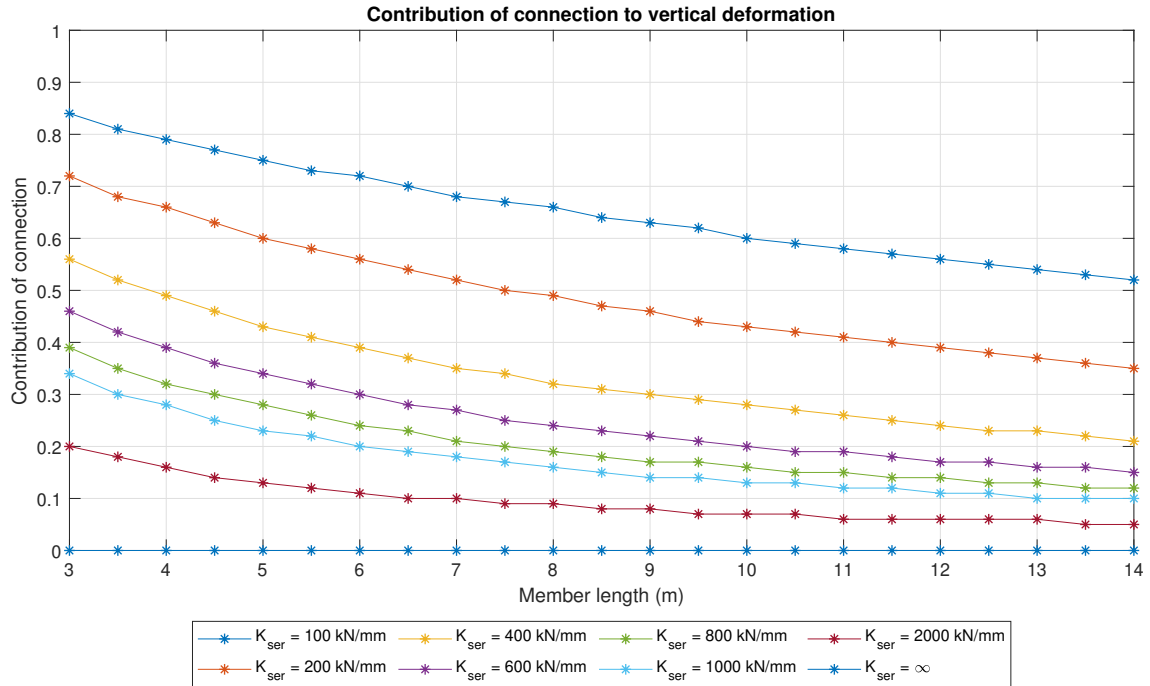


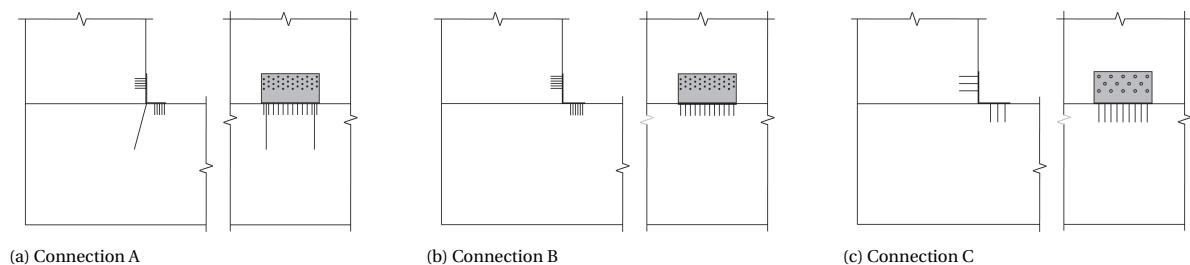
Figure 7.3: Contribution of a connection to the total vertical deformation

The contribution of the connections to the total vertical deformation decreases for greater lengths of the members. Furthermore, an increase in stiffness gives a decrease of the contribution of the connection. As can be seen, a connection which has a stiffness of 100 kN/mm will cover 50% of the total vertical deformation and thus this connection will double the deformation compared to a member with a fully rigid connection. Hence, the stiffness of the connection can have great influence on the total vertical deformation of the members.

## 7.2. Shear connection between corners of walls

Two types of connections are examined, namely connections which transfer either shear or tension forces. First shear connections are discussed, after which the tension connections are looked at. For this comparison, it is assumed that the walls have a thickness of 495 millimetres.

In the following Figure 7.4, 2 walls can be seen in both side views, where in the corner between the elements a connection is applied to transfer shear forces.



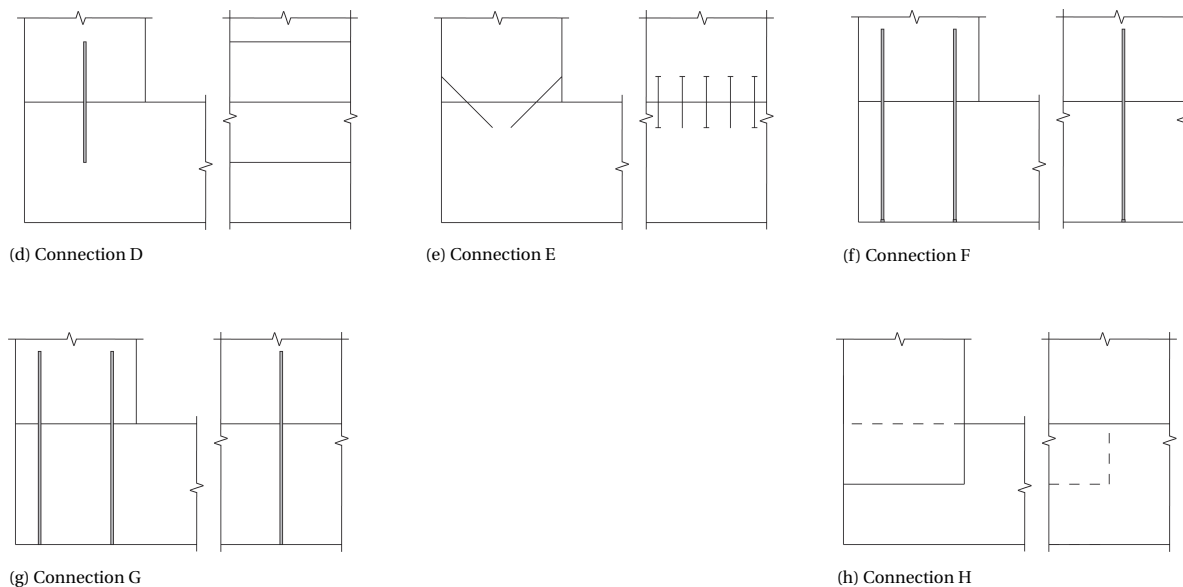


Figure 7.4: Side views of commonly used connection between wall segments to transfer shear forces

The connections can be described in the following way:

- Connection A: This connection consists of an angle bracket with full thread screws which can take up tensile and shear loads. The connection named Titan V (TTV240) is provided by the company Rothoblaas. The screws have a diameter of 5 millimetres and a length of 50 millimetres [54].
- Connection B: For this connection also an angle bracket is used which can only transfer shear forces, but this connection is fastened using  $\phi 5\text{mm}$  nails instead of screws with a length of 60 millimetres. Its named Titan N (TTN240) and provided by the company Rothoblaas [54].
- Connection C: A similar connection is shown as connection b, however  $\phi 8\text{mm}$  screws with a length of 80 millimetres are used instead of nails. The connection is provided under the name Titan S (TTS240) by the company Rothoblaas [54].
- Connection D: This connection is marketed by Rothoblaas under de name XEPOX. A cut is made in the wall segments, where a steel plate is placed. This steel plate is glued to the timber by using a two components epoxy adhesive, which has higher strength properties than the timber [53].
- Connection E: Screws are applied at a 45 degrees angle between the 2 wall segments. This is done on both sides. In this case, screws with a diameter of 11 millimetres and a length of 300 millimetres are used.
- Connection F: 2 screws are fully drilled through one wall segment, after which the screws are attached to the second wall segment. The screws have a total length of 800 millimetres, so the screw is attached to the second wall segment over a length of 305 millimetres.
- Connection G: This connection is similar to connection f, but the screws are replaced by glued-in threaded rods with the same diameter as the screws.
- Connection H: Teeth are cut in the timber to obtain a shear connection without using steel parts. Because of the cuts, only half the area of the timber can be fully loaded in shear.

### 7.2.1. Strength and stiffness properties

For all connections listed above, the design strength and stiffness in the direction of the shear stresses can be determined, which are depended on the centre-to-centre distance (ctc) between the fasteners. Therefore, this is done for different ctc, namely 1000, 500 and 240 millimetres for the connections which use brackets and 200 millimetres, 100 millimetres and the minimum spacing for connections consisting of either screws or rods. Thus, the ctc's for the different connections are shown in Table 7.2. The strength and stiffness properties

of the connections A, B and C are based on experiments performed by Rothoblaas [54] and are depicted in Figure 7.5. All other connections and their corresponding properties are calculated using formulas provided by NEN-EN 1995-1-1 [31].

In addition to corner connections, it is also possible that connections between walls next or on top of each other need to transfer shear forces. All connections, except connection A, B and C, can be used in a similar way for transferring shear forces. The strength and stiffness properties are the same as those found for the corner connections.

Numbers are assigned to each specific connection which correspond with the numbers shown in Figure 7.5.

Table 7.2: ctc for all shear connections

Connection	Number	ctc (mm)	Connection	Number	ctc. (mm)
A	1	1000	E	11	200
	2	500		12	100
	3	240		13	50
B	4	1000	F	14	200
	5	500		15	100
	6	240		16	50
C	7	1000	G	17	200
	8	500		18	100
	9	240		19	55
D	10		H	20	

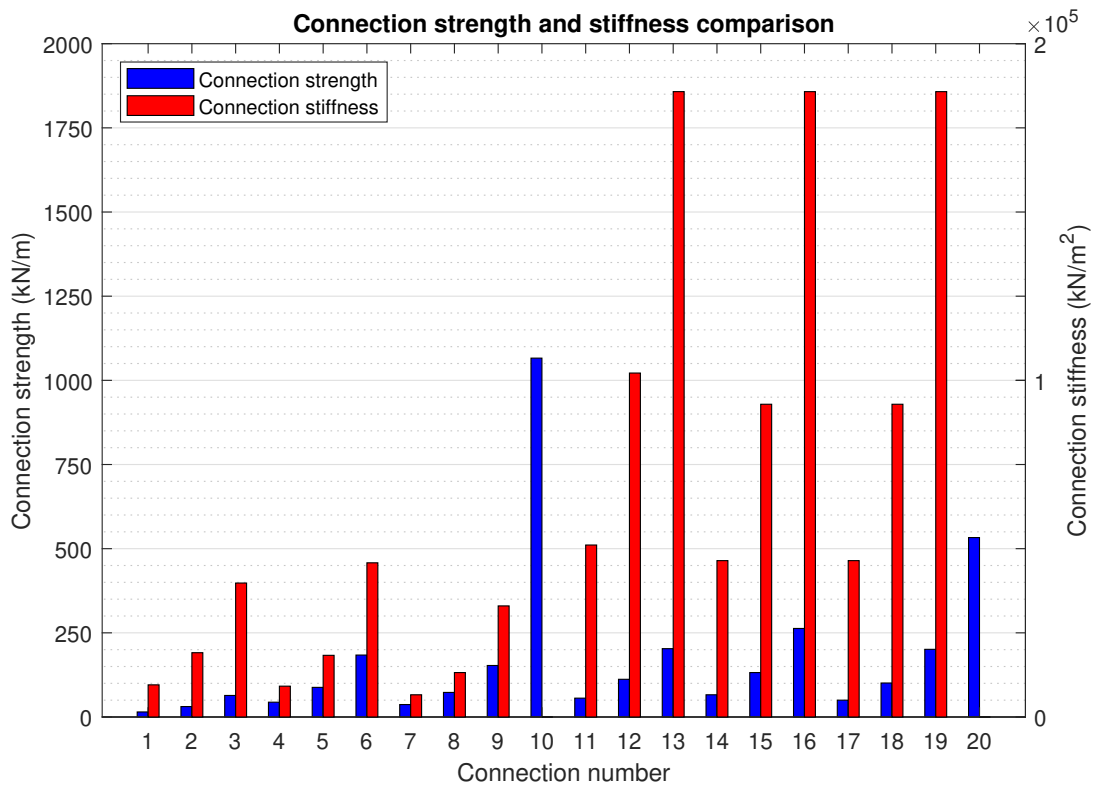


Figure 7.5: Connection strength and stiffness for different connections

Connection D, which uses a XEPOX plate, has the highest shear capacity. The full shear capacity of the timber

can be used and thus the connection does not cause a decrease in shear resistance. Using a toothed connection results in half the connection strength of the connection with a XEPOX plate, because due to the teeth only half of the area of the timber can be used. The connections using screws and rods (connection E, F and G) have similar shear resistances for each ctc, where the connections with the lowest ctc have the highest shear capacity. The other connections provided by Rothoblaas (connection A, B and C) have the worst performance in this comparison with regard to transferring shear forces.

The stiffness of connection D and H are not shown in the graph, because the it is assumed to be infinite. The connections using screws and rods (connection E, F and G) have a lower stiffness than connection D and H, but have similar stiffness for each ctc compared to each other. The connections A, B and C have the lowest stiffness. When using these connections with the minimum ctc, the stiffness are similar to the screws and rods connections with the greatest ctc. It should be noticed that it is highly unlikely that the shear brackets are positioned directly next to each other.

### 7.2.2. Influence of connection stiffness on structure

The influence of the stiffness of shear connections between walls is investigated by checking what the contribution of the connection stiffness is to the total horizontal displacements of the structure. Therefore, 3 walls are considered which are connected using similar connections, which are distributed over the whole height of the walls. These walls have a width of 12000 millimetres and a depth of 9100 millimetres, which is shown in Figure 7.6.

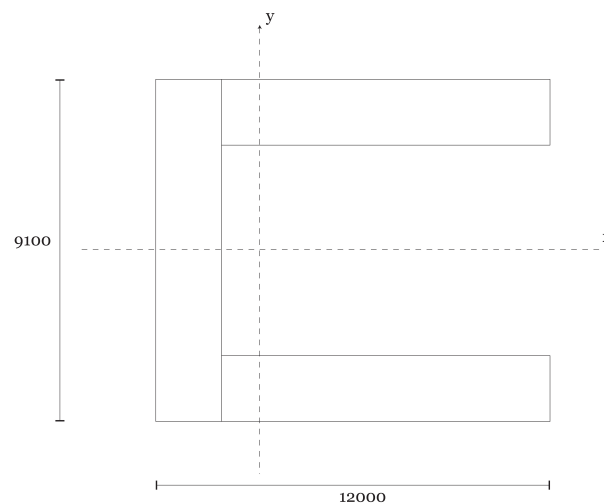


Figure 7.6: Top view of the investigated structure

The horizontal displacements are checked in both x- and y-direction by using the theory of mechanically jointed beams, which was also used in subsection 6.5.2. This is done for connection stiffness varied from 10 to 200  $N/mm^2$  for different building heights. The results are shown in Figure 7.7 and Figure 7.8.

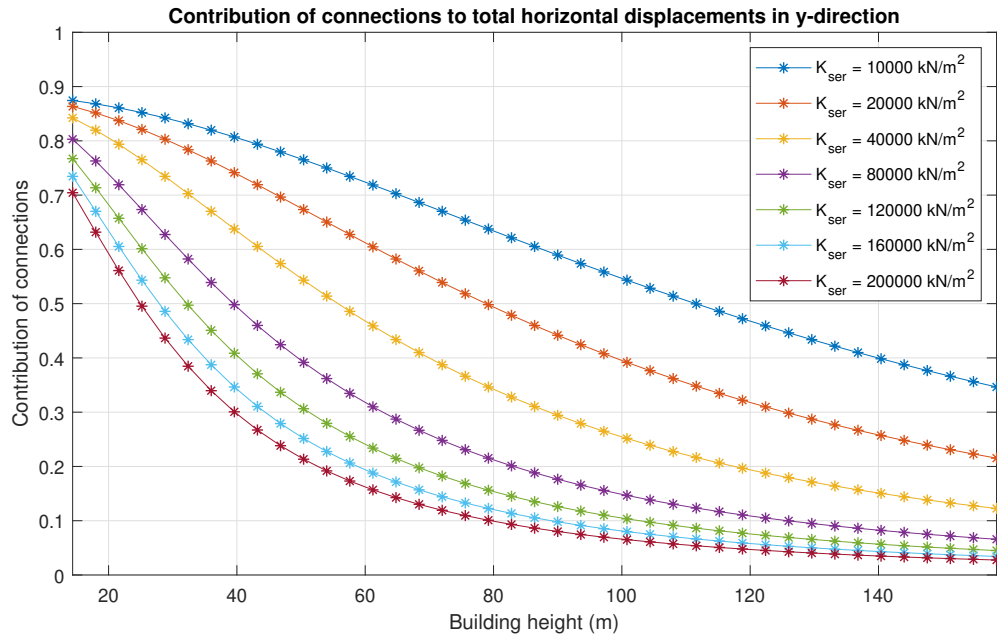


Figure 7.7: Contribution of connections to total horizontal displacements in y-direction

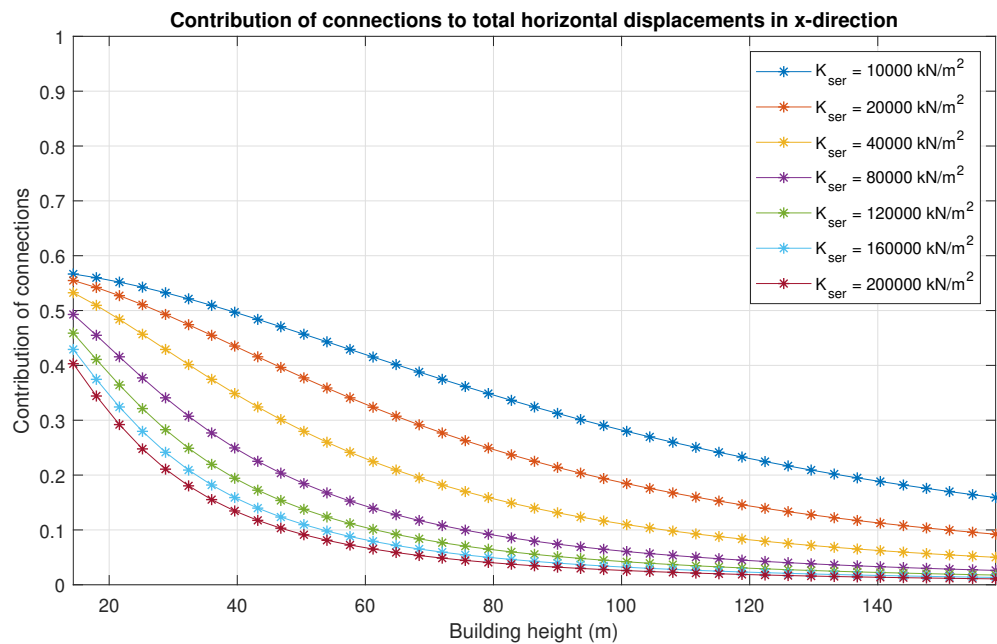


Figure 7.8: Contribution of connections to total horizontal displacements in x-direction

The contribution of the connection stiffness on the total horizontal displacements is greater in y- than in x-direction and decreases for greater building heights. Furthermore, greater stiffness results in less contribution. When using a corner connection with a stiffness of  $20000 \text{ kN/m}^2$  gives a 40% contribution in y-direction and 20% in x-direction for a 100-metres high building and will reduce to 20% and 10% contribution in x- and y-direction respectively.

### 7.3. Tension and shear connections between stacked walls

A number of connections which can be used to transfer tension forces between walls which are stacked on top of each other are discussed. Side views of these connections can be observed in Figure 7.9.

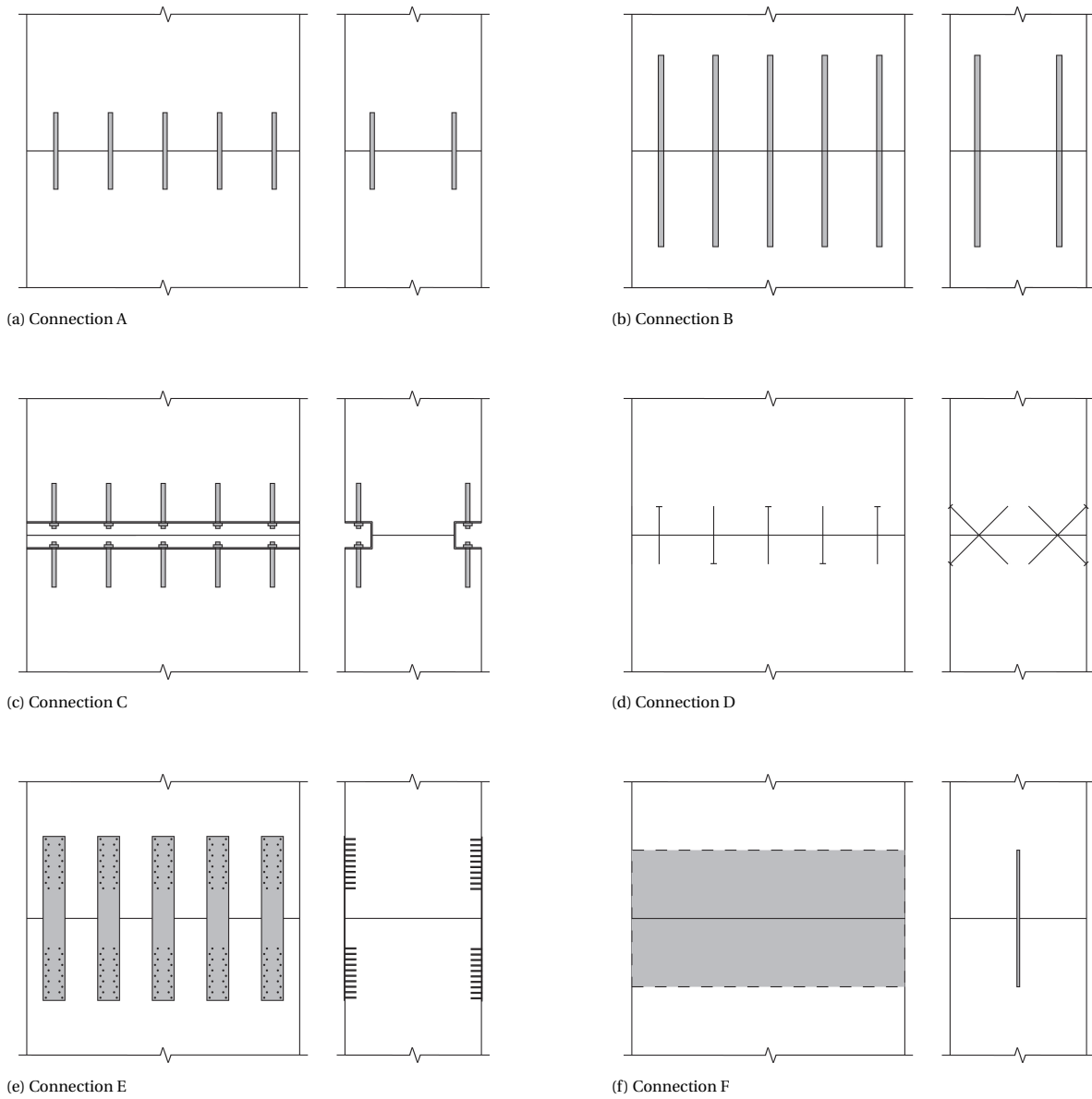
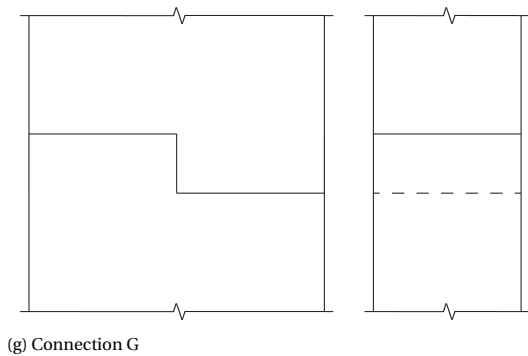


Figure 7.9: Overview of tension connections between wall elements



The connections can be described as:

- Connection A: This connection was also used in section 7.1, but in this case the connection is continuous along the walls. The tension and shear forces are transferred by the rods, while the compression resistance is determined by the timber area.
- Connection B: This connection is similar to connection A, but here the characteristics of the connection used in subsection 6.5.2 are considered.
- Connection C: Steel profiles are added to each side of the wall, where the glued-in threaded rods can be bolted to. The glued-in rods have the same properties as those of connection A, the timber area is reduced by the width of the steel profiles.
- Connection D: Screws applied in a 45 degrees angle are adopted between the wall segments on both sides. In this comparison, screws with a diameter of 11 millimetres and a length of 300 millimetres are considered.
- Connection E: Perforated plates combined with anker nails can also be continuously used to transfer the tension forces. This connection is already discussed in section 7.1.
- Connection F: A XEPOX plate which is glued between 2 wall segments transfers the tension forces. Because the adhesive between the steel plate and the timber has higher strength properties than the timber, the full tensile resistance of the timber can be used when a plate with sufficient length is applied. The compression forces are taken up by the timber.
- Connection G: This connection is comparable to connection H discussed in section 7.2. This connection can be combined with other fasteners such as screws.

To determine the strength properties of these connections, the ctc between the fasteners is important. Therefore, for each connection type, different ctc are considered. The strength and stiffness properties are compared in Table 7.3.

Table 7.3: Strength and stiffness properties of connections

Connection	ctc	Tension resistance (kN/m)	Shear resistance (kN/m)	Vertical stiffness ( $kN/m^2$ )	Horizontal stiffness ( $kN/m^2$ )
A	500	69	47	$\infty$	29721
	250	139	94	$\infty$	59442
	80	433	292	$\infty$	185757
B	500	116	47	$\infty$	29721
	250	233	94	$\infty$	59442
	100	582	234	$\infty$	185757
C	500	69	47	$\infty$	42032
	250	139	94	$\infty$	84064
	80	433	292	$\infty$	262700
D	500	43	56	20000	20433
	250	86	112	41000	40866
	55	389	203	186000	185757
E	500	66	-	149000	-
	250	131	-	297000	-
	80	411	-	929000	-
F	-	2659	1066	$\infty$	$\infty$
H	-	-	533	-	$\infty$

Connection F has the highest tensile strength, because the full tensile resistance of the timber can be used. All other connections have similar strength, with connection B having the second highest resistance of 582 kN/m. Connection A and C have the equal tension force capacity of 433 kN/m, followed by connection E with

a resistance of 411 kN/m. Connection D has the worst performance with a tensile strength of 389 kN/m. It should be noticed that it is not common that the perforated plates of connection E are placed directly next to each other.

Connection F can use the full shear resistance of the timber and thus has the highest shear strength. The shear resistance of the other connections are comparable, with a maximum shear strength of 292 kN/m for connection A and C using the minimum spacing. No values are given for connection E, because these are not provided by the manufacturer Rothoblaas and these connections are not designed to transfer shear forces.

All connections, except connection C, can transfer the full compression resistance of the timber. Connection C has a reduced cross-section area of the timber between the steel profiles, which causes a compression strength reduction of 40%.

Connection D and D are connections which cannot be considered infinite stiff in vertical direction. Connection D has a maximum stiffness of  $186000 \text{ kN/m}^2$  using the minimum spacing of 55 millimetres, while connection E is much stiffer with a maximum value of  $929000 \text{ kN/m}^2$ .

All connections, except connection F and H, have a finite stiffness in horizontal direction. The connections using glued-in threaded rods and the connections using screws have similar stiffness, where the connection using an additional steel profile is slightly stiffer than the other connections.

### 7.3.1. Influence of connection stiffness on structure

The influence of the connections on the structure is investigated for both horizontal and vertical direction. A horizontal stiffness will give additional shear deformation, while the stiffness in vertical direction will cause extra vertical deformation when the connection is loaded in tension, which leads to horizontal deformation of the structure.

#### Horizontal stiffness

To check the influence of the horizontal connection stiffness, structures with a width of 10 and 20 metres are modelled in 2 as shown in Figure 7.10.

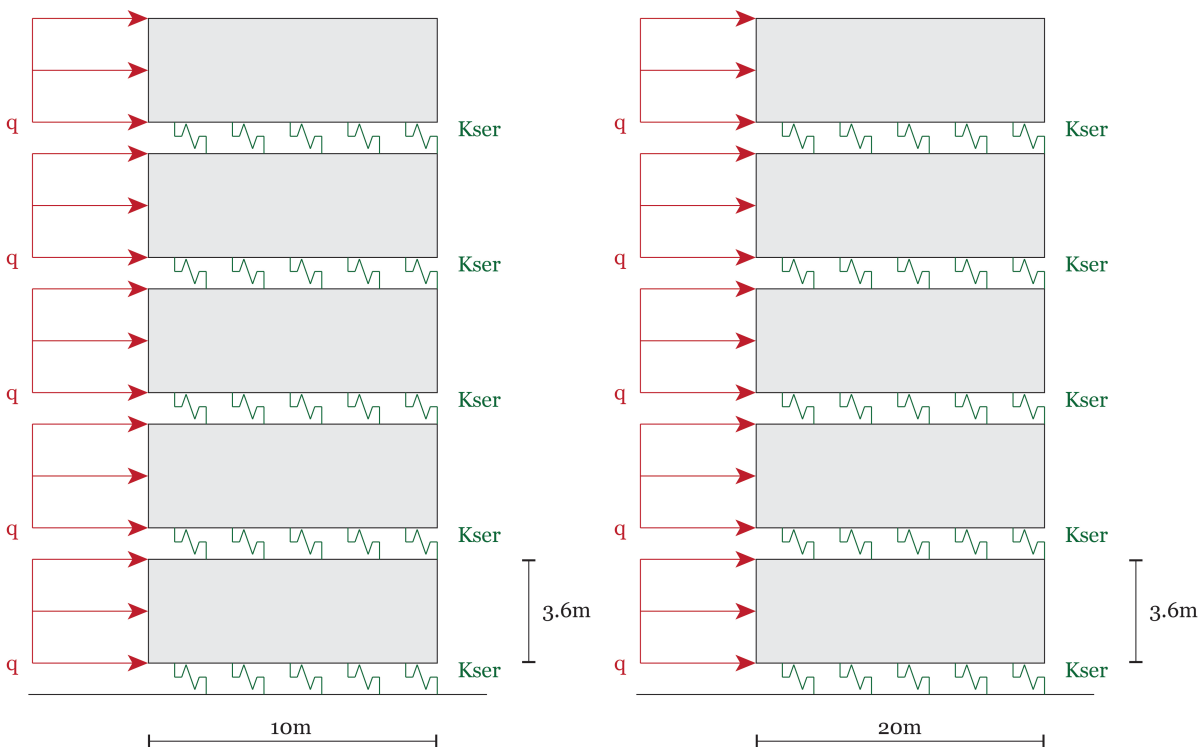


Figure 7.10: Models as used to determine influence of vertical connection stiffness on the structures

The same amount of fasteners is applied on each level. Then the bending deformations and displacements caused by the connections are calculated. The spring stiffness is varied between 10000 and 180000  $kN/m^2$ , because these values were found in this section for typical connections. The contribution of the connection to the total vertical displacement of the top of the walls is determined and the results for the 10- and 20-metres width wall are shown in Figure 7.11 and Figure 7.12 respectively.

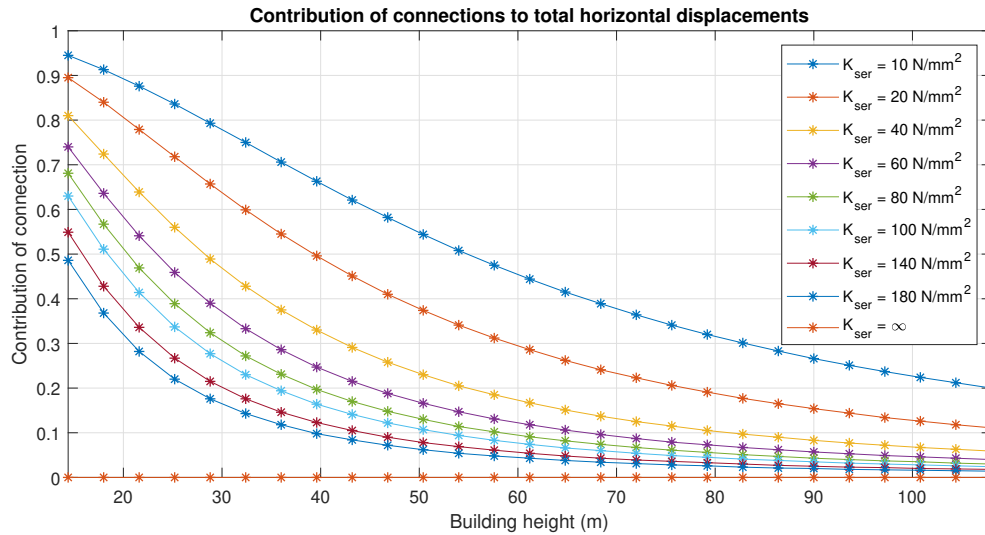


Figure 7.11: Contribution of connection to total horizontal displacements of 10-metres width wall

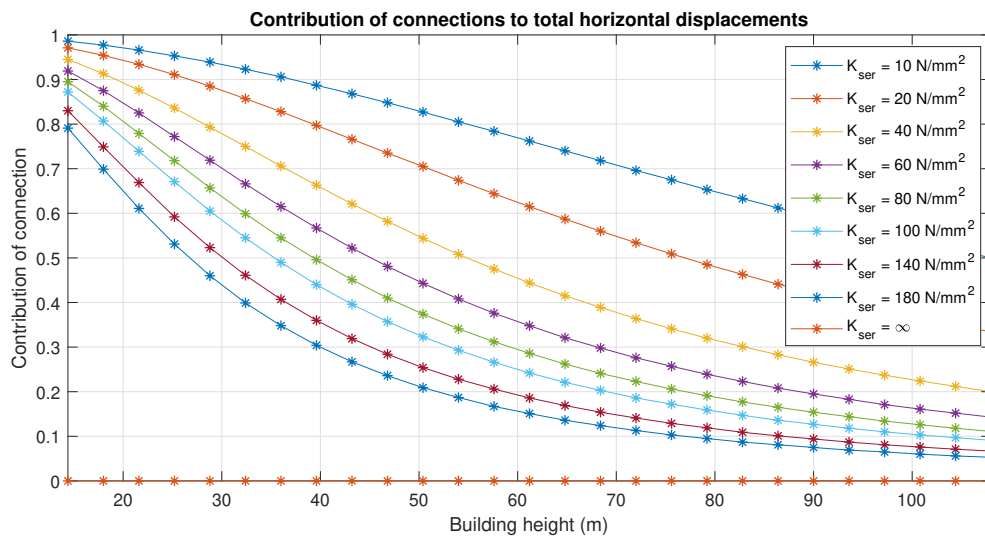


Figure 7.12: Contribution of connection to total horizontal displacements of 20-metres width wall

The contribution of the connections to the total vertical deformation decreases for greater amounts of levels. This is because for higher walls the horizontal displacement by bending becomes more important than the horizontal displacements by shear. The connections will have more influence on the total vertical deformation if the bending stiffness of the walls is greater, i.e. the contribution of the connections will be greater for a 20-metres wall than for a 10-metres width wall. Thus, the horizontal stiffness of the connections can have great influence on the total horizontal deformation. For example, a connection with a stiffness of 40  $kN/m^2$  can have a contribution of 20% to the total displacements.

### Vertical stiffness

To check the influence of the vertical connection stiffness, a structure with a width of 10 metres is modelled in RFEM as depicted in Figure 7.13. A spring is applied between each 3.6-metres high wall, which will extend when its subjected to tension, while the spring will be infinitely stiff when loaded in compression.

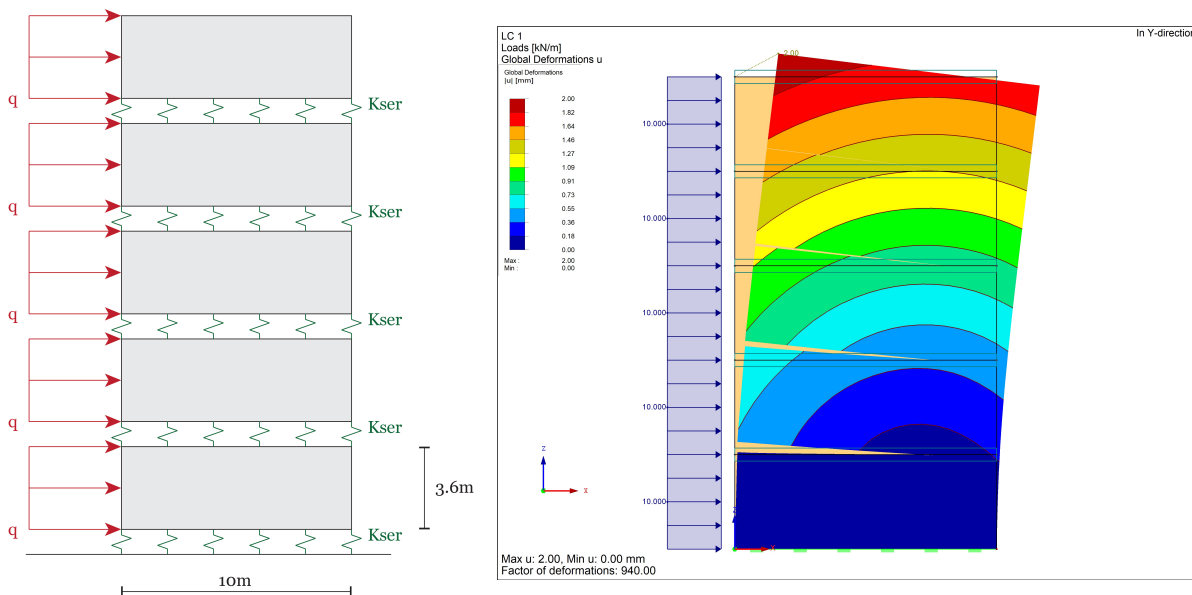


Figure 7.13: Models as used to determine influence of vertical connection stiffness on the structures

Also in this case the same amount of fasteners is applied on each level. The connection stiffness is varied between 10000 to 800000  $kN/m^2$ . The results of the RFEM model are displayed in Figure 7.14.

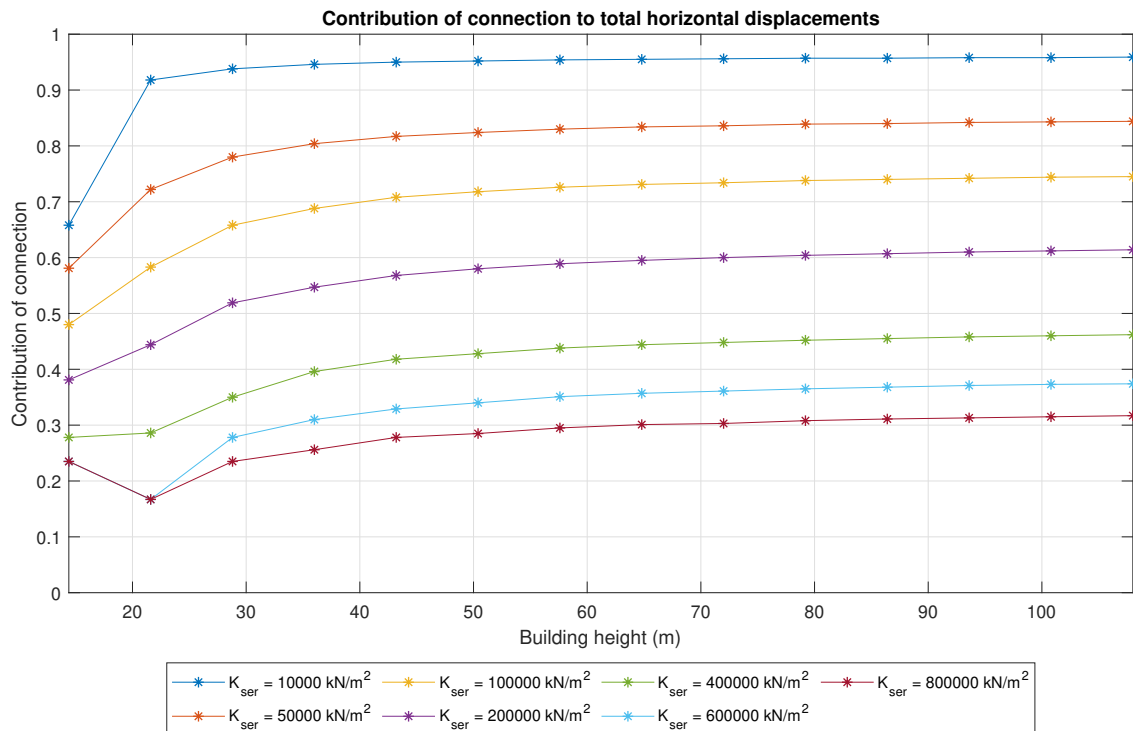


Figure 7.14: Contribution of connection to total horizontal displacements of 10-metres width wall

It is clear that a greater stiffness of the connection results in a smaller contribution to the total horizontal displacements of the top of the wall. For an increase in building height, the contribution of the connection increases slightly, but remains rather constant. For example, a horizontal connection stiffness of  $400000 \text{ kN/m}^2$  contributes 50% to the total horizontal displacements, which implies that the connections doubles the displacements compared to a fully rigid connection.

# 8

## Results of parametric study

In this chapter the parametric study is performed for single and combined stability systems. This is done for the basic design elaborated in section 6.1, which consists of an office building with a width of 32.4 metres and a depth of 28.8 metres.

First the design strategy is explained, whereafter the results regarding dimensions of the structural elements, unity checks for all stresses and dynamic behaviour are elaborated using the specific connection characteristics determined in chapter 6.

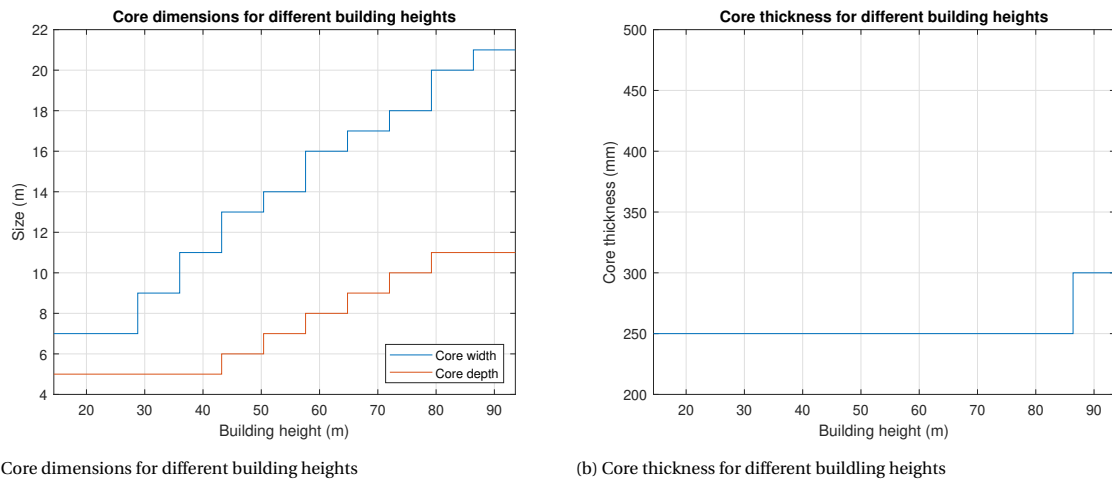
### **8.1. Structure with concrete stability core**

#### **8.1.1. Design strategy**

The dimensions of the core are changed when the horizontal deformations are greater than allowed according to SLS requirements. The width of the core is changed when the maximum deformation in x-direction exceeds the SLS limit and furthermore the depth of the core is changed when the maximum deformation in y-direction exceeds the SLS limit. When the stresses in the core are greater than the resistance of the material, the thickness of the core is increased. Also, when horizontal deformations do not match the SLS requirements, but the core already reached its maximum dimensions, the thickness of the core is increased until the maximum thickness of 450 millimetres is reached. .

#### **8.1.2. Results of parametric study**

The minimum core dimensions for different building heights is displayed in Figure 8.1a, together with the wall thickness in Figure 8.1b.



(a) Core dimensions for different building heights

(b) Core thickness for different building heights

Figure 8.1: Core properties for different building heights

The core keeps its minimum width of 7 metres and depth of 5 metres until a height of 28.8 metres. After that, the core increases in width and depth for each increase in building height to ensure that the building complies with SLS requirements. These dimensions guarantee that the UC in ULS always stays well below 1.0.

A building with a height of 86.4 metres requires a core width of 21 metres and a depth of 11 metres, which corresponds to 24.8% of the total area of the building, which is equal to the limitation stated in section 6.1. When using these core dimensions with the minimum core thickness, the structure will not satisfy the SLS conditions. Therefore, the thickness of the core is increased to 300 millimetres and from this point, only the core wall thickness can further be increased. For a 100.8-meter structure, a thickness of 400 millimetres is reached and the maximum building height is reached, which is equal to 93.6 metres.

The unity checks (UC) are determined by using the calculated mean stresses in the small rectangles at the bottom of the core and the maximum allowed stresses determined in Table 6.11. They are displayed in Figure 8.2. The maximum compressive and tensile stress are determined by taking the minimum and maximum values of the stresses in vertical direction respectively. The shear stress is determined by taking the maximum value of the shear stresses in all directions.

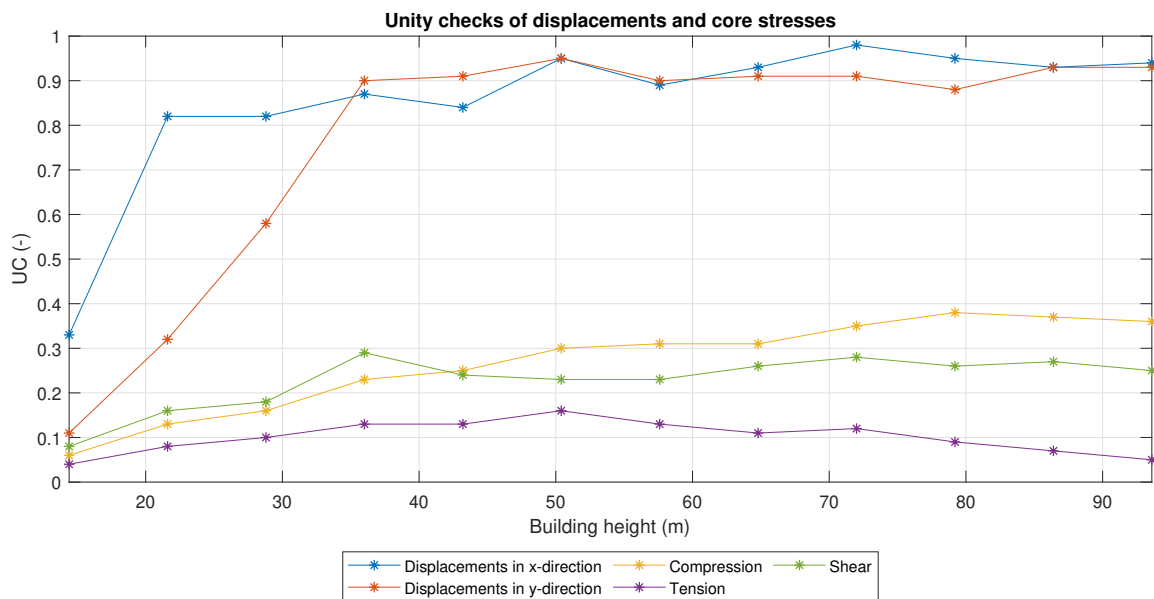


Figure 8.2: Unity check of core stresses for different building heights

The unity check for compression will increase for every increase of building height. The tensile stresses will first increase to a maximum UC of 0.16 for a 50.4-meter building and will then decrease for each increment of the building height. The tensile stresses due to wind loads will increase, while this increment will be compensated by the fact that the self weight of the building raises and the core becomes larger. The shear stresses will increase linear to a maximum value of 0.29. All unity checks will reduce for a building larger than 79.2 metres, due to the fact that the core walls become thicker.

As shown in Figure 8.3, the column dimensions will enlarge from 400 millimetres for a building smaller than 36 metres to a 500x500 millimetres column for buildings of 36 to 64.8 metres. From there on, the column width will remain 600 millimetres until the maximum building height is reached.

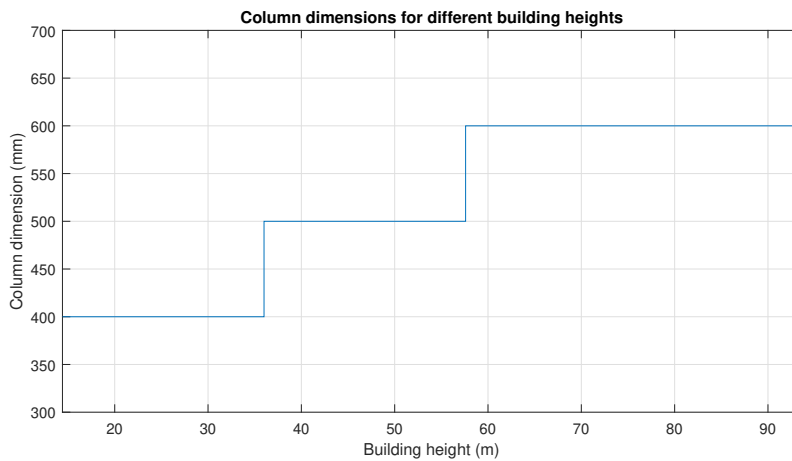
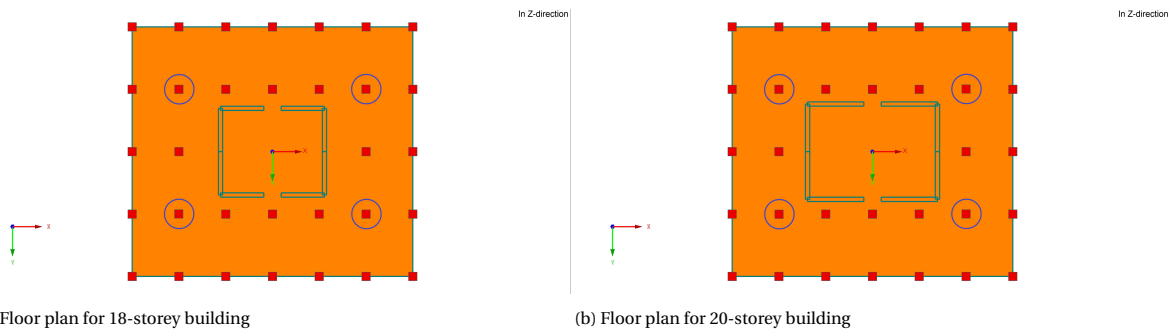


Figure 8.3: Column dimensions for different building heights

The column size is determined by the compression forces acting on these columns. The compression forces increase linearly between a 4-storey and a 20-storey building. From there, a decrease in force can be seen. This is caused by the fact that the core walls are getting closer to the heaviest loaded columns. The core walls will therefore take up more compression forces. This is demonstrated in Figure 8.4a and Figure 8.4b. The heaviest loaded columns are indicated by a blue circle and the different positions of the core walls can be seen.



(a) Floor plan for 18-storey building

(b) Floor plan for 20-storey building

Figure 8.4: Increase in core size for 18-storey and 20-storey building

The natural frequencies together with the corresponding maximum acceleration of the top level are calculated and depicted in Figure 8.5.

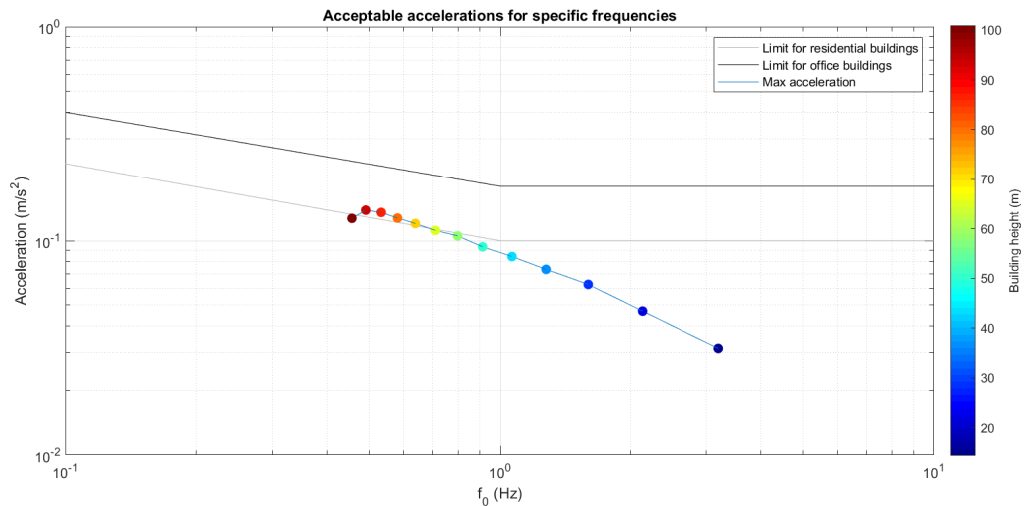


Figure 8.5: Maximum accelerations of top level for different building heights

The natural frequency of the structure depends on the height of the building and will decrease for an increase in height. The maximum acceleration depends on the height of the building, its natural frequency and its mass per unit of height. The acceleration will become greater for an increase in height, but will never exceed the limit for office buildings. Until a height of 64.8 metres, the maximum acceleration is even below the limit for residential buildings.

## 8.2. Structure with CLT stability core

### 8.2.1. Design strategy

The same procedure is used for the CLT stability core as for the concrete core. The only difference is that the thickness of the CLT walls is not changed and will remain 495 millimetres in all cases.

### 8.2.2. Results of parametric study

The minimum core dimensions for different building heights is displayed in Figure 8.6.

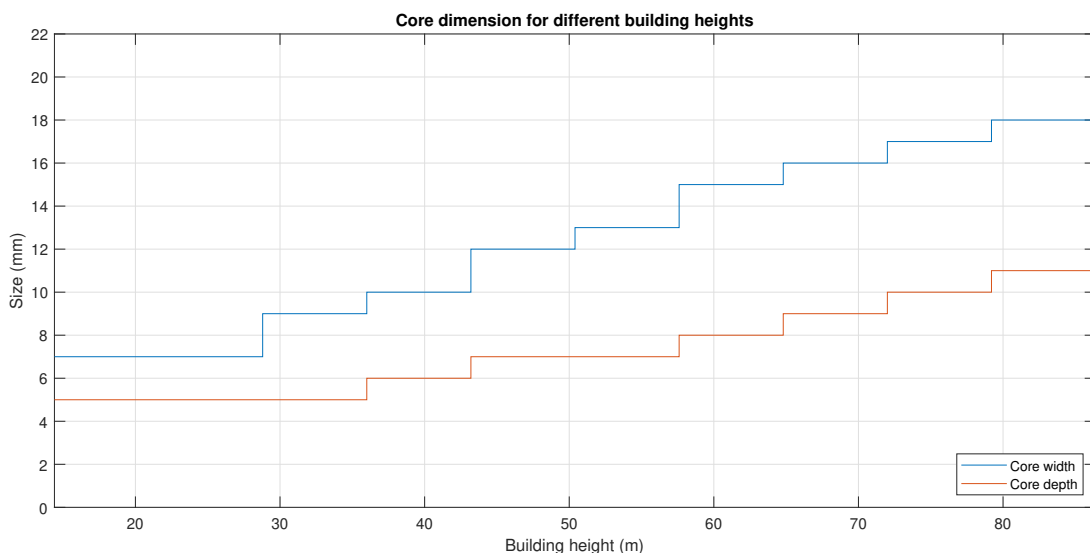


Figure 8.6: Core properties for different building heights

On a similar note as the structure with a concrete core, the dimensions of the CLT core start at the minimum

width of 7 metres and a depth of 5 metres. This is the case until the building reaches a height of 28.8 metres. Subsequently, the core increases in size for each increase in building height. A core width of 19 metres combined with a core depth of 12 metres is needed for a 86.4-metres building and will result in a core area equal to 24.4% of the total area of the building. For a 93.3-metres structure, a core with a width of 19 metres and a depth of 12 metres is not sufficient to meet the SLS requirements. Because the core has a fixed thickness, by reaching the maximum core dimensions the maximum building height is reached as well, which is equal to 86.4 metres.

It should be noticed that the core dimensions found in this particular case are partly determined by the assumed connection characteristics between the core walls. A less rigid connection would mean the the wall elements cooperation is less, which results in greater core dimensions.

The same method is used to determine the core stresses as applied for the concrete core structure. Therefore, the maximum compressive and tensile stress are determined by taking the minimum and maximum values of the stresses in vertical direction respectively. The maximum shear stress in the toothed connection is resolved by taking the maximum value of the stress in horizontal direction and the maximum shear stress in the corners of the core are calculated by using the shear stress. The results are shown in Figure 8.7.

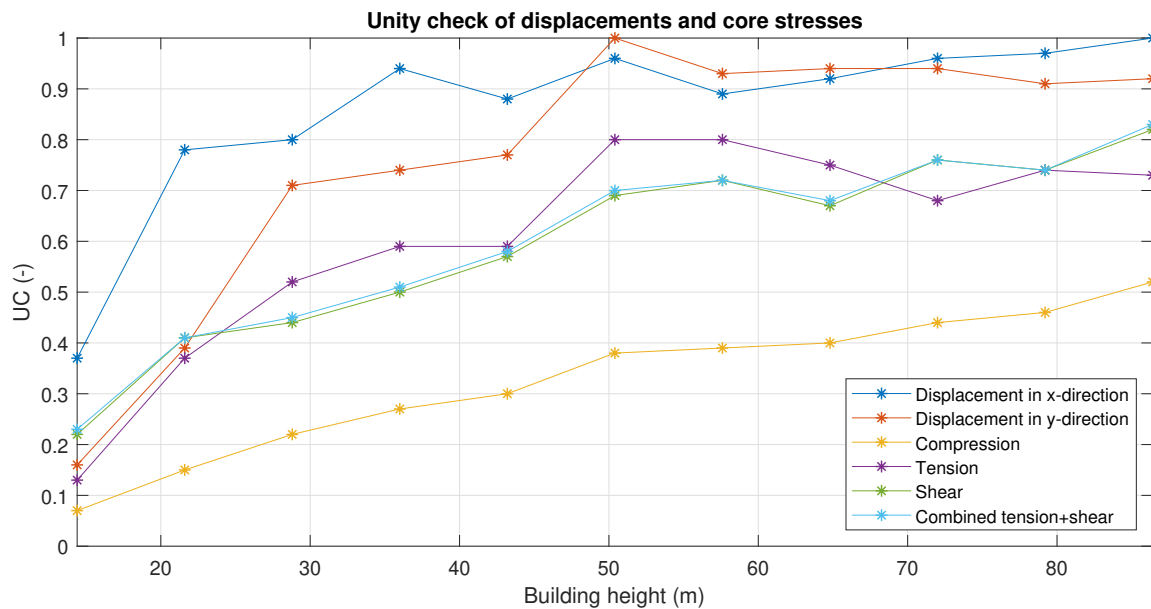
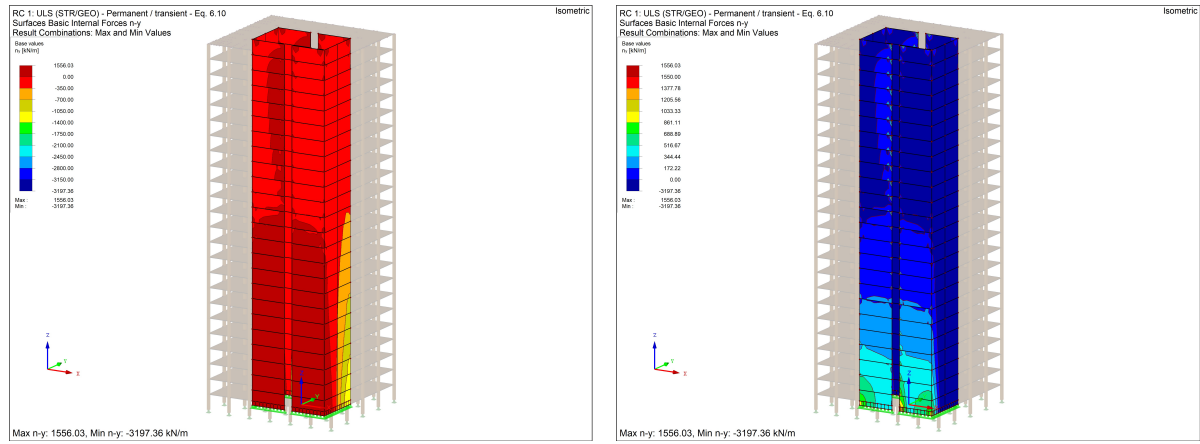


Figure 8.7: Unity check of core stresses for different building heights

The compressive stress will increase linearly for every raise of building height. The unity check for tensile stresses will increase until a building height of 50.4 metres. Thereupon, the tension will decrease. The unity check for tension has a maximum value of 0.73, thus not that many rods are needed as stated in subsection 6.5.2. Furthermore, the tensile stress will be lower for core walls which are located higher in the structure. At those locations, even fewer rods are necessary then needed at the supports. The distribution of the compressive and tensile stresses are displayed in Figure 8.8.



(a) Compressive stresses

(b) Tensile stresses

Figure 8.8: Stresses in the core walls

The unity checks for the shear toothed and shear corner connections increase for each increment of building height. All unity checks will stay below 1.0 and the dimensions of the cores are not adjusted to meet the requirements in ULS, they are only based on the maximum allowed horizontal displacement of the structure in SLS. This means that for transferring the shear forces in the corners, fewer screws are required than assumed and the spacing between the screws can therefore be increased. However, this causes a reduction of the connection stiffness and thus can result in additional deflection of the structure. This implies that the minimum spacing between the screws is still necessary, because the maximum building height is determined by the deflection of the building and thus the connection requires its rigidity.

The columns will have a width and depth of 400 millimetres for a building smaller than 36 metres, thereafter the column size increases to 500 millimetres for a building with a height between 36 and 57.6 metres and reaches a maximum of 600 millimetres for a building higher than 57.6 metres. Thus, the column sizes are almost similar to those of the concrete core system. This is demonstrated in Figure 8.9.

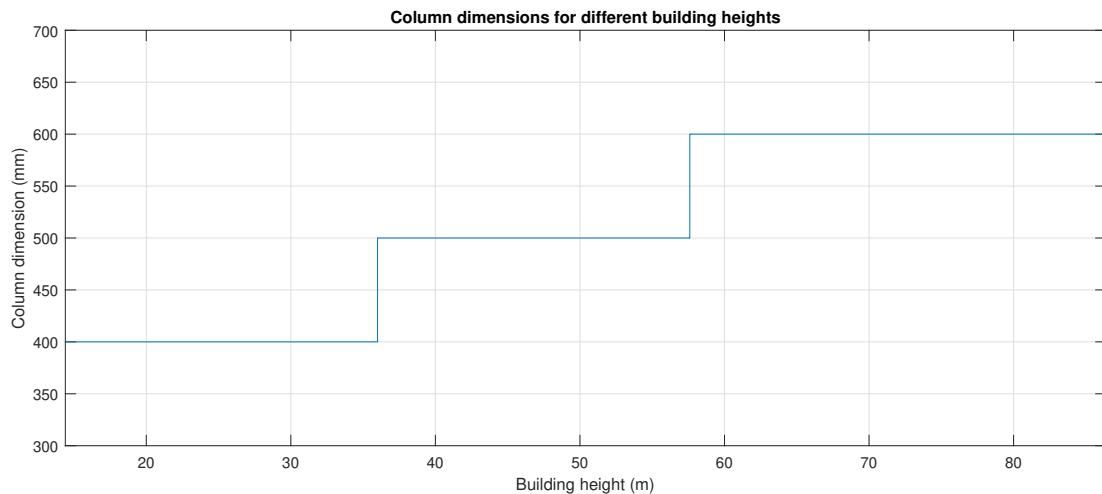


Figure 8.9: Column dimensions for different building heights

The natural frequencies and the corresponding maximum acceleration of the top level are calculated by using the mass, height, depth and width of the structure, displayed in Figure 8.10.

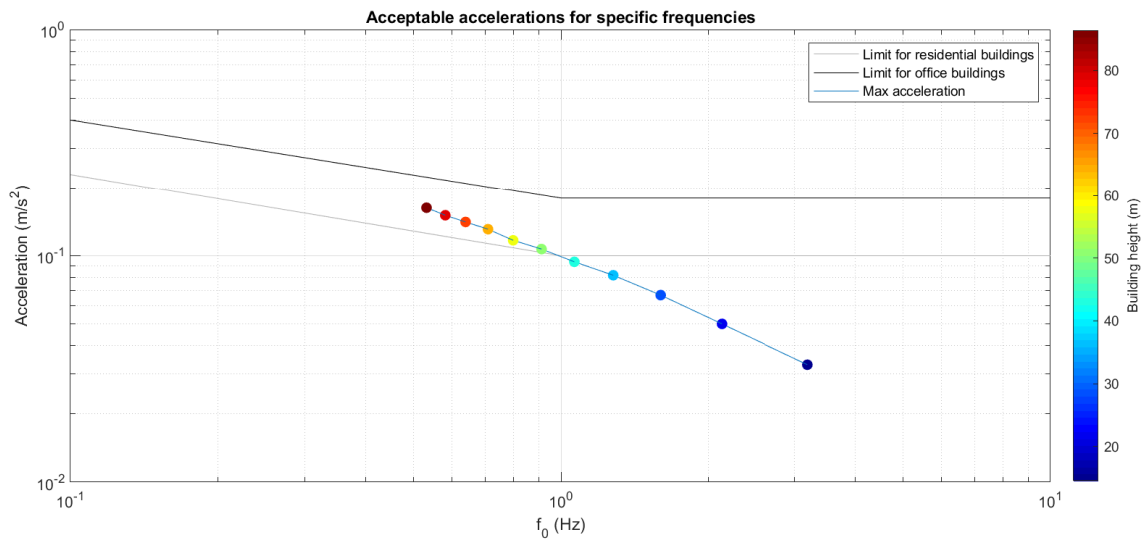


Figure 8.10: Maximum accelerations of top level for different building heights

The structure with CLT core walls will have a lower mass compared to a building with concrete core walls, but will have the same eigenfrequency using the same building height. Consequently, the maximum acceleration will also be higher. However, in all cases the building’s acceleration stays below the limit for office building.

### 8.3. Structure with diagrid using glued-in threaded rods connections

#### 8.3.1. Design strategy

To prevent that checking the feasibility of a diagrid system becomes a time-consuming process because of the presence of many variables, an optimum diagonal angle is used, which is determined by Panchal et al [46].

Panchal et al. investigated a building with a 36x36m plan for which displacement, storey drift, shear force and material usage are checked for different building heights and several diagonal angles. A building with 24, 36, 48 and 60 floors is examined with diagonal angles varying between 50.2 degrees and 82.1 degrees. The angle is defined as depicted in Figure 8.11.

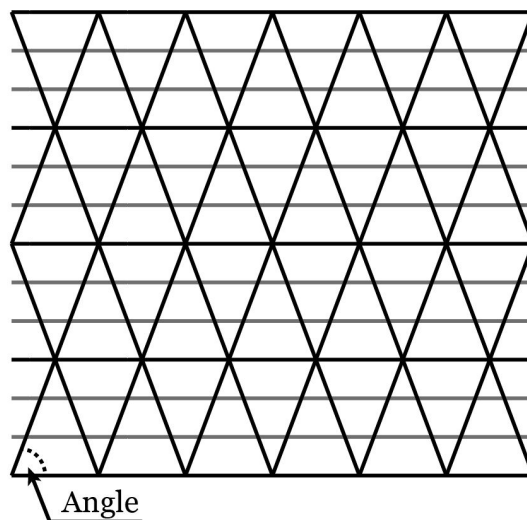


Figure 8.11: Definition of the angle of a diagonal

Panchal et al. concluded that a diagonal angle between 65 and 75 degrees insures less top level displace-

ment, inter-storey drift, storey shear and material consumption. Therefore, for investigating the feasibility of a structure with a diagrid, an fixed angle of 70 degrees is used.

Diagrids consisting of diagonals spanning 4, 6 and 8 storeys are investigated. For example, in Figure 8.11, the diagonal spans 6 storeys. Consequently, the inputs used for the different diagrids are defined in Table 8.1.

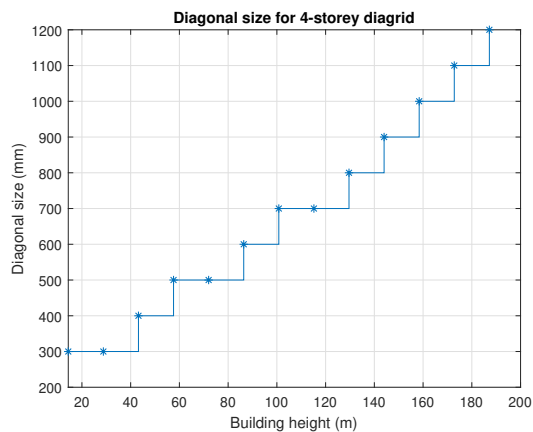
Table 8.1: Inputs for different diagrids

Diagrid type	Storeys per diagrid cross	Diagonal crosses in width	Diagonal crosses in depth
4-storey diagonals	4	6	6
6-storey diagonals	6	4	4
8-storey diagonals	8	3	3

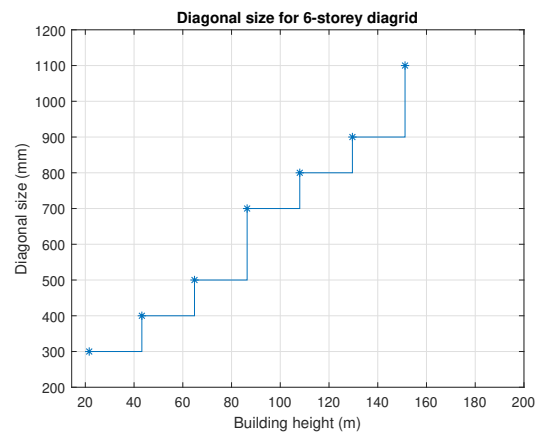
The dimensions of the diagonals are increased when the forces in the diagonals are greater than the resistance of the connection in ULS or when the building does not satisfy the requirements regarding deflections in SLS. The maximum building height is reached when the diagonals cannot increase in size, thus have a width and depth of 1200 millimetres.

### 8.3.2. Results of parametric study

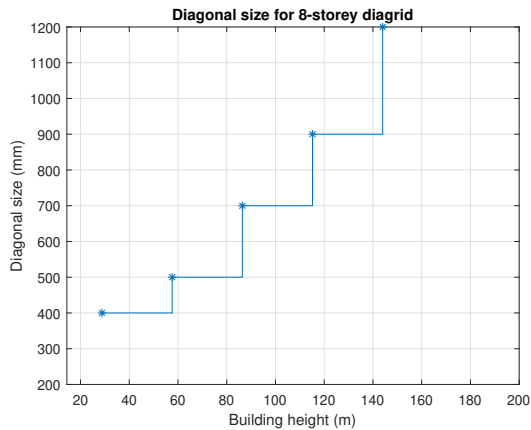
First the required diagonal size per building height is examined. The results for each diagrid type are depicted in Figure 8.12. For each graph, a different starting point can be observed. This is due to the fact that a minimum building height is required for each type of diagrid. For example, for an 8-storey diagrid, a minimum of 8 stories is required, which is equal to 28.8 metres.



(a) Diagonal size for 4-storey diagrid



(b) Diagonal size for 6-storey diagrid

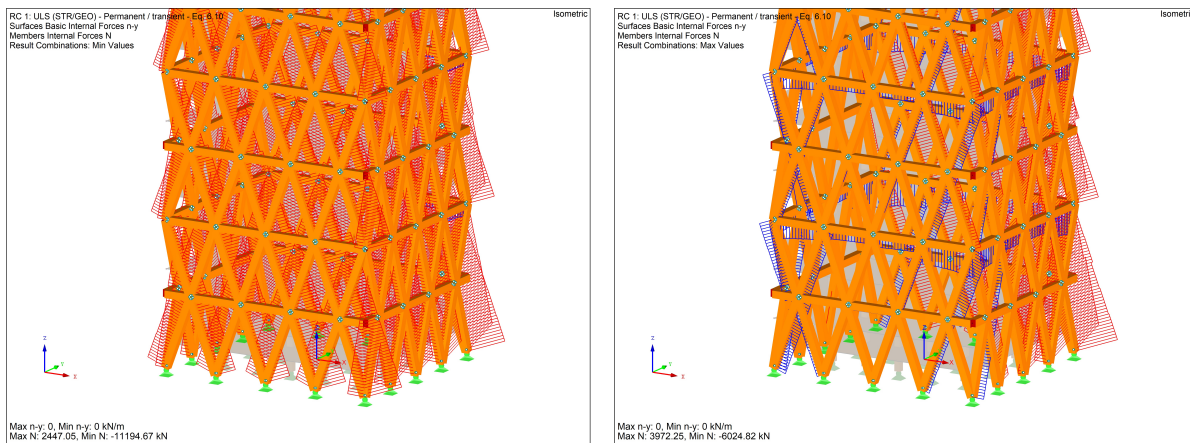


(c) Diagonal size for 8-storey diagrid

Figure 8.12: Diagonal size for each diagrid

For the 4-storey diagrid, a minimum diagonal size of 300 millimetres is required for a building height up to 28.8 metres. The dimensions will increase approximately 100 millimetres for each building height increment of 14.4 metres. The maximum diagonal width of 1200 millimetres is reached for a structure with a height of 158.4 metres. Only a 1100 millimetres diagonal is necessary for a 6-storey diagrid to reach its maximum height of 151.2 metres. An 8-storey diagrid has a top elevation of 144 metres.

During the process of examining the different building heights, the model gave feedback regarding diagonal dimensions. It is interesting to notice that when the feedback states that a greater dimension is necessary, this is always based on the fact that the occurring tensile forces in the diagonals exceed the maximum tensile resistance of the connection. In Figure 8.13 the enveloping forces are shown for all load combinations. It can be seen that the tensile forces occur in both the horizontally and vertically oriented diagonals. Thus, an increase in dimensions was never caused by an exceedance of the compression resistance or displacement limitations.



(a) Minimum forces in diagonals

(b) Maximum forces in diagonals

Figure 8.13: Forces in diagonals

Each diagrid type show the same column dimensions for each building height. Therefore the results are combined in Figure 8.14 as a single plot. It can be seen that the columns have a minimum width of 400 millimetres for a 28.8 metres high building and will increase to 800 millimetres for a building height between 115.2 and 144 metres. For the maximum building height of 187.2 metres the column has a width and depth of 1000 millimetres. It should be noticed that these column dimensions are greater than those found for the same building heights using a core system.

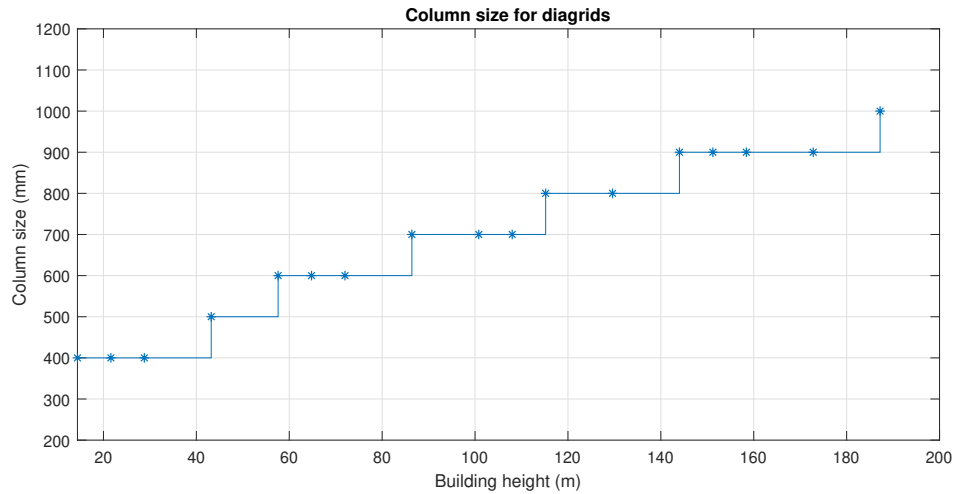
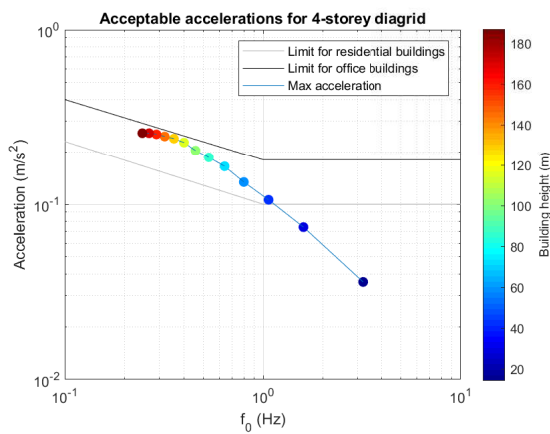
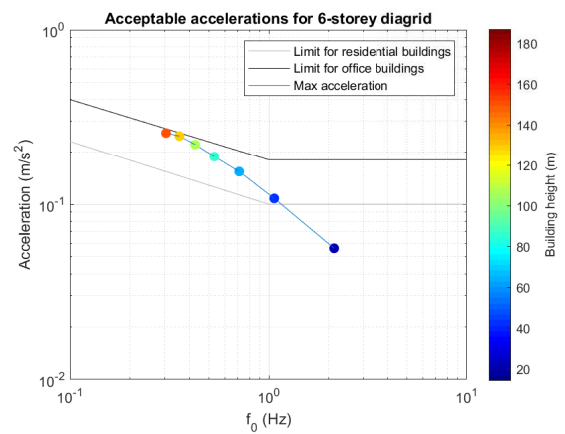


Figure 8.14: Column dimensions for all diagrid types

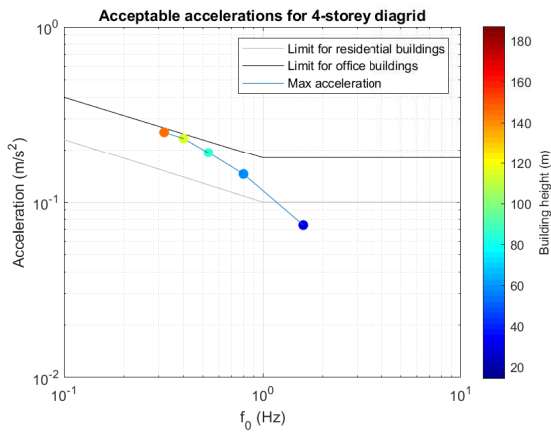
The natural frequencies and the corresponding maximum acceleration of the top level are determined for each diagrid type, which can be seen in Figure 8.15. Compared to structures with a stability core, the accelerations are higher due to a lower building mass. Although they are higher and approach the limits for office buildings, the acceleration for each height will remain below the maximum allowed accelerations.



(a) Max acceleration for 4-storey diagrid



(b) Max acceleration for 6-storey diagrid



(c) Max acceleration for 8-storey diagrid

Figure 8.15: Maximum acceleration of the top level for each diagrid type

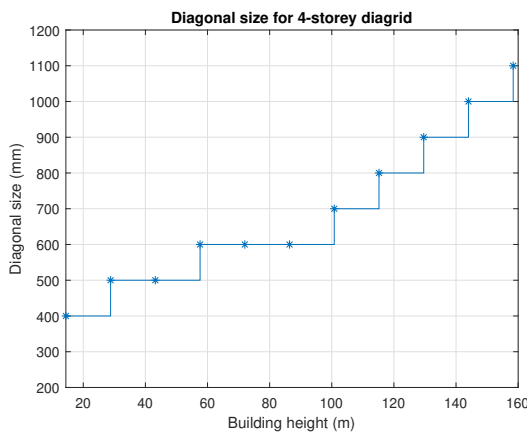
## 8.4. Structure with diagrid using steel plates and dowel connections

### 8.4.1. Design strategy

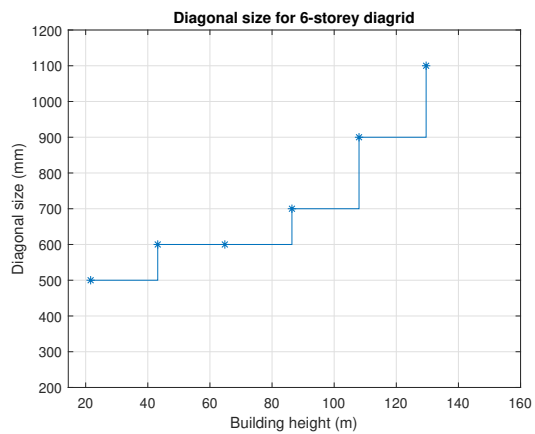
The same procedure is followed as described in subsection 8.3.1.

### 8.4.2. Results of parametric study

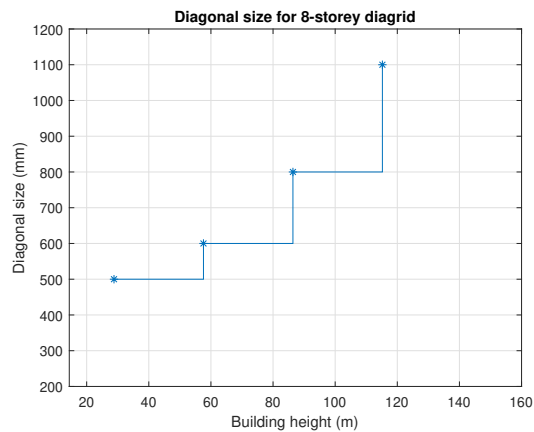
The required diagonal dimensions are shown in Figure 8.16 for each diagrid type.



(a) Diagonal size for 4-storey diagrid



(b) Diagonal size for 6-storey diagrid



(c) Diagonal size for 8-storey diagrid

Figure 8.16: Diagonal size for each diagrid

The diagonals have a minimum width of 400, 500 and 500 millimetres for a 4-, 6- and 8-storey diagrid respectively. These dimensions are greater compared to a diagrid with glued-in threaded rods, because the dimensions for these building heights are solely determined by the compression force in the diagonals and the compression resistance of connections with steel plates and dowels is considerably lower than the connection with glued-in threaded rods.

For buildings higher than approximately 100 metres, not the compression force in the member will be decisive, but the deflection of the building determines the dimensions of the diagonal. This differs from the diagrid structure using glued-in rods connections, where the tension forces in the diagonals are decisive for the size. This leads to larger cross sections compared to the other diagrid system. This results in maximum overall heights of the structures which are lower than those of the diagrids with glued-in rods connections. With a 4-storey diagrid, a maximum height of 158.4 metres can be reached. A 6-storey diagrid has a lower maximum height with 129.6 metres. An elevation of 115.2 metres can be reached with an 8-storey diagrid. All diagrid types require a diagonal width of 1100 millimetres for reaching the maximum height.

It should be noticed that a conservative assumption is made regarding the stiffness of the diagonals. A reduction of the Young's modulus of 30% is used, which is the average reduction for a member with a length of 3600 millimetres. However, the diagonals used in this study have greater lengths and thus this reduction can be less. The dimensions found in this parametric study are based on this reduction and therefore this assumption has influence on the diagonal dimensions.

The same column dimensions are observed as for the diagrid system with glued-in rods connections. The same minimum width of 400 millimetres is used for a building lower than 43.2 metres. The column reaches dimensions of 900 by 900 millimetres for the maximum height of 158.4 metres.

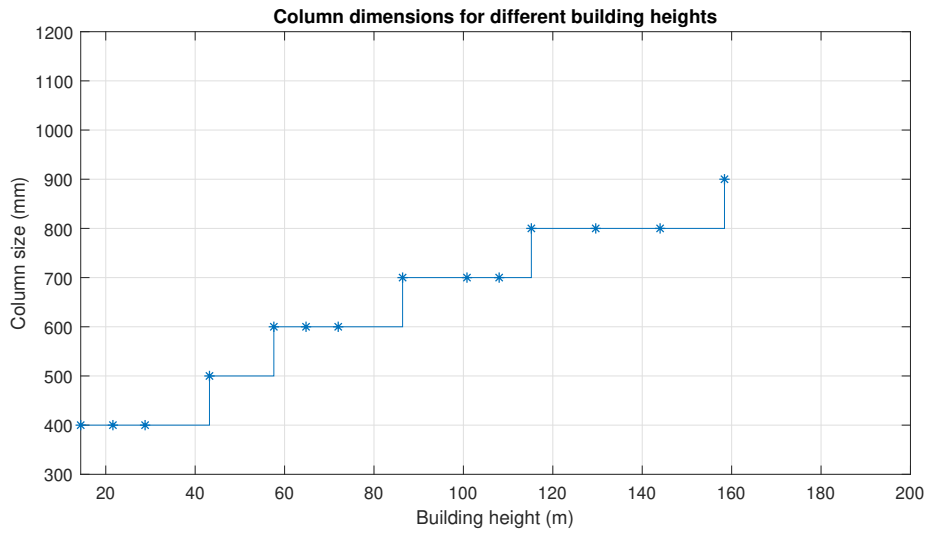
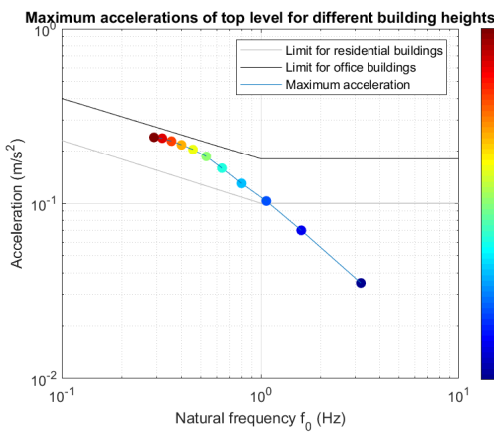
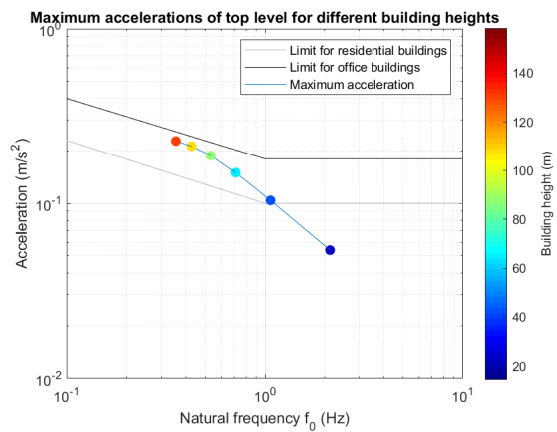


Figure 8.17: Column dimensions for different building heights

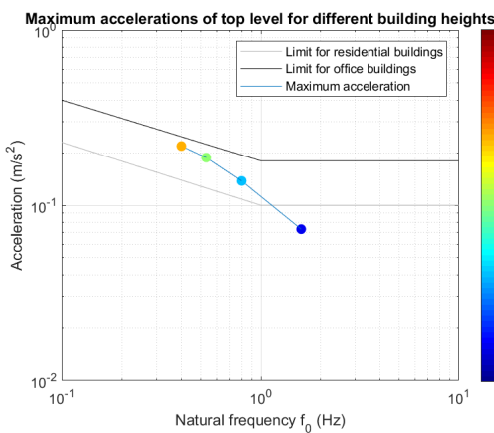
The maximum accelerations of each diagrid type are shown in Figure 8.18. It can be seen that these accelerations are similar to those found for the diagrid system with glued-in rods connections.



(a) Max acceleration for 4-storey diagrid



(b) Max acceleration for 6-storey diagrid



(c) Max acceleration for 8-storey diagrid

Figure 8.18: Maximum acceleration of the top level for each diagrid type

## 8.5. Structure with tube system

### 8.5.1. Design strategy

The width and depth of the building and the thickness of the facade elements are fixed. Thus, in addition to the dimensions of the columns, there are no other variables which are varied during the parametric study. The maximum height is reached when the SLS requirements are exceeded or the stresses in the facade elements become too high.

### 8.5.2. Results of the parametric study

First the column dimensions, shown in Figure 8.19, are examined.

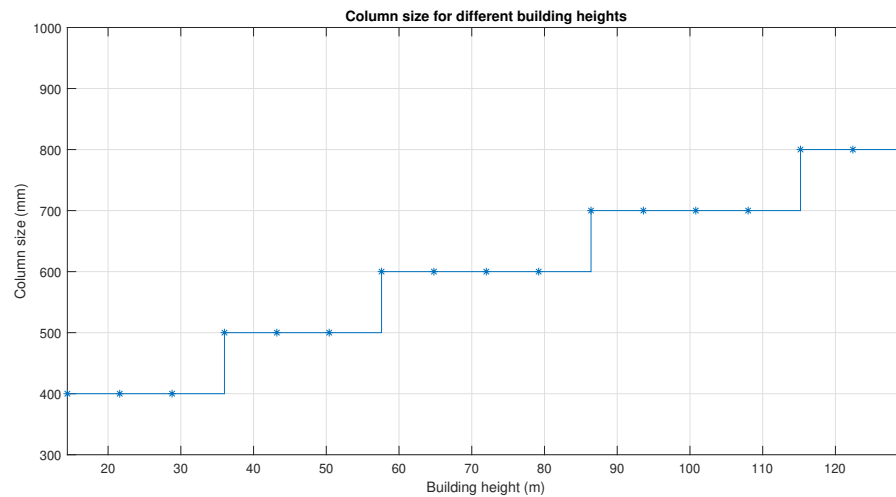


Figure 8.19: Column size for different building heights

The column width starts at 400 millimetres and will increase approximately 100 millimetres per 25 metres building height increment. They will reach a maximum width of 800 millimetres for a structure higher than 115.2 metres. The maximum building height found using this stability system is equal to 129.6 metres.

The maximum stresses which occur in the facade elements are checked. This is done for compression, tension and shear stresses, where for the shear stresses a distinction is made between the horizontal toothed connection and the connection in the corners of the building. The results are shown in Figure 8.20.

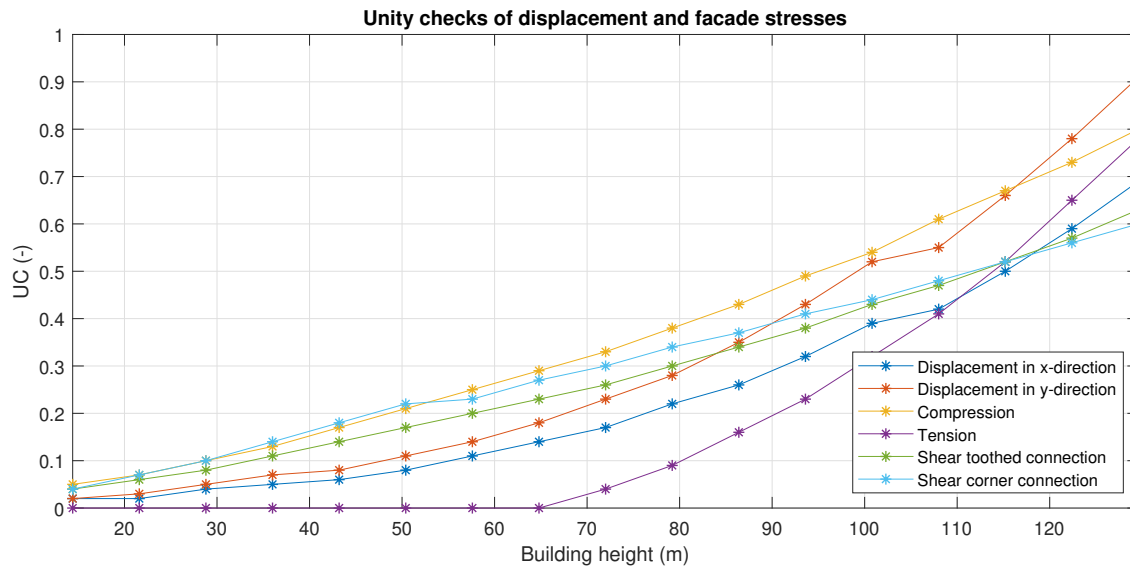


Figure 8.20: Unity checks of stresses

It is clear that all stresses are below 1.0 and the stresses are not decisive on the maximum height which can be reached using this stability system. All stresses will increase quadratically with an increment in height. The unity check for compression has a maximum value of 0.80. The unity check for tension will be zero until a height of 64.8 metres, because the self weight of the structure will eliminate the tensile stresses due to wind loads. It will eventually reach a maximum value of 0.78. This means that the amount of rods which transfer the tensile forces is not necessary and can be lowered. Furthermore, the tensile stresses between the elements will be the highest in the lower part of the structure, thus the amount of rods needed in the upper part of the structure can be lower than the quantity needed in the lower part of the building. Also the compressive stresses will be higher in the lower part of the facade, but this has no effect on the number of fasteners needed. The distribution of the compressive and tensile stresses can be seen in Figure 8.21.

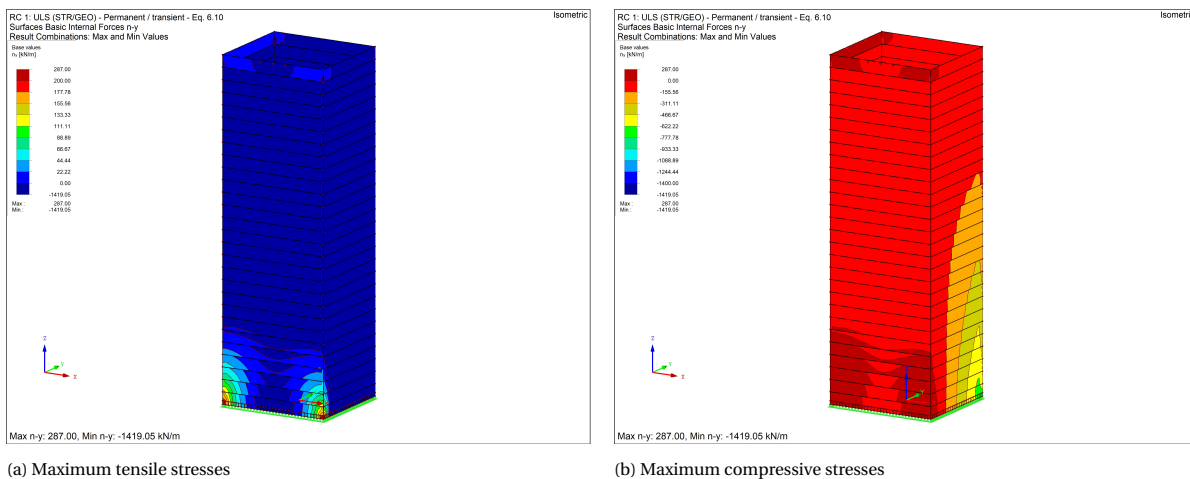


Figure 8.21: Stresses in facade

The toothed connection can easily transfer the shear forces between the elements, for which a maximum unity check of 0.63 is found. Also the shear connection in the corners of the building are capable of transferring all shear forces with a unity check of 0.51 for a building height of 129.6 metres. Therefore, the minimum spacing between the screws is not necessary regarding ULS requirements. However, an increase in spacing between the screws will cause a decrease of the stiffness of this connection and thus can cause extra deflection of the structure.

The natural frequency and the corresponding maximum acceleration of the top level are calculated and depicted in Figure 8.22. It can be seen that the acceleration will increase quadratically, but will never exceed the limits stated for an office building. Until a height of 50.4 metres, the accelerations also satisfy the requirements for residential buildings. The structure has the lowest maximum acceleration for each building height compared to all other system types. The mass of the building is the highest of all systems investigated.

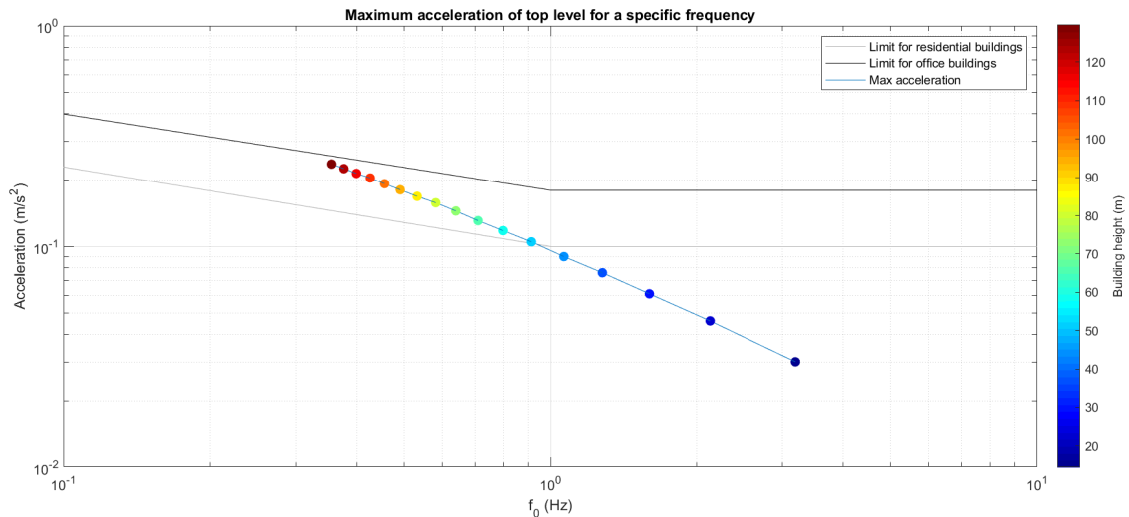


Figure 8.22: Max acceleration of the top level

## 8.6. Structure with combined stability systems

Instead of using a single stability systems, also a combination of different systems can be used. A CLT stability core can be either used with a tube system or diagrid system. The diagrid system cant be used with the diagrid system because both systems are present in the facade.

To check which maximum building heights can be reached with combined systems, the maximum core dimensions of 19 by 12 metres are used, which were found during the CLT stability core study, while the diagonals will have its maximum dimensions of 1200 by 1200 metres. The maximum building height is reached when either the diagonals exceed their maximum resistance in ULS, the stresses in the core or facade are too high or the displacements of the structure exceed the requirements in SLS. The results are shown in Table 8.2.

Table 8.2: Maximum height of combined stability systems

Number	Type of stability systems	Max height (m)
1	Tube + CLT stability core	151.2
2	4-storey diagrid with glued-in rods connection + CLT stability core	187.2
3	6-storey diagrid with glued-in rods connection + CLT stability core	172.8
4	8-storey diagrid with glued-in rods connection + CLT stability core	144
5	4-storey diagrid with steel plates and dowels connection + CLT stability core	172.8
6	6-storey diagrid with steel plates and dowels connection + CLT stability core	151.2
7	8-storey diagrid with steel plates and dowels connection + CLT stability core	144

Combining 2 stability systems ensures an increase in the maximum building height of at most 28.8 metres with an 8-storey diagrid with steel plates and dowels connections, 21.6 metres for 6-storey diagrid systems and 14.4 metres for a tube system combined with a CLT stability core. No increase in maximum height is observed for a 4- and 8-storey diagrid with glued-in rods connections when used with a CLT stability core.

For the core and facade walls the unity checks for different stresses are calculated if present, which can be found in Figure 8.23.

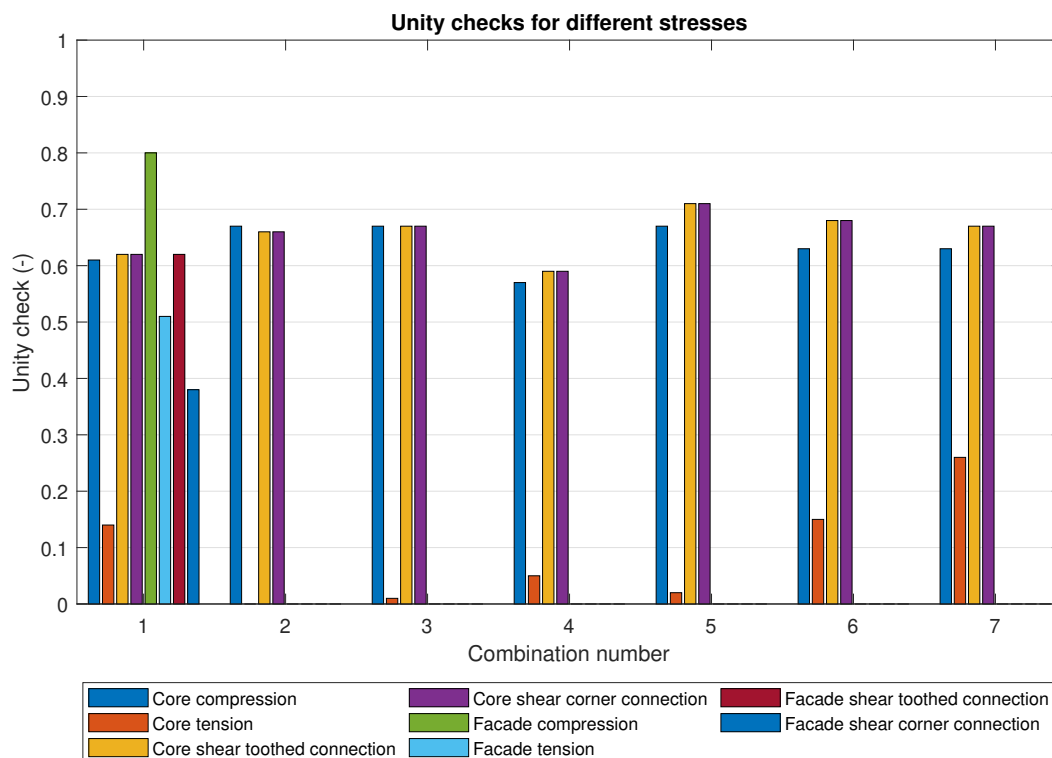


Figure 8.23: Unity checks for different stresses

All unity checks are far below 1.0, with a maximum value of 0.80 for the compression in the facade. What stand out are the unity checks for tensile stresses. These are considerably higher for a diagrid with steel plates and dowels connections than for a diagrid with glued-in rods connections. This is caused by the lower stiffness of the diagonals when using steel plates and dowels, which causes the core to transfer more forces. In the core walls of a 4-storey diagrid with glued-in rods connections there are no tensile stresses present at all. The requirements in SLS ensure that the maximum dimensions of the diagonals of 1200 by 1200 millimetres are needed, while these cross-sections are not necessary to transfer the occurring forces.

For all combinations, the maximum acceleration of the top level is calculated. This can be seen in Figure 8.24. It is clear that all structures meet the requirements for an office building.

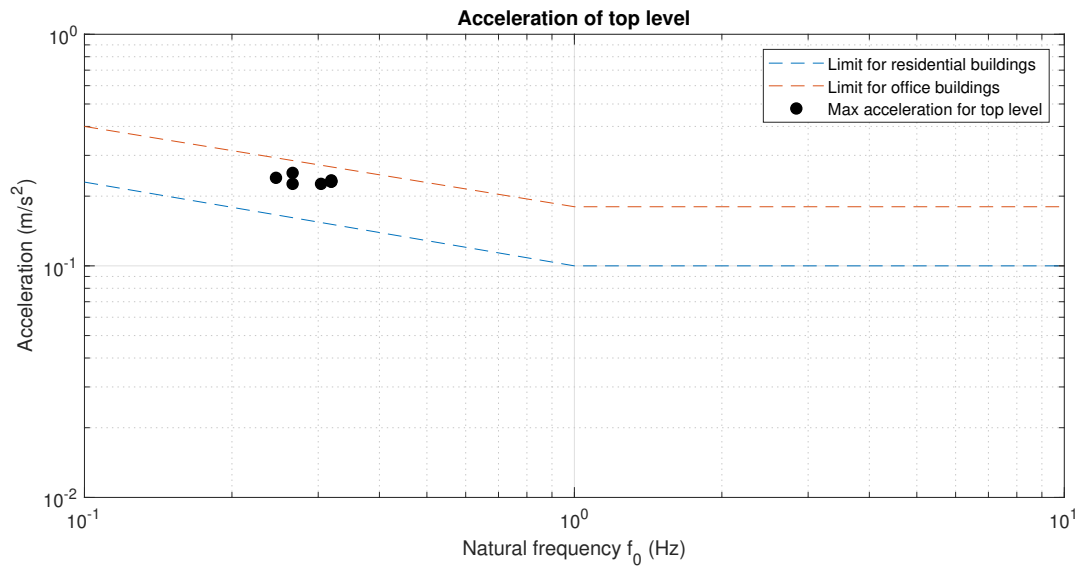


Figure 8.24: Maximum acceleration of the top level

# 9

## Comparison between the stability systems

In this chapter, the results found in chapter 8 are compared regarding maximum height of the structures and material usage. Also, the results of this thesis are compared to results found by other reports.

### 9.1. Maximum building height and slenderness

The maximum building heights for the different stability systems, which are found in chapter 8, are graphically summarized in Figure 9.1.

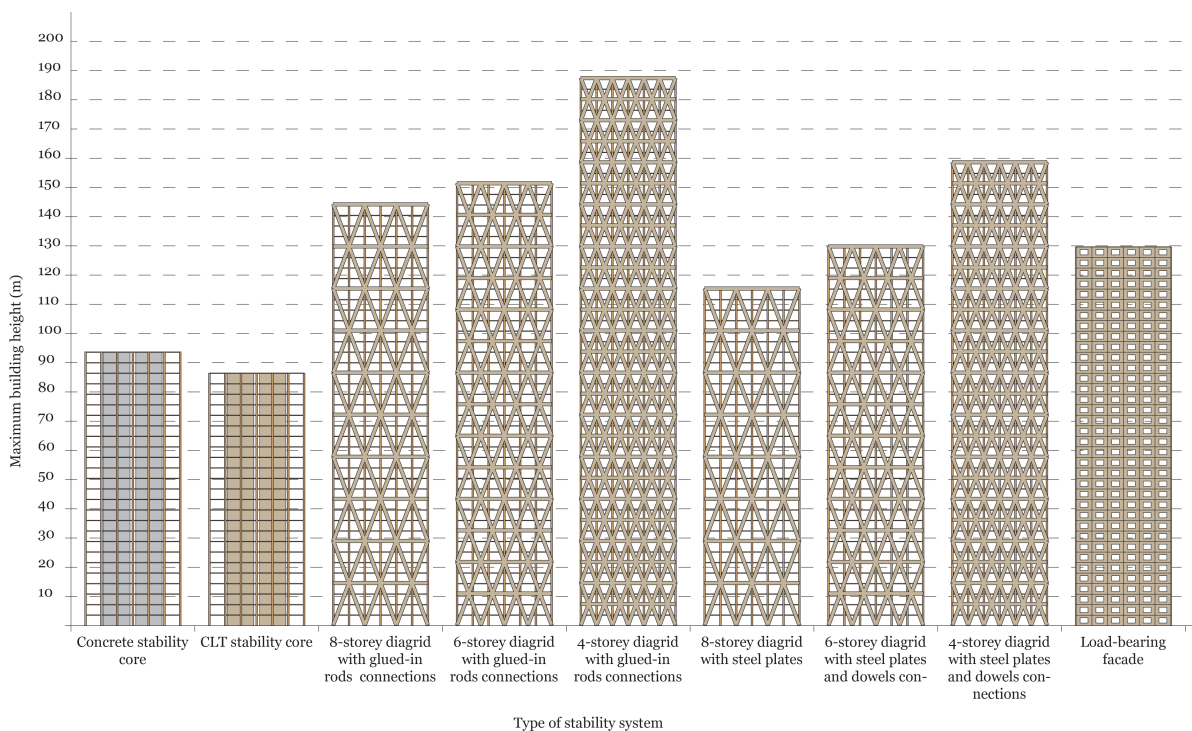


Figure 9.1: Maximum building height for each type of stability system

The lowest building height can be reached using a CLT stability core, which is equal to 86.4 metres. The tube system has a better performance regarding building height with a maximum of 129.6 metres. If a diagrid system is used, diagonals spanning fewer floors will give a greater maximum height. Thus, the 4-storey diagrid can reach higher altitudes than an 8-storey diagrid, with 187.2 and 144 metres respectively. In addition, the use of glued-in rods connections between the diagonals will ensure a greater height than when connections with steel plates and dowels are used.

A combination of stability systems is briefly examined and discussed in chapter 8. A combination of a CLT stability core with either a diagrid or tube system is looked at. The results are summarized in Figure 9.2.

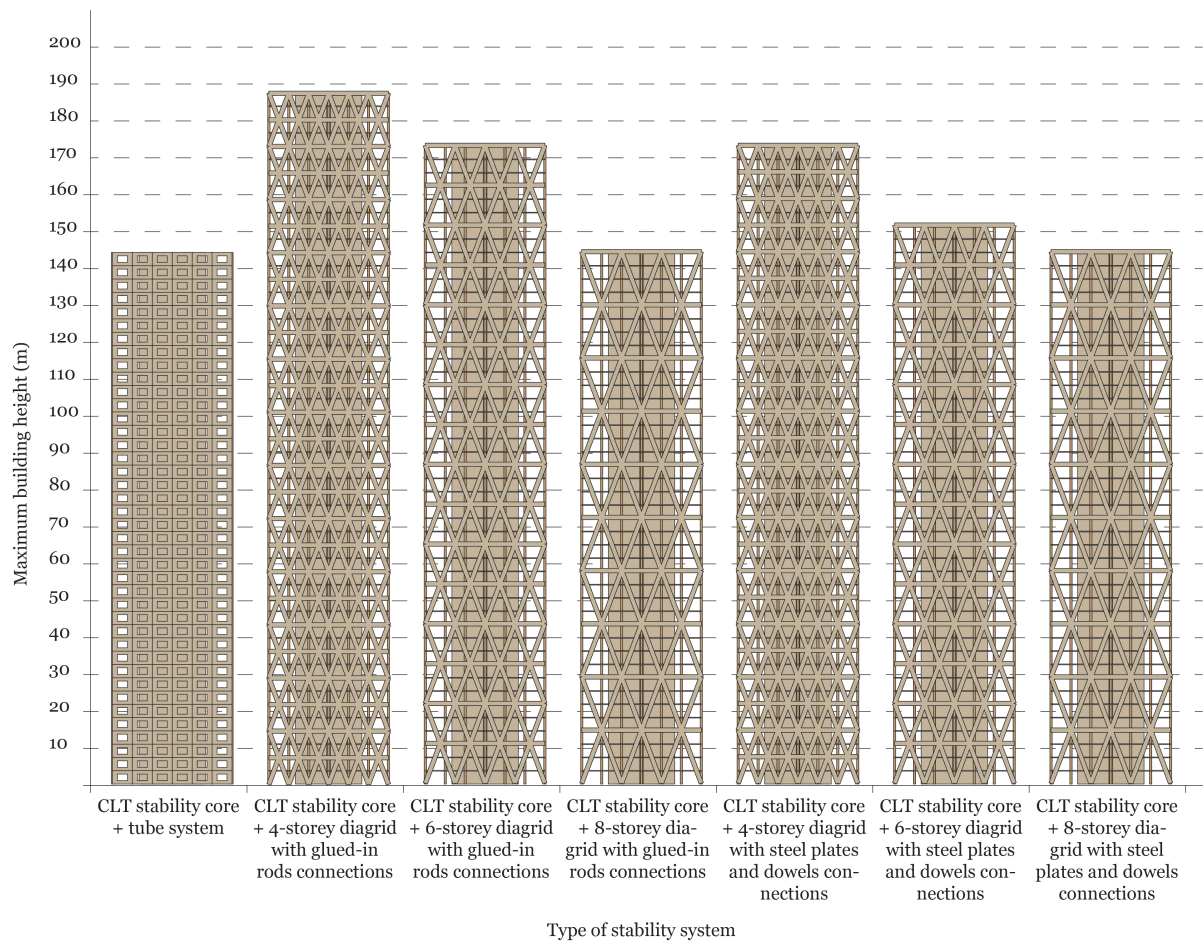


Figure 9.2: Maximum building height for combinations of stability systems

For some combined systems, additional building height can be achieved compared to single stability systems. The greatest increase in height can be observed for an 8-storey diagrid with steel plates and dowels connections with an increment of 28.8 metres. Both 6-storey diagrid systems reach an extra elevation of 21.6 metres. When combining a CLT stability core with a tube system or a 4-storey diagrid with steel plates and dowels, a raise of 14.4 metres can be seen. For a 4- and 8-storey diagrid with glued-in rods connections, no additional height is achieved by combining it with a CLT stability core system.

The width and depth of the building influences the maximum building height. To eliminate this influence, the slenderness of the building can be used, which is defined as the height divided by the lesser of the width and depth of the building. Thus, the height is divided by 28.8 metres.

The values of the slenderness of each stability system are shown in Table 9.1 and Table 9.1.

Table 9.1: Maximum building height and slenderness of single stability systems

Type of stability system	Max height (m)	Slenderness (-)
Concrete stability core	100.8	3.5
CLT stability core	86.4	3.0
8-storey diagrid with glued-in rods connections	144	5.0
6-storey diagrid with glued-in rods connections	151.2	5.25
4-storey diagrid with glued-in rods connections	187.2	6.5
8-storey diagrid with steel plates and dowels connections	115.2	4.0
6-storey diagrid with steel plates and dowels connections	129.6	4.5
4-storey diagrid with steel plates and dowels connections	158.4	5.5
CLT load-bearing facade	129.6	4.5

Table 9.1: Maximum building height and slenderness of combined stability systems

Type of stability systems	Max height (m)	Slenderness (-)
CLT load-bearing facade + CLT stability core	144	5.0
8-storey diagrid with glued-in rods connection + CLT stability core	144	5.0
6-storey diagrid with glued-in rods connection + CLT stability core	172.8	6.0
4-storey diagrid with glued-in rods connection + CLT stability core	187.2	6.5
8-storey diagrid with steel plates and dowels connection + CLT stability core	172.8	6.0
6-storey diagrid with steel plates and dowels connection + CLT stability core	151.2	5.25
4-storey diagrid with steel plates and dowels connection + CLT stability core	144	5.0

A minimum slenderness of 3.0 for a CLT stability core system and a maximum of 6.5 for a 4-storey diagrid with glued-in rods connections can be observed.

## 9.2. Timber material usage

It is also convenient to compare the different systems by looking at the total material usage to reach certain building heights. First a comparison is made between the total timber volume of each system, then the same is done for the total steel mass used for all connections.

The total usage of timber volume for each stability system is determined by calculating the total volume of all columns, floor slabs and components of the stability system, such as walls and diagonal members. The results are displayed in Figure 9.3.

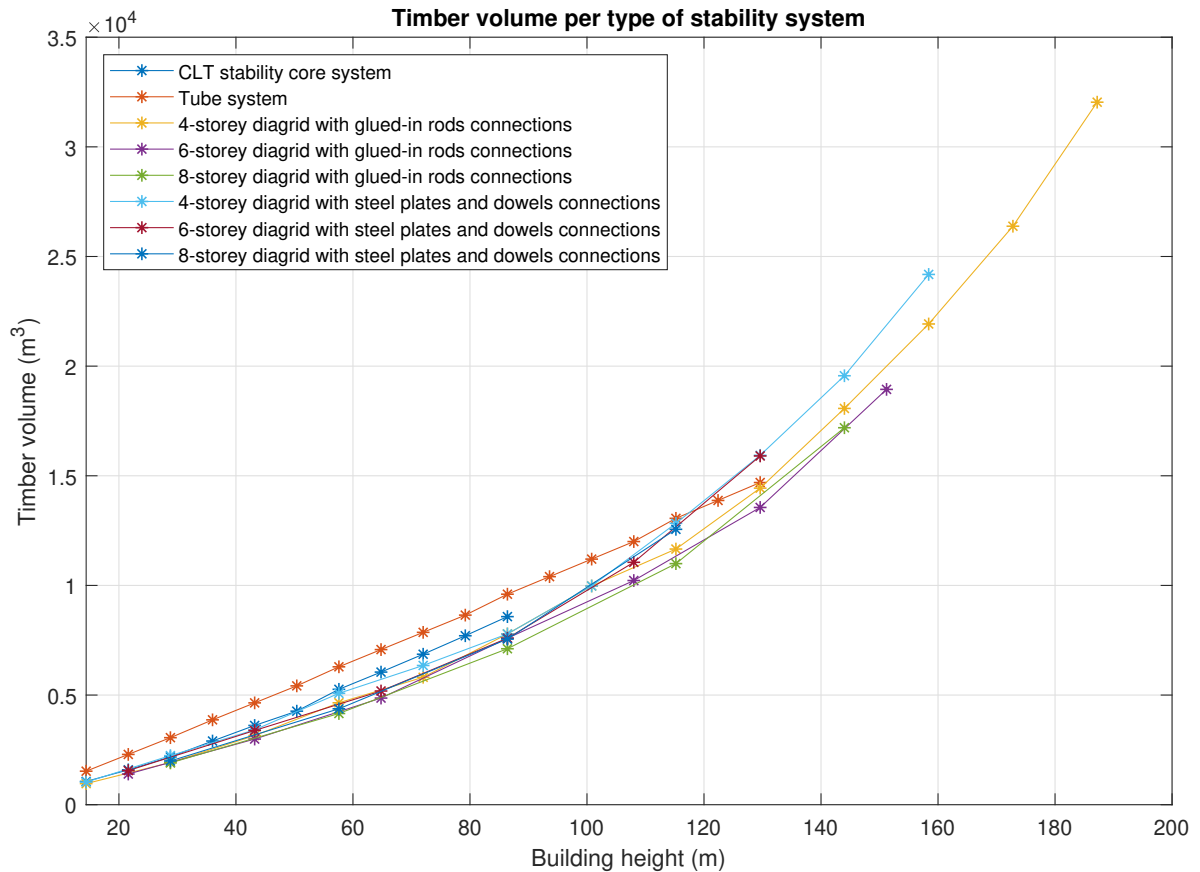


Figure 9.3: Volume of timber per type of stability system

All systems, except the tube system, show a quadratic increment in timber volume with an increase in height. The CLT stability core and tube system show the largest volume in timber, while for lower building heights the material usage of the diagrid systems are similar to each other. For elevations greater than 100 metres, the diagrid system with steel plates and dowels connections have a greater timber volume than the diagrids with glued-in rods connections. The tube system will then have a smaller material usage than some diagrid structures.

Because the timber volume consists of different components, it is interesting to look at the contribution of the different parts of the structure to the total volume of the building. A comparison is shown in Figure 9.5, which represents a structure with a height of 75.6 metres.

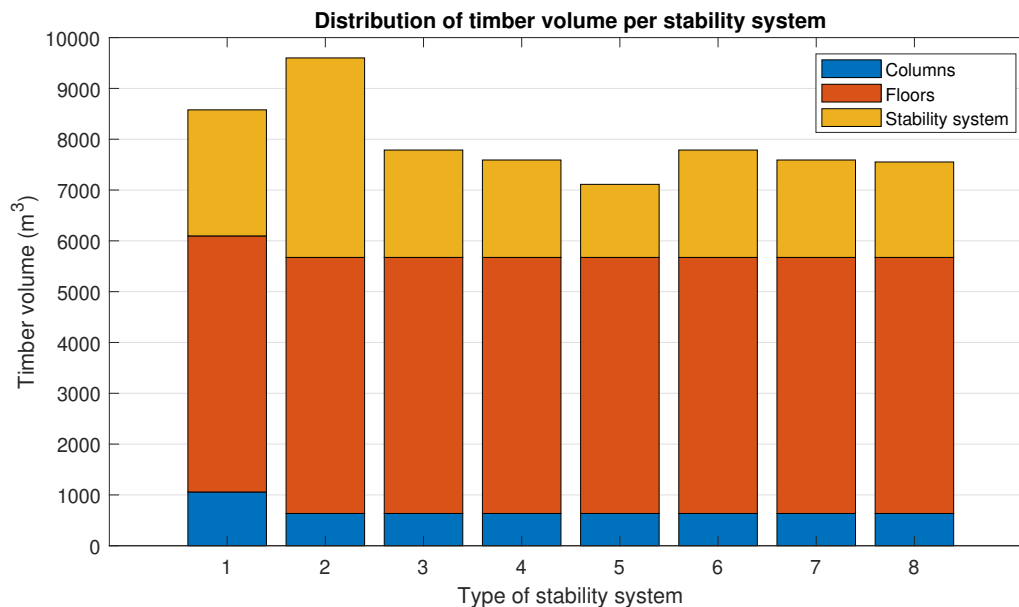


Figure 9.4: Distribution of volume for different type of stability systems

The type of stability system is indicated by a number, which represent the following types:

- 1 CLT stability core
- 2 Tube system
- 3 4-storey diagrid with glued-in rods connections
- 4 6-storey diagrid with glued-in rods connections
- 5 8-storey diagrid with glued-in rods connections
- 6 4-storey diagrid with steel plates and dowels connections
- 7 6-storey diagrid with steel plates and dowels connections
- 8 8-storey diagrid with steel plates and dowels connections

All systems use the same floor slabs and therefore it is clear that the volume of the floors is equal for all systems. This amount forms a significant part of the total timber volume, with a minimum of 52.5% of the total for a tube system and a maximum of 65% for the 8-storey diagrid with glued-in rods connections. These quantities will be relatively greater for lower heights and less for higher structures.

All systems use the same column dimensions of 600x600 millimetres, yet a greater volume of columns can be seen for a system with a CLT stability core. This is caused by the columns which are present on the perimeter of the building, which are not present in all other systems.

The contribution of the stability system to the total volume of the structure is the greatest for a tube system, which almost uses three times the amount of timber compared to an 8-storey diagrid with glued-in rods connections. It should be mentioned that windows and other finishing of the facade can be integrated in the tube elements and therefore this system requires less material to complete the facade compared to the other systems. This can also be said about the diagrid systems and in particular for the diagonals that are placed close together, i.e. the 4-storey diagonals.

The diagrid systems use the least material for the stability systems. It can also be seen that the systems with smaller diagonal crosses require more material, even though they require smaller diagonal dimensions. Thus the 4-storey diagrid requires the most and the 8-storey diagrid the least material. While no difference in volume can be observed between the 4-storey diagrids and the 6-storey diagrids, there is a difference between the 8-storey diagrids. The systems with steel plates and dowels connections require more timber volume than the systems with glued-in rods connections.

### 9.3. Steel material usage

Instead of looking at the total timber volume of each system, moreover it is possible to look at the amount of steel found in each structure. The amount of steel consists of the quantities used for rods, screws, plates and dowels if present. The results are displayed in Figure 9.5.

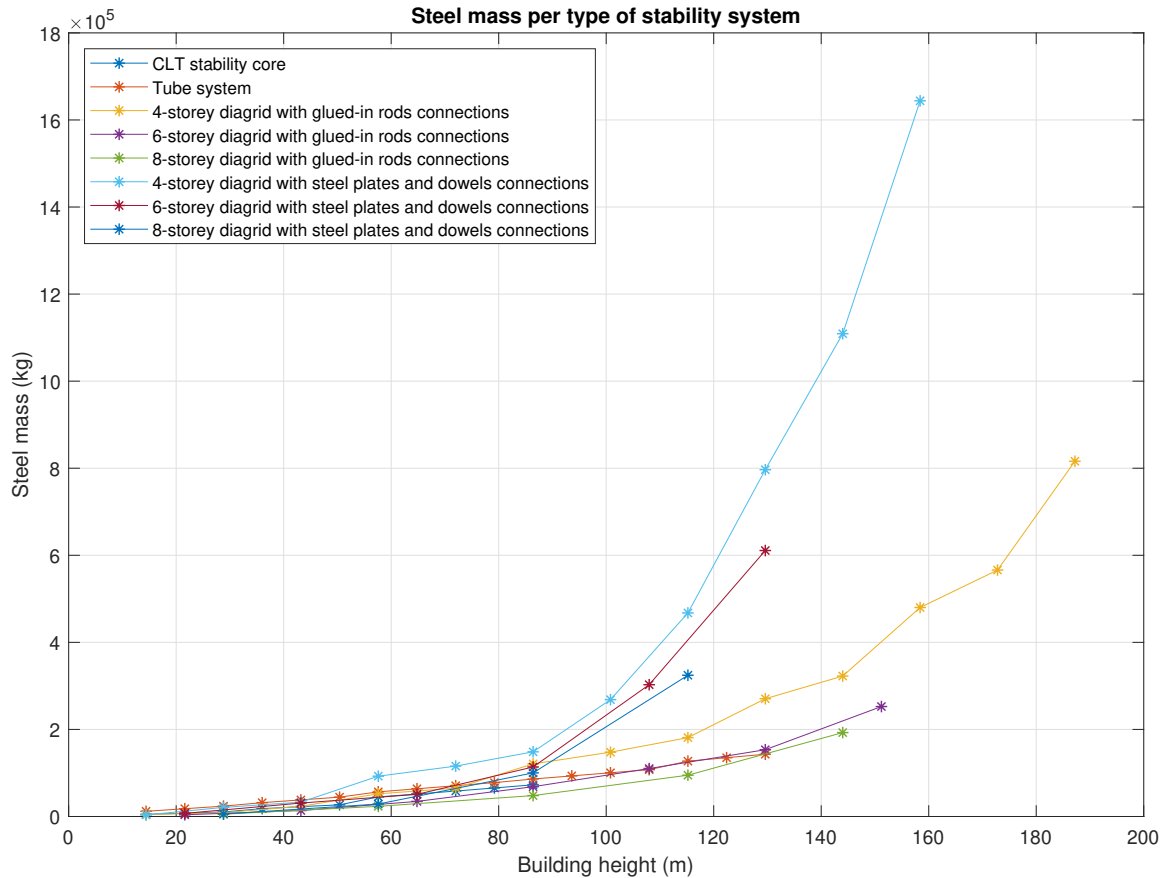


Figure 9.5: Steel volume for different building heights

It is clear that the systems using steel plates and dowels have a much higher usage of steel than all other systems, especially for greater building heights. The diagrid systems with smaller diagonal crosses require more material, so a 4-storey diagrid requires the most and the 8-storey diagrid the least steel mass. This is also the case for diagrids with glued-in rods connections, but these structures require significantly less steel compared to a diagrid with steel plates and dowels connections. A structure with a CLT stability core requires the least steel mass for all building heights. The CLT load-bearing facade system has a higher steel mass than the diagrids with glued-in rods, but will approach the other systems for greater building heights. For a maximum height of 158.4 metres, the steel plates and dowels connections require 6 times more steel compared to the glued-in rods connections.

The steel mass is made up of the steel used in the connections between the columns and in the connections between the different elements of the stability system. The distribution of these 2 connections is shown for a 75.6-metres high building in Figure 9.6.

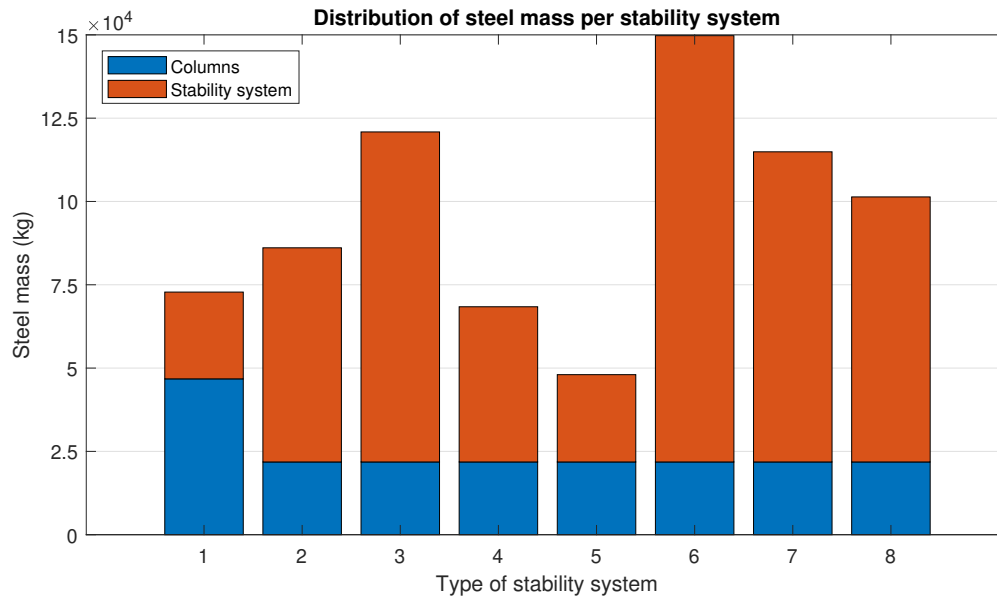


Figure 9.6: Distribution of steel mass per stability system

The type of stability system is indicated by a number, which represent the following types:

- 1 CLT stability core
- 2 Tube system
- 3 4-storey diagrid with glued-in rods connections
- 4 6-storey diagrid with glued-in rods connections
- 5 8-storey diagrid with glued-in rods connections
- 6 4-storey diagrid with steel plates and dowels connections
- 7 6-storey diagrid with steel plates and dowels connections
- 8 8-storey diagrid with steel plates and dowels connections

As was the case with the timber volume of the systems, a larger quantity of steel can be seen for the CLT stability core system in comparison with the other systems due to the presence of more columns. For all other systems, the steel mass is largely determined by the steel used in the stability system.

## 9.4. Comparison with other stability systems

It is interesting to compare the results from this research with existing timber high-rise, buildings which are in development and other research case studies. Therefore in Figure 9.7 the number of floors of several buildings are compared, with their corresponding building materials. The numbers on the x-axis correspond with the different building descriptions in Table 9.2.

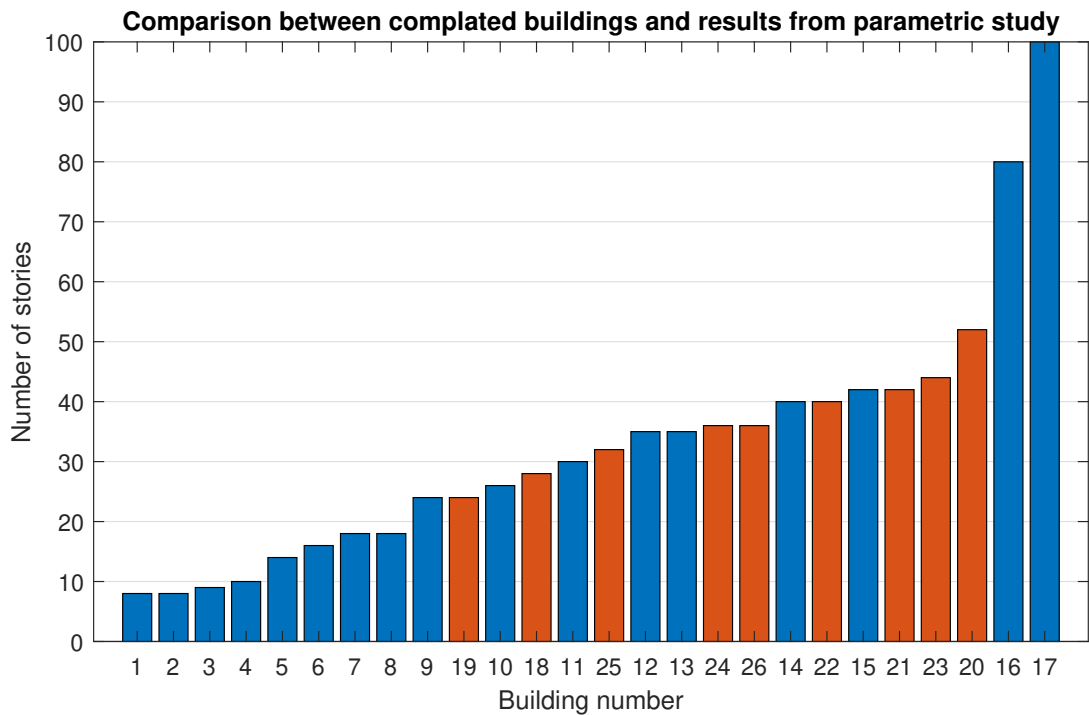


Figure 9.7: Comparison between completed buildings and results from parametric study

The completed buildings and other research case studies are summarized in Table 9.2.

Table 9.2: Completed buildings and other case studies [10, 36, 50]

Number	Completed build-ings and studies	City	Number of stories	Materials
1	Life Cycle Tower	Dornbirn	8	Timber, concrete
2	Stadthaus	London	8	Timber
3	Jakarta Hotel	Amsterdam	9	Timber
4	Forte Tower	Melbourne	10	Timber
5	Treet	Bergen	14	Timber
6	Kulturhuset Skelleftea	Skelleftea	16	Timber, steel
7	Mjostarnet	Brumunddal	18	Timber
8	BrockCommons Tallwood Building	Vancouver	18	Timber, concrete
9	HAUT	Amsterdam	24	Timber, concrete
10	HoHo	Vienna	26	Timber, concrete
11	Abebe Court Tower	lagos	30	Timber, steel
12	Tratoppen	Stockholm	35	Timber
13	Baobab	Paris	35	Timber, steel
14	vd Kuilen case study	-	40	Timber
15	SOM Timber Tower Research Project	-	42	Timber, concrete
16	River Beech Tower	Chicago	80	Timber
17	Slooten Timber Research Thesis	-	100	Timber, concrete

The results of the parametric study are described in Table 9.3.

Table 9.3: Results from parametric study

Number	Parametric study structures	Number of stories	Materials
18	Concrete core system	28	Timber, concrete
19	CLT core system	24	Timber
20	4-storey diagrid with glued-in rods connections	52	Timber
21	6-storey diagrid with glued-in rods connections	42	Timber
22	8-storey diagrid with glued-in rods connections	40	Timber
23	4-storey diagrid with steel plates and dowels connections	44	Timber
24	6-storey diagrid with steel plates and dowels connections	36	Timber
25	8-storey diagrid with steel plates and dowels connections	32	Timber
26	Tube system	36	Timber

Three buildings are listed which use a concrete core as stability system, namely the BrockCommons Tallwood Building, HAUT and HoHo. The heights of the buildings are comparable to that of the result from the parametric study. There are 2 more buildings shown in Table 9.2 which use timber and concrete, namely The SOM Timber Tower Research Project and the Slooten Timber Research Thesis, which reach a much greater height, namely 42 and 100 stories respectively. However, these buildings use an outrigger system and therefore they cannot be compared with the results of the parametric study.

Several buildings are described which use CLT walls as stability systems, which are the Stadthaus in London, Jakarta Hotel in Amsterdam and Forte Tower in Melbourne. However, these systems are not build around a core but use CLT walls which are spread over the whole floor. Furthermore, it is not clear what kind of connections are used in these buildings, which has a great influence on the behaviour of the structure. Nevertheless, it can be seen that the result for the maximum building height found in chapter 8 is slightly higher than the building heights found in Table 9.2.

Only 1 building using a diagrid is found, namely the River Beech Tower in Chicago. This proposed building will consist of 80 floors, which is more than what is found in the parametric study for diagrid systems. In addition, this building is still a concept and it is not clear which kind of connections are used in the diagrid system. Furthermore, the building uses a 2-storey diagrid system which is not investigated in this research.

Two buildings which have a tube system are Trätoppen and Abebe Court Tower, with a height of 30 and 35 floors respectively. A maximum of 36 stories for a tube system is observed in this thesis, thus is comparable to the other buildings.



# 10

## Conclusions and Recommendations

### 10.1. Conclusions

Two main research questions were elaborated in chapter 1. The first research question states:

*How can a parametric model be used to examine the possibilities of timber high-rise?*

The conclusions that followed from this research question are summarized:

- A parametric model which can generate timber high-rise structures is developed using Dynamo. A plug-in made by the company Arcadis is used to connect the parametric software with a FEA application called RFEM to perform a structural analysis.
- The model is able to generate 3 different stability systems, namely a shear core, diagrid and tube system. These systems can be used independently or combined and different properties of the structure can easily be modified.
- To take into account stiffness of connections between members and surfaces in different directions, the Young's modulus of the relevant elements must be adjusted. The magnitude of this reduction in Young's modulus can be determined by different methods, such as the method of equivalent spring stiffness or the theory of mechanically jointed beams.
- A case study is performed on the Brockcommons Tallwood House which showed that the parametric model produces adequate results.

The second main research question which is examined states:

*What are the possibilities of timber high-rise regarding maximum building height in The Netherlands?*

The following conclusions can be drawn from the parametric study which was performed to answer this research question:

- When looking at the influence of the assumed connections on the behaviour of the structural elements, it follows that:
  - No reduction in strength due to fire resistance is needed when unprotected members or wall elements have a width and depth of at least 326 millimetres and the fasteners are placed 93 millimetres from the edges of the elements. Wall elements will have a separating function of 120 minutes when the thickness is greater than 330 millimetres.
  - When using a connection with steel plates and dowels between members, an average stiffness reduction of the members of 30% is found caused by the connections for a member with a length of 3600 millimetres. This reduction decreases for greater lengths.

- A bending stiffness decrease of 40% for a building lower than 20 metres and a minimal bending stiffness decrease of 5% for a building higher than 76 metres is found for U-shaped CLT core walls when shear connections in the corners with  $K_{ser} = 186N/mm^2$  are used.
- The facade elements have a 50% stiffness reduction if 25% of the area is used as openings. Taken into account the corner connections ( $K_{ser} = 186N/mm^2$ ) and vertical connections between facade elements ( $K_{ser} = 743N/mm^2$ ) results in a total maximum decrease in stiffness of 70% for a building lower than 19 metres and a minimum decrease in stiffness of 55% for higher buildings.
- The following conclusions can be drawn from the research into the influence of connection characteristics on the structure:
  - The stiffness of connections between structural elements can have great influence on the total strength and stiffness of the structure. It is quite possible that the stiffness of a structure including connection stiffness is a quarter of the stiffness of a structure without the connection stiffness included.
  - The influence of shear connections between corners of wall elements on the total stiffness of the structure will reduce for greater building heights if the connections are evenly distributed over the whole height.
  - The influence of shear connections between stacked wall elements on the total stiffness of the structure will reduce for greater building heights because bending deformation will become more decisive than shear deformation.
  - For each building height, the influence of tensile connections between stacked wall elements on the total stiffness of the structure remains rather constant.
- A building with a width of 32.4 metres, a depth of 28.8 metres with a specific floor plan and connection characteristics is used to investigate the possibilities regarding maximum building height. These leads to the following conclusions:
  - Specific connections are used which provide high or infinite stiffness. These connections have a major influence on the outcome of this study.
  - The lowest maximum building height of 86.4 metres can be reached using a system with a CLT stability core. The greatest height of 187.2 metres can be obtained by adopting a 4-storey diagrid with glued-in rods connections.
  - Diagonals which span less floors can reach greater elevations. The difference in maximum building height for a 4-storey and 8-storey diagrid is 43.2 metres for both types of diagonal connections.
  - The dimensions of the diagonals with steel plates and dowels connections are determined by the maximum allowed deflection of the structure while the dimensions of the diagonals using glued-in rods connections are determined by the tensile resistance of the connection.
  - By combining 2 stability systems, greater building heights can be reached. When a combination of a CLT stability core system with a diagrid or tube system is used, a maximum extra elevation of 28.8 metres can be achieved.
  - The maximum building height of 187.2 metres is not changed by combining different systems.
  - The number of fasteners between the wall elements are only necessary for the required stiffness of the structure and thus not for the strength of the connection.
  - No additional measures had to be taken to ensure that each structure complied with the maximum acceleration limit for office buildings. Systems with higher mass, such as a system with a concrete or CLT core, have lower accelerations.
  - All systems, except the tube system, show a quadratic increment in timber volume with an increase in height. The tube system becomes more efficient in material usage for building heights over 100 metres. The floor slabs form a significant part of the total timber volume.
  - The systems using steel plates and dowels have a much higher usage of steel compared to all other systems, especially for higher buildings. For a height of 158.4 metres, a diagrid with steel plates and dowels connections require 6 times more steel compared to a diagrid with glued-in rods connections.

## 10.2. Recommendations

Based on the research performed in this report several recommendations can be formulated, which are summarized below.

- Arcadis is still developing the plug-in used in this thesis and therefore new functions will be added in the future. As a result, the following aspects can be improved:
  - Several assumptions have been made to include structural elements that could not be modelled. For example, connections that are not infinitely stiff have been taken into account by lowering the Young's modulus of certain structural elements. In the future it will be possible to model springs in RFEM by Dynamo. This makes it possible to model the connections between the elements and thus the assumptions made to include the connections are then no longer needed. This enables you to easier investigate the influence of these connections on the behaviour of the building.
  - The possibility of modelling springs in RFEM by Dynamo will also ensure that a foundation can be added with the correct strength and stiffness properties instead of using a conservative approach that says that half of the displacements of the building is caused by the foundation. This will lead to more realistic results of the model.
  - It would be useful to develop a function that allows you to model anisotropic surfaces such as CLT plates in RFEM by Dynamo. In the parametric study, the CLT plates are assumed to be isotropic with stiffness properties equal to the in-plane stiffness of the plate. This leads to good results with regard to the displacements of the stability system, but cannot be used to calculate deflections of the CLT floor slabs.
- The maximum building heights are determined for stability systems using a core made of either concrete or CLT, a diagrid or a tube with specific connection characteristics. This is also done for combinations of stability systems. However, an outrigger system was also discussed in chapter 2. Several studies, for example Slooten [51] and SOM [50], have shown that great heights can be achieved with the use of this particular system in combination with concrete elements. It would be interesting to discover the possibilities of this system by using only timber as structural material. In addition, it is also valuable to see whether this system can be combined with other stability systems.
- Properties of the specific connections used in the parametric study have been determined by making use of MATLAB, which optimized the configurations of the connections for compressive and tensile resistance. However, the parametric study has shown that not the strength but the stiffness of the connections are decisive. It would therefore be interesting to perform this investigation again, but then to optimize for stiffness instead. Subsequently, it should be checked if these connection configurations lead to greater possible building heights.
- In chapter 7 different connections together with their strength and stiffness properties were discussed.
  - It followed that connections between stacked wall elements can have a major influence on the strength and stiffness of the structure. It would be interesting to check what the possibilities regarding maximum building height are when including shear and tension connections between stacked wall elements with a finite stiffness.
  - In addition to the connections used in the parametric model, another connection also showed good properties in terms of strength and stiffness, namely the XEPOX connection. It would be interesting to investigate the possibilities of structures using this type of connection regarding maximum building height and material use.
- The dynamic behaviour is determined by using equations provided by the Dutch National annex of the Eurocode. A rule of thumb is used to approximate the natural frequency of the building. However, this rule is mainly based on concrete high-rise buildings and not specifically on timber buildings. It would therefore be interesting to investigate whether this approach corresponds with values which can be found using structural software, such as RFEM.

Furthermore, it is assumed that office buildings are examined in the parametric study and therefore all structures meet the dynamic requirements for this specific function. However, none of the structures are able to meet the maximum acceleration limit of a residential building and it would be interesting to investigate what measures are needed to satisfy the dynamic requirements for residential use.

# Bibliography

- [1] Rune Abrahamsen. Mjostarnet - construction of an 81 m tall timber building, 2017.
- [2] Rune B Abrahamsen and Kjell Arne Malo. Structural design and assembly of Treet - a 14-storey timber residential building in Norway. 2014.
- [3] National Precast Concrete Association Australia. *Precast Concrete Handbook*. NPCAA & CIA, Australia, 2 edition, 2009.
- [4] Hans Joachim Blass and Carmen Sandhaas. *Timber Engineering, Principles for Design*. KIT Scientific Publishing, 2017.
- [5] Eric Borgström. *Design of timber structures - Structural aspects of timber construction*, volume 1. Swedish Forest Industries Federation, 2 edition, 2016.
- [6] Bouwen en uitvoering. Nationaal militair museum, 2016. URL <https://bouwenuitvoering.nl/varia/militair-museum-wint-staalprijs-utiliteitsbouw/>. [Online accessed February 28 , 2019].
- [7] Scott Breneman. Structural CLT floor and Roof Design. 2017. URL <http://www.woodworks.org/wp-content/uploads/17DS04-BRENEMAN-Structural-CLT-Floor-and-Roof-Design-WDS-171116.pdf>.
- [8] I. Pečanac. The possibilities of structural parametric design in structural engineering. - analysis of variant studies, 2019.
- [9] MyTiCon Timber Connectors. Assy vg csk | timber connector | myticon timber connectors, 2019.
- [10] J.W.G. Van de Kuilen, A. Ceccotti, Zhouyan Xia, and Minjuan He. Very tall wooden buildings with cross laminated timber, 2011.
- [11] Sofia Teixeira de Vasconcelos Feist. A-bim: Algorithmic-based building information modelling, 2016.
- [12] B. Dujic, S. Klobcar, and R. Zarnic. Influence of openings on shear capacity of wooden walls. CIB W-18, 2007.
- [13] Inc. Encyclopaedia Britannica. High-rise building - architecture | britannica, 2020. URL <https://www.britannica.com/technology/high-rise-building>.
- [14] Per Feldt and Axel Thelin. Glued-in rods in timber structures - finite element analyses of adhesive failure, 2018.
- [15] Forestry Innovation Investment (FII), Binational Softwood Lumber Council (BSLC), and Perkins+Will. Summary report: Survey of international tall wood buildings. 2018.
- [16] International Organization for Standardization. *ISO 10137:2007 - Bases for design of structures - Serviceability of buildings and walkways against vibrations*. 2007.
- [17] Forest and Wood Products Australia Ltd. Lifecycle tower one - 8 stories of wood-concrete | woodsolutions, 2020. URL <https://www.woodsolutions.com.au/inspiration-case-study/lifecycle-tower-one-8-stories-wood-concrete>. [Online accessed March 03, 2020].
- [18] Deutsches Institut für Normung. *DIN 1052 - Entwurf, Berechnung und Bemessung von Holzbauwerken - Allgemeine Bemessungsregeln und Bemessungsregeln für den Hochbau*. 2004.
- [19] Deutsches Institut für Normung. *Eurocode 5: Bemessung und Konstruktion von Holzbauten - Teil 1-1: Allgemeines - Allgemeine Regeln und Regeln für den Hochbau; Deutsche Fassung EN 1995-1-1:2004/A2:2014*. 2014.

- [20] Andrea Frangi, Jurgen Konig, and Dhionis Dhima. *Fire safety in timber buildings - technical guideline for Europe, SP report 2010:19 - excerpt of chapters 5-7 on structural fire design*. SP Technical Research Institute of Sweden, 2019.
- [21] Emporis GMBH. "high-rise building|emporis standards|emporis", 2019. URL <https://www.emporis.com/building/standard/3/high-rise-building>.
- [22] Holz Schiller GmbH. Glued laminated timber beam, 2018. URL [https://holz-schiller.de/images/pics/profi\\_it/brettschichtholz\\_astarm/brettschichtholz\\_k.jpg](https://holz-schiller.de/images/pics/profi_it/brettschichtholz_astarm/brettschichtholz_k.jpg). [Online accessed February 26, 2019].
- [23] Nederlands Normalisatie Instituut. *NEN-EN 1990:2002 en, Eurocode: Grondslagen van het constructief ontwerp*. 2002.
- [24] Nederlands Normalisatie Instituut. *NEN-EN 1990+A1+A1/C2:2011/NB:2011 nl, Nationale bijlage bij NEN-EN 1990+A1+A1/C2: Eurocode: Grondslagen van het constructief ontwerp*. 2002.
- [25] Nederlands Normalisatie Instituut. *NEN-EN 1991-1-1+C1:2011 nl, Eurocode 1: Belastingen op constructies - Deel 1-1: Algemene belastingen - Volumieke gewichten, eigen gewicht en opgelegde belastingen voor gebouwen*. 2002.
- [26] Nederlands Normalisatie Instituut. *NEN-EN 1991-1-4+A1+C2:2011 nl, Eurocode 1: Belastingen op constructies - Deel 1-4: Algemene belastingen - Windbelasting*. 2002.
- [27] Nederlands Normalisatie Instituut. *NEN-EN 1991-1-2+C1:2011/NB:2011 nl, Nationale bijlage bij NEN-EN 1991-1-4+A1+C2: Eurocode 1: Belastingen op constructies - Deel 1-4: Algemene belastingen - Windbelasting*. 2002.
- [28] Nederlands Normalisatie Instituut. *NEN-EN 1990+A1+A1/C2/NB (nl), Nationale bijlage bij NEN-EN 1990+A1+A1/C2: Eurocode: Grondslagen van het constructief ontwerp*. 2007.
- [29] Nederlands Normalisatie Instituut. *NEN-EN 1991-1-3+C1 (nl), Eurocode 1: Belastingen op constructies - Deel 1-3: Algemene belastingen - Sneeuwbelasting*. 2007.
- [30] Nederlands Normalisatie Instituut. *NEN-EN 1993-1-1 (en), Eurocode 3: Design of steel structures - Part 1-1: General rules and rules for buildings*. 2007.
- [31] Nederlands Normalisatie Instituut. *NEN-EN 1995-1-1 (en), Eurocode 5: Ontwerp en berekening van houtconstructies - Deel 1-1: Algemeen - Gemeenschappelijke regels en regels voor gebouwen*. 2007.
- [32] Nederlands Normalisatie Instituut. *NEN-EN 1995-1-2 (en), Eurocode 5: Ontwerp en berekening van houtconstructies - Deel 1-2: Algemeen - Ontwerp en berekening van constructies bij brand*. 2007.
- [33] Nederlands Normalisatie Instituut. *NEN-EN 1995-1-2/NB (nl) - Nationale bijlage bij NEN-EN 1995-1-2 Eurocode 5: Ontwerp en berekening van houtconstructies - Deel 1-2: Algemeen - Ontwerp en berekening van constructies bij brand (inclusief C1:2006 en C2:2009)*. 2007.
- [34] Nederlands Normalisatie Instituut. *NEN-EN 1995-1-1+C1+A1/NB (nl) - Nationale bijlage bij NEN-EN 1995-1-1+C1+A1, Eurocode 5: Ontwerp en berekening van houtconstructies - Deel 1-1: Algemeen - Gemeenschappelijke regels en regels voor gebouwen (inclusief NEN-EN 1995-1-1+C1+A1/C1:2012)*. 2013.
- [35] ir. M.W. Kamerling. Bibliotheek tudelft - analyse draagconstructie, 2014.
- [36] CTBUH Journal. Tall buildings in numbers - tall timber: A global audit, 2017.
- [37] LEVER Architecture. Cross-laminated timber floor slab, 2019. URL [https://images.adsttc.com/media/images/5c1a/bca5/08a5/e516/a300/0b44/slideshow/AlbinaYard\\_10\\_LEVER.jpg?1545256091](https://images.adsttc.com/media/images/5c1a/bca5/08a5/e516/a300/0b44/slideshow/AlbinaYard_10_LEVER.jpg?1545256091). [Online accessed February 26, 2019].
- [38] Andrew Livingstone. Timber connections, 2015.
- [39] Will Lowry. Heco-ws(ws = wood and steel) self-drilling dowels, 2018. URL <https://www.fastenerandfixing.com/media/35147/111-con-fix-013.jpg>. [Online accessed May 27, 2019].

- [40] KLH UK Ltd. Klh: Stadthaus, murray grove, 2019. URL <http://www.klhuk.com/portfolio/residential/stadthaus,-murray-grove.aspx>.
- [41] XLam Australia Pty Ltd. Xlam Australian Cross Laminated Timber Panel Structural Guide, 2017.
- [42] Yamada M. and Goto. Proc. pan pacific tall buildings conference. In *The criteria to motions in Tall Building*, pages 233–244, 1975.
- [43] Richard McLain and Scott Breneman. Fire design of mass timber members - code applications, construction types and fire ratings, 2019.
- [44] University of British Columbia. Brock Commons Tallwood house - The advent of tall wood structures in Canada - a case study, 2013.
- [45] The University of British Columbia. Brock Commons Tall Wood building - Introduction, 2016.
- [46] Nishith B. Panchal, dr. V.R. Patel, and dr. I.I. Pandya. Optimum angle of diagrid structural system. *International Journal of engineering and technical research (IJETR)*, 2014. ISSN 2321-0869.
- [47] Martin Uhre Pedersen. *Dowel Type Timber Connections, Strength modelling*. 2002.
- [48] Angelique Pilon, Aletha Utimati, and Jessica Jin. Brock commons phase 1: Overview - design and pre-construction of a tall wood building, 2016.
- [49] Cambridge University Press. High-rise | meaning in the cambridge english dictionary, 2020. URL <https://dictionary.cambridge.org/dictionary/english/high-rise>.
- [50] Owings Skidmore and Merrill LLP. Timber tower research project - final report, 2013.
- [51] EC Slooten. Feasibility study of a wood-concrete hybrid super tall building and optimization of its wind-induced behaviour, 2018.
- [52] Simonin Wood Solutions. Resix - hidden and high tech fastening systems, 2016.
- [53] Rotho Blaas Srl. Xepox - timber, steel and concrete structures, 2018.
- [54] Rotho Blaas Srl. Screws and connectors for wood - carpentry, structures and outdoor, 2019.
- [55] Rotho Blaas SRL. High bond nail | lba, 2019. URL <https://www.rothoblaas.com/products/fastening/brackets-and-plates/nails-and-staples/lba>.
- [56] M. Stepinac, F Hunger, R. Tomasi, E. Serrano, V. Rajcic, and J. van de Kuilen. Comparison of design rules for glued-in rods and design rule proposal for implementation in european standards, 2013.
- [57] Structurlam. Crosslam clt - technical design guide, 2019.
- [58] TRADA Technology Ltd. Case Study | Stadthaus, Murray Grove, London. 2009.
- [59] Ingunn Utne. Numerical Models for Dynamic Properties of a 14-storey timber building, 2012.
- [60] Ir. P.C. van Staalduinen. *TNO-rapport - B-90-0483 - Achtergronden van de windbelastingen volgens NEN 6702:1991*. 1993.
- [61] M. van Telgen. Parametrisch model gekoppeld aan rekenprogramma. *Cement*, pages 26–29, 2018.
- [62] Okke Willebrands. Differential vertical shortening in timber-concrete high-rise structures, 2017.



# A

## Connections

### A.1. MATLAB script for determining strength of slotted-in steel plates and dowels connection

```
clear;

%Timber and steel properties
fc0k = 31 ; %N/mm^2
ft0k = 26; %N/mm^2
fv0k = 2.5; %N/mm^2
rhok = 450; %kg/m^3
kmod = 0.6; %Permanent
ym = 1.3;
fy = 355; %N/mm^2
fu = 450; %N/mm^2
hp = 0; %mm

%Char layer depth
tres = 120; %min
if hp > 0
    tch = 2.8 * hp - 14;
    ta = min(2*tch,25/(2*0.7) + tch);
    t120 = (tres - ta) * 0.7 + 25;
else
    t120 = 7+0.7*tres;
end

Steelplates = 2;

Width_column = 400; %mm
Depth_column = Width_column; %mm

maxlength = Width_column; %Max length connection
Diameter_dowel = 15; %mm
Steelplate_thickness = 10; %mm
Cols = 4;

edge_distance = max(6 * Diameter_dowel,2*t120);
Rows = floor( (Width_column - edge_distance) / (3*Diameter_dowel) );

%Compression or tension of the net timber area
Anet = (Width_column - Rows*Diameter_dowel) * (Depth_column - Steelplates * ...
    Steelplate_thickness);
Fmaxc(1) = fc0k * Anet / 1000;
Fmaxt(1) = 0.4*ft0k * Anet / 1000;

%Max force in steel plates
Fmaxc(2) = fy * Steelplates * Steelplate_thickness * (Width_column-2*t120) / 1000;
```

```

Fmaxt(2) = fy * Steelplates * Steelplate_thickness * (Width_column-2*t120) / 1000;

%Max force for dowel failure or embedment failure
fh = 0.082 * (1 - 0.01 * Diameter_dowel) * rhok;
t1 = Width_column * 1/3 - t120; t2 = Width_column * 1/3; d = Diameter_dowel; My = (1/6) * ...
    Diameter_dowel^3 * fy;

Fdowel(1) = 0.25 * (2 * t1 + t2) * d * fy;
Fdowel(2) = (-0.5 * t1 + t2 / 4 + sqrt(0.5 * t1^2 + My/(d*fh)) * d * fh );
Fdowel(3) = sqrt(4* My * d * fy);
Fdowel(4) = (0.5 * t1 + 0.5 * sqrt(t1^2 + 2 * My/(d*fy))) * d * fh;
Fdowel(5) = (sqrt(My/(d*fh)) + 0.5 * t1) * d * fh;
Fdowel(6) = (sqrt(My / (d*fy)) + 0.25 * t2) * d * fh;
Fdowel(7) = (-0.5 * t1 + sqrt(0.5 * t1^2 + My/(d*fh)) + sqrt(My / (d*fh) ))*d*fh;

nef = min(Cols, Cols^0.9 * (5/13)^0.25);

Fmaxc(3) = 4 * nef * Rows * min(Fdowel)/1000;
Fmaxt(3) = 4 * nef * Rows * min(Fdowel)/1000;

%Block shear and plug shear
lt = Width_column - edge_distance;
Anett = lt * (t1+t2+t1);
Fbs1 = 1.5 * Anett * ft0k / 1000;

lv = 2 * (5*d * (Cols-1) + max(7*d,80));
tef = 2 * sqrt( (My) / (fh * d));

Anetv = min(lv/2 * (lt + 2 * (2*tef + t2)), lv * (t1+t2+t1));
Fbs2 = 0.7 * Anetv * fv0k / 1000;

Fmaxt(4) = max(Fbs1, Fbs2);
Fmaxt(5) = 0.9 * fu/1000 * (Steelplates * Steelplate_thickness * ...
    (Width_column-2*t120-Rows*Diameter_dowel))/1.25;
%Fmaxt(5) = NuRd(c);

Connection_length = max(7*d,80) + 5*d*(Cols-1);

if Connection_length > Width_column
    Fmaxc(1) = 0;
    Fmaxt(1) = 0;
    disp('Connection too long. ');
end

%Connection resistance
Rcmax = kmod * min(Fmaxc) / ym;
Rtmax = kmod * min(Fmaxt) / ym;

%Resistance during fire
firet = ft0k * 1.1 * (Width_column-2*t120)^2 / 1000 / 0.45;
firec = fc0k * 1.1 * (Width_column-2*t120)^2 / 1000 / 0.45;

%Member resistance
normalt = ft0k * kmod * Width_column^2 / 1000 / ym;
normalc = fc0k * kmod * Width_column^2 / 1000 / ym;

mintension = min([Rtmax, firet, normalt]);
mincompression = min([Rcmax, firec, normalc]);

disp(['Max compression force: ', num2str(mincompression), ' kN']);
disp(['Max tension force: ', num2str(mintension), ' kN']);

```

## A.2. MATLAB script for determining strength of glued-in rod connection

```

clear;

%%Properties of the connection
tres = 120; %min
hp = 3*16; %mm

d = 16; %mm
anchorlength = 140; %mm
rods = 2; %Number of rods in 1 direction
kmod = 0.6;
fyd = 235; %N/mm2
ft0k = 26; %N/mm2
fc0k = 31; %N/mm2

width = 265; %mm

%Char layer depth
if hp > 0
    tch = 2.8 * hp - 14;
    ta = min(2*tch, 25/(2*0.7) + tch);
    t120 = (tres - ta) * 0.7 + 25;
else
    t120 = 7+0.7*tres;
end

%Minimum anchorlength
lmin = max(0.5*d^2, 10*d);
lad = max(lmin, anchorlength);

if lad < 250
    fk1 = 4.0;
elseif lad > 500
    fk1 = 3.5 - 0.0015 * lad;
else
    fk1 = 5.25 - 0.005 * lad;
end

slenderness = lad / d;

if slenderness < 15
    if slenderness > 7.5
        Aef = rods * rods * 0.25 * pi * d^2;
        Aeftimber = min(width*width - rods*Aef, rods*d^2);
        Failure1 = rods*rods*pi*d*lad*fk1 / 1000;
        Failure2 = rods*rods*fyd * Aef / 1000;
        Failure3 = Aeftimber*ft0k;
        Rtmax = kmod * min([Failure1, Failure2, Failure3])/1.3;
        Rcmx = min(kmod * fc0k * width * width / 1.3, 1.1 * fc0k * (width - t120)^2 / ...
            0.45) / 1000;

        disp(['Max tension force: ', num2str(Rtmax), ' kN']);
        disp(['Max compression force: ', num2str(Rcmx), ' kN'])
    else
        disp('Slenderness not OK');
    end
else
    disp('Slenderness not OK');
end

```

### A.3. MATLAB script for determining maximum strength of slotted-in steel plates and dowels connection

```

clear;
warning('off')

%Timber and steel properties
%GL24h + S355 steel plate
fc0k = 24; %N/mm^2
ft0k = 16.5; %N/mm^2
fv0k = 3.5; %N/mm^2
rhok = 385; %kg/m^3
kmod = 0.8; %Permanent
ym = 1.3;
E = 11500;
fy = 355; %N/mm^2
fu = 450; %N/mm^2
t = 120;
fireprotection = 7+0.7*t; %Minimum distance from edge for fire safety.
c = 1;
Steelplates = 2;
rhom = 420;

Width_column = 800;
Depth_column = Width_column;
maxlength = Width_column; %Max length connection
for b = 1:100
    Steelplate_thickness = 2 + (b-1);

    %Different dowel diameters
    Diameter_dowel = linspace(6,30,25);
    for i = 1:length(Diameter_dowel)
        %Different number of dowel columns
        for a = 1:80
            %Max number of columns by using minimum spacing for tension
            %Also fire safety could be used here as minimum spacing at
            %the edges?
            Rows = floor( (Width_column - 2*fireprotection - 6 * Diameter_dowel(i)) / ...
                (3*Diameter_dowel(i)) + 1);
            Cols = a;

            %Compression or tension of the net timber area
            Anet = (Width_column - Rows*Diameter_dowel(i)) * (Depth_column - Steelplates ...
                * Steelplate_thickness);
            Fmaxc(1) = fc0k * Anet / 1000;
            Fmaxt(1) = ft0k * Anet / 1000;

            %Max force in steel plates
            Fmaxc(2) = fy * Steelplates * Steelplate_thickness * ...
                (Width_column-2*fireprotection) / 1000;
            Fmaxt(2) = fy * Steelplates * Steelplate_thickness * ...
                (Width_column-2*fireprotection) / 1000;

            %Max force for dowel failure or embedment failure
            fh = 0.082 * (1 - 0.01 * Diameter_dowel(i)) * rhok;
            t1 = Width_column * 1/3 - fireprotection; t2 = Width_column * 1/3; d = ...
                Diameter_dowel(i); My = (1/6) * Diameter_dowel(i)^3 * fy;

            Fdowel(1) = 0.25 * (2 * t1 + t2) * d * fy;
            Fdowel(2) = (-0.5 * t1 + t2 / 4 + sqrt(0.5 * t1^2 + My/(d*fh)) * d * fh );
            Fdowel(3) = sqrt(4* My * d * fy);
            Fdowel(4) = (0.5 * t1 + 0.5 * sqrt(t1^2 + 2 * My/(d*fy))) * d * fh;
            Fdowel(5) = (sqrt(My/(d*fh)) + 0.5 * t1) * d * fh;
            Fdowel(6) = (sqrt(My / (d*fy)) + 0.25 * t2) * d * fh;
            Fdowel(7) = (-0.5 * t1 + sqrt(0.5 * t1^2 + My/(d*fh)) + sqrt(My / (d*fh) ))*d*fh;

            nef = min(Cols,Cols^0.9 * (5/13)^0.25);
        end
    end
end

```

```

Fmaxc(3) = 4 * nef * Rows * min(Fdowel)/1000;
Fmaxt(3) = 4 * nef * Rows * min(Fdowel)/1000;

%Block shear and plug shear
lt = Width_column - max(6 * d, fireprotection);
Anett = lt * (t1+t2+t1);
Fbs1 = 1.5 * Anett * ft0k / 1000;

lv = 2 * (5*d * (Cols-1) + max(7*d,80));
tef = 2 * sqrt( (My) / (fh * d));

Anetv = min(lv/2 * (lt + 2 * (2*tef + t2)), lv * (t1+t2+t1));
Fbs2 = 0.7 * Anetv * fv0k / 1000;

Fmaxt(4) = max(Fbs1,Fbs2);
Fmaxt(5) = 0.9 * fu/1000 * (Steelplates * Steelplate_thickness * ...
    (Width_column-2*fireprotection-Rows*Diameter_dowel(i)))/1.25;
%Fmaxt(5) = NuRd(c);

Connection_length(c) = max(7*d,80) + 5*d*(Cols-1)+3*d;

if Connection_length(c) > Width_column
    Fmaxc(1) = 0;
    Fmaxt(1) = 0;
end

tsteelplate(c) = Steelplate_thickness;
t_dowel(c) = d;
dowels(c) = Cols*Rows;
[zc(c),Failureindexc(c)] = min(Fmaxc);
[zt(c),Failureindext(c)] = min(Fmaxt);
zc(c) = zc(c) * kmod / ym;
zt(c) = zt(c) * kmod / ym;
dowelcols(c) = Cols;
dowelrows(c) = Rows;
kser(c) = 4*Cols*Rows * (2*rhom)^1.5 * d / (1000*23);
c = c+1;
end
end
end
firet = ft0k * 1.1 * (Width_column-2*fireprotection)^2 / 1000 / 0.45;
firec = fc0k * 1.1 * (Width_column-2*fireprotection)^2 / 1000 / 0.45;

normalt = ft0k * 0.6 * Width_column^2 / 1000 / 1.25;
normalc = fc0k * 0.6 * Width_column^2 / 1000 / 1.25;

for i = 1:max(zc)-1
    [a,b] = max(zt .* ge(zc,i));
    failure_modet(i) = Failureindext(b);
    failure_modec(i) = Failureindexc(b);
    failure_steelplate(i) = tsteelplate(b);
    failure_dowel(i) = t_dowel(b);
    failure_cols(i) = dowelcols(b);
    failure_rows(i) = dowelrows(b);
    failure_dowels(i) = dowelcols(b) * dowelrows(b);
    failure_length(i) = Connection_length(b);
    failure_tension(i) = min([firet,a, normalt]);
    failure_compression(i) = min([firec,i,normalc]);
    failure_kser(i) = kser(b);
end

%figure;
%plot(zc,zt, '.,','MarkerSize',4);
hold on;
plot(failure_compression,failure_tension,'LineWidth',1);

xlabel('Max compression force (kN)');
ylabel('Max tension force (kN)');

```

```

title(['Compression and tension strength ...
      ',num2str(Width_column),'x',num2str(Width_column),'mm']);
%title('Compression and tension strength');
grid on;
xlim([0 i]);
ylim([0 1.1*max(failure_tension)]);

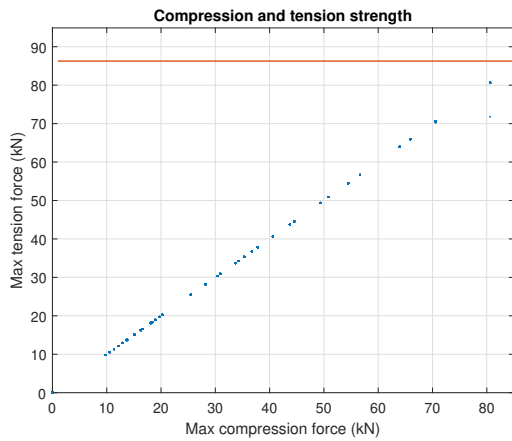
disp(['Max compression force: ',num2str(max(failure_compression)),' kN']);
disp(['Max tension force (for max compression): ...
      ',num2str(round(failure_tension(max(failure_compression)))),' kN']);

disp('Properties for connection with max compression:');
disp(['Dowel diameter: ',num2str(failure_dowel(max(i))),' mm']);
disp(['Steelplate thickness: ',num2str(failure_steelplate(i)),' mm']);
disp(['Connection length: ',num2str(failure_length(i)),' mm']);
disp(['Number of dowel columns: ',num2str(failure_cols(i))]);
disp(['Number of dowel rows: ',num2str(failure_rows(i))]);
disp(['Total dowels: ',num2str(failure_cols(i) * failure_rows(i))]);
disp(['Kser: ',num2str(round(failure_kser(i))),' kN/mm']);
disp(['EA/l = ',num2str(E * Width_column * Depth_column / 3000000),' kN/mm']);
disp(['Keq = ',num2str( (2/failure_kser(i) + 1/(E * Width_column * Depth_column / ...
      3000000))^-1 / (E * Width_column * Depth_column / 3000000))]);

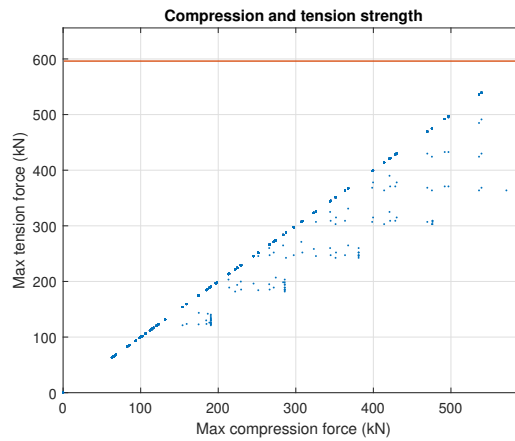
%figure(2);
%hold on;
%plot(failure_compression,failure_kser);
%ylim([0 inf])

```

### A.4. Maximum strength of slotted-in steel plates and dowels connection

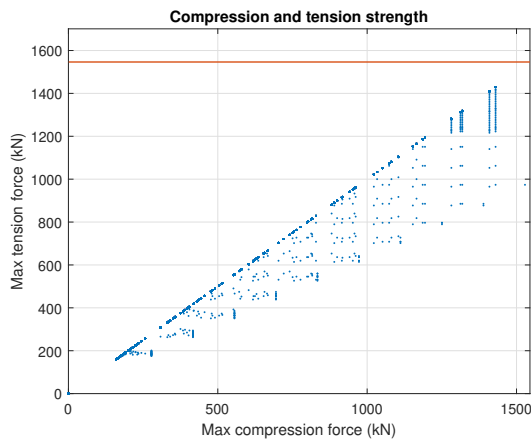


(a) Compression and tension strength for 300x300mm member

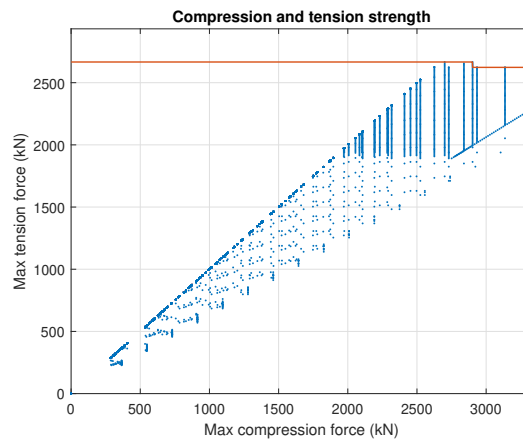


(b) Compression and tension strength for 400x400mm member

Figure A.1: Compression and tension strength for 300x300mm and 400x400mm member

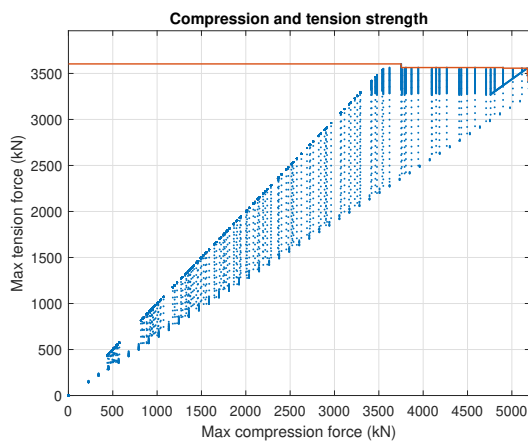


(a) Compression and tension strength for 500x500mm member

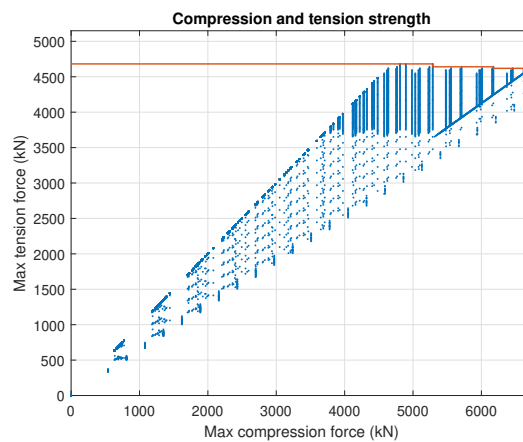


(b) Compression and tension strength for 600x600mm member

Figure A.2: Compression and tension strength for 500x500mm and 600x600mm member

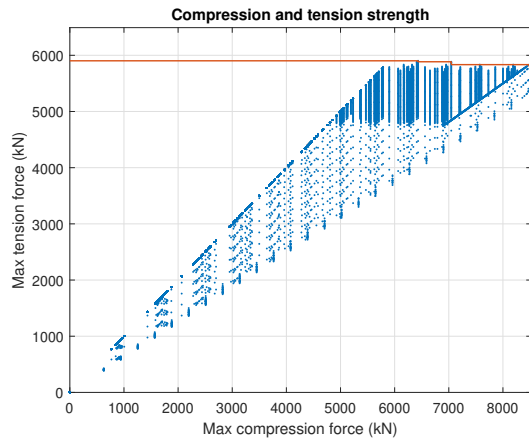


(a) Compression and tension strength for 700x700mm member

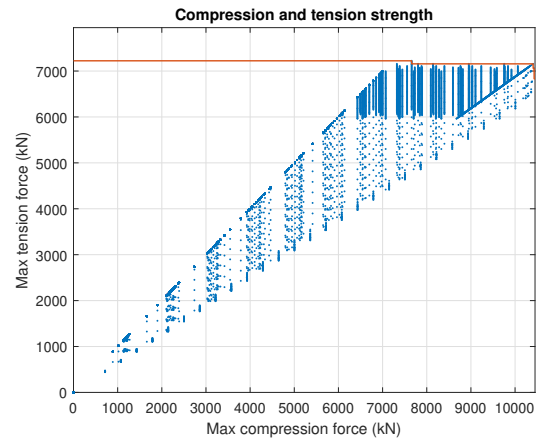


(b) Compression and tension strength for 800x800mm member

Figure A.3: Compression and tension strength for 700x700mm and 800x800mm member

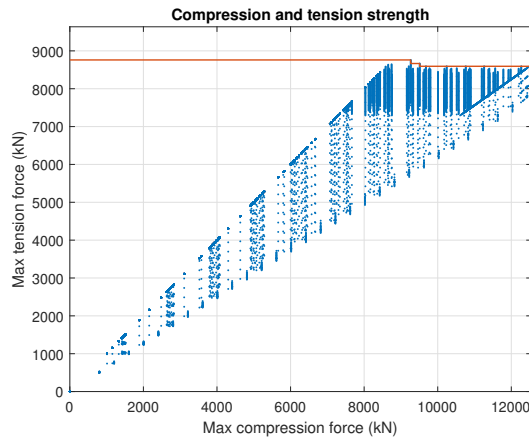


(a) Compression and tension strength for 900x900mm member

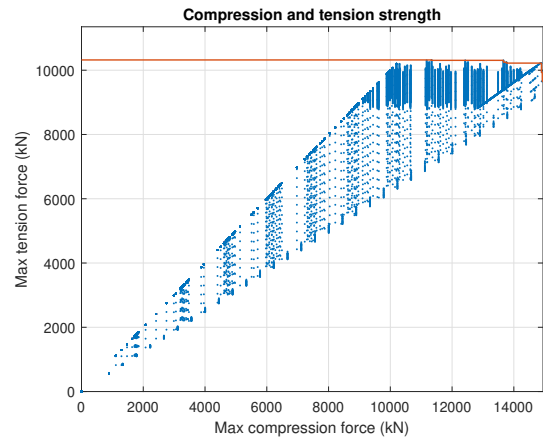


(b) Compression and tension strength for 1000x1000mm member

Figure A.4: Compression and tension strength for 900x900mm and 1000x1000mm member



(a) Compression and tension strength for 1100x1100mm member



(b) Compression and tension strength for 1200x1200mm member

Figure A.5: Compression and tension strength for 1100x1100mm and 1200x1200mm member

## A.5. MATLAB script for determining maximum strength of glued-in rods connection

```

clear; close all;
fyd = 355;
c = 1;
ft0k = 16.5;
fc0k = 24;
Width = 1200;
tfire = 120;
hp = 0;
kmod = 0.8;

if hp > 0
    tch = 2.8 * hp - 14;
    ta = min(2*tch, 25/(2*0.7) + tch);
    fireprotection = max((tfire - ta) * 0.7 + 25, 0);
else
    fireprotection = 7+0.7*tfire;
end

Rc = min(kmod * (Width)^2 * fc0k/1000 / 1.3, 1.1 * (Width - 2*fireprotection)^2 * ...
    fc0k/1000 / 1 / 0.45);

for d = 6:30
    maxrods = floor((Width - (2*(max(2.5*d, fireprotection))))/(5*d))+1;
    for rods = 1:maxrods
        lmin = max(0.5*d^2, 10*d);
        for lad = lmin:Width
            if lad < 250
                fk1 = 4.0;
            elseif lad > 500
                fk1 = 3.5 - 0.0015 * lad;
            else
                fk1 = 5.25 - 0.005 * lad;
            end
            slenderness = lad / d;

            if slenderness < 15
                if slenderness > 7.5
                    diameter(c) = d;
                    length(c) = lad;
                    numofrods(c) = rods;
                    Aef(c) = rods * rods * 0.25 * pi * diameter(c)^2;
                    Aeftimber(c) = min(Width*Width - rods*Aef(c), rods*d^2);
                    Failure1(c) = rods*rods*pi*d*lad*fk1 / 1000;
                    Failure2(c) = rods*rods*fyd * Aef(c) / 1000;
                    Failure3(c) = Aeftimber(c)*ft0k;
                    mrods(c) = rods;
                    Raxd(c) = 0.8 * min([Failure1(c), Failure2(c), Failure3(c)])/1.3;
                    Rvxd(c) = 0.8 * rods * rods * d * lad / 1000 * 3.5 / 1.3;
                end
            end
            c = c + 1;
        end
    end
end

ftmax = min([max(Raxd), ft0k * 0.8 / 1.25 * (Width^2) / 1000, 1.1 * ft0k * ...
    (Width-2*fireprotection)^2 / 1000 / 0.45]);
fcmx = min(fc0k * 0.8 / 1.25 * (Width^2) / 1000, 1.1 * fc0k * (Width-2*fireprotection)^2 ...
    / 1000 / 0.45);

figure;
scatter3(diameter, length, Raxd, 1, Raxd);
h = colormap(jet);
h = colorbar;
ylabel(h, 'Tensile strength (kN)')

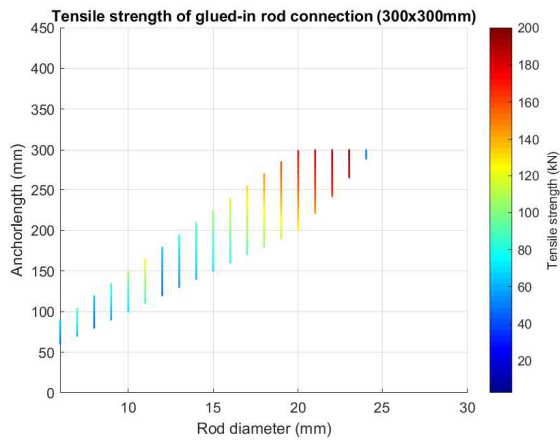
```

```
view(2);
xlabel('Rod diameter (mm)');
ylabel('Anchorlength (mm)');

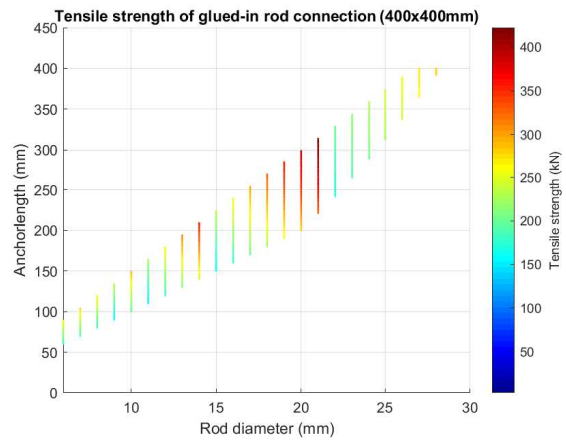
title(['Tensile strength of glued-in rod connection ...
      ', num2str(Width), 'x', num2str(Width), 'mm']);

disp(['Max tension: ', num2str(round(max(ftmax))), ' kN']);
disp(['Max compression: ', num2str(round(Rc)), ' kN']);
disp(['Diameter for max: ', num2str(diameter(Raxd == max(Raxd)))]);
disp(['Number of rods for max: ', num2str(mrods(Raxd == max(Raxd)))]);
disp(['Length of rods for max: ', num2str(length(Raxd == max(Raxd)))]);
disp(['Max shear force: ', num2str(round(Rvxd(Raxd == max(Raxd))), ' kN');
```

### A.6. Maximum strength of glued-in rods connection

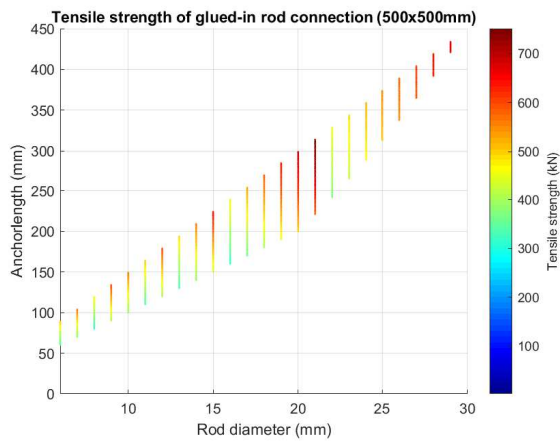


(a) Tensile strength for 300x300mm member

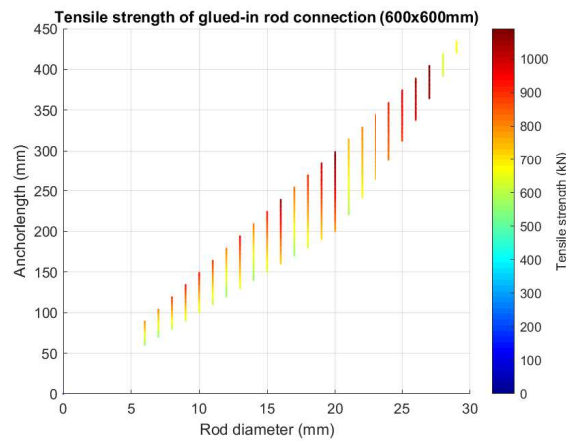


(b) Tensile strength for 400x400mm member

Figure A.6: Tensile strength for 300x300mm and 400x400mm member

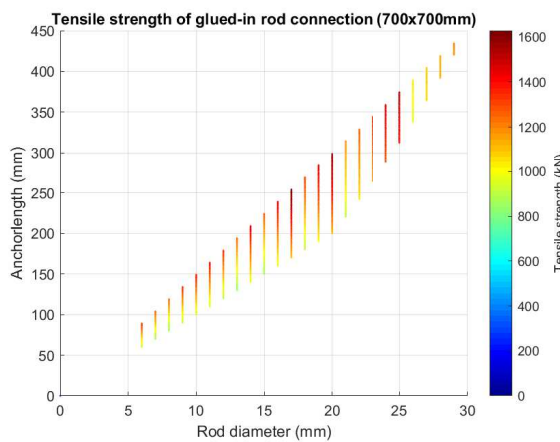


(a) Tensile strength for 500x500mm member

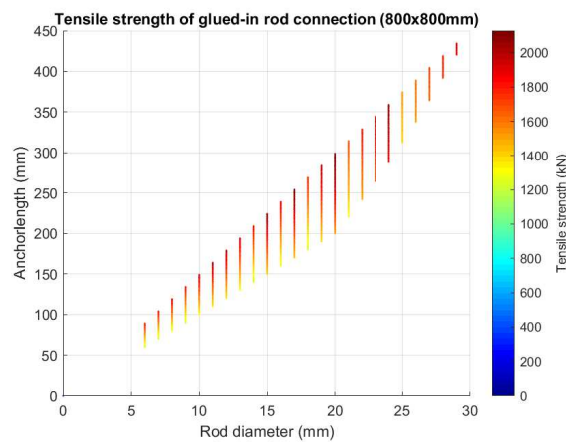


(b) Tensile strength for 600x600mm member

Figure A.7: Tensile strength for 500x500mm and 600x600mm member

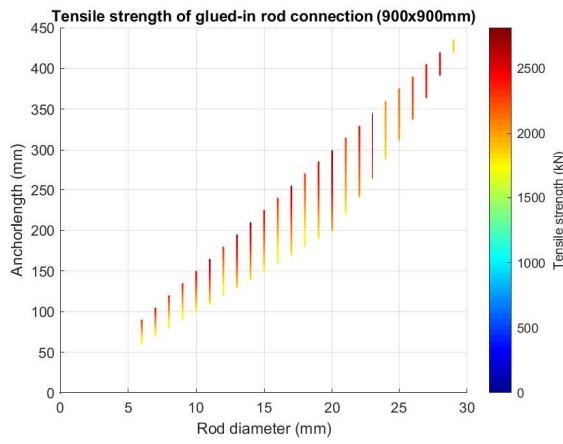


(a) Tensile strength for 700x700mm member

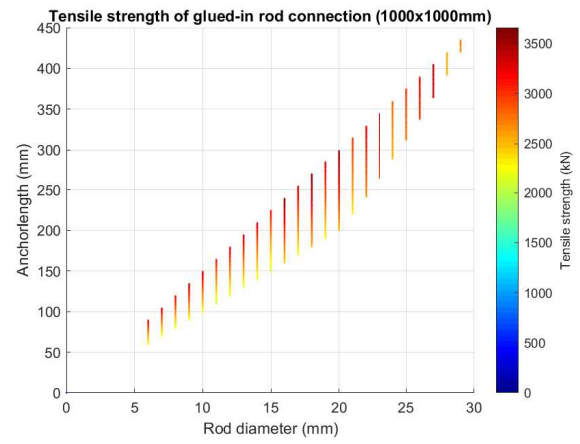


(b) Tensile strength for 800x800mm member

Figure A.8: Tensile strength for 700x700mm and 800x800mm member

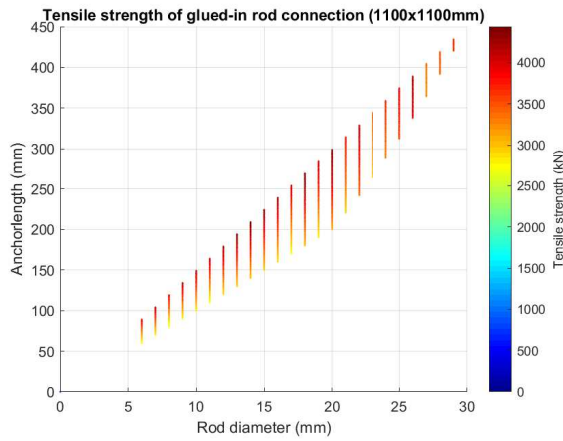


(a) Tensile strength for 900x900mm member

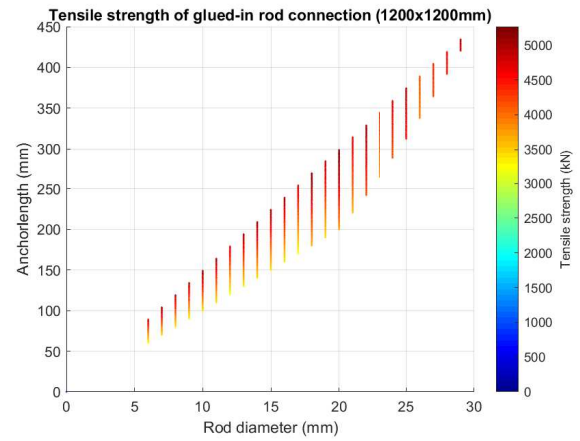


(b) Tensile strength for 1000x1000mm member

Figure A.9: Tensile strength for 900x900mm and 1000x1000mm member



(a) Tensile strength for 1100x1100mm member



(b) Tensile strength for 1200x1200mm member

Figure A.10: Tensile strength for 1100x1100mm and 1200x1200mm member

## A.7. MATLAB script for determining shear resistance of screwed connection

```

clear;

t1 = 495; %Length in element 1
t2 = 305; %Length in element 2
d = 10;
alpha = 90;
rhok = 485;
fu = 1000; %Ultimate strength screw
MyRk = 0.3 * fu * d^2.6;

fh1k = 0.082*(1-0.01*d)*rhok / ((1.35 + 0.015*d) * sind(alpha)^2 + cosd(alpha)^2);
fh2k = fh1k;
beta = fh1k/fh2k;

FaxRk = (pi * d * t2)^0.8 * 3.6e-3 * rhok^1.5 / (sind(alpha)^2 + 1.5*cosd(alpha)^2)

%6 failure modes without rope effect
option1 = fh1k * t1 * d;
option2 = fh2k * t2 * d;
option3 = (fh1k * t1 * d)/(1 + beta) * (sqrt(beta + 2 * beta^2 * (1 + t2/t1 + (t2/t1)^2 + ...
    beta^3 * (t2/t1)^2 - beta*(1+t2/t1))));
option4 = 1.05 * fh1k * t1 * d / (2+beta) * (sqrt(2*beta*(1+beta) + (4*beta*(2+beta) * ...
    MyRk)/(fh1k * d * t1^2)) - beta);
option5 = 1.05 * fh1k * t2 * d / (2+beta) * (sqrt(2*beta*(1+beta) + (4*beta*(2+beta) * ...
    MyRk)/(fh1k * d * t2^2)) - beta);
option6 = 1.15 * sqrt(2*beta / (1+beta)) * sqrt(2 * MyRk * fh1k * d);

%Include rope effect
rope = FaxRk/4;
option3 = option3 + min(option3,FaxRk/4);
option4 = option4 + min(option4,FaxRk/4);
option5 = option5 + min(option5,FaxRk/4);
option6 = option6 + min(option6,FaxRk/4);

%Total force in connection
maxFv = 0.8 * min([option1,option2,option3,option4,option5,option6]) / 1.3
maxFvs = maxFv*2 / (5 * d * 495) %Stress with minimum spacing

```



# B

## Structural elements calculations

### B.1. Structural analysis of floor beam

The structural calculations is performed below to check if the floor beam satisfies all conditions for ULS and SLS. It is considered that the beam is simply supported and has a span of 8 metres.

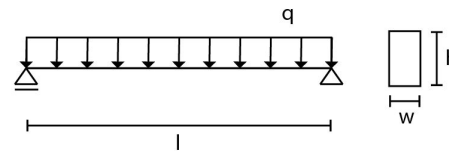


Figure B.1: Simply supported floor beam

Table B.1: Structural calculations of the floor beam

Length	8	m		
Height	0.7	m		
Width	0.4	m		
<b>Loads</b>				
Dead load	Beam	$0.400 \cdot 0.700 \cdot 5$	1.40	kN/m
	Floor slab	$1.7 \cdot 6$	10.20	kN/m
	Add. load	$1.0 \cdot 6$	6.00	kN/m
Live load	Floor slab	$(2.5 + 0.5) \cdot 6$	18.00	kN/m
Total		$1.2 \cdot \text{DL} + 1.5 \cdot \text{LL}$	48.12	kN/m
<b>Moment resistance</b>				
Maximum moment in the beam		$(1/8) \cdot q \cdot l^2$	384.96	kNm
Moment of resistance	$W$	$(1/6) \cdot b \cdot h^2$	0.03	$m^3$
Bending stress capacity	$f_{b,d}$	$0.8 \cdot 24 / 1.25$	15.36	$N/mm^2$
Bending stress	$\sigma_b$	$M/W$	11.78	$N/mm^2$
UC		$\sigma_b / f_{b,d}$	0.77	(-)
<b>Shear resistance of the beam</b>				
Maximum shear force		$q \cdot l/2$	192.48	kN
Maximum shear capacity	$f_{v,d}$	$k_{mod} \cdot f_{v,k} / \gamma_m$	2.24	$N/mm^2$
Effective shear area	$A_{ef}$	$0.67 \cdot b \cdot h$	0.20	$m^2$
Shear stress	$\sigma_v$	$1.5 \cdot V / A_{ef}$	1.44	$N/mm^2$
UC		$\sigma_v / f_{v,d}$	0.64	(-)
<b>Resistance at support</b>				
Effective support area	$A_{ef}$	$(0.150 + 0.030) \cdot 0.400$	0.07	$m^2$
Maximum stress		$F_{c,90,d} / A_{ef}$	2.67	$N/mm^2$

Max allowed stress		$k_{c,90} * k_{mod} * f_{c,90,k} / \gamma_m$	2.80	$N/mm^2$
UC			0.95	(-)
Deflection				
Instantaneous deflection	$w_{inst}$	$(5/384) * q * l^4 / EI$	19.52	mm
Maximum instantaneous deflection	Max $w_{inst}$	$1/300 * l$	26.67	mm
Final deflection	$w_{inf}$	$(5/384) * q * l^4 / (E / (1 + k_{def}) * I)$	31.23	mm
Maximum final deflection	Max $w_{inf}$	$1/250 * l$	32.00	mm

## B.2. Strength of glued-in rod connection of Brockcommons Tallwood Building

The compressive and tensile strength is calculated below. The connection is shown in Figure B.2.

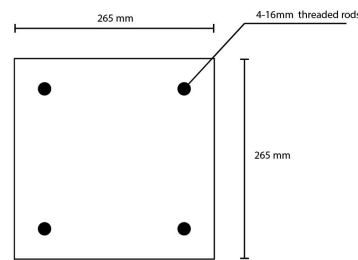


Figure B.2: Column connection of Brockcommons Tallwood Building

Table B.2: Calculation of resistance of glued-in rod connection

Number of rods	n	4	(-)
Diameter rod	d	16	mm
Anchorlength	$l_{ad}$	140	mm
Width column	w	265	mm
Fire protective gypsum layer		3x16	mm
Char layer depth	d	12	mm
Characteristic compression resistance	$f_{c,0,k}$	32	$N/mm^2$
Characteristic tension resistance	$f_{t,0,k}$	10	$N/mm^2$
	$k_{mod}$	0.8	(-)
	$\gamma_m$	1.3	(-)
Bond joint strength	$f_{k,1}$	4.00	$N/mm^2$
Yield strength rod	$f_{y,d}$	235	$N/mm^2$
Area rods	$A_{ef}$	804	$mm^2$
Maximum tension force in rods	$F_{ax,Rd}$	113	kN
Maximum tension force in timber	$F_{t,timber}$	369	kN
Design tension resistance	$F_{t,d}$	69	kN
Design compression resistance	$F_{c,d}$	1383	kN

## B.3. Shear strength of screwed corner connection

The shear strength of the corner connection between 2 core or facade walls is calculated below.

Table B.3: Shear strength of screwed corner connection

$n$	2		
$d$	10	mm	
$\rho_k$	485	$kg/m^3$	
$t_1$	495	mm	
$t_2$	305	mm	
$\alpha$	90	degrees	
Stiffness			
$K_1$	9288	$N/mm$	
$K_{ser}$	186	$N/mm^2$	
Strength			
$F_{ax,Rd}$	58.90	kN	per screw
$F_{v,Rk}$	11.81	kN	failure mode a
	72.78	kN	failure mode b
	108.45	kN	failure mode c
	56.32	kN	failure mode d
	40.61	kN	failure mode e
	17.36	kN	failure mode f
$f_{v,Rk}$	1.40	$N/mm^2$	for 2 screws
$f_{v,Rd}$	0.86	$N/mm^2$	

### B.4. Tensile strength of glued-in rods connection

The tensile strength of the connections between wall segments using glued-in rods is shown below.

Table B.4: Tensile resistance of glued-in rods

$n$	2		
$d$	20	mm	
$l_{ef}$	350	mm	
$f_{k,1}$	3.5	$N/mm^2$	
$F_{t,Rk}$	76.97	kN	per rod
Spacing	100	mm	
Wall thickness	49	mm	
$f_{t,Rk}$	3.11	$N/mm^2$	
$f_{t,Rd}$	1.91	$N/mm^2$	

## B.5. Separating function of wall assembly

### B.5.1. Position coefficients

Material	Position coefficient $k_{\text{pos,exp,i}}$ and $k_{\text{pos,exp,n}}$	
Cladding (gypsum, timber)	$k_{\text{pos,exp,n}}$ for $t_{\text{ins,n}}$	
	$1 - 0,6 \cdot \frac{\sum t_{\text{prot,n-1}}}{t_{\text{ins,0,n}}}$	for $\sum t_{\text{prot,n-1}} \leq \frac{t_{\text{ins,0,n}}}{2}$
	$0,5 \cdot \sqrt{\frac{t_{\text{ins,0,n}}}{\sum t_{\text{prot,n-1}}}}$	for $\sum t_{\text{prot,n-1}} > \frac{t_{\text{ins,0,n}}}{2}$
	$k_{\text{pos,exp,i}}$ for $t_{\text{prot,i}}$	
Stone wool insulation	$1 - 0,6 \cdot \frac{\sum t_{\text{prot,i-1}}}{t_{\text{prot,0,i}}}$	for $\sum t_{\text{prot,i-1}} \leq \frac{t_{\text{prot,0,i}}}{2}$
	$0,5 \cdot \sqrt{\frac{t_{\text{prot,0,i}}}{\sum t_{\text{prot,i-1}}}}$	for $\sum t_{\text{prot,i-1}} > \frac{t_{\text{prot,0,i}}}{2}$
	$k_{\text{pos,exp,i}}$ for $t_{\text{prot,i}}$	
	$1 - 0,8 \cdot \frac{\sum t_{\text{prot,i-1}}}{t_{\text{prot,0,i}}}$	for $\sum t_{\text{prot,i-1}} \leq \frac{t_{\text{prot,0,i}}}{4}$
Glass wool insulation for $h_i \geq 40$ mm	$(0,001 \cdot \rho_i + 0,27) \cdot \left[ \frac{t_{\text{prot,0,i}}}{\sum t_{\text{prot,i-1}}} \right]^{(0,75 - 0,002 \cdot \rho_i)}$	for $\sum t_{\text{prot,i-1}} > \frac{t_{\text{prot,0,i}}}{4}$

Figure B.3: Position coefficients of exposed wall assembly

Material of the layer considered	$k_{\text{pos,unexp},i}$ for layers backed by cladding made of gypsum or timber	$k_{\text{pos,unexp},i}$ for layers backed by insulation
Gypsum plasterboard, gypsum fibre board	1,0	$0,5 \cdot h_i^{0,15}$
Solid timber, cross-laminated timber, LVL	1,0	$0,35 \cdot h_i^{0,21}$
Particleboard, fibreboard	1,0	$0,41 \cdot h_i^{0,18}$
OSB, plywood	1,0	$0,5 \cdot h_i^{0,15}$
Stone wool insulation	1,0	$0,18 \cdot h_i^{(0,001\rho_i+0,08)}$
Glass wool insulation	1,0	$0,01 \cdot h_i - \frac{h_i^2}{30000} + \rho_i^{0,09} - 1,3$

Figure B.4: Position coefficients of unexposed wall assembly

### B.5.2. Joint coefficients

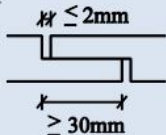
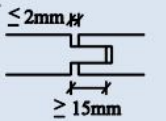
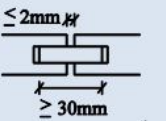
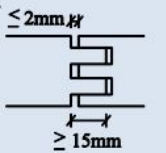
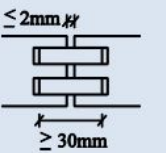
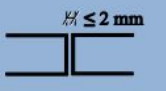
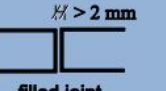
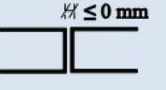
Material	Joint type	$k_{j,n}$ for $t_{ins,n}$	$k_{j,i}$ for $t_{prot,i}$	
			Layer backed by a void cavity	Layer backed by battens or panels or structural members or insulation
Cladding (timber)		0,3	0,3	1,0
		0,4	0,4	1,0
				
		0,6	0,6	1,0
				
	no joint	1,0	1,0	1,0
Gypsum plasterboard, gypsum fibre board		0,8	0,8	1,0
				
	no joint	1,0	1,0	1,0
Insulation (mineral wool insulation)		-	0,8	1,0
	no joint	-	1,0	1,0

Figure B.5: Joint coefficients for wall assembly

### B.5.3. Separating function of wall assembly with multiple 45mm thick layers

Table B.5: Separating function for 135 millimetres thick wall

Layer i	$t_{prot,0,i}(min)$	$t_{ins,n}(min)$	$k_{pos,exp,i}$	$k_{i,j}$	$t(min)$
1	73.20	-	1.0	0.6	43.92
2	73.20	-	0.4	0.6	17.57
3	-	59.13	0.32	0.6	11.27
Total time (min)					72.76

Table B.6: Separating function for 225 millimetres thick wall

Layer i	$t_{prot,0,i}(min)$	$t_{ins,n}(min)$	$k_{pos,exp,i}$	$k_{i,j}$	$t(min)$
1	73.20	-	1.0	0.6	43.92
2	73.20	-	0.4	0.6	17.57
3	73.20	-	0.35	0.6	15.53
4	73.20	-	0.29	0.6	12.68
5	-	59.13	0.22	0.6	7.97
Total time (min)					97.67

Table B.7: Separating function for 315 millimetres thick wall

Layer i	$t_{prot,0,i}(min)$	$t_{ins,n}(min)$	$k_{pos,exp,i}$	$k_{i,j}$	$t(min)$
1	73.20	-	1.0	0.6	43.92
2	73.20	-	0.4	0.6	17.57
3	73.20	-	0.35	0.6	15.53
4	73.20	-	0.29	0.6	12.68
5	73.20	-	0.25	0.6	10.98
6	73.20	-	0.22	0.6	9.82
7	-	59.13	0.18	0.6	6.51
Total time (min)					117.01

Table B.8: Separating function for 405 millimetres thick wall

Layer i	$t_{prot,0,i}(min)$	$t_{ins,n}(min)$	$k_{pos,exp,i}$	$k_{i,j}$	$t(min)$
1	73.20	-	1.0	0.6	43.92
2	73.20	-	0.4	0.6	17.57
3	73.20	-	0.35	0.6	15.53
4	73.20	-	0.29	0.6	12.68
5	73.20	-	0.25	0.6	10.98
6	73.20	-	0.22	0.6	9.82
7	73.20	-	0.20	0.6	8.97
8	73.20	-	0.19	0.6	8.30
9	-	59.13	0.16	0.6	5.64
Total time (min)					133.4

Table B.9: Separating function for 495 millimetres thick wall

Layer i	$t_{prot,0,i}(min)$	$t_{ins,n}(min)$	$k_{pos,exp,i}$	$k_{i,j}$	$t(min)$
1	73.20	-	1.0	0.6	43.92
2	73.20	-	0.4	0.6	17.57
3	73.20	-	0.35	0.6	15.53
4	73.20	-	0.29	0.6	12.68
5	73.20	-	0.25	0.6	10.98
6	73.20	-	0.22	0.6	9.82
7	73.20	-	0.20	0.6	8.97
8	73.20	-	0.19	0.6	8.30
9	73.20	-	0.18	0.6	7.76
10	73.20	-	0.17	0.6	7.32
11	-	59.13	0.14	0.6	5.04
Total time (min)					147.89

## B.6. Connection study

The complete calculations of the resistance and stiffness of the different connections discussed in chapter 7 are shown here. For all connections, a  $k_{mod}$  value of 0.8 is used and a partial safety factor of 1.3. The columns are made of GL24h, which has the properties shown in Table 2.2.

### B.6.1. Connections between members

The calculations for determining the stiffness and resistance of the connections between 2 members discussed in section 7.1 are shown here.

#### Connection A

The compression force is determined by the timber area of the column. So:

$$F_{c,d} = 0.8 \cdot 400 \cdot 400 \cdot 24 / 1.3 = 2363 \text{ kN} \quad (\text{B.1})$$

The tension resistance is determined by the 4 glued-in threaded rods.

Table B.10: Calculation of resistance of glued-in rod connection

Number of rods	n	4	(-)
Diameter rod	d	16	mm
Anchorlength	$l_{ad}$	140	mm
Width column	w	400	mm
Fire protective layer		0	mm
Char layer depth	d	91	mm
Characteristic compression resistance	$f_{c,0,k}$	24	$N/mm^2$
Characteristic tension resistance	$f_{t,0,k}$	16.5	$N/mm^2$
	$k_{mod}$	0.8	(-)
	$\gamma_m$	1.3	(-)
Bond joint strength	$f_{k,1}$	4.00	$N/mm^2$
Yield strength rod	$f_{y,d}$	235	$N/mm^2$
Area rods	$A_{ef}$	804	$mm^2$
Maximum tension force in rods	$F_{ax,Rd}$	113	kN
Maximum tension force in timber	$F_{t,timber}$	608	kN
Design tension resistance	$F_{t,d}$	69	kN

#### Connection B

The compression force is determined by the reduced timber area of the column between the steel profiles.

$$F_{c,d} = 0.8 \cdot (0.5 \cdot 400) \cdot 400 \cdot 24 / 1.3 = 1182 \text{ kN} \quad (\text{B.2})$$

The tension resistance is determined by the 4 glued-in threaded rods. Thus, the tension resistance is the same as for connection 1.

$$F_{t,d} = 69 \text{ kN} \quad (\text{B.3})$$

### Connection C

Both the compression and tension resistance are determined by the steel plates and dowels. The different failure mechanisms are examined.

Compression and tension of the net timber area:

Table B.11: Compression and tension of the net timber area

Net timber area	$A_{net}$	142080	$\text{mm}^2$
Max compression force	$F_{c,max,1}$	3410	kN
Max tension force	$F_{t,max,1}$	2344	kN

Resistance of the steel plates:

Table B.12: Compression and tension of the net timber area

Max compression force	$F_{c,max,2}$	1504	kN
Max tension force	$F_{t,max,2}$	1504	kN

Resistance of dowels (both dowel failure and embedment failure):

Table B.13: Resistance of dowels (both dowel failure and embedment failure)

Embedment strength	$f_h$	26.83	$\text{N/mm}^2$
Plastic moment of dowel	$M_y$	132190	Nmm
Dowel length	t	133.33	mm
Failure mode 1	$F_{dowel,1}$	352.50	kN
Failure mode 2	$F_{dowel,2}$	38.61	kN
Failure mode 3	$F_{dowel,3}$	43.17	kN
Failure mode 4	$F_{dowel,4}$	53.73	kN
Failure mode 5	$F_{dowel,5}$	34.13	kN
Failure mode 6	$F_{dowel,6}$	15.88	kN
Failure mode 7	$F_{dowel,7}$	19.10	kN
Minimum of failure modes	$F_{dowel,max}$	15.88	kN
Effective number of dowel columns	$n_{ef}$	1.47	
Max compression force	$F_{c,max,3}$	186.72	kN
Max tension force	$F_{t,max,3}$	186.72	kN

Block shear and plug shear failure:

Table B.14: Block shear and plug shear failure

Block shear length	$l_t$	220	mm
Block shear area	$A_{net,t}$	88000	$\text{mm}^2$
Block shear resistance	$F_{bp,1}$	2178	kN
Plug shear length	$l_v$	360	mm
Effective dowel length		36.24	mm
Plug shear area	$A_{net,v}$	113700	$\text{mm}^2$
Plug shear resistance	$F_{bp,2}$	278.55	kN
Block and plug shear resistance	$F_{t,max,4}$	278.55	kN

Tension in the net area of the steel plates:

Table B.15: Tension in the net area of the steel plates

Tension resistance of steel plates net area	$F_{t,max,5}$	1918	kN
---	---------------	------	----

So the maximum characteristic compression resistance is the minimum of  $f_{c,max,1}$ ,  $f_{c,max,2}$  and  $f_{c,max,3}$ , which is equal to 186.72 kN. The design compression resistance is 114.90 kN. The maximum characteristic tension resistance is the minimum of  $f_{t,max,1}$ ,  $f_{t,max,2}$ ,  $f_{t,max,3}$ ,  $f_{t,max,4}$  and  $f_{t,max,5}$ , which is equal to 186.72 kN. The design tension resistance is 114.9 kN.

#### Connection D

For this connection, the same tension resistance holds as connection 3, which is 114.9 kN. However, the compression force will be transferred by the steel end plate. Thus:

$$F_{c,d} = 0.8 \cdot 400 \cdot 400 \cdot 24 / 1.3 = 2363 \text{ kN} \quad (\text{B.4})$$

#### Connection E

The maximum compression force is determined by the timber area of the member. So:

$$F_{c,d} = 0.8 \cdot 400 \cdot 400 \cdot 24 / 1.3 = 2363 \text{ kN} \quad (\text{B.5})$$

The maximum tension force is determined by the total tensile resistance of the screws. A  $\phi 11$ mm-300mm full threaded screw with cylindrical head (Rothoblaas VGZ11300) gives a characteristic tensile resistance of 18.75 kN [54]. A total of 14 screws per connection is used, which results in a total maximum tension force in the connection of:

$$F_{t,d} = 0.8 \cdot 8 \cdot 18.75 / 1.3 = 92.31 \text{ kN} \quad (\text{B.6})$$

#### Connection F

A perforated plate Rothoblaas LBV80600 is used, with a width of 80 mm, thickness of 1.5 mm and a total height of 600 millimetres. Anker nails Rothoblaas LBA440 are considered with a diameter of 4 millimetres and a length of 40 millimetres. From [54] follows that the characteristic tensile strength of the plate and the nail group is equal to 26.7 kN and 31.92 kN respectively. Two plates are used, which gives a minimum design tensile resistance of:

$$F_{t,d} = 2 \cdot 0.8 \cdot 26.7 / 1.3 = 39.29 \text{ kN} \quad (\text{B.7})$$

The compression forces are transferred via the timber material, thus gives a total compression resistance of:

$$F_{c,d} = 0.8 \cdot 400 \cdot 400 \cdot 24 / 1.3 = 2363 \text{ kN} \quad (\text{B.8})$$

#### Connection G

The properties of this connection are already determined in subsection 6.3.1.

#### Connection H

The properties of this connection are already determined in section 6.2.

### B.6.2. Shear connections in corners between walls

The calculations for determining the stiffness and shear resistance of the connections between 2 wall segments discussed in section 7.2 are shown here.

#### Connection A

The characteristics values of the resistance and stiffness of a TTV240 connection are found in the catalogue of Rothoblaas [54] and thus the design values can be calculated. This is done for different ctc:

Table B.16: Strength and stiffness of TTV240

ctc (mm)	$F_{v,d}$ (kN/m)	$f_{v,d}$ (N/mm <sup>2</sup> )	$K_{ser}$ (kN/m <sup>2</sup> )
1000	$0.8 \cdot 59.70 / 1.3 \cdot 1000 / 1000 = 37$	0.07	$6.60 \cdot 1000 / 1000 = 6600$
500	$0.8 \cdot 59.70 / 1.3 \cdot 1000 / 500 = 73$	0.15	$6.60 \cdot 1000 / 500 = 13200$
240	$0.8 \cdot 59.70 / 1.3 \cdot 1000 / 240 = 153$	0.31	$6.60 \cdot 1000 / 240 = 33000$

## Connection B

The characteristics values of the resistance and stiffness of a TTN240 connection are found in the catalogue of Rothoblaas [54] and thus the design values can be calculated. This is done for different ctc:

Table B.17: Strength and stiffness of TTN240

ctc (mm)	$F_{v,d}$ (kN/m)	$f_{v,d}$ (N/mm <sup>2</sup> )	$K_{ser}$ (kN/m <sup>2</sup> )
1000	$0.8 \cdot 71.90 / 1.3 \cdot 1000 / 1000 = 44$	0.09	$9.16 \cdot 1000 / 1000 = 9160$
500	$0.8 \cdot 71.90 / 1.3 \cdot 1000 / 500 = 88$	0.18	$9.16 \cdot 1000 / 500 = 18320$
240	$0.8 \cdot 71.90 / 1.3 \cdot 1000 / 240 = 184$	0.37	$9.16 \cdot 1000 / 240 = 45800$

## Connection C

The characteristics values of the resistance and stiffness of a TTS240 connection are found in the catalogue of Rothoblaas [54] and thus the design values can be calculated. This is done for different ctc:

Table B.18: Strength and stiffness of TTS240

ctc (mm)	$F_{v,d}$ (kN/m)	$f_{v,d}$ (N/mm <sup>2</sup> )	$K_{ser}$ (kN/m <sup>2</sup> )
1000	$0.8 \cdot 25.00 / 1.3 \cdot 1000 / 1000 = 15$	0.03	$9.55 \cdot 1000 / 1000 = 9550$
500	$0.8 \cdot 25.00 / 1.3 \cdot 1000 / 500 = 31$	0.06	$9.55 \cdot 1000 / 500 = 19100$
240	$0.8 \cdot 25.00 / 1.3 \cdot 1000 / 240 = 64$	0.13	$9.55 \cdot 1000 / 240 = 39792$

## Connection D

The full shear resistance of the timber can be used, therefore:

$$f_{v,d} = 0.8 \cdot 3.5 / 1.3 \cdot 495 = 1066 \text{ kN/m} = 2.15 \text{ N/mm}^2 \quad (\text{B.9})$$

## Connection E

The characteristic shear resistance of a single screw is determined by Rothoblaas [54] and is equal to 9.06 kN. Therefore, the design strength for different ctc are:

Table B.19: Strength of connection E

ctc (mm)	$F_{v,d}$ (kN/m)	$f_{v,d}$ (N/mm <sup>2</sup> )
200	$0.8 \cdot 2 \cdot 9.06 / 1.3 \cdot 1000 / 200 = 55.75$	0.11
100	$0.8 \cdot 2 \cdot 9.06 / 1.3 \cdot 1000 / 100 = 112$	0.23
55	$0.8 \cdot 2 \cdot 9.06 / 1.3 \cdot 1000 / 55 = 203$	0.41

## Connection F

The strength and stiffness properties are calculated in Table B.20.

Table B.20: Strength and stiffness of connection F

$n$	2		
$d$	10	mm	
$\rho_k$	485	$kg/m^3$	
$t_1$	495	mm	
$t_2$	305	mm	
$\alpha$	90	degrees	
Stiffness			
$K_1$	9288	$N/mm^2$	
$K_{ser}$	186	$N/mm^2$	
Strength			
$F_{ax,Rd}$	58.90	kN	per screw
$F_{v,Rk}$	11.81	kN	failure mode a
	72.78	kN	failure mode b
	108.45	kN	failure mode c
	56.32	kN	failure mode d
	40.61	kN	failure mode e
	17.36	kN	failure mode f
$f_{v,Rk}$	1.40	$N/mm^2$	for 2 screws
$f_{v,Rd}$	0.86	$N/mm^2$	

## Connection G

The strength and stiffness properties of connection G are calculated in Table B.21.

Table B.21: Strength and stiffness of connection G

$n$	2		
$d$	10	mm	
$\rho_k$	485	$kg/m^3$	
$t_1$	495	mm	
$t_2$	305	mm	
$\alpha$	90	degrees	
Stiffness			
$K_1$	9288	$N/mm^2$	
$K_{ser}$	186	$N/mm^2$	
Strength			
$F_{ax,Rd}$	18.46	kN	per screw
$F_{v,Rk}$	11.81	kN	failure mode a
	72.78	kN	failure mode b
	98.34	kN	failure mode c
	46.21	kN	failure mode d
	30.50	kN	failure mode e
	13.30	kN	failure mode f
$f_{v,Rk}$	1.07	$N/mm^2$	for 2 glued-in rods
$f_{v,Rd}$	0.66	$N/mm^2$	

## Connection H

Due to the teeth, half of the shear resistance of the timber can be used, thus:

$$f_{v,d} = 0.8 \cdot 3.5 / 1.3 \cdot 495 / 2 = 533 \text{ kN/m} = 1.08 \text{ N/mm}^2 \quad (\text{B.10})$$

### B.6.3. Tension connections between walls

The calculations for determining the stiffness and tension resistance of the connections between 2 wall segments discussed in section 7.3 are shown here.

#### Connection A

The same glued-in threaded rods are used as for connection A in section 7.1. In this case, 2 rods are placed in the depth of the wall. Using the calculation of subsection B.6.1:

$$F_{c,d} = 0.8 \cdot 495 \cdot 1000 \cdot 24 / 1.3 = 7311 \text{ kN/m} = 14.77 \text{ N/mm}^2 \quad (\text{B.11})$$

The tensile resistance per rod is equal to:

$$F_{t,d} = 69 / 4 = 17.25 \text{ kN} \quad (\text{B.12})$$

For the different c.t.c. distances, the tensile resistance is therefore equal to:

Table B.22: Strength of connection B

ctc (mm)	$F_{t,d}$ (kN/m)	$f_{t,d}$ (N/mm <sup>2</sup> )
500	$2 \cdot 17.25 \cdot 1000 / 500 = 69$	0.14
250	$2 \cdot 17.25 \cdot 1000 / 250 = 138$	0.28
80	$2 \cdot 17.25 \cdot 1000 / 80 = 431$	0.87

#### Connection B

The compression force is determined by the timber area of the column. So:

$$F_{c,d} = 0.8 \cdot 495 \cdot 1000 \cdot 24 / 1.3 = 7311 \text{ kN/m} = 14.77 \text{ N/mm}^2 \quad (\text{B.13})$$

The tension resistance is determined by the glued-in threaded rods.

Table B.23: Calculation of resistance of glued-in rod connection

Number of rods	n	1	(-)
Diameter rod	d	20	mm
Anchorlength	$l_{ad}$	350	mm
Characteristic compression resistance	$f_{c,0,k}$	24	N/mm <sup>2</sup>
Characteristic tension resistance	$f_{t,0,k}$	16.5	N/mm <sup>2</sup>
	$k_{mod}$	0.8	(-)
	$\gamma_m$	1.3	(-)
Bond joint strength	$f_{k,1}$	3.50	N/mm <sup>2</sup>
Yield strength rod	$f_{y,d}$	235	N/mm <sup>2</sup>
Area rod	$A_{ef}$	201	mm <sup>2</sup>
Maximum tension force in rods	$F_{ax,Rd}$	47	kN
Design tension resistance	$F_{t,d}$	29	kN

2 rods are placed in the depth of the wall segments, for the different c.t.c. distances, the tensile resistance is therefore equal to:

Table B.24: Strength of connection B

ctc (mm)	$F_{t,d}$ (kN/m)	$f_{t,d}$ (N/mm <sup>2</sup> )
500	$2 \cdot 29 \cdot 1000 / 500 = 116$	0.23
250	$2 \cdot 29 \cdot 1000 / 250 = 232$	0.47
100	$2 \cdot 29 \cdot 1000 / 100 = 580$	1.17

### Connection C

The same rods are used as for connection A, therefore the tensile resistance will be the same. However, the compression resistance is reduced because of the reduced area of the timber. Thus:

$$F_{c,d} = 0.8 * (495 - 2 \cdot 100) \cdot 24/1.3 = 4357 \text{ kN/m} = 8.80 \text{ N/mm}^2 \quad (\text{B.14})$$

### Connection D

The same screws are used as for connection E in section 7.1. The compression forces are transferred by the timber area.

$$F_{c,d} = 0.8 \cdot 495 \cdot 1000 \cdot 24/1.3 = 7311 \text{ kN/m} = 14.77 \text{ N/mm}^2 \quad (\text{B.15})$$

One screw is used per side with a characteristic tensile resistance of 18.75 kN, thus using different c.t.c. distances, the tensile resistance of the connection is equal to:

Table B.25: Strength of connection D

ctc (mm)	$F_{t,d}$ (kN/m)	$f_{t,d}$ (N/mm <sup>2</sup> )
500	$0.8 \cdot 2 \cdot 18.75/1.3 \cdot 1000/500 = 46$	0.09
250	$0.8 \cdot 2 \cdot 18.75/1.3 \cdot 1000/250 = 92$	0.19
55	$0.8 \cdot 2 \cdot 18.75/1.3 \cdot 1000/55 = 420$	0.85

### Connection E

The same perforated plates and nails are used as Connection F in section 7.1. The compression forces are transferred via the timber material:

$$F_{c,d} = 0.8 \cdot 495 \cdot 1000 \cdot 24/1.3 = 7311 \text{ kN/m} = 14.77 \text{ N/mm}^2 \quad (\text{B.16})$$

The characteristic tensile resistance of a single perforated plate is equal to 26.7 kN. Thus, for the different c.t.c. distances:

Table B.26: Strength of connection E

ctc (mm)	$F_{t,d}$ (kN/m)	$f_{t,d}$ (N/mm <sup>2</sup> )
500	$0.8 \cdot 2 \cdot 26.7/1.3 \cdot 1000/500 = 66$	0.13
250	$0.8 \cdot 2 \cdot 26.7/1.3 \cdot 1000/250 = 131$	0.26
80	$0.8 \cdot 2 \cdot 26.7/1.3 \cdot 1000/80 = 411$	0.83

### Connection F

The full compression and tensile resistance of the timber can be used, therefore:

$$F_{c,d} = 0.8 \cdot 24 \cdot (6/11) \cdot 495/1.3 = 3988 \text{ kN/m} = 8.06 \text{ N/mm}^2 \quad (\text{B.17})$$

$$F_{t,d} = 0.8 \cdot 16.5 \cdot (6/11) \cdot 495/1.3 = 2659 \text{ kN/m} = 5.37 \text{ N/mm}^2 \quad (\text{B.18})$$

# C

## Dynamo model overview

## C.1. Dynamo model overview

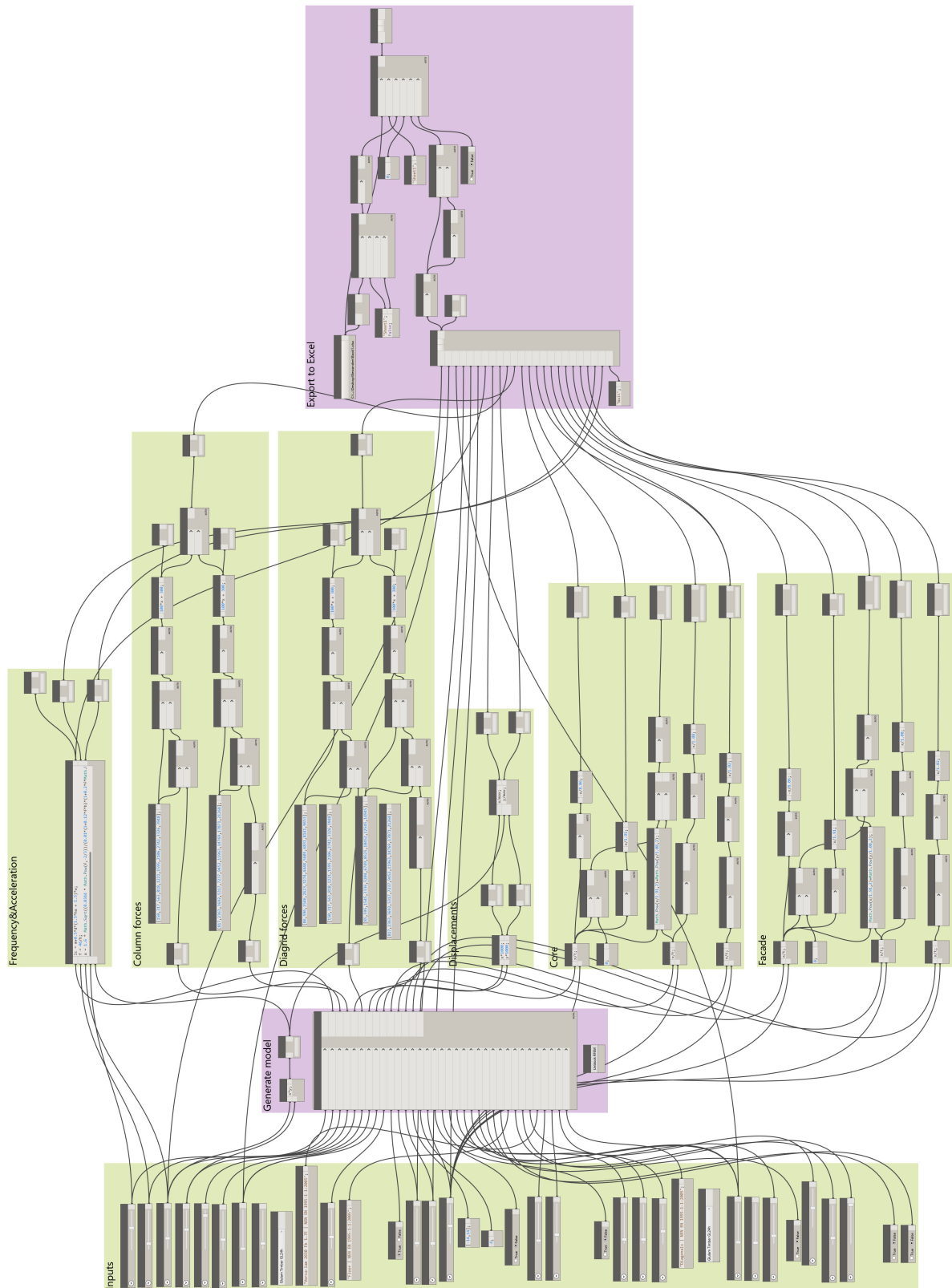


Figure C.1: Dynamo model overview

## C.2. Dynamo model custom node

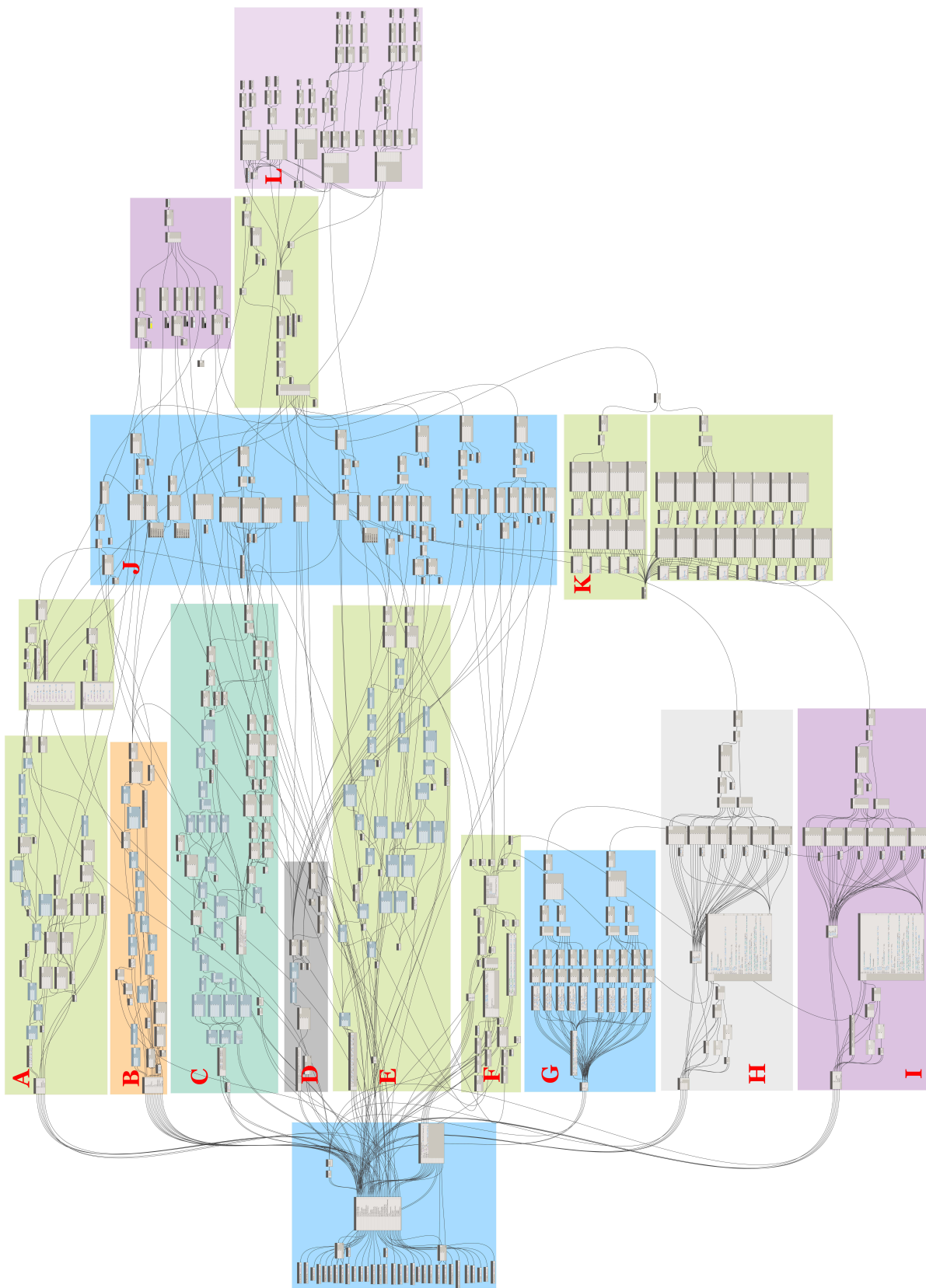


Figure C.2: Dynamo custom node overview



### C.3. Dynamo model facade element research

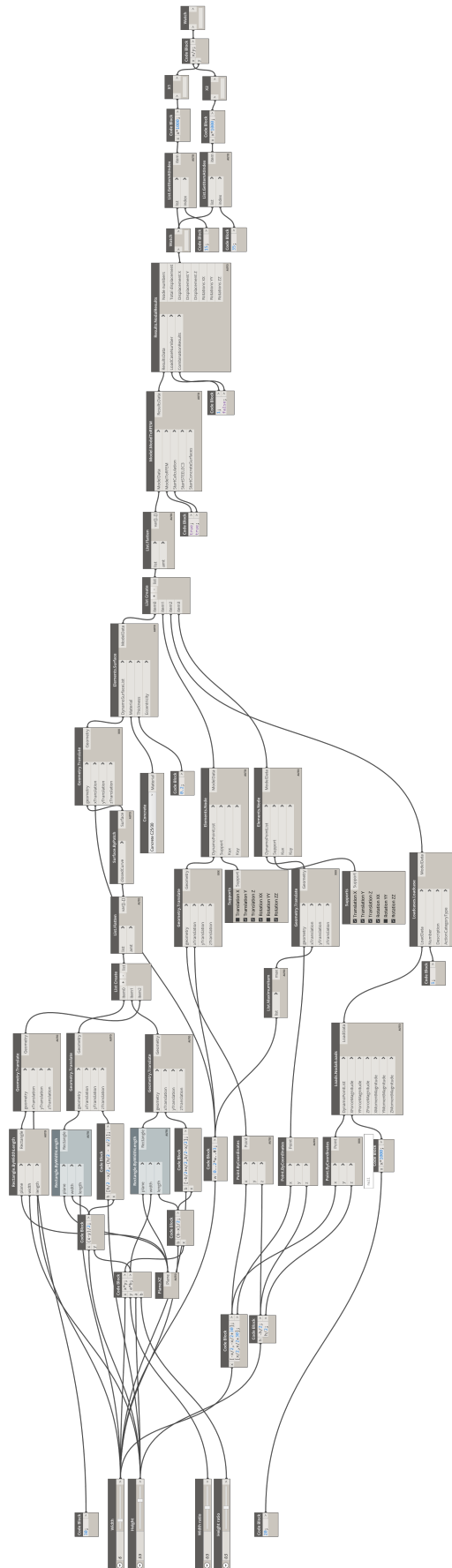


Figure C.3: Dynamo window research



# D

## Parametric study results

### D.1. RFEM results for structure with concrete stability core

Storeys	Column size (mm)	Core width (m)	Core depth (m)	Core thickness (mm)	Building weight (kN)	UC displ. X	UC displ. Y	Advised column size (mm)	Core UC compression	Core UC tension	Core UC shear	Eigenfrequency (Hz)	Acceleration (m/s <sup>2</sup> )
4	400	7	5	250	15635	0.33	0.11	400	0.06	0.04	0.08	3.194	0.032
6	400	7	5	250	23378	0.82	0.32	400	0.13	0.08	0.16	2.130	0.048
8	400	7	5	250	31121	1.51	0.71	400	0.21	0.17	0.24	1.597	0.065
8	400	8	5	250	31481	1.10	0.64	400	0.20	0.14	0.17	1.597	0.064
8	400	9	5	250	31841	0.82	0.58	400	0.16	0.10	0.18	1.597	0.063
10	400	9	5	250	39763	1.33	1.09	500	0.24	0.18	0.24	1.278	0.079
10	500	9	5	250	40314	1.30	1.09	500	0.24	0.18	0.24	1.278	0.078
10	500	10	5	250	40674	1.10	0.98	500	0.26	0.17	0.22	1.278	0.077
10	500	11	5	250	41124	0.87	0.90	500	0.23	0.13	0.29	1.278	0.076
12	500	11	5	250	49319	1.31	1.49	500	0.32	0.23	0.40	1.065	0.091
12	500	11	6	250	49859	1.24	1.03	500	0.28	0.19	0.30	1.065	0.090
12	500	12	6	250	50399	1.01	0.96	500	0.28	0.15	0.23	1.065	0.089
12	500	13	6	250	50939	0.84	0.91	500	0.25	0.24	0.24	1.065	0.088
14	500	13	6	250	59404	1.18	1.39	500	0.33	0.20	0.29	0.913	0.102
14	500	13	7	250	60034	1.13	1.02	500	0.30	0.15	0.24	0.913	0.101
14	500	14	7	250	60664	0.95	0.95	500	0.30	0.16	0.23	0.913	0.100
16	500	14	7	250	69309	1.27	1.34	600	0.37	0.21	0.25	0.799	0.113
16	600	14	7	250	70323	1.27	1.32	600	0.37	0.21	0.25	0.799	0.111
16	600	14	8	250	71043	1.21	1.00	600	0.33	0.17	0.26	0.799	0.110
16	600	15	8	250	71763	1.03	0.94	600	0.33	0.15	0.23	0.799	0.109
16	600	16	8	250	72483	0.89	0.90	600	0.31	0.13	0.23	0.799	0.108
18	600	16	8	250	81525	1.11	1.23	600	0.38	0.18	0.27	0.710	0.121
18	600	16	9	250	82335	1.07	0.95	600	0.33	0.12	0.26	0.710	0.119
18	600	17	9	250	83145	0.93	0.91	600	0.31	0.11	0.26	0.710	0.118
20	600	17	9	250	92367	1.16	1.20	600	0.37	0.14	0.29	0.639	0.130
20	600	17	10	250	93267	1.12	0.96	600	0.36	0.11	0.28	0.639	0.129
20	600	18	10	250	94167	0.98	0.91	600	0.35	0.12	0.28	0.639	0.128
22	600	18	10	250	103568	1.20	1.18	600	0.41	0.16	0.31	0.581	0.139
22	600	19	10	250	104558	1.06	1.13	600	0.42	0.16	0.27	0.581	0.138
22	600	19	11	250	105548	1.02	0.92	600	0.39	0.11	0.25	0.581	0.137
22	600	20	11	250	106253	0.95	0.88	600	0.38	0.09	0.26	0.581	0.136
24	600	20	11	250	115899	1.14	1.12	600	0.44	0.12	0.28	0.532	0.147
24	600	21	11	250	116979	1.03	1.08	600	0.42	0.11	0.31	0.532	0.145
24	600	21	11	300	123891	0.93	0.93	600	0.37	0.07	0.27	0.532	0.137
26	600	21	11	300	134203	1.10	1.17	600	0.42	0.10	0.31	0.491	0.147
26	600	21	11	350	141691	1.01	1.04	600	0.38	0.07	0.28	0.491	0.139
26	600	21	11	400	149179	0.94	0.93	600	0.36	0.05	0.25	0.491	0.132
28	600	21	11	400	160643	1.11	1.15	600	0.40	0.07	0.28	0.456	0.141
28	600	21	11	450	168707	1.04	1.05	600	0.37	0.05	0.26	0.456	0.135

### D.2. RFEM results for structure with CLT stability core

Storeys	Column size (mm)	Core width (m)	Core depth (m)	Core thickness (mm)	Building weight (kN)	UC displ. X	UC displ. Y	Advised column size (mm)	Core UC compression	Core UC tension	Core UC shear	Core UC shear corner	Eigenfrequency (Hz)	Acceleration (m/s <sup>2</sup> )
4	400	7	5	495	14897	0.37	0.16	400	0.07	0.13	0.22	0.23	3.194	0.033
6	400	7	5	495	22751	0.78	0.39	400	0.15	0.37	0.41	0.41	2.130	0.050
8	400	7	5	495	29645	1.40	0.87	400	0.27	0.74	0.61	0.61	1.597	0.068
8	400	8	5	495	29788	1.03	0.78	400	0.24	0.61	0.45	0.46	1.597	0.067
8	400	9	5	495	29931	0.80	0.71	400	0.22	0.52	0.44	0.45	1.597	0.067
10	400	9	5	495	36897	1.20	1.17	500	0.34	0.90	0.59	0.60	1.278	0.085
10	500	10	6	495	38332	0.94	0.74	500	0.27	0.59	0.50	0.51	1.278	0.082
12	500	10	6	495	46867	1.38	1.22	500	0.38	0.92	0.63	0.64	1.065	0.096
12	500	11	7	495	47295	1.07	0.82	500	0.31	0.70	0.64	0.64	1.065	0.095
12	500	12	7	495	47508	0.88	0.77	500	0.30	0.59	0.57	0.58	1.065	0.094
14	500	12	7	495	56151	1.15	1.06	500	0.40	0.89	0.68	0.69	0.913	0.108
14	500	13	7	495	56400	0.96	1.00	500	0.38	0.80	0.69	0.70	0.913	0.107
16	500	13	7	495	63580	1.29	1.40	600	0.47	1.02	0.73	0.74	0.799	0.123
16	600	13	8	495	66502	1.22	1.04	600	0.40	0.91	0.71	0.72	0.799	0.118
16	600	14	8	495	66787	1.03	0.98	600	0.39	0.83	0.71	0.72	0.799	0.117
16	600	15	8	495	67072	0.89	0.93	600	0.39	0.80	0.72	0.72	0.799	0.117
18	600	15	8	495	74359	1.11	1.27	600	0.48	1.01	0.81	0.82	0.710	0.132
18	600	15	9	495	74680	1.07	0.99	600	0.41	0.81	0.66	0.67	0.710	0.132
18	600	16	9	495	75000	0.92	0.94	600	0.40	0.75	0.67	0.68	0.710	0.131
20	600	16	9	495	84516	1.15	1.25	600	0.48	0.94	0.75	0.76	0.639	0.142
20	600	16	10	495	84872	1.10	0.99	600	0.46	0.73	0.75	0.76	0.639	0.142
20	600	17	10	495	85228	0.96	0.94	600	0.44	0.68	0.76	0.76	0.639	0.141
22	600	17	10	495	94815	1.14	1.17	600	0.53	0.84	0.84	0.85	0.581	0.152
22	600	17	11	495	95207	1.11	0.96	600	0.49	0.70	0.76	0.77	0.581	0.151
22	600	18	11	495	95599	0.97	0.91	600	0.46	0.74	0.74	0.74	0.581	0.151
24	600	18	11	495	103100	1.17	1.16	600	0.53	0.90	0.81	0.82	0.532	0.165
24	600	19	11	495	103527	1.04	1.11	600	0.55	0.90	0.84	0.85	0.532	0.164
24	600	19	12	495	103955	1.00	0.92	600	0.52	0.73	0.82	0.83	0.532	0.163
26	600	19	12	495	111527	1.18	1.15	600	0.60	0.88	0.90	0.91	0.491	0.177
26	600	19	12	495	103975	1.17	1.14	600	0.59	0.88	0.76	0.90	0.491	0.190
26	600	20	12	495	104101	1.08	1.09	600	0.58	0.80	0.77	0.91	0.491	0.190

### D.3. RFEM results for diagrid structure with glued-in rods connections

#### D.3.1. 4-storey diagrid

Storeys	Column size (mm)	Diagonal size (mm)	Building weight (kN)	UC displ. X	UC displ. Y	Advised column size (mm)	Advised diagonal size (mm)	Eigenfrequency (Hz)	Acceleration n (m/s <sup>2</sup> )
4	400	300	13696	0.20	0.24	400	300	3.194	0.036
8	400	300	27243	0.32	0.42	400	300	1.597	0.074
12	400	300	40790	0.52	0.70	500	400	1.065	0.110
12	500	400	42109	0.29	0.39	500	400	1.065	0.106
16	500	400	56096	0.45	0.59	600	500	0.799	0.140
16	600	500	58332	0.29	0.38	600	500	0.799	0.134
20	600	500	72877	0.40	0.55	600	500	0.639	0.165
24	600	500	87423	0.56	0.78	700	600	0.532	0.194
24	700	600	91493	0.39	0.55	700	600	0.532	0.186
28	700	600	106717	0.54	0.75	700	700	0.456	0.213
28	700	700	111168	0.40	0.56	700	700	0.456	0.204
32	700	700	127028	0.53	0.75	800	700	0.399	0.229
32	800	700	128324	0.53	0.75	800	700	0.399	0.227
36	800	700	144346	0.70	0.99	800	800	0.355	0.250
36	800	800	150949	0.54	0.76	800	800	0.355	0.239
40	800	800	167704	0.70	0.99	900	900	0.319	0.261
40	900	900	177855	0.55	0.78	900	900	0.319	0.246
44	900	900	195625	0.70	1.00	900	1000	0.290	0.266
44	900	1000	205847	0.61	0.82	900	1000	0.290	0.253
48	900	1000	224547	0.72	1.03	900	1100	0.266	0.272
48	900	1100	236873	0.59	0.85	900	1100	0.266	0.257
52	900	1100	256600	0.74	1.06	1000	1200	0.246	0.274
52	1000	1200	273891	0.62	0.89	1000	1200	0.246	0.257
56	1000	1200	294948	0.76	1.09	1000	1300	0.228	0.272

D.3.2. 6-storey diagrid

Storeys	Column size (mm)	Diagonal size (mm)	Building weight (kN)	UC displ. X	UC displ. Y	Advised column size (mm)	Advised diagonal size (mm)	Eigenfrequency (Hz)	Acceleration n (m/s <sup>2</sup> )
6	400	300	20250	0.62	0.73	400	300	2.130	0.056
12	400	300	40350	0.91	1.18	500	400	1.065	0.111
12	500	400	41326	0.53	0.68	500	400	1.065	0.108
18	500	400	61915	0.84	1.12	600	500	0.710	0.159
18	600	500	63770	0.53	0.71	600	500	0.710	0.154
24	600	500	84977	0.85	1.17	700	700	0.532	0.200
24	700	700	90515	0.43	0.60	700	700	0.532	0.188
30	700	700	113107	0.69	0.96	700	800	0.426	0.228
30	700	800	116775	0.53	0.74	700	800	0.426	0.221
36	700	800	140100	0.81	1.14	800	900	0.355	0.258
36	800	900	146547	0.64	0.90	800	900	0.355	0.247
42	800	900	170946	0.93	1.33	900	1000	0.304	0.280
42	900	1000	179379	0.76	1.08	900	1100	0.304	0.267
42	900	1100	186569	0.63	0.89	900	1100	0.304	0.257
48	900	1100	213200	0.89	1.27	900	1200	0.266	0.286
48	900	1200	222200	0.75	1.07	900	1200	0.266	0.274

## D.3.3. 8-storey diagrid

Storeys	Column size (mm)	Diagonal size (mm)	Building weight (kN)	UC displ. X	UC displ. Y	Advised column size (mm)	Advised diagonal size (mm)	Eigenfrequency (Hz)	Acceleration (m/s <sup>2</sup> )
8	400	300	26803	1.23	1.48	400	400	1.597	0.075
8	400	400	27145	0.82	0.97	400	400	1.597	0.074
16	400	400	54142	1.14	1.43	600	500	0.799	0.145
16	600	500	55886	0.73	0.92	600	500	0.799	0.145
24	600	500	83755	1.20	1.63	700	700	0.532	0.203
24	700	700	88118	0.60	0.81	700	700	0.532	0.193
32	700	700	117442	1.05	1.47	800	900	0.399	0.248
32	800	900	124998	0.64	0.90	800	900	0.399	0.233
40	800	900	156210	1.09	1.55	900	1100	0.319	0.281
40	900	1100	167828	0.74	1.05	900	1100	0.319	0.261
40	900	1200	173453	0.62	0.88	900	1200	0.319	0.253
48	900	1200	208114	0.99	1.43	900	1300	0.266	0.293

### D.4. RFEM results for diagrid structure with steel plates and dowels connections

#### D.4.1. 4-storey diagrid

Storeys	Column size (mm)	Diagonal size (mm)	Building weight (kN)	UC displ. X	UC displ. Y	Advised column size (mm)	Advised diagonal size (mm)	Eigenfrequency (Hz)	Acceleration n (m/s <sup>2</sup> )
4	400	300	13696	0.25	0.32	400	400	3.194	0.036
4	400	400	14038	0.13	0.17	400	400	3.194	0.035
8	400	400	27928	0.24	0.32	400	500	1.597	0.072
8	400	500	28808	0.15	0.20	400	500	1.597	0.070
12	400	500	43138	0.26	0.35	500	500	1.065	0.104
12	500	500	43430	0.26	0.35	500	500	1.065	0.103
16	500	500	57856	0.41	0.54	600	600	0.799	0.135
16	600	600	60484	0.28	0.38	600	600	0.799	0.130
20	600	600	75567	0.40	0.55	600	600	0.639	0.159
24	600	600	90651	0.56	0.78	700	600	0.532	0.187
24	700	600	91493	0.56	0.78	700	600	0.532	0.186
28	700	600	106717	0.76	1.07	700	700	0.456	0.213
28	700	700	111168	0.56	0.79	700	700	0.456	0.204
32	700	700	127028	0.76	1.07	700	700	0.399	0.229
32	800	700	128324	0.76	1.06	700	700	0.399	0.227
32	800	800	134193	0.58	0.82	700	700	0.399	0.217
36	800	800	150949	0.77	1.08	800	800	0.355	0.239
36	800	900	158432	0.61	0.86	800	800	0.355	0.228
40	800	900	176019	0.78	1.11	800	900	0.319	0.249
40	800	1000	185312	0.64	0.90	800	900	0.319	0.237
44	800	1000	203828	0.81	1.16	900	1000	0.290	0.256
44	900	1000	205847	0.81	0.81	900	1000	0.290	0.253
44	900	1100	217146	0.67	0.96	900	1000	0.290	0.240
48	900	1100	236873	0.84	1.21	900	1100	0.266	0.257
48	900	1200	250372	0.71	1.02	900	1100	0.266	0.244

## D.4.2. 6-storey diagrid

Storeys	Column size (mm)	Diagonal size (mm)	Building weight (kN)	UC displ. X	UC displ. Y	Advised column size (mm)	Advised diagonal size (mm)	Eigenfrequency (Hz)	Acceleration (m/s <sup>2</sup> )
6	400	300	20250	0.67	0.83	400	500	2.130	0.056
6	400	500	21032	0.26	0.32	400	500	2.130	0.054
12	400	500	41915	0.44	0.58	500	600	1.065	0.107
12	500	600	43283	0.30	0.40	500	600	1.065	0.104
18	500	600	64850	0.51	0.69	600	600	0.710	0.152
18	600	600	65384	0.51	0.69	600	600	0.710	0.150
24	600	600	87129	0.83	1.15	700	700	0.532	0.195
24	700	700	90515	0.61	0.85	700	700	0.532	0.188
30	700	700	113107	0.97	1.36	700	800	0.426	0.228
30	700	800	116775	0.75	1.05	700	800	0.426	0.221
30	700	900	120932	0.59	0.83	700	800	0.426	0.213
36	700	900	145089	0.91	1.28	800	900	0.355	0.249
36	800	1000	152122	0.74	1.04	800	1000	0.355	0.238
36	800	1100	158285	0.61	0.86	800	1000	0.355	0.228
42	800	1100	184641	0.89	1.27	900	1100	0.304	0.259
42	900	1200	194443	0.75	1.07	900	1100	0.304	0.246

## D.4.3. 8-storey diagrid

Storeys	Column size (mm)	Diagonal size (mm)	Building weight (kN)	UC displ. X	UC displ. Y	Advised column size (mm)	Advised diagonal size (mm)	Eigenfrequency (Hz)	Acceleration n (m/s <sup>2</sup> )
8	300	300	26652	1.45	1.78	400	500	1.597	0.076
8	400	500	27586	0.66	0.79	400	500	1.597	0.073
16	400	500	55022	0.99	1.25	600	600	0.799	0.142
16	600	600	56962	0.67	0.85	600	600	0.799	0.138
24	600	600	85369	1.15	1.56	700	800	0.532	0.199
24	700	800	90319	0.63	0.87	700	800	0.532	0.188
32	700	800	120376	1.14	1.61	800	900	0.399	0.242
32	800	900	124998	0.90	1.28	800	1000	0.399	0.233
32	800	1000	128715	0.74	1.04	800	1000	0.399	0.226
32	800	1100	132824	0.61	0.86	800	1000	0.399	0.219
40	800	1100	165992	1.04	1.49	900	1100	0.319	0.264
40	900	1100	167828	1.04	1.48	900	1100	0.319	0.261
40	900	1200	173453	0.88	1.25	900	1200	0.319	0.253

## D.5. RFEM results for structure with tube system

Storeys	Column size (mm)	Building weight (kN)	UC displ. X	UC displ. Y	Advised column size (mm)	Façade UC compression	Façade UC tension	Façade UC shear	Façade UC corner	Eigenfrequency (Hz)	Acceleration (m/s <sup>2</sup> )
4	400	16528	0.02	0.02	400	0.05	0.00	0.04	0.04	3.194	0.030
6	400	24717	0.02	0.03	400	0.07	0.00	0.06	0.07	2.130	0.046
8	400	32906	0.04	0.05	400	0.10	0.00	0.08	0.10	1.597	0.061
10	400	41096	0.05	0.07	500	0.13	0.00	0.11	0.14	1.278	0.076
10	500	41339	0.05	0.07	500	0.13	0.00	0.11	0.14	1.278	0.076
12	500	49577	0.06	0.08	500	0.17	0.00	0.14	0.18	1.065	0.090
14	500	57814	0.08	0.11	500	0.21	0.00	0.17	0.22	0.913	0.105
16	500	66052	0.11	0.14	600	0.25	0.00	0.20	0.24	0.799	0.119
16	600	66528	0.11	0.14	600	0.25	0.00	0.20	0.23	0.799	0.118
18	600	74825	0.14	0.18	600	0.29	0.00	0.23	0.27	0.710	0.131
20	600	83122	0.17	0.23	600	0.33	0.04	0.26	0.30	0.639	0.145
22	600	91420	0.22	0.28	600	0.38	0.09	0.30	0.34	0.581	0.158
24	600	99717	0.27	0.35	700	0.43	0.15	0.34	0.37	0.532	0.170
24	700	100559	0.26	0.35	700	0.43	0.16	0.34	0.37	0.532	0.169
26	700	108927	0.32	0.43	700	0.49	0.23	0.38	0.41	0.491	0.181
28	700	117294	0.39	0.52	700	0.54	0.32	0.43	0.44	0.456	0.193
30	700	125662	0.42	0.55	700	0.61	0.41	0.47	0.48	0.426	0.205
32	700	134029	0.50	0.66	800	0.67	0.52	0.52	0.52	0.399	0.217
32	800	135325	0.50	0.66	800	0.67	0.52	0.52	0.52	0.399	0.215
34	800	143774	0.59	0.78	800	0.73	0.65	0.57	0.56	0.376	0.226
36	800	152222	0.69	0.91	800	0.80	0.78	0.63	0.60	0.355	0.237
38	800	160671	0.80	1.07	800	0.87	0.92	0.68	0.64	0.336	0.248



## D.7. Timber volume for different type of stability systems

Number of floors	Timber volume per type of stability system (m <sup>3</sup> )								
	Concrete stability core	CLT stability core	Tube system	4-storey diagrid with glued-in rods connections	6-storey diagrid with glued-in rods connection	8-storey diagrid with glued-in rods connection	4-storey diagrid with steel plates and dowels connections	6-storey diagrid with steel plates and dowels connections	8-storey diagrid with steel plates and dowels connections
4	976	1061	1529	962	1400	1905	1031	1556	1994
6	1464	1591	2293	1925	2994	4159	2238	3385	4374
8	1980	2178	3057	3151	4863	7112	3415	5185	7552
10	2658	2904	3870	4648	5811	9975	5079	7591	11054
12	3232	3614	4644	5419	6288	7787	6349	9975	12832
14	3847	4266	5419	6288	7074	9975	7787	11054	15904
16	4454	5262	6288	7074	8646	10400	9975	12832	17191
18	5350	6048	7074	8646	9600	11200	9975	12832	19562
20	5980	6862	7860	9600	10400	12000	9975	12832	24182
22	6658	7705	8646	10400	11200	13059	9975	12832	
24	7392	8577	9600	11200	12000	13875	9975	12832	
26	8289		10400	12000	13059	14692	9975	12832	
28	9834		11200	13059	14692		9975	12832	
30			12000	14437	18940		9975	12832	
32			13059	18071			9975	12832	
34			13875	21923			9975	12832	
36			14692	26381			9975	12832	
38				32037			9975	12832	
40							9975	12832	
42							9975	12832	
44							9975	12832	
46							9975	12832	
48							9975	12832	
50							9975	12832	
52							9975	12832	

